Journal of Function Spaces

Fractional Differentiation and Integration: Above Power Law, Exponential Decay and the Generalized Mittag-Leffler Kernels

Lead Guest Editor: Badr Saad T. Alkaltani
Guest Editors: Pranay Goswami and Ilknur Koca

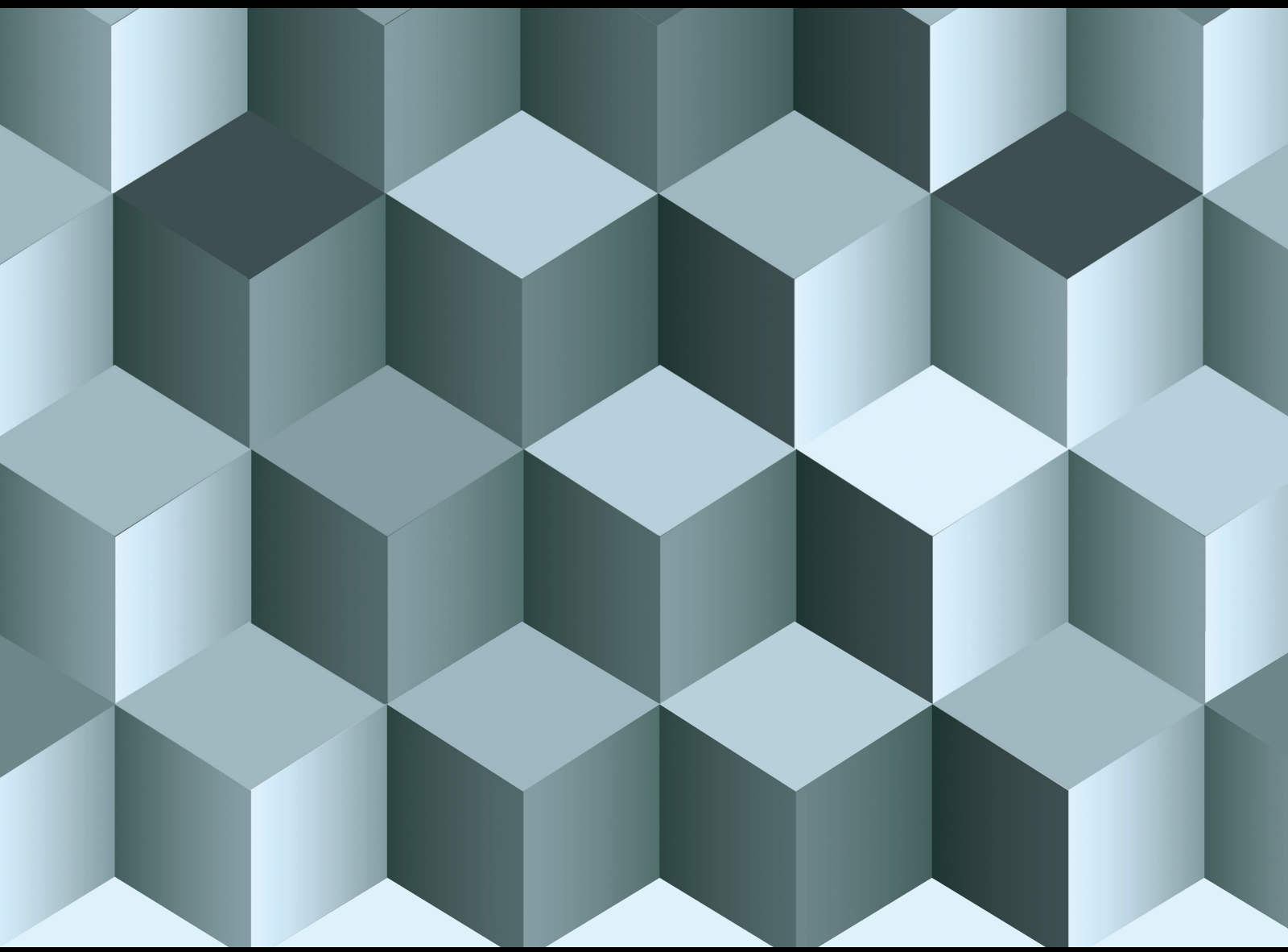

Fractional Differentiation and Integration: Above Power Law, Exponential Decay and the Generalized Mittag-Leffler Kernels

Journal of Function Spaces

Fractional Differentiation and Integration: Above Power Law, Exponential Decay and the Generalized Mittag-Leffler Kernels

Lead Guest Editor: Badr Saad T. Alkaltani
Guest Editors: Pranay Goswami and Ilknur Koca

Contents

Hindawi
Journal of Function Spaces
Volume 2022, Article ID 3771137, 21 pages
https://doi.org/10.1155/2022/3771137

Research Article

Stability Analysis and Optimal Control Strategies of Giving Up Relapse Smoking Model with Bilinear and Harmonic Mean Type of Incidence Rates

Badr Saad T. Alkahtani

Department of Mathematics, College of Science, King Saud University, P.O. Box 1142, Riyadh 11989, Saudi Arabia

Correspondence should be addressed to Badr Saad T. Alkahtani; balqahtani1@ksu.edu.sa

Received 5 September 2021; Revised 12 December 2021; Accepted 9 February 2022; Published 14 April 2022

Academic Editor: Richard I. Avery

In this manuscript, a giving-up smoking model is develop using bilinear incidence rate, harmonic mean type of incidence rate and keeping in view the relapse factor associated to smoking. It is shown that the model' solution is bounded and positive for the appropriate initial data. The equilibria of the model are obtained, and it is proved that the smoking-free equilibrium is both locally and globally asymptotically stable for R_0 less than unity. It is shown that the model has a positive light smoker present equilibrium whenever R_0 is greater than one, and it is locally asymptotically stable if we have $1 < R_0 < 1 + 2\beta_1(\mu + d + \delta)/\Lambda\beta_2$. Conditions for the global stability of light smoker present equilibrium are rigorously investigated. Also, it is proved that the model has a smoking present equilibrium when R_0 satisfies some condition which is investigated both for local and global behavior. By considering a few control measures, optimal control strategies are achieved with the help of Pontryagin's maximum principle. The analytical results are verified numerically, and effectiveness of the control program is presented.

1. Introduction

Among other diseases, infectious diseases are the most alarming threat to humanity from the last few centuries. The plague of Athens is considered to be the first ever epidemic which affects human life to a great extent [1, 2]. The life in Egypt and Roman was completely demolished by the smallpox in 165-180 C.E. in which millions of people died [3]. The epidemic Black Death in Europe is observed to be the first well-documented epidemic which killed more than 50 millions of people that region and Mediterranean. Various other epidemics affected human life throughout the history, and the current corona virus disease is the last epidemic whose disasters are in front of us. Thus, it is very crucial to understand the dynamics of such infectious disease (particularly the emerging epidemics) and to control its spread in early transmission phase. In the context of these extensive illnesses, the tobacco pandemic is one of the world's most serious health threats. According to statistics, up to 50% of smokers die as a result of their habit, a tobacco-related mortality occurs every 8 seconds, and 10 percent of the adult population dies as a result of tobacco-related illnesses [4].

Smoking habit grows and spreads across a society in the same way as an epidemic illness does, and generally, it nearly follows the same process. To be specific, people are prone to smoking at first, then become active users, and eventually recover through certain control methods or self-abandonment of its usage. In the early twentieth century, William Hamer's work on mathematical modeling of infectious illnesses achieved substantial progress. Perhaps, Hamer was the first who introduces mass action law in epidemic modeling. However, Sir Ronald Ross is considered the father of today's mathematical biology due to his work on malaria. In 1911, he published a book regarding malaria in which he used mathematical models for describing the dynamics of the infection and calculated the threshold parameters. The formal mathematical biology started with the work of Kermack

and McKendrick [5], and then, significant contributions were made in the subject, for instance, one can see [6–11].

To study the transmission of smoking habits and its control in the society, numerous researchers used the tools of mathematical modeling and optimal control theory. Castillo-Garrsow et al. [12] used a model of SIR type and well-presented the qualitative aspects of the model under discussion. Sharomi and Gumel [13] extended the work of Castillo-Garrsow et al. and introduced temporary quit class into the model. Zaman [14] incorporated the light smoker compartment and rigorously investigated the model from mathematical perspectives. Subsequently, considering various features and characteristics of smoking, sophisticated models have been developed and investigated, for example, [15–18].

Incidence rate plays a crucial role while investigating the dynamics of any epidemic disease. The bilinear and saturated incidence rates were widely used in case of epidemic diseases and smoking models, for instance, one can see [12, 19, 20]. The authors in [17, 21, 22] used the square root incidence rate and discussed the models from various mathematical aspects. In the sequel, Rahman et al. [4] used harmonic mean type of incidence rate in his giving-up smoking model, investigated the dynamics of the model, and set the controlling strategies for reducing the smoking habit. Similarly, Alzaid and Alkahtani used the same incidence rate and studied the effect of relapse [23]. This work as well as the work of Rahman et al. assumed that potential smokers will start smoking only if they make a contact with light smoker. However, this is usually not the case. A person (potential smoker) may start smoking when he/she comes into contact with a smoker. In this work, the authors intend to overcome this gap. We shall assume that smoking habit may spread in the population via two roots; (i) contacts of potential smoker and light smokers and (ii) contact between smoker and light smokers. For the former type of spread, we will use the usual harmonic mean type of incidence rate, and for the later, the standard bilinear incidence rate will be utilized. By doing so, the present model will cover models [4, 23] as a subcase.

The rest of the work is organized as follows. The model formulation and essential biological features to the model are discussed in Section 2. The smoking generation number and equilibria of the model are presented in Section 3. We investigated the local stability of each equilibrium point in Section 4, whereas the criteria for global dynamics of smoking-free, light smoker present, and smoking-present equilibria are derived in Section 5. The local sensitivity will be performed in Section 6. Based on sensitivity analysis, we take into account some control variables and formulated a control problem for further analysis in Section 7. The desired goals were obtained, and the results are verified through simulations in Section 8. Finally, we presented the conclusion of the work.

2. Model Formulation and Well-Posedness

To formulate the model, we will divide the entire population into four compartments, namely, the potential smokers $P = P(t)$, the light (or occasional) smokers $L = L(t)$, the smokers $S = S(t)$, and the quit smokers $Q = Q(t)$. That is, if $T(t)$ denotes the total population, and then, $T(t) = P + L + S + Q$. We assumed that smoking habit spread in the population through (i) contact between potential smokers and light smokers and (ii) contact between the light smokers and chain smokers. The former contact is mathematically described by harmonic mean type of incidence rate. The reason for taking such type of contact is that the potential smokers may start smoking at a slower rate whenever they come into contact with the light smokers. Due to tendency of light smokers towards smoking, the light smokers will come into contact with smokers frequently and the rate will obey the mass action law. Hence, we assumed the bilinear incidence rate between light smokers and smokers. Furthermore, the harmonic mean type of incidence rate takes into account the behavioral changes of potential smokers and the crowding effect of the light smokers which prevent the unboundedness of the contact rate by choosing suitable parameters. Also, it is very hard to become a light smoker (because many social/cultural variables can restrict the contacts of light smokers with potential smokers), and mathematically, this phenomenon can be modeled by using the harmonic mean type of incidence rate instead of using bilinear incidence rate (because $PL/P + L \leq PL$ whenever P and L are positive). Besides this type of spread, we take into account the spread arising from contact between potential smokers and smokers which is described by bilinear incidence rate. It is also assumed that the quitting of smoking is not permanent, and an individual may start smoking again. These assumptions lead to the following system of ODEs representing the dynamics of smoking habit in a population.

$$\begin{cases} \dfrac{dP(t)}{dt} = \Lambda - 2\beta_1 \dfrac{P(t)L(t)}{P(t)+L(t)} - (d+\mu)P(t) + \gamma Q(t), \\ \dfrac{dL(t)}{dt} = 2\beta_1 \dfrac{P(t)L(t)}{P(t)+L(t)} - \beta_2 L(t)S(t) - (d+\mu)L(t), \\ \dfrac{dS(t)}{dt} = \beta_2 L(t)S(t) - (d+\mu+\delta)S(t), \\ \dfrac{Q(t)}{dt} = \delta S(t) - (d+\mu+\gamma)Q(t), \end{cases} \tag{1}$$

with initial conditions

$$P_0 > 0, L_0 \geq 0, S_0 \geq 0, Q_0 \geq 0, \tag{2}$$

where P_0, L_0, S_0, and Q_0 stand for the initial size of the population of the respective compartments. The description of parameters used in model (1) is shown in Table 1.

By adding the governing equations of model (1), we obtain the conservation law

$$\frac{dT(t)}{dt} = \Lambda - (d_0 + \mu)T(t), \tag{3}$$

with $T(0) = T_0 = P_0 + L_0 + S_0 + Q_0$.

Table 1: Interpretation of parameters of model (1).

Parameter	Interpretation
Λ	Constant recruitment into the potential smokers
β_1	The contact rate of occasional and potential smokers
β_2	The contact rate between smokers and light smokers
μ	The natural mortality rate
d_0	Death rate due to smoking
δ	Temporarily quitting rate of smokers

Theorem 1. *For the nonnegative initial data, if a solution to model (1) exists, it must be positive.*

Proof. Consider the second equation in model (1), and its solution is given by

$$L(t) = L_0 e^{2\beta_1 P(t)/P(t)+L(t)-\beta_2 S(t)-(d+\mu)} \geq 0. \tag{4}$$

By using this relation in the third equation of system (1), we have $S(t) \geq 0$ which assures the positivity of $Q(t)$. Finally, using these facts in the first equation, we have $P(t) \geq 0$. □

Theorem 2. *For nonnegative initial conditions that are not identically zero on any interval, all possible solutions of system (1) are bounded in the region*

$$D = \left\{ (P(t), L(t), S(t), Q(t)) \in R_+^4 : P(t) + L(t) + S(t) + Q(t) \leq \frac{\Lambda}{\mu} \right\}. \tag{5}$$

Since each compartment denotes the size of population and thus must be nonnegative, the desired solution space is $D = \{(P(t), L(t), S(t), Q(t)) \in R_+^4\}$. Thus, the each component in the vector $(P(t), L(t), S(t), Q(t))$ is bounded below by zero, and thus, we have to find the upper bound for the solution. From the conservation equation (3), we have

$$\frac{dT(t)}{dt} = \Lambda - (d_0 + \mu)T(t) \leq \Lambda - \mu T(t). \tag{6}$$

By solving this differential inequality, we get

$$T(t) \leq T(0)e^{-\mu t} + \frac{\Lambda}{\mu}. \tag{7}$$

Letting $t \longrightarrow \infty$, we get $T(t) \leq \Lambda/\mu$. Thus, all solutions of the model are bounded by 0 and Λ/μ, and hence, the desired feasible set is (4).

Theorem 3. *For system (1), the nonnegative space R_+^4 is positive invariant.*

Proof. Consider the vector $\Psi = (P, L, S, Q)$; then, in matrix form, we can write model (1) in the form

$$\frac{d\Psi(t)}{dt} = \mathscr{A}\Psi + \mathscr{B}, \tag{8}$$

where

$$\mathscr{A} = \begin{pmatrix} -\left(\frac{2\beta_1}{P+L}L + d_0 + \mu\right) & 0 & 0 & \gamma \\ \frac{2\beta_1}{P+L}L & -(d_0+\mu) - \beta_2 S & 0 & 0 \\ 0 & \beta_2 S & -(d_0+\mu+\delta) & 0 \\ 0 & 0 & \delta & -(d_0+\mu+\gamma) \end{pmatrix},$$
$$\mathscr{B} = \begin{pmatrix} \Lambda \\ 0 \\ 0 \\ 0 \end{pmatrix}. \tag{9}$$

Clearly, the nondiagonal entries of matrix $\mathscr{A}$ are nonnegative which guarantees that $\mathscr{A}$ is Metzler matrix [24]. Further, $\mathscr{B} \geq 0$, and thus, system (1) is positively invariant in the desired space. In the next section, we intended to find the smoking generation number (an important parameter describing the behavior of a system) as well as the possible equilibria of the proposed system. □

3. Equilibria of the Model and Smoker Generation Number

In order to find the equilibria of the proposed model (1), we set

$$\Lambda - 2\beta_1 \frac{P(t)L(t)}{P(t)+L(t)} - (d+\mu)P(t) + \gamma Q(t) = 0, \tag{10}$$

$$2\beta_1 \frac{P(t)L(t)}{P(t)+L(t)} - \beta_2 L(t)S(t) - (d+\mu)L(t) = 0, \tag{11}$$

$$\beta_2 L(t)S(t) - (d+\mu+\delta)S(t) = 0, \tag{12}$$

$$\delta S(t) - (d+\mu+\gamma)Q(t) = 0. \tag{13}$$

System of equations (10)–(13) always has a solution of the form

$$E_0 = \left(\frac{\Lambda}{\mu+d}, 0, 0, 0\right). \tag{14}$$

This fixed point is known as smoking-free equilibrium of the model.

To calculate the smoker generation number, we will follow the procedure of [25]. For this purpose, consider the smoker classes from system (1) and assume $y = (L(t), S(t))^T$, that is,

$$\frac{dy}{dt} = F - W, \tag{15}$$

where

$$F = \begin{pmatrix} \frac{2\beta_1}{P+L} PL - \beta_2 LS \\ \beta_2 LS \end{pmatrix}, W = \begin{pmatrix} (d+\mu)L(t) \\ (d+\mu+\delta)S(t) \end{pmatrix}. \tag{16}$$

Considering the Jacobians of these two matrices at DFE, we get

$$\tilde{F} = \begin{pmatrix} 2\beta_1 & 0 \\ 0 & 0 \end{pmatrix}, \tilde{W} = \begin{pmatrix} d+\mu & 0 \\ 0 & d+\mu+\delta \end{pmatrix}, \tag{17}$$

and thus,

$$\tilde{W}^{-1} = \begin{pmatrix} \frac{1}{d+\mu} & 0 \\ 0 & \frac{1}{d+\mu+\delta} \end{pmatrix}. \tag{18}$$

Let us consider $\mathcal{G} = \tilde{F}\tilde{W}^{-1}$; thus,

$$\mathcal{G} = \begin{pmatrix} \frac{2\beta_1}{d+\mu} & 0 \\ 0 & 0 \end{pmatrix}. \tag{19}$$

Since R_0 (the smoking generation) is the dominant eigenvalue of the next generation matrix $\mathcal{G}$, hence

$$R_0 = \frac{2\beta_1}{d+\mu}. \tag{20}$$

By using the number R_0, we can obtain other possible equilibria of system (1) using equation (3).

Theorem 4.

(1) If $R_0 > 1$, then model (1) has a positive light smoker present equilibrium given by

$$E_l = (P_l, L_l, S_l, Q_l) = \left(\frac{\Lambda}{2\beta_1}, \frac{\Lambda}{2\beta_1}(R_0 - 1), 0, 0\right). \tag{21}$$

(2) If $R_0 < 1$, then the model has a smoking-free equilibrium given by (14)

(3) Whenever $R_0 = 1$, then again, the model has the smoking-free equilibrium given by (14)

Proof. By solving systems (10)–(13) and keeping in view that there are no smokers (i.e., $S(t) = 0$) in the community, we obtained the light smoker present equilibrium (21). However, for $R_0 < 1$, the light smoker becomes negative and hence, the model will have just the smoking-free equilibrium (14). In the similar way, if we assume $R_0 = 1$, then the fixed point (21) becomes the smoking-free equilibrium as we have $\Lambda/2\beta_1 = \Lambda/(\mu + d)R_0$. □

Theorem 5. *There exists a positive smoking present equilibrium of model (1) blue if $R_0 \geq 1$ and $\beta_2 S_* < \mu + d$.*

Proof. System (1) has a positive solution of the form

$$E_* = (P_*, L_*, S_*, Q_*), \tag{22}$$

where

$$\begin{aligned} P_* &= \frac{\Lambda}{\mu+d} + \frac{\gamma\delta S_*}{(\mu+d)(\mu+d+\gamma)} - \frac{(\mu+d+\delta)}{\beta_2(\mu+d)}(\beta_2 S_* - (\mu+d)), \\ L_* &= \frac{\mu+d+\delta}{\beta_2}, \\ Q_* &= \frac{\delta S_*}{\mu+d+\gamma}, \end{aligned} \tag{23}$$

and S_* is a positive root of

$$\begin{aligned} &\beta_2 \frac{d+\mu+\gamma+\delta}{d+\mu+\gamma} S_*^2 - \left[\frac{(d+\mu)(R_0-1)(d+\mu+\gamma+\delta)}{d+\mu+\gamma} + \frac{\Lambda\beta_2}{\mu+d}\right] S_* \\ &+ \Lambda(R_0 - 1) + R_0 \frac{(\mu+d)(\mu+d+\delta)}{\beta_2} = 0, \end{aligned} \tag{24}$$

which surely exist by Descartes' rule of signs whenever $R_0 > 1$ and $\beta_2 S_* < \mu + d$. Further, if we set $R_0 = 1$, then both solutions of equation (24) are positive and real and hence the theorem. □

4. Local Stability Analysis of Equilibria

To find out the local stability of system (1) at each equilibrium point, first, we will calculate the Jacobian matrix

$$J = \begin{pmatrix} -\frac{2\beta_1 L^2}{(L+P)^2} - (d+\mu) & -\frac{2\beta_1 P^2}{(L+P)^2} & 0 & \gamma \\ \frac{2\beta_1 L^2}{(L+P)^2} & \frac{2\beta_1 P^2}{(L+P)^2} - \beta_2 S - (d+\mu) & -\beta_2 L & 0 \\ 0 & \beta_2 S & \beta_2 L - (d+\mu+\delta) & 0 \\ 0 & 0 & \delta & -(d+\mu+\gamma) \end{pmatrix}. \tag{25}$$

Theorem 6. *The SFE (14) of system (1) is locally asymptotically stable for $R_0 < 1$.*

From relation (25), the Jacobian of system (1) at E_0 is given by

$$J(E_0) = \begin{pmatrix} -(d+\mu) & 2\beta_1 & 0 & \gamma \\ 0 & 2\beta_1 - (d+\mu) & 0 & 0 \\ 0 & 0 & -(d+\mu+\delta) & 0 \\ 0 & 0 & \delta & -(d+\mu+\gamma) \end{pmatrix}. \tag{26}$$

Matrix (26) has eigenvalues $t_1 = -(\mu + d)$, $t_2 = -(\mu + d + \delta)$, $t_3 = 2\beta_1 - (\mu + d)$, and $t_4 = -(\mu + d + \gamma)$. As the parameters of the model assume positive values, thus the eigenvalues t_1, t_2, and t_4 are negative and $t_3 = (\mu + d)(2\beta_1/\mu + d - 1) = (\mu + d)(R_0 - 1)$ is negative only if $R_0 < 1$. Hence, for $R_0 < 1$, all of the eigenvalues of the Jacobian matrix at E_0 are negative and so E_0 is locally asymptotically stable. Further, if $R_0 = 1$, then $t_3 = 0$. However, if we assume $R_0 > 1$, then E_0 becomes unstable as one of the eigenvalues is positive in such case.

Theorem 7. *The local smoking present equilibrium (LSPE) (21) of system (1) is locally asymptotically stable for $1 < R_0 < 1 + 2\beta_1(\mu + d + \delta)/\Lambda\beta_2$.*

Proof. From relation (25), the Jacobian of system (1) at E_l is given by

$$J(E_l) = \begin{pmatrix} -\frac{2\beta_1 L_l^2}{(L_l+P_l)^2} - (d+\mu) & -\frac{2\beta_1 P_l^2}{(L_l+P_l)^2} & 0 & \gamma \\ \frac{2\beta_1 L_l^2}{(L_l+P_l)^2} & \frac{2\beta_1 P_l^2}{(L_l+P_l)^2} - (d+\mu) & -\beta_2 L_l & 0 \\ 0 & 0 & \beta_2 L_l - (d+\mu+\delta) & 0 \\ 0 & 0 & \delta & -(d+\mu+\gamma) \end{pmatrix}. \tag{27}$$

The eigenvalues of matrix (30) are $t_1 = -(\mu + d)$, $t_2 = -(\mu + d)(R_0 - 1)$, $t_3 = -(\mu + d + \gamma)$, and $t_4 = (R_0 - 1)\Lambda\beta_2/2\beta_1 - (\mu + d + \delta)$. Now, for positive parameters of the model and for $R_0 > 1$, the eigenvalues t_1, t_2, and t_3 are negative. However, t_4 is negative only for $R_0 < 1 + 2\beta_1(\mu + d + \delta)/\Lambda\beta_2$. Hence, if $1 < R_0 < 1 + 2\beta_1(\mu + d + \delta)/\Lambda\beta_2$, all of the eigenvalues of the Jacobian matrix at E_l are negative and so E_l is locally asymptotically stable. Moreover, for $R_0 = 1$, we have $t_2 = 0$. In the case of $R_0 < 1$, t_2 becomes positive and thus, the equilibrium E_l will be unstable. □

Theorem 8. *The smoking present equilibrium (SPE) is locally asymptotically stable of if $1 < R_0 < 1 + \beta_2 S_*/\mu + d$.*

Proof. The Jacobian at SPE is given by

$$J = \begin{pmatrix} -a_{11} & -a_{12} & 0 & \gamma \\ a_{21} & -a_{22} & -\beta_2 L_* & 0 \\ 0 & a_{32} & \beta_2 L_* - (d+\mu+\delta) & 0 \\ 0 & 0 & \delta & -a_{44} \end{pmatrix}, \tag{28}$$

where

$$a_{11} = \frac{2\beta_1 L_*^2}{(L_* + P_*)^2} + (d + \mu), \tag{29}$$

$$a_{12} = \frac{2\beta_1 P_*^2}{(L_* + P_*)^2}, \tag{30}$$

$$a_{21} = \frac{2\beta_1 L_*^2}{(L_* + P_*)^2}, \tag{31}$$

$$a_{22} = \beta_2 S_* + (d + \mu) - \frac{2\beta_1 P_*^2}{(L_* + P_*)^2}, \tag{32}$$

$$a_{32} = \beta_2 S_*, \tag{33}$$

$$a_{44} = (d + \mu + \gamma). \tag{34}$$

The characteristic equation of matrix (28) is given by

$$\begin{aligned} &\tau^4 + (a_{44} + a_{22} + a_{11})\tau^3 + (a_{32}(d + \delta + \mu) + a_{11}(a_{22} + a_{44}) \\ &+ a_{12}a_{21} + a_{22}a_{44})\tau^2 + ((da_{32} + \delta a_{32} + \mu a_{32}) \times (a_{11} + a_{44}) \\ &+ a_{44}(a_{11}a_{22} + a_{12}a_{21}))\tau + (d + \delta)a_{11}a_{32}a_{44} - \delta a_{32}a_{21}\gamma \\ &+ \mu a_{11}a_{32}a_{44} = 0. \end{aligned} \tag{35}$$

Clearly, a_{11}, a_{12}, a_{21}, a_{32}, and a_{44} are positive and

$$\begin{aligned} a_{22} &= \beta_2 S_* + (d + \mu) - \frac{2\beta_1 P_*^2}{(L_* + P_*)^2}, \geq \beta_2 S_* + (d + \mu) - 2\beta_1, \\ &= \beta_2 S_* - (d + \mu)(R_0 - 1) > 0, \end{aligned} \tag{36}$$

only if $\beta_2 S_* > (d + \mu)(R_0 - 1)$. Thus, all of the coefficients of the characteristic equation (35) are positive, and hence, by Descartes' rule of signs, this equation has no positive real solution. By using $-\tau$ in place of τ in equation (35) and utilizing Descartes' rule of signs, we get that all of the eigenvalues of this equation are negative or complex conjugates with dominant negative real part. Therefore, the SPE is locally asymptotically stable whenever $R_0 < 1 + \beta_2 S_*/\mu + d$. Further, for the existence of SPE, we must assume that $R_0 > 1$. Moreover, the case $R_0 = 1$ does not affect the stability of the equilibrium point; however, this condition will challenge the existence of smoking-present equilibrium. □

5. Global Stability Analysis of the Equilibria

Theorem 9. *Let $R_0 \leq 1$; then, the smoking-free equilibrium (SFE) E_0 of model (1) is globally asymptotically stable (GAS).*

Proof. For proving the required result, the Lyapunov function of the following form is assumed:

$$\mathscr{V}_1(P, L, S, Q) = L(t) + S(t) + Q(t). \tag{37}$$

By considering the derivative of (37) with respect to time t and using model (1), we have

$$\begin{aligned}\frac{d\mathscr{V}_1}{dt} &= \frac{dL(t)}{dt} + \frac{dS(t)}{dt} + \frac{dQ(t)}{dt},\\ &= 2\beta_1 \frac{P(t)L(t)}{P(t)+L(t)} - \beta_2 L(t)S(t) - (d+\mu)L(t)\\ &\quad + \beta_2 L(t)S(t) - (d+\mu+\delta)S(t) + \delta S(t) - (d+\mu+\gamma)Q(t),\\ &\le 2\beta_1 L(t) - (d+\mu)L(t) - (d+\mu+\delta)S(t) + \delta S(t) - (d+\mu+\gamma)Q(t),\end{aligned} \tag{38}$$

because $P(t)/P(t)+L(t) \le 1$. Thus,

$$\begin{aligned}\frac{d\mathscr{V}_1}{dt} &\le (2\beta_1 - (d+\mu))L(t) - (d+\mu)S(t) - (d+\mu+\gamma)Q(t),\\ &= (\mu+d)(R_0-1)L(t) - (d+\mu)S(t) - (d+\mu+\gamma)Q(t).\end{aligned} \tag{39}$$

Hence,

$$\frac{d\mathscr{V}_1}{dt} < 0, \tag{40}$$

only if $R_0 \le 1$, and thus, by LaSalle's invariant principle [26], E_0 is globally asymptotically stable in the feasible region. □

Theorem 10. *If $1 < R_0 < \beta_2\Lambda + 2\beta_1(d+\mu)/\beta_2\Lambda$, then the local smoking present equilibrium (LSPE) E_l of model (1) is globally asymptotically stable (GAS).*

Proof. To prove the main result, we will take into consideration the Lyapunov function of the form

$$\mathscr{V}_2(P,L,S,Q) = L - L_l - L_l \ln \frac{L(t)}{L_l} + S(t) + Q(t). \tag{41}$$

The third additive compound matrix of J_* is given by

$$J_*^{|3|} = \begin{pmatrix} A_{11} & 0 & 0 & \gamma \\ \delta & A_{22} & -\beta_2 L^* & 0 \\ 0 & \beta_2 S_* & A_{33} & -2\beta_1 \dfrac{P_*^2}{(P_*+L_*)^2} \\ 0 & 0 & 2\beta_1 \dfrac{L_*^2}{(P_*+L_*)^2} & A_{44} \end{pmatrix}, \tag{44}$$

where

$$\begin{aligned}A_{11} &= -\left(d+\mu+2\beta_1\frac{(L_*)^2}{(P_*+L_*)^2}\right) + \left(\frac{R_0P_*^2}{(P_*+L_*)^2} - 1\right)\\ &\quad \cdot (d+\mu) - \beta_2 S_* + \beta_2 L_* - (d+\mu+\delta),\end{aligned}$$

By considering the derivative of (37) with respect to time t and using model (1), we have

$$\begin{aligned}\frac{d\mathscr{V}_2}{dt} &= \frac{dL(t)}{dt} - \frac{L_l}{L(t)}\frac{dL(t)}{dt} + \frac{dS(t)}{dt} + \frac{dQ(t)}{dt},\\ &= 2\beta_1\frac{P(t)L(t)}{P(t)+L(t)} - \beta_2 L(t)S(t) - (d+\mu)L(t)\\ &\quad - \frac{L_l}{L(t)}\left[2\beta_1\frac{P(t)L(t)}{P(t)+L(t)} - \beta_2 L(t)S(t) - (d+\mu)L(t)\right]\\ &\quad + \beta_2 L(t)S(t) - (d+\mu+\delta)S(t) + \delta S(t) - (d+\mu+\gamma)Q(t),\\ &\le (\mu+d)(1-R_0)L(t) - (\mu+d)(R_0-1)L_l\\ &\quad + (\beta_2 L_l - (d+\mu))S(t) - (d+\mu+\gamma)Q(t), <0,\end{aligned} \tag{42}$$

for $R_0 > 1$ and so by LaSalle's invariant principle, the light smoker present equilibrium E_l is globally asymptotically stable. By considering relation (42) and the case of $R_0 = 1$, we will reach to the conclusion of Theorem 9 (as the case of $R_0 = 1$ does not guarantee the existence of LSPE). □

Theorem 11. *If $R_0 > 1$, $\beta_2 S_* < \mu + d$ and $R_0 P_*^2/(P_*+L_*)^2 < 1$, then (1) is GAS at SPE E_*.*

Proof. By considering the Jacobean (25) of the system at the SPE, we have

$$\begin{aligned}A_{22} &= -\left(d+\mu+2\beta_1\frac{(L_*)^2}{(P_*+L_*)^2}\right) + \left(\frac{R_0(P_*)^2}{(P_*+L_*)^2} - 1\right)\\ &\quad \cdot (d+\mu) - \beta_2 S_* - (d+\mu+\gamma),\end{aligned}$$

$$\begin{aligned}A_{33} &= -\left(d+\mu+2\beta_1\frac{(L_*)^2}{(P_*+L_*)^2}\right)\\ &\quad + \beta_2 L_* - (d+\mu+\gamma) - (d+\mu+\delta),\end{aligned}$$

$$\begin{aligned}A_{44} &= \left(\frac{R_0(P_*)^2}{(P_*+L_*)^2} - 1\right)(d+\mu) - \beta_2 S_* + \beta_2 L_*\\ &\quad - (d+\mu+\gamma) - (d+\mu+\delta).\end{aligned} \tag{45}$$

Consider $\rho(\chi) = \text{diag}\{Q,S,L,P\}$ such that $\rho(\chi^{-1}) = \text{diag}\{1/Q, 1/S, 1/L, 1/P\}$ and time derivative is $\rho_f(\chi) = \text{diag}$

$\{\dot{Q}, \dot{S}, \dot{L}, \dot{P}\}$. Therefore,

$$\rho_f \rho^{-1} = \operatorname{diag}\left\{\frac{\dot{P}}{P}, \frac{\dot{L}}{L}, \frac{\dot{S}}{S}, \frac{\dot{Q}}{Q}\right\}, \tag{46}$$

and hence,

$$\rho J^{[3]} \rho^{-1} = \begin{pmatrix} A_{11} & 0 & 0 & \gamma \dfrac{Q}{P} \\ \delta \dfrac{S}{Q} & A_{22} & -\beta_2 S & 0 \\ 0 & \beta_2 L & A_{33} & -2\beta_1 \dfrac{LP}{(P+L)^2} \\ 0 & 0 & 2\beta_1 \dfrac{LP}{(P+L)^2} \dfrac{Q}{S} & A_{44} \end{pmatrix}. \tag{47}$$

By defining $B = \rho_f \rho^{-1} + |2| \rho^{-1}$ so that

$$B = \begin{pmatrix} b_{11} & 0 & 0 & b_{14} \\ b_{21} & b_{22} & b_{23} & 0 \\ 0 & b_{32} & b_{33} & b_{34} \\ 0 & 0 & b_{43} & b_{44} \end{pmatrix}, \tag{48}$$

where

$$b_{11} = \frac{\dot{Q}}{Q} - \left(d + \mu + 2\beta_1 \frac{L_*^2}{(P_* + L_*)^2}\right) + \left(\frac{R_0 P_*^2}{(P_* + L_*)^2} - 1\right) \cdot (d + \mu) - \beta_2 S_* + \beta_2 L_* - (d + \mu + \delta),$$

$$b_{14} = \gamma \frac{Q}{P} = \frac{\dot{P}}{P} - \frac{\Lambda}{P} + 2\beta_1 \frac{L}{P + L} + (d + \mu),$$

$$b_{21} = \delta \frac{S}{Q} = \frac{\dot{Q}}{Q} + (d + \mu + \gamma),$$

$$b_{22} = \frac{\dot{S}}{S} - \left(d + \mu + 2\beta_1 \frac{L_*^2}{(P_* + L_*)^2}\right) + \left(\frac{R_0 P_*^2}{(P_* + L_*)^2} - 1\right) \cdot (d + \mu) - \beta_2 S_* - (d + \mu + \gamma),$$

$$b_{23} = -\beta_2 S,$$

$$b_{32} = \beta_2 L,$$

$$b_{33} = \frac{\dot{L}}{L} - \left(d + \mu + 2\beta_1 \frac{L_*^2}{(P_* + L_*)^2}\right) + \beta_2 L_* - (d + \mu + \delta) - (d + \mu + \gamma),$$

$$b_{34} = -\left(2\beta_1 \frac{LP}{(P + L)^2}\right),$$

$$b_{43} = \left(2\beta_1 \frac{LP}{(P + L)^2}\right),$$

$$b_{44} = \frac{\dot{P}}{P} + \left(\frac{R_0 P_*^2}{(P_* + L_*)^2} - 1\right)(d + \mu) - \beta_2 S_* + \beta_2 L_* - (d + \mu + \delta) - (d + \mu + \gamma). \tag{49}$$

Consequently,

$$h_1(t) = b_{11} + \sum_{j=2}^{4} |b_{1j}|,$$

$$h_1(t) = \frac{\dot{Q}}{Q} - \left(d + \mu + 2\beta_1 \frac{L_*^2}{(P_* + L_*)^2}\right) + \left(\frac{R_0 P_*^2}{(P_* + L_*)^2} - 1\right) \cdot (d + \mu) - \beta_2 S_* + \beta_2 L_* - (d + \mu + \delta) + \gamma \frac{Q}{P},$$
$$\leq \frac{\dot{P}}{P} + \frac{\dot{Q}}{Q} + \left(\frac{R_0 P_*^2}{(P_* + L_*)^2} - 1\right)(d + \mu),$$

$$h_2(t) = b_{22} + \sum_{j=1 \text{ and } j \neq 2}^{4} |b_{2j}|,$$

$$h_2(t) = \frac{\dot{S}}{S} - \left(d + \mu + 2\beta_1 \frac{L_*^2}{(P_* + L_*)^2}\right) + \left(\frac{R_0 P_*^2}{(P_* + L_*)^2} - 1\right) \cdot (d + \mu) - \beta_2 S_* - (d + \mu + \gamma) + \delta \frac{S}{Q} + \beta_2 S + \frac{\dot{Q}}{Q} + (d + \mu + \gamma),$$
$$\leq \frac{\dot{S}}{S} + \frac{\dot{Q}}{Q} + \left(\frac{R_0 P_*^2}{(P_* + L_*)^2} - 1\right)(d + \mu),$$

$$h_3(t) = b_{33} + \sum_{j=1 \text{ and } j \neq 3}^{4} |b_{3j}|,$$

Table 2: Sensitivity indices of R_0 w.r.t and the parameters β_1, μ, and d.

Parameters	Sensitivity index	Value
β_1	S_{β_1}	1
μ	S_μ	−0.999500
d	S_d	−0.00049975

$$\begin{aligned} h_3(t) &= \frac{\dot{L}}{L} - \left(d+\mu+2\beta_1\frac{L_*^2}{(P_*+L_*)^2}\right) + \beta_2 L_* - (d+\mu+\delta) \\ &\quad - (d+\mu+\gamma) + \beta_2 L + \left(2\beta_1\frac{LP}{(P+L)^2}\right), \\ &\le \frac{\dot{L}}{L} - (d+\mu+\gamma), \end{aligned}$$

$$h_4(t) = b_{44} + \sum_{j=1}^{3}|b_{4j}|,$$

$$\begin{aligned} h_4(t) &= \frac{\dot{P}}{P} + \left(\frac{R_0P_*^2}{(P_*+L_*)^2} - 1\right)(d+\mu) - \beta_2 S_* + \beta_2 L_* \\ &\quad - (d+\mu+\delta) - (d+\mu+\gamma) + \left(2\beta_1\frac{LP}{(P+L)^2}\right), \\ &\le \frac{\dot{P}}{P} + \left(\frac{R_0P_*^2}{(P_*+L_*)^2} - 1\right)(d+\mu). \end{aligned} \tag{50}$$

Now we have

$$\begin{aligned} \lim_{t\longrightarrow\infty}\operatorname{supsup}\frac{1}{t}\int \lim_0^t h_1(t)dt &< \lim_{t\longrightarrow\infty}\frac{1}{t}\log\frac{P(t)}{P(0)} \\ &\quad + \lim_{t\longrightarrow\infty}\frac{1}{t}\log\frac{Q(t)}{Q(0)} + \left(\frac{R_0P_*^2}{(P_*+L_*)^2} - 1\right)(d+\mu), \\ &< \left(\frac{R_0P_*^2}{(P_*+L_*)^2} - 1\right)(d+\mu), \end{aligned}$$

$$\begin{aligned} \lim_{t\longrightarrow\infty}\operatorname{supsup}\frac{1}{t}\int \lim_0^t h_2(t)dt &< \lim_{t\longrightarrow\infty}\frac{1}{t}\log\frac{S(t)}{S(0)} \\ &\quad + \lim_{t\longrightarrow\infty}\frac{1}{t}\log\frac{Q(t)}{Q(0)} + \left(\frac{R_0P_*^2}{(P_*+L_*)^2} - 1\right)(d+\mu), \\ &< \left(\frac{R_0P_*^2}{(P_*+L_*)^2} - 1\right)(d+\mu), \end{aligned}$$

$$\begin{aligned} \lim_{t\longrightarrow\infty}\operatorname{supsup}\frac{1}{t}\int \lim_0^t h_3(t)dt &< \lim_{t\longrightarrow\infty}\frac{1}{t}\log\frac{L(t)}{L(0)} \\ &\quad - (d+\mu+\gamma), < -(d+\mu+\gamma), \end{aligned}$$

$$\begin{aligned} \lim_{t\longrightarrow\infty}\operatorname{supsup}\frac{1}{t}\int \lim_0^t h_4(t)dt &< \lim_{t\longrightarrow\infty}\frac{1}{t}\log\frac{P(t)}{P(0)} \\ &\quad + \left(\frac{R_0P_*^2}{(P_*+L_*)^2} - 1\right)(d+\mu), \\ &< \left(\frac{R_0P_*^2}{(P_*+L_*)^2} - 1\right)(d+\mu). \end{aligned} \tag{51}$$

By combining the preceding four inequalities, we have the following inequality.

$$\bar{q} = \lim_{t\longrightarrow\infty}\operatorname{supsup}\frac{1}{t}\int_0^t \mu(B)dt < 0, \tag{52}$$

and we denote the Lozinskii measure by $\mu(B) = h_i$, $i = 1, 2, 3, 4$, and hence, it shows that the SPE is GAS. □

6. Local Sensitivity Analysis

The term R_0 is generally influenced by the inconsistencies in data gathering and estimated values. Sensitivity analysis is used to assess the relative impact of epidemic factors for disease propagation and control.

Definition 12. For the basic reproduction number, the normalized sensitivity index of a parameter ψ (which depends on the partial derivative of R_0 *w.r.t* ψ) is of the following form:

$$S_\psi = \frac{\psi}{R_0}\frac{\partial R_0}{\partial \psi}. \tag{53}$$

By calculating the sensitivity index, we may determine R_0's responsiveness. To find the sensitivity of each parameter for R_0, we will employ equation (53) which was suggested by Tilahun et al. [27]. On the basis of parameter values $\beta_1 = 0.006$, $d = 0.00004$, and $\mu = 0.08$, we have the sensitivity indices of the form

$$\begin{aligned} S_{\beta_1} &= \frac{\beta_1}{R_0}\frac{\partial R_0}{\partial \beta_1} = \frac{\beta_1}{R_0}\frac{2}{\mu+d} = 1, \\ S_\mu &= \frac{\mu}{R_0}\frac{\partial R_0}{\partial \mu} = -\frac{\mu}{\mu+d} = -0.999500 < 0, \\ S_d &= \frac{d}{R_0}\frac{\partial R_0}{\partial d} = -\frac{d}{\mu+d} = -0.00049975 < 0. \end{aligned} \tag{54}$$

These indices enable us to determine the relevance of numerous variables involved in disease transmission, as well as the relative change in the number of reproductions as a function of parameter changes. Using such indices, we may identify the characteristics that have a significant impact on R_0 and are critical for disease prevention.

Table 2 suggests that there is a positive relation between R_0 and β_1 while negative influence of μ and d on R_0. The same argument is supported by Figure 1. This means that if you raise or reduce the value of parameter β_1 by 10%, it

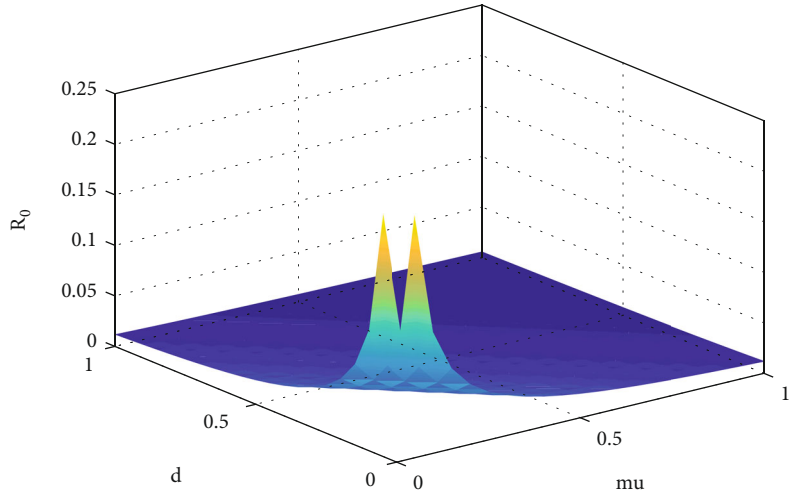

(a) R_0 verses μ and d at fixed $\beta_1 = 0.006$

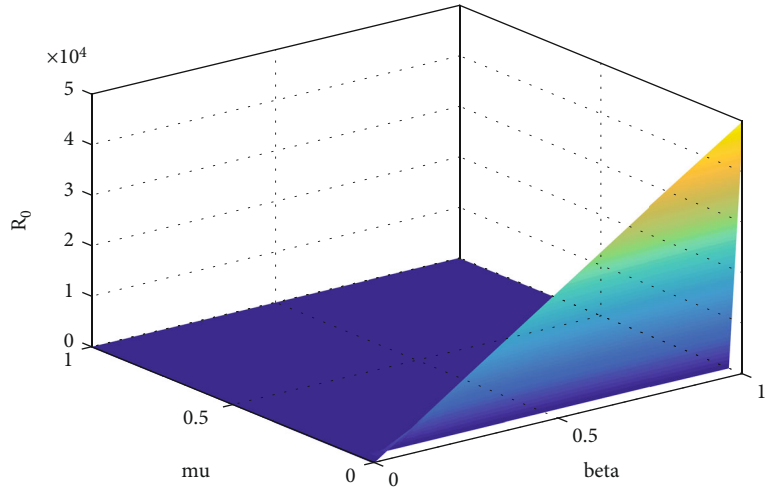

(b) R_0 verses β and d at fixed $\mu = 0.08$

FIGURE 1: Sensitive parameters β, μ, and d and its impact on R_0.

will rise or decrease R_0 by 10%. Similarly, if we reduce or increase μ and d by 1 percent, its relative inverse impact on R_0 will be 99.9% and 0.04%, respectively. To prevent smoking from the population, we must consider those parameters which have high sensitivity indices. Based on the sensitivity indices, we concluded that β_1 will directly affect R_0 (100%) whereas μ affects R_0 inversely about 99%. Thus, to reduce smoking habit, we must focus on the contacts between potential smokers and light smokers. It is simple to develop a control mechanism program for eradication of smoking habit based on this study.

7. Formulation and Analysis of Optimal Control Problem

In this part, we simulate the eradication of smoking habit from the population by using the tools of control theory [9, 28]. We focus on reducing transmission, which has a sensitivity index of 1, to develop a control plan based on local sensitivity analysis. Further, to make the control program more effective, we take into consideration the following four control measures.

The first control measure is the education campaign which is denoted by $u_1(t)$, and its aim is to reduce the size of potential smokers. The second control variable $u_2(t)$ shows physically antismoking gum, and it will reduce the number of light smokers. The third and fourth control variables are antinicotive drug $u_3(t)$ and ban on smoking particularly in public places by the government $u_4(t)$. These measures will be imposed on the smoking compartment. It is observed that whenever the law enforcement personnel came into contact with light smokers (which smoke in public places), the light smokers will tend to quit smoking in public places. That is, by increasing the law enforcement personnel in public places, the size of light smokers will tend to decrease and hence, small number of individuals will tend to quit smoking. Therefore, we will use the term $1 - u_4(t)$ which will reduce the contacts between the law enforcement personnel with the light smokers. The control variables are subject to some

Table 3: Parameter values for verifying the global stability of smoking-free equilibrium.

Parameters	Values	Parameters	Values
Λ	10.25	μ	0.08
γ	0.006	β_1	0.008
β_2	0.00038	d	0.0019
δ	0.000274		

Table 4: Parameter values for verifying the global stability of light smoker present equilibrium.

Parameters	Values	Parameters	Values
Λ	10.25	μ	0.0111
γ	0.006	β_1	0.038
β_2	0.00038	d	0.0019
δ	0.041		

conditions; $u_i(t) \in [0, u_{i_{\max}}]$ for $i = 1, \cdots, 4$ and $u_1 \le u_4 \le u_2 \le u_3$. These control variables are the main measures which could help in reducing the smoking habit [29]. Based on the control measures, we have the following governing equations for the control problem:

$$\begin{cases} \frac{dP(t)}{dt} = \Lambda - 2\beta_1 \frac{P(t)L(t)}{P(t)+L(t)} - (d + \mu + u_1(t))P(t) + \gamma Q(t), \\ \frac{dL(t)}{dt} = 2\beta_1 \frac{P(t)L(t)}{P(t)+L(t)} - \beta_2 L(t)S(t) - (d + \mu + u_2(t) + (1 - u_4(t)))L(t), \\ \frac{dS(t)}{dt} = \beta_2 L(t)S(t) - (d + \mu + \delta + u_3(t) + qu_4(t))S(t), \\ \frac{Q(t)}{dt} = \delta S(t) - (d + \mu + \gamma)Q(t) + (u_3(t) + qu_4(t))S(t) + (u_2(t) + 1 - u_4(t))L(t) + u_1(t)P(t), \end{cases} \tag{55}$$

with the conditions

$$P_0 > 0, L_0 \ge 0, S_0 \ge 0, Q_0 \ge 0, \tag{56}$$

Our optimum control strategy is to reduce/minimize the number of potential smokers, light smokers, and smokers while increasing the number of people who quit smoking. Keeping in view the control problem (55), our cost functional is given by the following:

$$J(u_1, u_2, u_3, u_4) = \int_0^T \left[D_1 L + D_2 S + D_3 P - D_4 Q + \frac{1}{2}\left(F_1 v_1^2(t) + F_2 v_2^2(t) + F_3 v_3^2(t) + F_4 v_4^2(t)\right) \right] dt. \tag{57}$$

Equation (60) denotes a nonlinear system (the proposed control problem) with bounded coefficients. Set

$$\mathcal{K} = \mathcal{L}\psi + \mathcal{X}(\psi). \tag{62}$$

Table 5: Parameter values are used for showing the effectiveness of the control program.

Parameters	Values	Parameters	Values
Λ	10.25	μ	0.0111
γ	0.006	β_1	0.9
β_2	0.00038	d	0.0019
δ	0.000274	q	0.2

In the cost functional (57), D_i's are positive constants describing the balancing factors, whereas F_i's are the cost associated to the control measures. Clearly, the cost functional has a goal to reduce smoker population and to enhance the size of quit smokers. Our main focus is to find a set of functions $\{u_1^\star, u_2^\star, u_3^\star, u_4^\star\}$ in such a way that

$$J(u_1^\star, u_2^\star, u_3^\star, u_4^\star) = \min_{u_i \in V} J(u_i), \tag{58}$$

where the set V is the admissible control set and is define by

$$V = \left\{ u_i(t) \in L^2[0, T] : 0 \le u_i(t) \le u_{i_{\max}} \le 1 \text{ for } i = 1, \cdots, 4 \right\}, \tag{59}$$

where $u_i(t)$ are the control variables described above, and these are Lebesgue measurable functions. To identify such control measures, we must first establish that actually they exist.

7.1. Existence of Solution to the Control Problem. For proving the desired result, we will take into consideration problems (55) and (56) and will show that actually this system has a solution. It is worthy to notice that nonnegative bounded solutions to the state system exist if we have bounded Lebesgue measurable control measures and nonnegative initial conditions [28]. Let

$$\frac{d\psi}{dt} = \mathcal{L}\psi + \mathcal{X}(\psi), \tag{60}$$

and here,

By considering the following,

$$\begin{aligned} |\mathcal{X}(\psi_1) - \mathcal{X}(\psi_2)| &\le 2\beta_1 |P_1 - P_2| + 2\beta_1 |L_1 - L_2| + \beta_2 |L_1 S_1 - L_2 S_2|, \\ &\le N_1 (|P_1 - P_2| + |L_1 - L_2| + |L_1 S_1 - L_2 S_2|), \end{aligned} \tag{63}$$

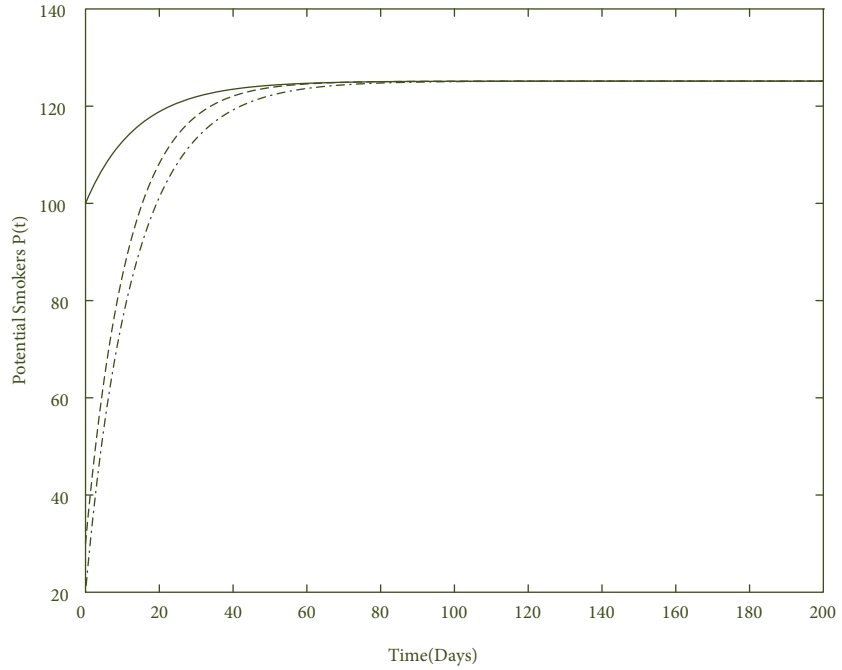

(a) Dynamics of potential smokers whenever $R_0 < 1$

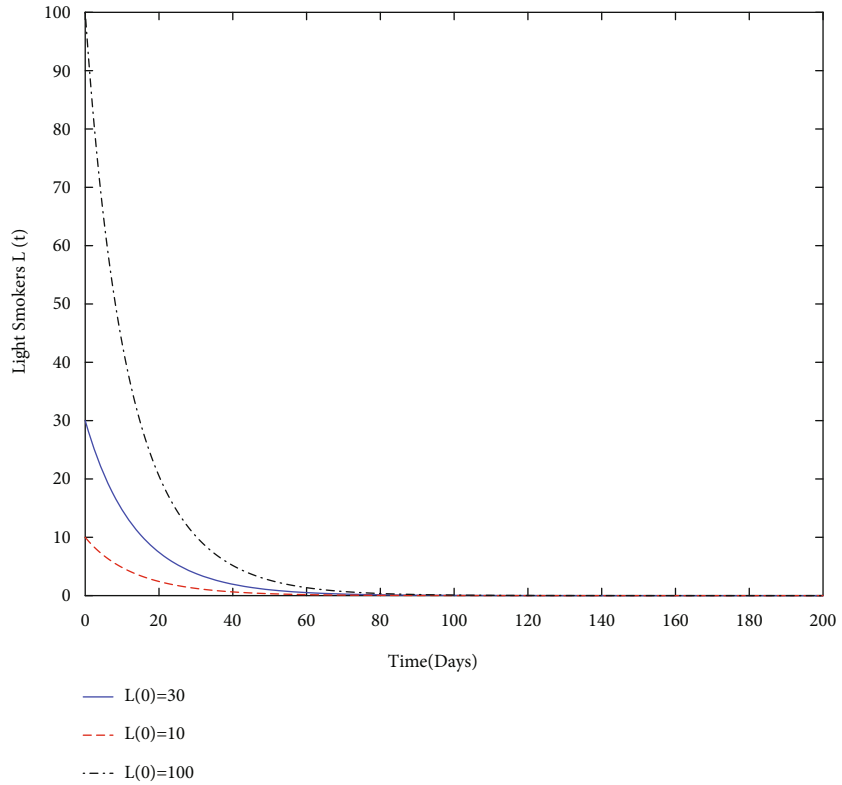

(b) The case of $R_0 < 1$ and evolution of light smokers

Figure 2: Continued.

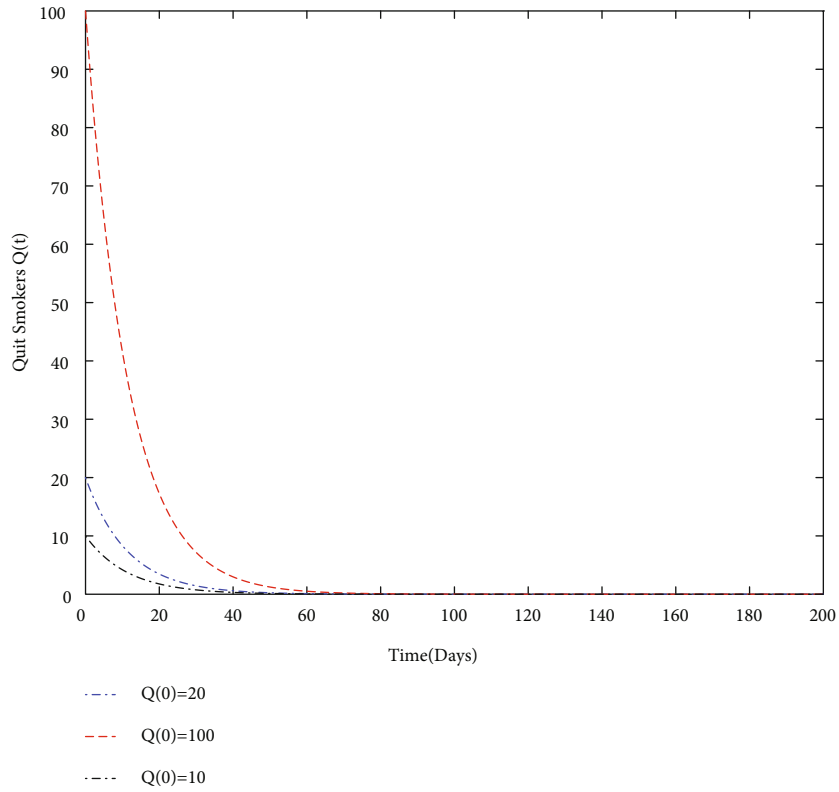

(c) Behavior of smoker population for $R_0 < 1$

FIGURE 2: Different initial size of compartments and its long-term behavior for $R_0 < 1$.

where $N_1 = \max(2\beta_1, \beta_2)$ is free from the state's variable. Also, one can write

$$|\mathcal{K}(\psi_1) - \mathcal{K}(\psi_2)| \leq \leq M_1(|\psi_1 - \psi_2|), \tag{64}$$

where $\infty > M_1 = \max(N_1, \|\mathcal{L}\|)$; thus, $\mathcal{X}$ is uniformly continuous function in the sense of Lipschitz. Further, for the definition of the control measures and conditions on the states $(P(t) > 0, L(t) \geq 0, S(t) \geq 0$ and $R(t) > 0)$, we can observe that a solution to the control problem (55) does really exist. The following conclusion holds for the existence of control variables in the optimum control problem.

Theorem 13. *There exists a control vector* $u^\star = (u_1^\star, u_2^\star, u_3^\star, u_4^\star) \in U$ *which minimizes the objective functional.*

Proof. In order to show that actually such control variables exist, we need to follow [28], as

(a) Both the state and control functions are nonnegative

(b) Convexity and closedness properties hold by the set of admissible controls

(c) The boundedness of the control model assures the compactness

(d) The function inside the integral in the objective functional (57) is convex in the control measures

Therefore, there exist the control variables $u_i(t)$ for $i = 1, 2, 3, 4$ which minimize the objective functional. □

7.2. Optimality Conditions. For deriving characterization of the control from the control problem (55) subject to the cost functional (57), first of all, we will define the Lagrangian and the Hamiltonian for this problem. Let $z = (P, L, S, Q)$ denote the vector whose components are the state functions and $u = (u_1, u_2, u_3, u_4)$ is the control vector. The Lagrangian $\mathcal{L}$ is given by

$$\mathcal{L}(z, u) = D_1 L + D_2 S + D_3 P - D_4 Q + \frac{1}{2}\left(F_1 v_1^2(t) + F_2 v_2^2(t) + F_3 v_3^2(t) + F_4 v_4^2(t)\right), \tag{65}$$

and the Hamiltonian $\mathcal{H}$ is given by

$$\mathcal{H}(z, u, \lambda) = L(z, u) + \lambda f(z, u), \tag{66}$$

where $\lambda = (\lambda_1, \lambda_2, \lambda_3, \lambda_4)$ and $f(z, u) = f_1(z, u) + f_2(z, u) + f_3(z, u) + f_4(z, u)$ with

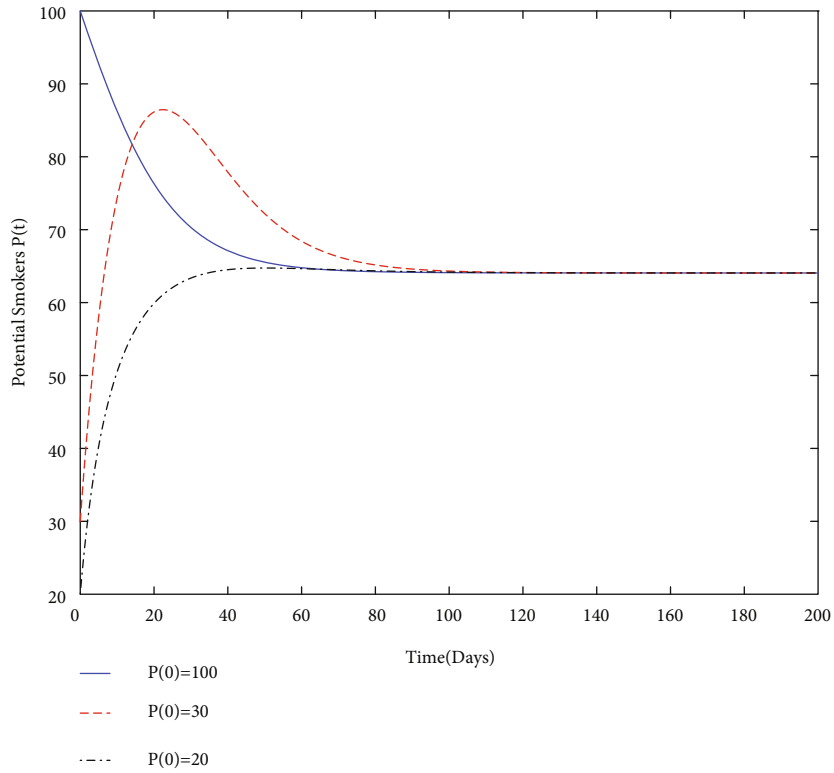

(a) The plot shows that $P \longrightarrow P_*$ when $R_0 > 1$

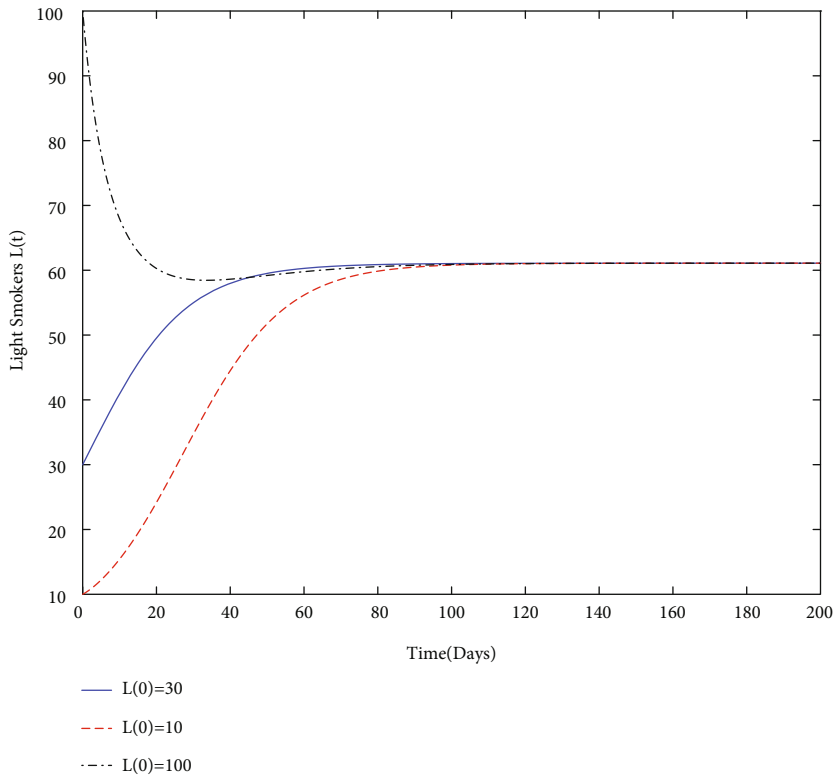

(b) Behavior of the light smokers for $R_0 > 1$

FIGURE 3: The plot describes stability of smoking present equilibrium $E_{\tilde{a}}$ when $R_0 > 1$.

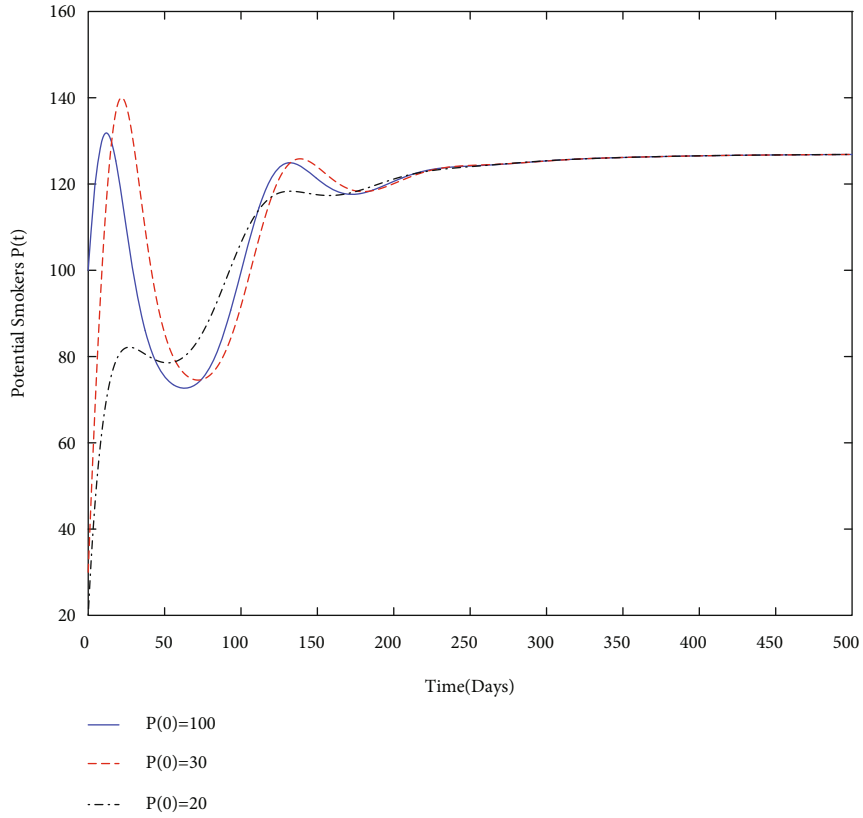

(a) The plot shows the overall effect of control variables on the class of potential smokers

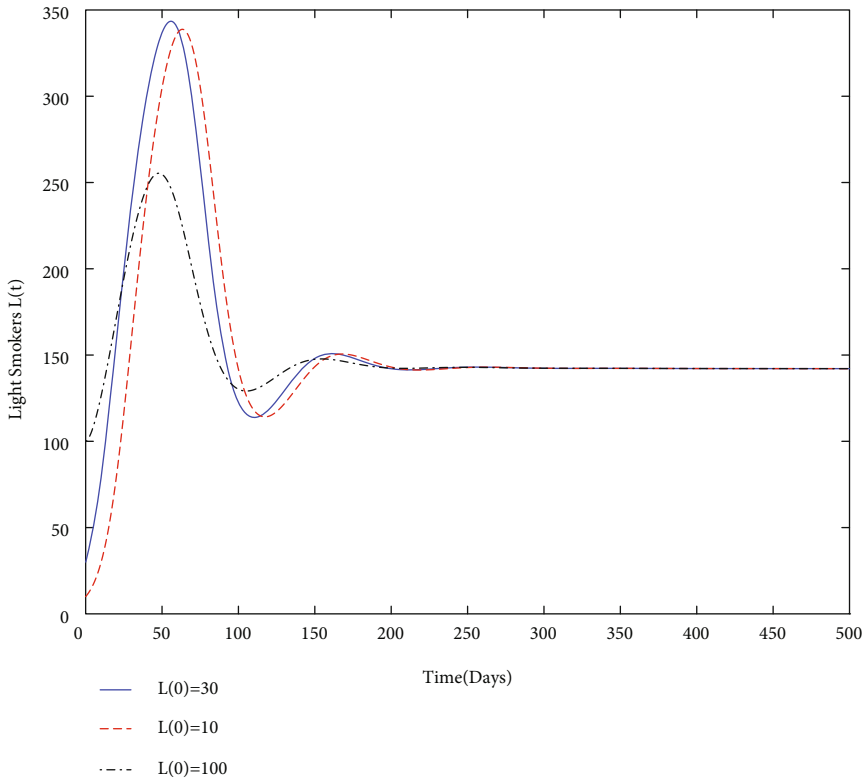

(b) Comparison of curves $L(t)$ both with and without control

FIGURE 4: Continued.

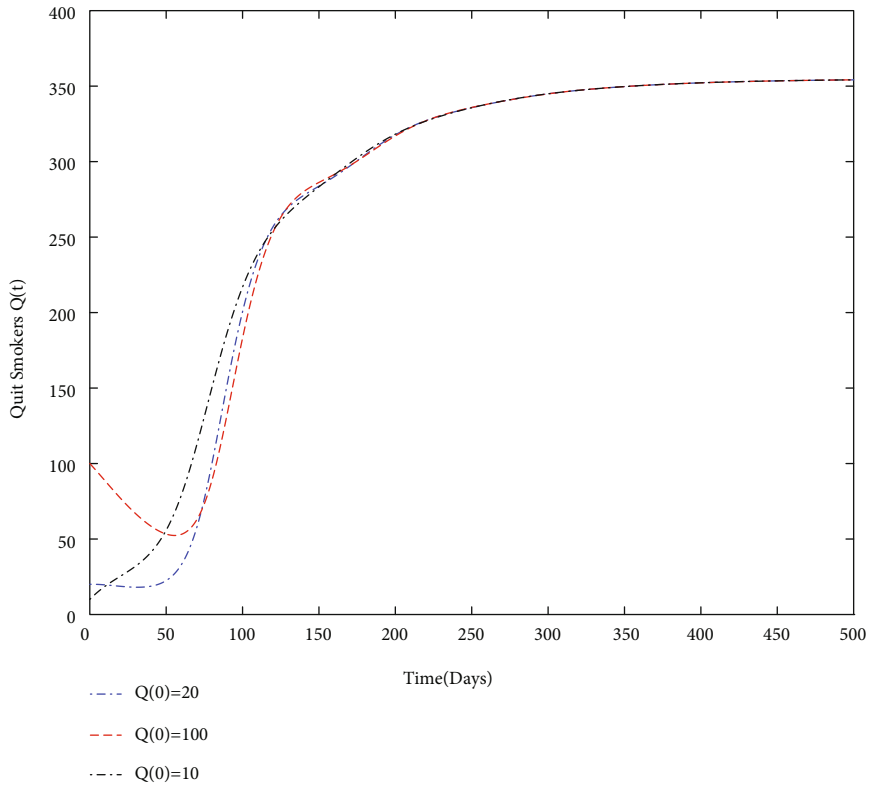

(c) Dynamics of smokers in the presence and absence of control variables

FIGURE 4: The plot presents a comparison of solution curves both with and without control.

$$\begin{cases} f_1(z,u) = \Lambda - 2\beta_1 \dfrac{P(t)L(t)}{P(t)+L(t)} - (d+\mu+u_1(t))P(t) + \gamma Q(t), \\ f_2(z,u) = 2\beta_1 \dfrac{P(t)L(t)}{P(t)+L(t)} - \beta_2 L(t)S(t) - (d+\mu+u_2(t)+(1-u_4(t)))L(t), \\ f_3(z,u) = \beta_2 L(t)S(t) - (d+\mu+\delta+u_3(t)+qu_4(t))S(t), \\ f_4(z,u) = \delta S(t) - (d+\mu+\gamma)Q(t) + (u_3(t)+qu_4(t))S(t) + (1-u_4(t))L(t) + u_1(t)P(t). \end{cases} \tag{67}$$

Thus,

$$\begin{aligned} \mathcal{H}(z,u,\lambda) &= D_1 L + D_2 S + D_3 P - D_4 Q + \frac{1}{2}\left(F_1 v_1^2(t)\right. \\ &\quad \left. + F_2 v_2^2(t) + F_3 v_3^2(t) + F_4 v_4^2(t)\right) + \lambda_1 \\ &\quad \cdot \left(\Lambda - 2\beta_1 \frac{P(t)L(t)}{P(t)+L(t)} - (d+\mu+u_1(t))P(t) + \gamma Q(t)\right) \\ &\quad + \lambda_2 \left(2\beta_1 \frac{P(t)L(t)}{P(t)+L(t)} - \beta_2 L(t)S(t)\right. \\ &\quad \left. - (d+\mu+u_2(t)+(1-u_4(t)))L(t)\right) \\ &\quad + \lambda_3(\beta_2 L(t)S(t) - (d+\mu+\delta+u_3(t) \\ &\quad + qu_4(t))S(t)) + \lambda_4(\delta S(t) - (d+\mu+\gamma)Q(t) \\ &\quad + (u_3(t)+qu_4(t))S(t) + (u_2(t) \\ &\quad + (1-u_4(t)))L(t) + u_1(t)P(t)). \end{aligned} \tag{68}$$

The Pontryagin maximum principle [28] is used to determine the best solution for our given optimum control problem.

If $(z^\star, u^\star)$ is the best solution for the control problem (55), then there exists a nonzero vector function λ such that the Hamiltonian system satisfies

$$\frac{dz^\star(t)}{dt} = \frac{\partial \mathcal{H}}{\partial \lambda}(z^\star(t), u^\star(t), \lambda(t)), \tag{69a}$$

$$\frac{\partial \mathcal{H}}{\partial u}(z^\star(t), u^\star(t), \lambda(t)) = 0, \tag{69b}$$

$$\frac{d\lambda(t)}{dt} = -\frac{\partial \mathcal{H}}{\partial z}(z^\star(t), u^\star(t), \lambda(t)), \tag{69c}$$

while holding the maximality and transversality conditions

$$\mathcal{H}(z^\star(t), u^\star(t), \lambda(t)) = \max_u \mathcal{H}(z^\star(t), u, \lambda(t)), \tag{70}$$

$$\lambda(T) = 0. \tag{71}$$

Theorem 14. *Let $P^\star$, $L^\star$, $S^\star$, and $Q^\star$ be optimal states associated with the optimal controls $(u_1^\star, u_2^\star, u_3^\star, u_4^\star)$ for problem (55). Then, there exist adjoint variables $\lambda_1(t)$, $\lambda_2(t)$, $\lambda_3(t)$, and $\lambda_4(t$*

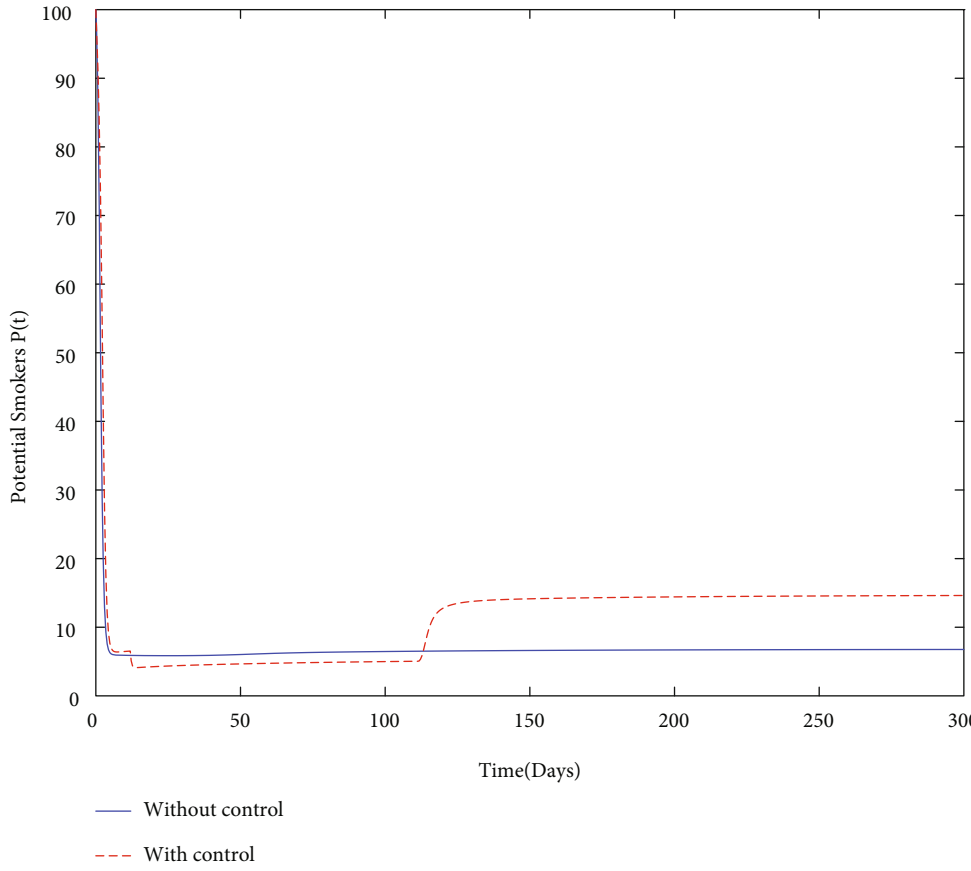

(a)

Figure 5: Continued.

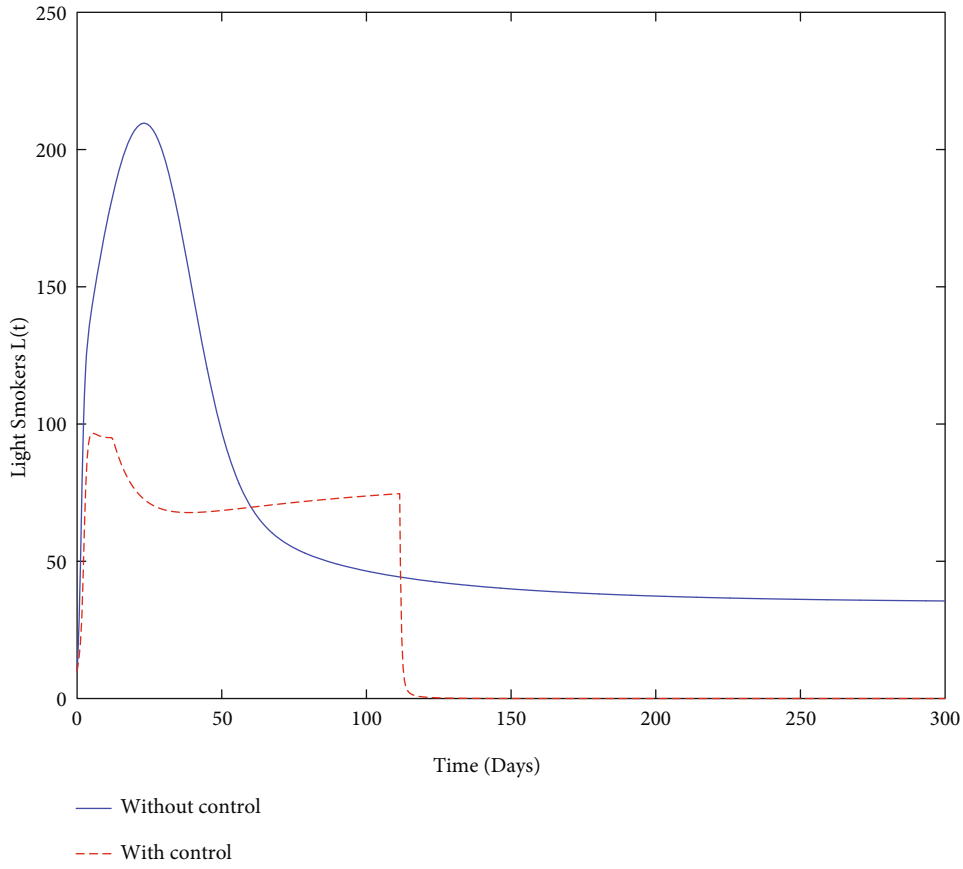

(b)

Figure 5: Continued.

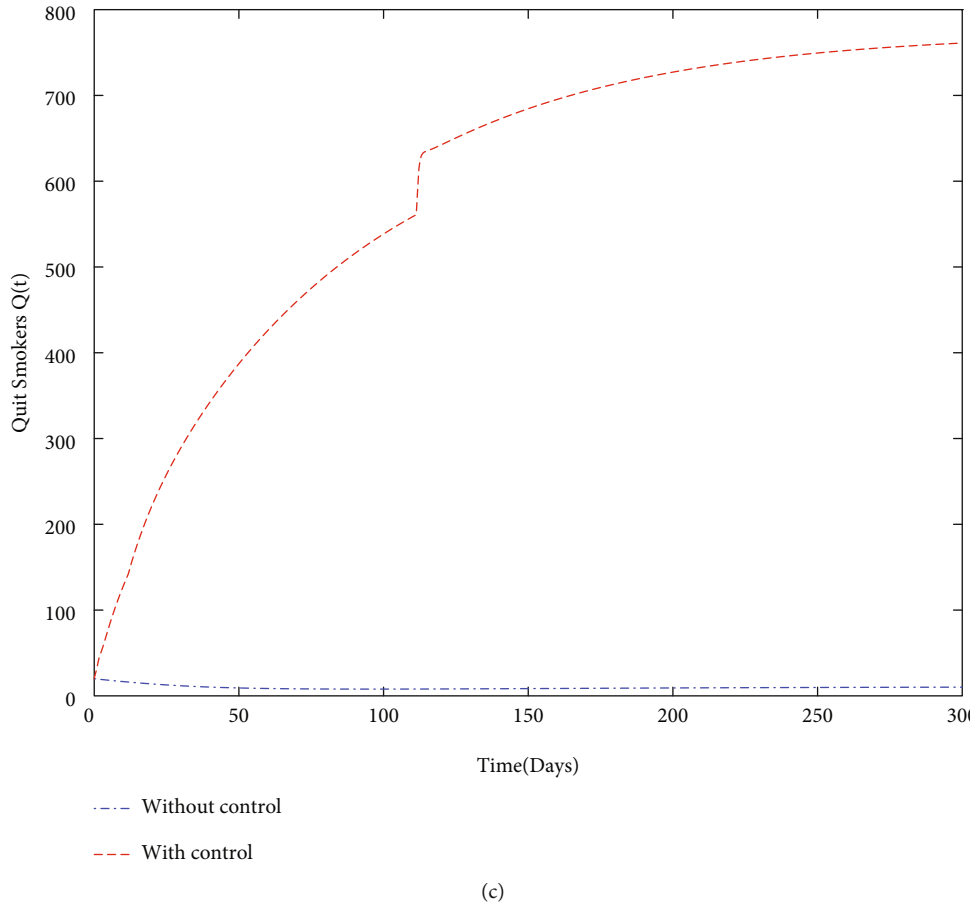

(c)

Figure 5: The plot describes stability of light smoker present equilibrium when $R_0 > 1$.

) *satisfying*

$$\frac{d\lambda_1(t)}{dt} = \left(2\beta_1 \frac{L^2(t)}{(P(t)+L(t))^2} + (d+\mu+u_1(t))\right)\lambda_1(t) - 2\beta_1 \frac{L^2(t)}{(P(t)+L(t))^2}\lambda_2(t) - u_1(t)\lambda_4(t) - D_3, \tag{72}$$

$$\frac{d\lambda_2(t)}{dt} = 2\beta_1 \frac{P^2(t)}{(P(t)+L(t))^2}\lambda_1(t) - 2\beta_1 \frac{P^2(t)}{(P(t)+L(t))^2}\lambda_2(t) + \beta_2 S(t)\lambda_2(t) + (d+\mu+u_2(t)+(1-u_4(t)))\lambda_2(t) - \beta_2 S(t)\lambda_3(t) - (u_2(t)+(1-u_4(t)))\lambda_4(t) - D_1, \tag{73}$$

$$\frac{d\lambda_3(t)}{dt} = \beta_2 L(t)\lambda_2(t) - \beta_2 L(t)\lambda_3(t) + (d+\mu+\delta+u_3(t) + qu_4(t))\lambda_3(t) + \delta\lambda_4(t) - (u_3(t)+qu_4(t))\lambda_4(t) - D_2, \tag{74}$$

$$\frac{d\lambda_4(t)}{dt} = -\gamma\lambda_1(t) + (d+\mu+\gamma)\lambda_4(t) + D_4, \tag{75}$$

with terminal conditions

$$\lambda_1(T) = 0, \lambda_2(T) = 0, \lambda_3(T) = 0, \lambda_4(T) = 0. \tag{76}$$

Further, the control measures are characterized by

$$u_1^\star(t) = \max\left\{\min\left\{c_1, \frac{(\lambda_1(t)-\lambda_4(t))}{F_1}P(t)\right\}, 0\right\}, \tag{77}$$

$$u_2^\star(t) = \max\left\{\min\left\{c_2, \frac{(\lambda_2-\lambda_4)}{F_2}L(t)\right\}, 0\right\}, \tag{78}$$

$$u_3^\star(t) = \max\left\{\min\left\{c_3, \frac{(\lambda_3-\lambda_4)}{F_3}S(t)\right\}, 0\right\}, \tag{79}$$

$$u_4^\star(t) = \max\left\{\min\left\{c_4, \frac{(\lambda_4-\lambda_2)L(t)+q(\lambda_3-\lambda_4)S(t)}{F_4}\right\}, 0\right\}. \tag{80}$$

Proof. The adjoint system (72) is obtained by using the adjoint equation (69c) in the maximum principles. The terminal conditions of (76) were derived as a direct consequence of equation (71). We took the partial derivatives of $\mathscr{H}$ with respect to the control measure u_i for $i = 1, \cdots, 4$ in turns and used (69b) for the derivation of (77)–(80). □

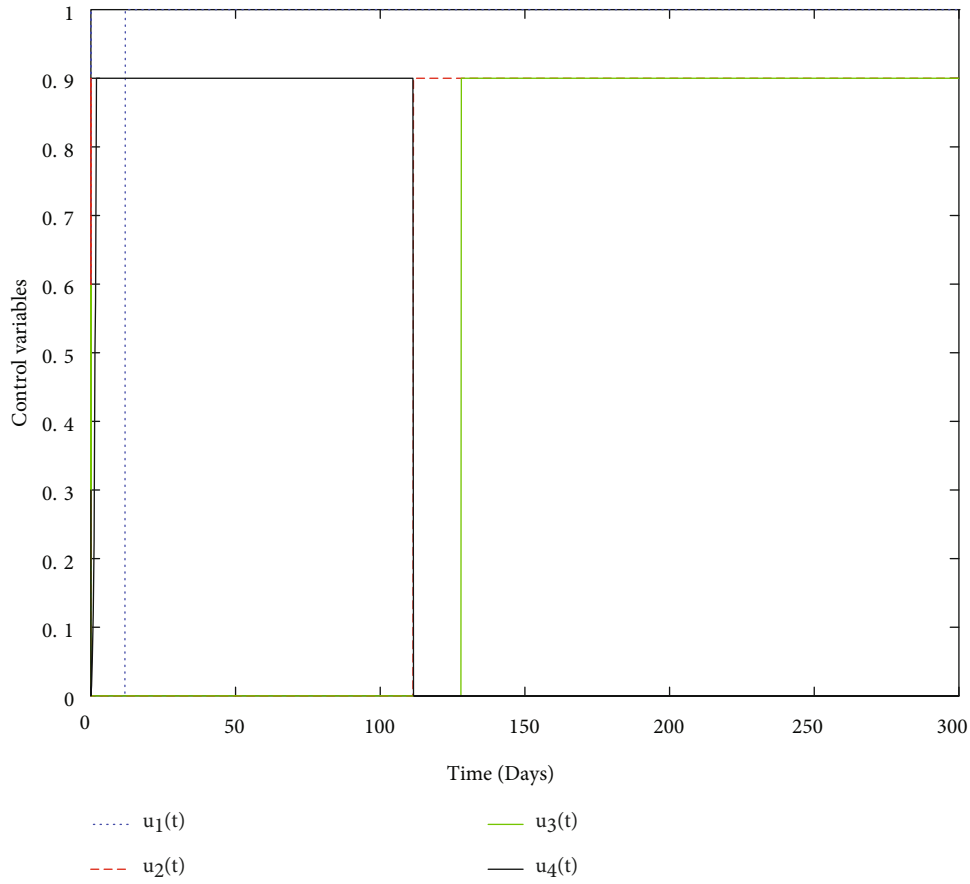

Figure 6: The dynamics of control variables.

8. Simulation Results

For solving the problems (both with and without controls), we used the standard RK method of fourth order. To verify numerically the key theorems on dynamical analysis, we utilized parameter values from Tables 3 and 4. Specifically, values of parameters from Table 3 were used to show the stability of smoking-free equilibrium, and sequentially, parameter values from Table 4 guarantee the stability of light smoker present equilibrium. For presenting the effect of control measures, we assumed values from Table 5. For simulating the control problem, firstly, we solved model (55) forward in time and then used backward RK4 method for solving the adjoint system (72) with the help of terminal conditions and characterization of the control variables (77)–(80). The simulation clearly illustrates the results on dynamical analysis (Figures 2 and 3) as well as on control theory (Figures 4 and 5).

By using values of parameter from Table 3, calculate the smoking generation number $R_0 = 0.1954$ and SFE $E_0 = (125.1526,0,0,0)$. It is clear from Figure 2 that each solution curve in the subplots tends to its SFE irrespective of the initial size of the population whenever $R_0 < 1$.

To show numerically the global stability of light smoker present equilibrium E_l (21), we assumed the same values of Table 3 except $\beta_1 = 0.08$ which gives $R_0 = 1.9536$ and as a result, $E_l = (P_l, L_l, S_l, Q_l) = (64.0625,61.0901,0,0)$. Thus, Figures 6(a)–6(d) shows a clear interpretation of Theorems 7 and 10, that is, if $R_0 > 1$, then $(P, L, S, Q) \longrightarrow (P_l, L_l, S_l, Q_l)$ as $t \longrightarrow \infty$.

Similarly, to show the long-term behavior of each class whenever $R_0 > 1$ and the side condition of Theorem 8 holds, we take into consideration values from Table 4. From these values of parameters, we calculated $R_0 = 12.3077 > 1$ and $(P_*, L_*, S_*, Q_*) = (127,142.1,164.5,354.9)$. Figure 3 proves the statement of Theorem 8 as well as the global stability of SPE numerically.

Finally, we used values from Table 5 and simulated both with and without control problems and presented the effect of the control variables. The simulation (in Figure 4) depicts in a clear way the effect of the control variables: to decrease the size of smoker population and to increase the number of quit smokers.

9. Concluding Remarks

In this work, we formulated and analyzed a giving-up smoking model utilizing three main factors related to smoking habit: the bilinear incidence rate showing the spread of smoking habit within the population from the contact of light smokers and smokers, the harmonic mean type of incidence rate (for incorporating contacts between potential smokers and occasional smokers), and the relapse factor associated to smoking.

After model formulation, we investigated the model for bounded and positive solution subject to appropriate initial conditions. The model was checked for possible fixed points, and three equilibria were derived under certain conditions, namely, the smoking-free equilibrium, light smoker present equilibrium, and smoking present equilibrium. It was shown that the smoking-free fixed point always exists and is both locally and globally asymptotically stable when $R_0 < 1$. The positive light smoker present equilibrium exists if we assume $R_0 > 1$, and the same fixed point is locally as well as globally asymptotically stable if we impose additional conditions on the basic reproduction number. Further, we proved that the model has a smoking present equilibrium whenever additional conditions are satisfied by R_0. Also, a criteria for the local analysis has been derived, and the global stability of smoking present equilibrium was presented both analytically and numerically. Keeping in mind a few control measures, we set a control problem and optimal control strategies were achieved with the help of Pontryagin's maximum principle. The obtained analytical results were verified through simulations and effectiveness of the control program is presented by comparing with and without control curves.

This work is indeed a very good contribution to the existing literature on smoking epidemics. However, this social evil has a dramatic impact on every society, and thus, one cannot ignore the memory effect while studying such and related problems. Keeping in view the importance of generalized fractional derivatives in this regard [10–30], the authors have a keen interest to formulate and analyze the fractional models for smoking epidemics in near future.

Data Availability

Data availability is not applicable to this research.

Conflicts of Interest

The author declares no conflicts of interest.

Acknowledgments

The author extends appreciation to the Deanship of Scientific Research at King Saud University for funding this work through research group no. RG-1437-017.

References

[1] P. E. Olson, C. S. Hames, A. S. Benenson, and E. N. Genovese, "The Thucydides syndrome: Ebola deja vu? (or Ebola reemergent?)," *Emerging Infectious Diseases*, vol. 2, no. 2, 1996.

[2] M. J. Papagrigorakis, C. Yapijakis, P. N. Synodinos, and E. Baziotopoulouy-valavani, "DNA examination of ancient dental pulp incriminates typhoid fever as a probable cause of the plague of Athens," *International Journal of Infectious Diseases*, vol. 10, no. 3, pp. 206–214, 2006.

[3] S. Alchon, *A Pest in the Land: New World Epidemic in a Global Perspective*, University of New Mexico Press, 2003.

[4] G. U. Rahman, R. P. Agarwal, and Q. Din, "Mathematical analysis of giving up smoking model via harmonic mean type incidence rate," *Applied Mathematics and Computation*, vol. 354, pp. 128–148, 2019.

[5] W. Kermack and A. Mckendrick, "Contributions to the mathematical theory of epidemics-I," *Bulletin of Mathematical Biology*, vol. 53, no. 1-2, pp. 33–55, 1991.

[6] H. W. Hethcote, "The mathematics of infectious diseases," *SIAM Review*, vol. 42, no. 4, pp. 599–653, 2000.

[7] K. A. Kabir, K. Kuga, and J. Tanimoto, "Analysis of SIR epidemic model with information spreading of awareness," *Chaos, Solitons & Fractals*, vol. 119, pp. 118–125, 2019.

[8] H. Inaba, "Mathematical analysis of an age-structured SIR epidemic model with vertical transmission," *Discrete & Continuous Dynamical Systems-B*, vol. 6, no. 1, pp. 69–96, 2006.

[9] A. P. Lemos-Paião, C. J. Silva, and D. F. Torres, "An epidemic model for cholera with optimal control treatment," *Journal of Computational and Applied Mathematics*, vol. 318, pp. 168–180, 2017.

[10] X.-Y. Wang, K. Hattaf, H.-F. Huo, and H. Xiang, "Stability analysis of a delayed social epidemics model with general contact rate and its optimal control," *Journal of Industrial & Management Optimization*, vol. 12, no. 4, pp. 1267–1285, 2016.

[11] K. Hattaf, A. A. Lashari, Y. Louartassi, and N. Yousfi, "A delayed sir epidemic model with a general incidence rate," *Electronic Journal of Qualitative Theory of Differential Equations*, vol. 3, no. 3, pp. 1–9, 2013.

[12] C. Castillo-Garsow, G. Jordan-Salivia, and A. R. Herrera, "Mathematical models for the dynamics of tobacco use, recovery and relapse, technical report series," 1997, https://qrlssp.asu.edu/sites/default/files/mathematical_models_for_dynamics_of_tobacco_use_recovery_relapse.pdf.

[13] O. Sharomi and A. B. Gumel, "Curtailing smoking dynamics: a mathematical modeling approach," *Applied Mathematics and Computation*, vol. 195, no. 2, pp. 475–499, 2008.

[14] G. Zaman, "Qualitative behavior of giving up smoking models," *Bulletin of the Malaysian Mathematical Sciences Society*, vol. 34, no. 2, pp. 403–415, 2011.

[15] J. Singh, D. Kumar, M. A. Qurashi, and D. Baleanu, "A new fractional model for giving up smoking dynamics," *Advances in Difference Equations*, vol. 2017, no. 1, 2017.

[16] Z. Alkhundhri, S. Al-Sheikh, and S. Al-Tuwairqi, "Global dynamics of a mathematical model on smoking," *International Scholarly Research Notices*, vol. 2014, Article ID 847075, 7 pages, 2014.

[17] Q. Din, M. Ozair, T. Hussain, and U. Saeed, "Qualitative behavior of a smoking model," *Advances in Difference Equations*, vol. 2016, no. 1, 2016.

[18] G. U. Rahman, R. P. Agarwal, L. Liu, and A. Khan, "Threshold dynamics and optimal control of an age-structured giving up smoking model," *Nonlinear Analysis: Real World Applications*, vol. 43, pp. 96–120, 2018.

[19] V. Capasso and G. Serio, "A generalization of the Kermack-Mckendrick deterministic epidemic model," *Mathematical Biosciences*, vol. 42, no. 1-2, pp. 43–61, 1978.

[20] S. G. Ruan and W. D. Wang, "Dynamical behavior of an epidemic model with a nonlinear incidence rate," *Journal of Differential Equations*, vol. 188, no. 1, pp. 135–163, 2003.

[21] R. E. Mickens, "SIR model with square-root dynamics: an NSFD scheme," *Journal of Difference Equations and Applications*, vol. 16, no. 2-3, pp. 209–216, 2010.

[22] A. Zeb, G. Zaman, and S. Momani, "Square-root dynamics of a giving up smoking model," *Applied Mathematical Modelling*, vol. 37, no. 7, pp. 5326–5334, 2013.

[23] S. S. Alzaid and B. S. T. Alkahtani, "Asymptotic analysis of a giving up smoking model with relapse and harmonic mean type incidence rate," *Results in Physics*, vol. 28, article 104437, 2021.

[24] S. Mushayabasa and C. P. Bhunu, "Modelling the effects of heavy alcohol consumption on the transmission dynamics of gonorrhea," *Nonlinear Dynamics*, vol. 66, no. 4, pp. 695–706, 2011.

[25] P. van den Driessche and J. Watmough, "Reproduction numbers and sub-threshold endemic equilibria for compartmental models of disease transmission," *Mathematical Biosciences*, vol. 180, no. 1-2, pp. 29–48, 2002.

[26] J. P. LaSalle, "The stability of dynamical systems," Society for Industrial and Applied Mathematics, 1976.

[27] G. T. Tilahun, O. D. Makinde, and D. Malonza, "Co-dynamics of pneumonia and typhoid fever diseases with cost effective optimal control analysis," *Applied Mathematics and Computation*, vol. 316, pp. 438–459, 2018.

[28] M. I. Kamien and N. L. Schwartz, *Dynamic Optimization, Advanced Textbooks in Economics, 31*, North-Holland Publishing Co., Amsterdam, second edition, 1991.

[29] Centers for Disease Control and Prevention (CDC), *Best Practices for Comprehensive Tobacco Control Programs*, Department of Health and Human Services, Atlanta GA, 2015.

[30] K. Hattaf, "A new generalized definition of fractional derivative with non-singular kernel," *Computation*, vol. 8, no. 2, p. 49, 2020.

Hindawi
Journal of Function Spaces
Volume 2022, Article ID 5877970, 11 pages
https://doi.org/10.1155/2022/5877970

Research Article

A Fractional-Order Investigation of Vaccinated SARS-CoV-2 Epidemic Model with Caputo Fractional Derivative

Badr Saad T. Alkahtani

Department of Mathematics, College of Science, King Saud University, P.O. Box 1142, Riyadh 11989, Saudi Arabia

Correspondence should be addressed to Badr Saad T. Alkahtani; balqahtani1@ksu.edu.sa

Received 19 September 2021; Revised 7 October 2021; Accepted 6 January 2022; Published 24 March 2022

Academic Editor: Feliz Minhos

In this paper, we consider a fractional-order mathematical system comprising four different compartments for the recent pandemic of SARS-CoV-2 with regard to global and singular kernels of Caputo fractional operator. The SARS-CoV-2 fractional mathematical model is analyzed for series-type solution by Laplace–Adomian decomposition techniques (LADM) and homotopy perturbation method (HPM). The whole quantity of each compartment is divided into small parts, and then the sum of these all parts is written as a series solution for each agent of the system, while the nonlinear part is decomposed using the Adomian polynomial. The model is also checked for approximate solution by HPM through a comparison of the parameter power, p, for each equation. The numerical simulation for both methods is provided in different fractional orders along with comparison with each other as well as with natural order 1.

1. Introduction

The novel coronavirus (SARS-CoV-2), considered the most dangerous virus of this decade, belong to family of severe acute respiratory syndrome (SARS) [1, 2]. Therefore, this new virus is related to the viruses associated with the syndrome. It has become a new novel strain of the SARS family, which was recognised in humans before [3, 4]. SARS-CoV-2 affected not only humans but also several animals. This virus has been transmitted from human to human, and it occurs similarly in animals. But many times, it has become a mystery that how the animals have been affected by it in certain security. Infected humans and different species of various animals are also recognised as an active cause of the spreading of the virus [5]. In the past, some similar viruses like the Middle East respiratory syndrome coronavirus (MERS-CoV) were spread from camels to the human population, and for SARS-CoV-1, the civet cats were recognised as the source of spreading into humans [6].

Mathematical models concerning infections have vastly been used since the last century to study the dynamics and transmission of various pandemics and epidemics and to apply valuable techniques for their control or minimization. Scholars investigating pandemics in the various areas of sciences are working to control these epidemics or reduce these negative impacts to a stable situation [7–9]. They also give the concept of the globalization of the ODEs that have the natural-order differentiation providing more degrees of freedom at any order. The equations which contain the FO differential equation δ, with FO $0 < \delta \leq 1$, may be studied in [10–12]. Mostly, in epidemiological problems, FDEs refer to models with memory effects [12]. Next, the fractional-order derivative has the term of integration providing the knowledge of the past spreading for an infection. We can expect the behavior of the transmission based on the previous results and studies. The hereditary and historical characteristics point to the past transmission of diseases, which is very beneficial for making predictions. Therefore, these characteristics can be tested by the application of noninteger order derivatives, and it impacts the transmission of an epidemic [10–12].

Modern calculus goods production arbitrary order may be used in different fields of clinical and physical sciences, such as goods production by engineering, control theory,

economics, financing, and infectious disease conditions. The extensive huge study of FODEs in modelling global phenomena is because of more attracting characteristics which are not explained in the natural order derivatives. The natural order differential equations are local in nature, while FDEs are concerned with nonlocality, which provides more globalization of their dynamics. Usage of integer operator is hot area and recently caught the researchers interest, whereas the noninteger order operators have been studied and used intensively. Infectious problems for the endemic are the most realistic area for the researchers as a research gap and are applied to test them in recent times. Moreover, the analysis for the mathematical models referring to the real-globe situation is made using the theory of stability, existence of solution, and with the optimal problem as in [13–15].

We proposed a new vaccinated SARS-CoV-2 epidemic model that has four quantities including the susceptible class $\mathbb{W}(t)$, the acutely infected class $\mathbb{X}(t)$, chronically infected class $\mathbb{Y}(t)$, and the recovered class $\mathbb{Z}(t)$, which takes the following form:

$$\begin{aligned}
\frac{d\mathbb{W}(t)}{dt} &= \Lambda - \beta\mathbb{W}(t)\mathbb{X}(t) - (\rho + \xi)\mathbb{W}(t),\\
\frac{d\mathbb{X}(t)}{dt} &= \beta\mathbb{W}(t)\mathbb{X}(t) - (\xi + \gamma + \lambda)\mathbb{X}(t),\\
\frac{d\mathbb{Y}(t)}{dt} &= \lambda\mathbb{X}(t) - (\xi + \delta + \kappa)\mathbb{Y}(t),\\
\frac{d\mathbb{Z}(t)}{dt} &= \gamma\mathbb{X}(t) + \kappa\mathbb{Y}(t) + \rho\mathbb{W}(t) - \xi\mathbb{Z}(t).
\end{aligned} \tag{1}$$

The parameters used in system (1) are described in Table 1:

The analysis of model (1) under fractional-order derivative with regard to the Caputo operator is given as

$$\begin{aligned}
{}^{\mathbb{C}}D_t^{\zeta}(\mathbb{W}(t)) &= \Lambda - \beta\mathbb{W}(t)\mathbb{X}(t) - (\rho + \xi)\mathbb{W}(t),\\
{}^{\mathbb{C}}D_t^{\zeta}(\mathbb{X}(t)) &= \beta\mathbb{W}(t)\mathbb{X}(t) - (\xi + \gamma + \lambda)\mathbb{X}(t),\\
{}^{\mathbb{C}}D_t^{\zeta}(\mathbb{Y}(t)) &= \lambda\mathbb{X}(t) - (\xi + \delta + \kappa)\mathbb{Y}(t),\\
{}^{\mathbb{C}}D_t^{\zeta}(\mathbb{Z}(t)) &= \gamma\mathbb{X}(t) + \kappa\mathbb{Y}(t) + \rho\mathbb{W}(t) - \xi\mathbb{Z}(t),
\end{aligned} \tag{2}$$

with general initial approximation $\mathbb{W}(0) = N_1$, $\mathbb{X}(0) = N_2$, $\mathbb{Y}(0) = N_3$, and $\mathbb{Z}(0) = N_4$.

In the seventeenth century, many researchers Euler, L'Hôpital, Fourier, Abels, Riemann–Liouville, etc., made fundamental contributions in this field of modern calculus and were known as the pioneers of fractional calculus. Besides them, many other scientists have made significant findings and discovered some fractional models as seen in [10–12]. Most of the basic properties needed for real phenomena such as memory, globality, and hereditary are involved in various fractional operators, while the integer-order differential operator have no such properties; therefore, modern calculus gives more realistic result. Modern calculus refers to the appliances of biological, physical, and engineering as in [11, 16–18]. Other properties of fractional operators like nonlocality, globality, singularity, and nonsingularity also attract the interest of many researchers. These properties are more applicable to most real-world problems.

Table 1: The description of different parameters given in model (1).

Parameter symbols	Description
Π	Rate of new birth or recruitment
ν	Rate of vaccination for SARS-CoV-2
μ	Rate of natural deaths
α	Rate of death due to SARS-CoV-2
η	Interaction rate of infectious and healthy population
γ	Recovered rate for acute infection
κ	Recovered rate for chronic infection
λ	Transferring rate acute class to chronic infection

It should be kept in mind that fractional operators do have not a unique definition and are formulated by different formulae. Most of the operators have the definite integral with singular and nonsingular kernels. These kernels can also be found in the various fractional integration formulae. These kernels are mostly taken from the Cauchy integral formula. These integral kernels present in the fractional operator may be analyzed by various techniques. Some researchers have used Laplace–Adomian decomposition techniques for both linear and nonlinear fractional differential models. For the terms of noninearity, Adomian polynomial is applied, which decomposes that term into a small one (see [19, 20]). Similarly, the homotopy perturbation techniques are also applied for a series solution, which can be obtained by perturbed by a small factor and then comparing the power of parameter $\zeta \in [0, 1]$ on both sides of the equation. For the iterative numerical solution of integer-order models, mostly Runge–Kutta techniques (RK4 and RK2) were used. They can be used for fractional-order equations by involving the fractional terms. In this article, we will apply Laplace transformation along with Adomian decomposition techniques by converting the while quantity into small ones. We will also apply the homotopy perturbation techniques (HPM) for the series solution of the said problem [21, 22].

Different global real-life situations may be represented by noninteger differential equations (FDEs) such as physics problems, problems of control theory, chemistry problems (polymerization, rheology, and electronics), physical biology, heat, aerodynamics, infectious diseases, electro-statics, electrical circuits, and blood flow [11, 23–25]. In the last few years, the interesting description of the existence of solutions of FDEs by changing the boundary conditions counting integer order phenomena, nonlocal, nonsingular kernel, periodic/antiperiodic, and multipoints has been investigated and has provided good supposition, as can be seen in [26–28]. Different researchers have tested the solution of the coupled models by differential equations of noninteger orders which gives the key role in applied fields of mathematics. This is the establishment for the model developed from biochemistry, biology, ecology, and other areas of engineering and physical sciences such as in [29].

2. Basic Definition

In this section, some definitions are written from [19, 20, 30].

Definition 1. Consider $\mathcal{Y} \in L^1([0,\infty)\mathbb{Z})$ to be a mapping; then, the Riemann–Liouville noninteger order integral of order ζ is as follows:

$$\mathbf{I}_t^{\zeta}\mathcal{Y}(t) = \frac{1}{\Gamma(\zeta)}\int_0^t \frac{\mathcal{Y}(\beta)}{(t-\beta)^{1-\zeta}}\mathrm{d}\beta, \quad \zeta > 0, \tag{3}$$

where the right integral must exist.

Definition 2. Let $\mathcal{Y}$ be an operator, then the Caputo noninteger order derivative can be defined as

$${}^{\mathbb{C}}\mathbf{D}_t^{\zeta}\mathcal{Y}(t) = \frac{1}{\Gamma(n-\zeta)}\int_0^t (t-\beta)^{n-\zeta-1}\mathcal{Y}^n(\beta)\mathrm{d}\beta, \tag{4}$$

and the R.H.S of the integration must exist and $n = [\zeta] + 1$. If $\zeta \in (0,1)$, then someone has

$${}^{\mathbb{C}}\mathbf{D}_t^{\zeta}\mathcal{Y}(t) = \frac{1}{\Gamma(1-\zeta)}\int_0^t \frac{\mathcal{Y}'(\beta)}{(t-\beta)^{\zeta}}\mathrm{d}\beta. \tag{5}$$

Lemma 1. *From the noninteger order differential equation, the following is satisfied:*

$$\mathbf{I}^{\zeta}\left[{}^{\mathbb{C}}\mathbf{D}^{\zeta}p\right](t) = p(t) + \gamma_0 + \gamma_1 t + \gamma_2 t^2 + \cdots + \gamma_{n-1}t^{n-1}. \tag{6}$$

Definition 3. With regard to the Caputo operator, the Laplace transformation can be written as

$$\mathscr{L}\left[{}^{\mathbb{C}}\mathbf{D}_t^{\zeta}p(t)\right] = s^{\zeta}P(s) - \sum_{j=0}^{m-1} s^{\zeta-j-1}p^k(0), \quad m-1 < \zeta < m, m \in \mathbb{N}. \tag{7}$$

Definition 4. On application of the homotopy perturbation techniques to an equation having linear L and nonlinear N classes, we may write a homotopy $v(r,g)$: $\Omega \times [0\times 1] \longrightarrow \mathbb{Z}$.

$$H(v,g) = (1-g)\left[L(v) - L(u_0)\right] + g\left[L(v) + N(v) - f(r)\right] = 0, \tag{8}$$

where $r \in \Omega$ and $q \in [0,1]$ is the embidding parameter.

3. Series Solution of Problem (2) via LADM

This section is devoted to the analysis of general-typed series techniques for the considered model (2) along with some starting conditions. On the application of the Laplace transformation to the considered problem (2), we get the following:

$$\begin{cases} \mathscr{L}\left[{}^{\mathscr{C}}D_t^{\zeta}(\mathbb{W}(t))\right] = \mathscr{L}[\Lambda - \beta\mathrm{SA} - (\rho+\xi)\mathbb{W}], \\ \mathscr{L}\left[{}^{\mathbb{C}}D_t^{\zeta}(\mathbb{X}(t))\right] = \mathscr{L}[\beta\mathrm{SA} - (\xi+\gamma+\lambda)\mathbb{X}], \\ \mathscr{L}\left[{}^{\mathbb{C}}D_t^{\zeta}(\mathbb{Y}(t))\right] = \mathscr{L}[\lambda\mathbb{X} - (\xi+\delta+\kappa)\mathbb{Y}], \\ \mathscr{L}\left[{}^{\mathbb{C}}D_t^{\zeta}(\mathbb{Z}(t))\right] = \mathscr{L}[\gamma\mathbb{X} + \kappa\mathbb{Y} + \rho\mathbb{W} - \xi\mathbb{Z}]. \end{cases} \tag{9}$$

Applying the initial approximation, problem (9) becomes

$$\begin{cases} \mathscr{L}[\mathbb{W}(t)] = \dfrac{N_1}{s} + \dfrac{1}{s^{\zeta}}\mathscr{L}[\Lambda - \beta\mathrm{SA} - (\rho+\xi)\mathbb{W}], \\ \mathscr{L}[\mathbb{X}(t)] = \dfrac{N_2}{s} + \dfrac{1}{s^{\zeta}}\mathscr{L}[\beta\mathrm{SA} - (\xi+\gamma+\lambda)\mathbb{X}], \\ \mathscr{L}[\mathbb{Y}(t)] = \dfrac{N_3}{s} + \dfrac{1}{s^{\zeta}}\mathscr{L}[\lambda\mathbb{X} - (\xi+\delta+\kappa)\mathbb{Y}], \\ \mathscr{L}[\mathbb{Z}(t)] = \dfrac{N_5}{s} + \dfrac{1}{s^{\zeta}}\mathscr{L}[\gamma\mathbb{X} + \kappa\mathbb{Y} + \rho\mathbb{W} - \xi\mathbb{Z}]. \end{cases} \tag{10}$$

Taking the infinite series solution for $\mathbb{W}, \mathbb{X}, \mathbb{Y}$, and $\mathbb{Z}$ as

$$\mathbb{W}(t) = \sum_{n=0}^{\infty}\mathbb{W}_n(t), \mathbb{X}(t) = \sum_{n=0}^{\infty}\mathbb{X}_n(t), \quad \mathbb{Y}(t) = \sum_{n=0}^{\infty}\mathbb{Y}_n(t), \mathbb{Z}(t) = \sum_{n=0}^{\infty}\mathbb{Z}_n(t), \tag{11}$$

the nonlinear term $\mathbb{W}(t)\mathbb{X}(t) = \sum_{n=0}^{\infty}X_n(t)$ can be decomposed as

$$X_n(t) = \frac{1}{n!}\frac{d^n}{d\lambda^n}\left[\sum_{k=0}^{n}\lambda^k\mathbb{W}_k(t)\sum_{k=0}^{n}\lambda^k\mathbb{X}_k(t)\right]_{\lambda=0}. \tag{12}$$

Substitute equations (11) and (12) into equation (10), and on comparing the terms on each side, we obtain

$$\begin{cases} \mathscr{L}[\mathbb{W}_0(t)] = \dfrac{N_1}{s}, \mathscr{L}[\mathbb{X}_0(t)] = \dfrac{N_2}{s}, \mathscr{L}[\mathbb{Y}_0(t)] = \dfrac{N_3}{s}, \mathscr{L}[\mathbb{Z}_0(t)] = \dfrac{N_4}{s}, \\ \mathscr{L}[\mathbb{W}_1(t)] = \dfrac{1}{s^{\zeta}}\mathscr{L}[\Lambda - \beta\mathbb{W}_0 A_0 - (\rho + \xi)\mathbb{W}_0], \\ \mathscr{L}[\mathbb{X}_1(t)] = \dfrac{1}{s^{\zeta}}\mathscr{L}[\beta\mathbb{W}_0 A_0 - (\xi + \gamma + \lambda)\mathbb{X}_0], \\ \mathscr{L}[\mathbb{Y}_1(t)] = \dfrac{1}{s^{\zeta}}\mathscr{L}[\lambda\mathbb{X}_0 - (\xi + \delta + \kappa)\mathbb{Y}_0], \\ \mathscr{L}[\mathbb{Z}_1(t)] = \dfrac{1}{s^{\zeta}}\mathscr{L}[\gamma\mathbb{X}_0 + \kappa\mathbb{Y}_0 + \rho\mathbb{W}_0 - \xi\mathbb{Z}_0], \\ \vdots \\ \mathscr{L}[\mathbb{W}_{n+1}(t)] = \dfrac{1}{s^{\zeta}}\mathscr{L}[\Lambda - \beta\mathbb{W}_n A_n - (\rho + \xi)\mathbb{W}_n], \\ \mathscr{L}[\mathbb{X}_{n+1}(t)] = \dfrac{1}{s^{\zeta}}\mathscr{L}[\beta\mathbb{W}_n A_n - (\xi + \gamma + \lambda)\mathbb{X}_n], \\ \mathscr{L}[\mathbb{Y}_{n+1}(t)] = \dfrac{1}{s^{\zeta}}\mathscr{L}[\lambda\mathbb{X}_n - (\xi + \delta + \kappa)\mathbb{Y}_n], \\ \mathscr{L}[\mathbb{Z}_{n+1}(t)] = \dfrac{1}{s^{\zeta}}\mathscr{L}[\gamma\mathbb{X}_n + \kappa\mathbb{Y}_n + \rho\mathbb{W}_n - \xi\mathbb{Z}_n]. \end{cases} \tag{13}$$

Upon using the inverse Laplace transform in expression (14), we get

$$\mathbb{W}_0(t) = \mathscr{L}^{-1}\left[\frac{N_1}{s}\right] = N_1, \mathbb{X}_0(t) = \mathscr{L}^{-1}\left[\frac{N_2}{s}\right] = N_2, \mathbb{Y}_0(t) = \mathscr{L}^{-1}\left[\frac{N_3}{s}\right] = N_3,, \mathbb{Z}_0(t) = \mathscr{L}^{-1}\left[\frac{N_4}{s}\right] = N_4,$$

$$\mathbb{W}_1(t) = \left[\Lambda - \beta N_1 N_2 - (\rho + \xi)N_1\right]\frac{t^{\zeta}}{\Gamma(\zeta+1)},$$

$$\mathbb{X}_1(t) = \left[\beta N_1 N_2 - (\xi + \gamma + \lambda)N_2\right]\frac{t^{\zeta}}{\Gamma(\zeta+1)},$$

$$\mathbb{Y}_1(t) = \left[\lambda N_2 - (\xi + \delta + \kappa)N_3\right]\frac{t^{\zeta}}{\Gamma(\zeta+1)},$$

$$\mathbb{Z}_1(t) = \left[\gamma N_2 + \kappa N_3 + \rho N_1 - \xi N_4\right]\frac{t^{\zeta}}{\Gamma(\zeta+1)}, \tag{14}$$

$$\mathbb{W}_2(t) = \frac{\Lambda t^{\zeta}}{\Gamma(\zeta+1)} - \left[\beta\left(N_1 G_{11} + N_2 K_{11}\right) - (\rho + \xi)G_{11}\right]\frac{t^{2\zeta}}{\Gamma(2\zeta+1)},$$

$$\mathbb{X}_2(t) = \left[\beta\left(N_1 G_{11} + N_2 K_{11}\right) - (\xi + \gamma + \lambda)K_{11}\right]\frac{t^{2\zeta}}{\Gamma(2\zeta+1)},$$

$$\mathbb{Y}_2(t) = \left[\lambda K_{11} - (\xi + \delta + \kappa)L_{11}\right]\frac{t^{\zeta^2}}{\Gamma(2\zeta+1)},$$

$$\mathbb{Z}_2(t) = \left[\gamma K_{11} + \kappa L_{11} + \rho G_{11} - \xi M_{11}\right]\frac{t^{2\zeta}}{\Gamma\left(2\zeta^{+}1\right)}.$$

In the same way, the remaining terms can be obtained, and the terms given in equation (14) are as follows:

$$\begin{aligned} G_{11} &= \Lambda - \beta N_1 N_2 - (\rho + \xi)N_1, \\ K_{11} &= \beta N_1 N_2 - (\xi + \gamma + \lambda)N_2, \\ L_{11} &= \lambda N_2 - (\xi + \delta + \kappa)N_3, \\ M_{11} &= \gamma N_2 + \kappa N_3 + \rho N_1 - \xi N_4. \end{aligned} \tag{15}$$

4. Approximate Solution for Problem (2) via HPM

Furthermore, we apply the HPM to obtain the approximate solution for the proposed problem (2), according to [20, 21] as follows:

$$\begin{cases} (1-q)\left[{}^{\mathbb{C}}D_t^{\zeta}(\mathbb{W}(t)) - {}^{\mathbb{C}}D_t^{\zeta}(\mathbb{W}_0(t))\right] + q\left[{}^{\mathbb{C}}D_t^{\zeta}(\mathbb{W}(t)) - \Lambda + \beta \mathrm{SA} + (\rho+\xi)\mathbb{W}\right] = 0, \\ (1-q)\left[{}^{\mathbb{C}}D_t^{\zeta}(\mathbb{X}(t)) - {}^{\mathbb{C}}D_t^{\zeta}(E_0(t))\right] + q\left[{}^{\mathbb{C}}D_t^{\zeta}(\mathbb{X}(t)) - \beta \mathrm{SA} + (\xi+\gamma+\lambda)\mathbb{X}\right] = 0, \\ (1-q)\left[{}^{\mathbb{C}}D_t^{\zeta}(\mathbb{Y}(t)) - {}^{\mathbb{C}}D_t^{\zeta}(I_0(t))\right] + q\left[{}^{\mathbb{C}}D_t^{\zeta}(\mathbb{Y}(t)) - \lambda\mathbb{X} + (\xi+\delta+\kappa)\mathbb{Y}\right] = 0, \\ (1-q)\left[{}^{\mathbb{C}}D_t^{\zeta}(\mathbb{Z}(t)) - {}^{\mathbb{C}}D_t^{\zeta}(\mathbb{Z}_0(t))\right] + q\left[{}^{\mathbb{C}}D_t^{\zeta}(\mathbb{Z}(t)) - \gamma\mathbb{X} - \kappa\mathbb{Y} - \rho\mathbb{W} + \xi\mathbb{Z}\right] = 0. \end{cases} \tag{16}$$

By applying $q = 0$ in equation: (16), a model of arbitrary differential equations can be obtained:

$$\begin{cases} {}^{\mathbb{C}}D_t^{\zeta}(\mathbb{W}(t)) - {}^{\mathbb{Y}}D_t^{\zeta}(\mathbb{W}_0(t)) = 0, \\ {}^{\mathbb{C}}D_t^{\zeta}(\mathbb{X}(t)) - {}^{\mathbb{Y}}D_t^{\zeta}(E_0(t)) = 0, \\ {}^{\mathbb{C}}D_t^{\zeta}(\mathbb{Y}(t)) - {}^{\mathbb{Y}}D_t^{\zeta}(I_0(t)) = 0, \\ {}^{\mathbb{C}}D_t^{\zeta}(\mathbb{Z}(t)) - {}^{\mathbb{Y}}D_t^{\zeta}(\mathbb{Z}_0(t)) = 0. \end{cases} \tag{17}$$

Solutions for the equation (17) are straightforward. If we use $q = 1$ in equation (16), we will obtain the same system as (2). The infinite series solution can be write in the following form as

$$\begin{aligned} \mathbb{W}(t) &= \sum_{n=0}^{\infty} q^n S_n(t), \mathbb{X}(t) = \sum_{n=0}^{\infty} q^n A_n(t), \mathbb{Y}(t) \\ &= \sum_{n=0}^{\infty} q^n C_n(t), \mathbb{Z}(t) = \sum_{n=0}^{\infty} q^n R_n(t). \end{aligned} \tag{18}$$

So, by comparing each term $q = 1$, in equation (18), we get the original model. Plugging equation (18) in to equation (16) and on comparison of each terms with the same power of q, we get

$$q^0 : \{\mathbb{W}_0(t) = N_1, \mathbb{X}_0(t) = N_2, \mathbb{Y}_0(t) = N_3, \mathbb{Z}_0(t) = N_4. \tag{19}$$

Similarly,

$$q^1 : \begin{cases} \mathbb{W}_1 = [\Lambda - \beta\mathbb{W}_0\mathbb{X}_0 - (\rho + \xi)\mathbb{W}_0]\dfrac{t^{\zeta}}{\Gamma(\zeta+1)}, \\ \mathbb{X}_1 = [\beta\mathbb{W}_0\mathbb{X}_0 - (\xi + \gamma + \lambda)\mathbb{X}_0]\dfrac{t^{\zeta}}{\Gamma(\zeta+1)}, \\ \mathbb{Y}_1 = [\lambda\mathbb{X}_0 - (\xi + \delta + \kappa)\mathbb{Y}_0]\dfrac{t^{\zeta}}{\Gamma(\zeta+1)}, \\ \mathbb{Z}_1 = [\gamma\mathbb{X}_0 + \kappa\mathbb{Y}_0 + \rho\mathbb{W}_0 - \xi\mathbb{Z}_0]\dfrac{t^{\zeta}}{\Gamma(\zeta+1)}, \end{cases} \tag{20}$$

$$q^2 : \begin{cases} \mathbb{W}_2 = [\Lambda - \beta\mathbb{W}_0\mathbb{X}_0\{\beta\mathbb{W}_0\mathbb{X}_0 - (\xi + \gamma + \lambda)\mathbb{X}_0\} - (\beta\mathbb{X}_0 + \rho + \xi)\{\Lambda - \beta\mathbb{W}_0\mathbb{X}_0 - (\rho + \xi)\mathbb{W}_0\}]\dfrac{t^{2\zeta}}{\Gamma(2\zeta+1)}, \\ \mathbb{X}_2 = [\{\mathbb{W}_0 - (\xi + \gamma + \lambda)\}\{\beta\mathbb{W}_0\mathbb{X}_0 - (\xi + \gamma + \lambda)\mathbb{X}_0\} + \mathbb{X}_0\{\Lambda - \beta\mathbb{W}_0\mathbb{X}_0 - (\rho + \xi)\mathbb{W}_0\}]\dfrac{t^{2\zeta}}{\Gamma(2\zeta+1)}, \\ \mathbb{Y}_2 = [\lambda\{\beta\mathbb{W}_0\mathbb{X}_0 - (\xi + \gamma + \lambda)\mathbb{X}_0\} - (\xi + \delta + \kappa)\{\lambda\mathbb{X}_0 - (\xi + \delta + \kappa)\mathbb{Y}_0\}]\dfrac{t^{2\zeta}}{\Gamma(2\zeta+1)}, \\ \mathbb{Z}_2 = [\gamma\{\beta\mathbb{W}_0\mathbb{X}_0 - (\xi + \gamma + \lambda)\mathbb{X}_0\} + \kappa\{\lambda\mathbb{X}_0 - (\xi + \delta + \kappa)\mathbb{Y}_0\} + \rho\{\Lambda - \beta\mathbb{W}_0\mathbb{X}_0 - (\rho + \xi)\mathbb{W}_0\} \\ \quad -\xi\{\gamma\mathbb{X}_0 + \kappa\mathbb{Y}_0 + \rho\mathbb{W}_0 - \xi\mathbb{Z}_0\}]\dfrac{t^{2\zeta}}{\Gamma(2\zeta+1)}. \end{cases} \tag{21}$$

Similarly, the high terms can be obtained, and the required terms are given in the part above. Hence, we obtain the same high terms as we obtained using LADM. Both the methods are applied as strong techniques for nonlinear fractional-order equations.

5. Discussion along with Numerical Simulation for the Proposed System (2)

Next, we compute the numerical solution for the considered system (2), by assigning different values for the parameter given in Table 1 used in problem (2).

The first four terms of the considered model (2), by using values from the table are given as follows:

$$\begin{cases} \mathbb{W}_0(t) = 6, \mathbb{X}_0(t) = 3, \mathbb{Y}_0(t) = 2, \mathbb{Z}_0(t) = 0, \\ \mathbb{W}_1(t) = \dfrac{-5.2}{\Gamma(\zeta+1)}t^{\zeta}, \mathbb{X}_1(t) =, \dfrac{5.3}{\Gamma(\zeta+1)}t^{\zeta}, \\ \mathbb{Y}_1(t) = \dfrac{0.8}{\Gamma(\zeta+1)}t^{\zeta}, \mathbb{Z}_1(t) = 0, \\ \mathbb{W}_2(t) = \dfrac{0.4}{\Gamma(\zeta+1)}t^{\zeta} + \dfrac{4.7}{\Gamma(2\zeta+1)}t^{2\zeta}, \\ \mathbb{X}_2(t) = \dfrac{-5.7}{\Gamma(2\zeta+1)}t^{2\zeta}, \mathbb{Y}_2(t) = \dfrac{2.25}{\Gamma(2\zeta+1)}t^{2\zeta}, \\ \mathbb{Z}_2(t) = \dfrac{0.15}{\Gamma(2\zeta+1)}t^{2\zeta}. \end{cases} \tag{22}$$

The solution for the first few terms are the following:

$$\begin{aligned} \mathbb{W}(t) &= 6 - \frac{5.2}{\Gamma(\zeta+1)}t^{\zeta} + \frac{4.876}{\Gamma(2\zeta+1)}t^{2\zeta} + \frac{0.3687\Gamma(2\zeta+1)}{\Gamma^2(\zeta+1)\Gamma(3\zeta+1)}t^{3\zeta}\ldots, \\ \mathbb{X}(t) &= 3 + \frac{5.3}{\Gamma(\zeta+1)}t^{\zeta} - \frac{5.765}{\Gamma(2\zeta+1)}t^{2\zeta} - \frac{0.3465\Gamma(2\zeta+1)}{\Gamma^2(\zeta+1)\Gamma(3\zeta+1)}t^{3\zeta}\ldots, \\ \mathbb{Y}(t) &= 2 + \frac{0.8}{\Gamma(\zeta+1)}t^{\zeta} + \frac{2.7654}{\Gamma(2\zeta+1)}t^{2\zeta} - \frac{0.6753}{\Gamma(3\zeta+1)}t^{3\zeta} + \ldots, \\ \mathbb{Z}(t) &= \frac{0.065}{\Gamma(2\zeta+1)}t^{2\zeta} - \frac{0.0076}{\Gamma(3\zeta+1)}t^{3\zeta} + \ldots. \end{aligned} \tag{23}$$

Now, evaluating equation (23) with $\zeta = 0.8$, we get

$$\begin{aligned} \mathbb{W}(t) &= 6 - 5.765470670t^{0.9} + 3.876379584t^{1.8} - 0.507094532t^{2.7} + \ldots, \\ \mathbb{X}(t) &= 2 - 4.543942654t^{0.9} - 2.655544765t^{1.8} - 0.5464427072t^{2.7} + \ldots, \\ \mathbb{Y}(t) &= 2 + 0.08768770670t^{0.9} + 0.876594565t^{1.8} - 0.8766862398t^{2.7} + \ldots, \\ \mathbb{Z}(t) &= 0.87656354145t^{1.8} - 0.00872947616t^{2.7} + \ldots. \end{aligned} \tag{24}$$

Similarly, for $\zeta = 0.6$, the approximate solution for (23) is

Table 2: Numerical values for the parameters given in model (2).

Parameters	Value
Λ	0.8
ρ	0.5
ξ	0.2
δ	0.5
β	0.4
γ	0.04
κ	0.05
λ	0.2

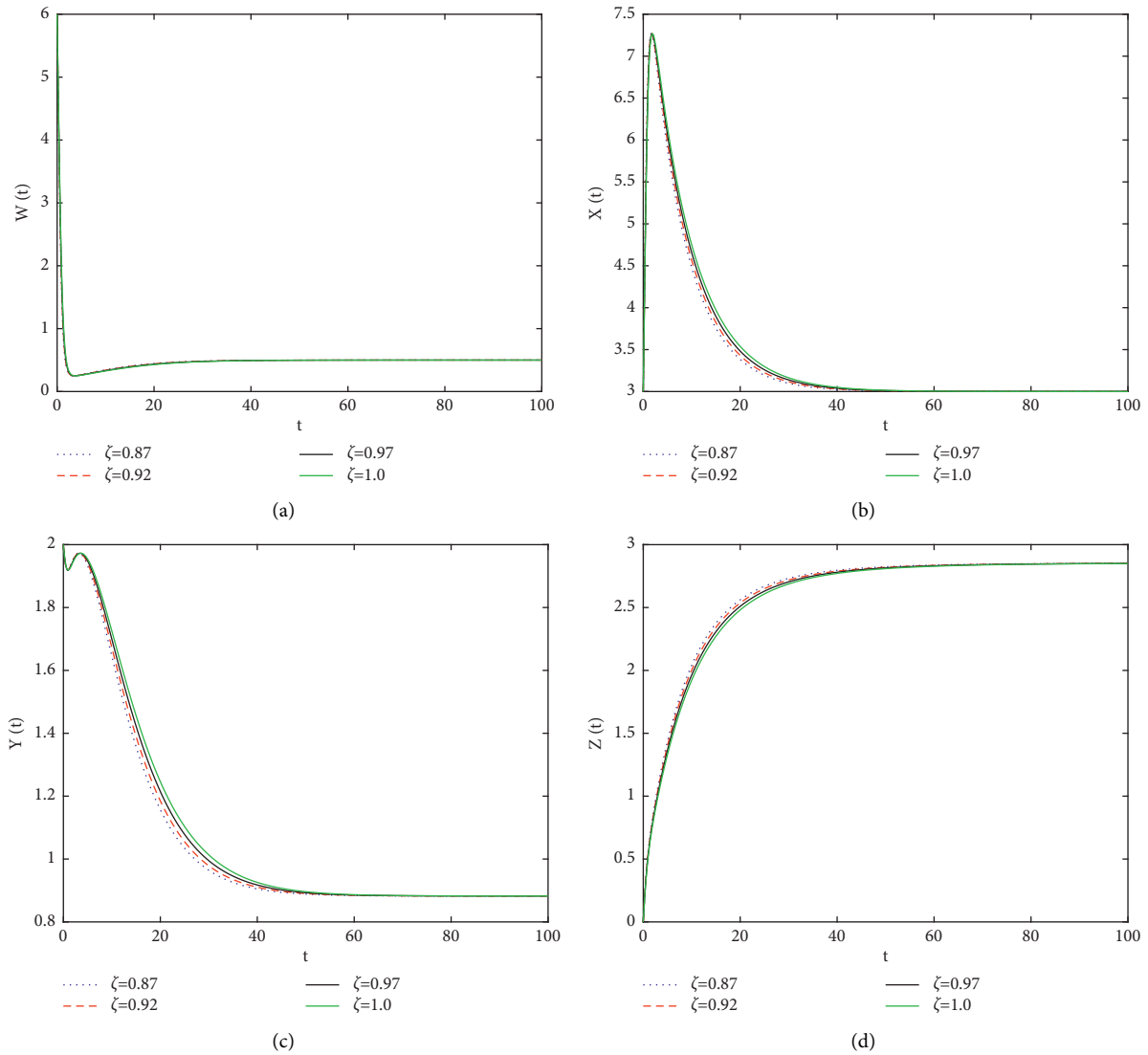

Figure 1: Graphical representation of the series solution of $(\mathbb{W}(t), \mathbb{X}(t), \mathbb{Y}(t), \mathbb{Z}(t))$ of the proposed system (2) for various arbitrary orders. (a) W(t): susceptible population. (b) X(t): acutely infected population. (c) Y(t): chronically infected population. (d) Z(t): recovered population.

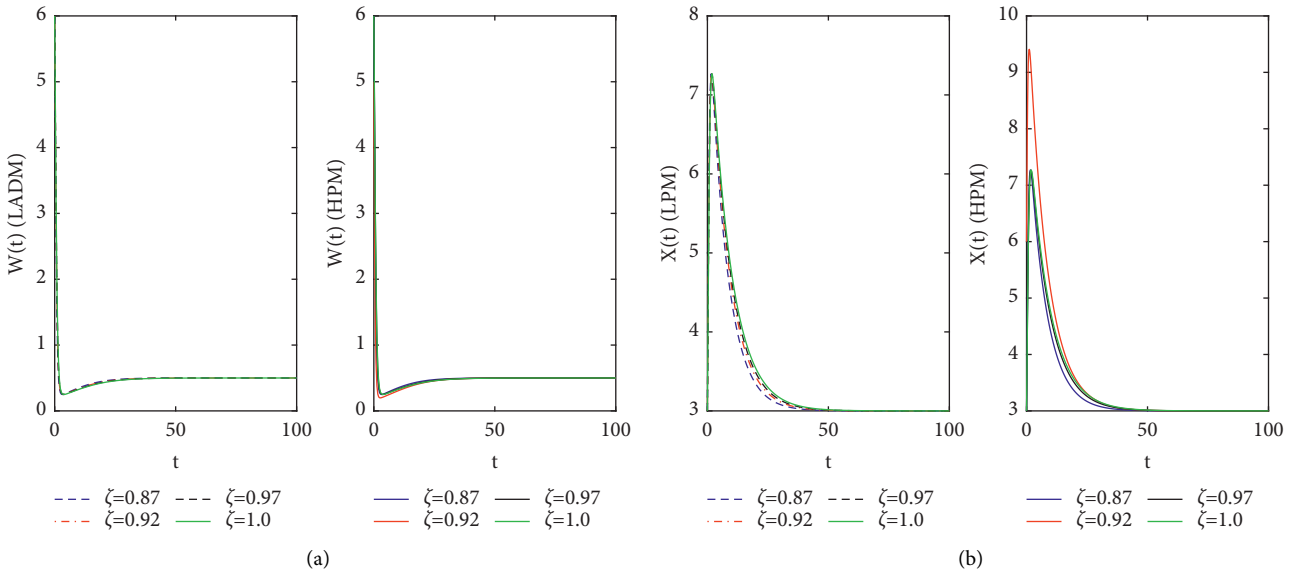

Figure 2: Comparison of LADM and HPM for the series solution of $(\mathbb{W}(t), \mathbb{X}(t))$ for various arbitrary orders of the considered model (2). (a) Comparison of LADM and HPM for the series solution of W(t) for various arbitrary orders. (b) Comparison of LADM and HPM for the series solution of X(t) for various arbitrary orders.

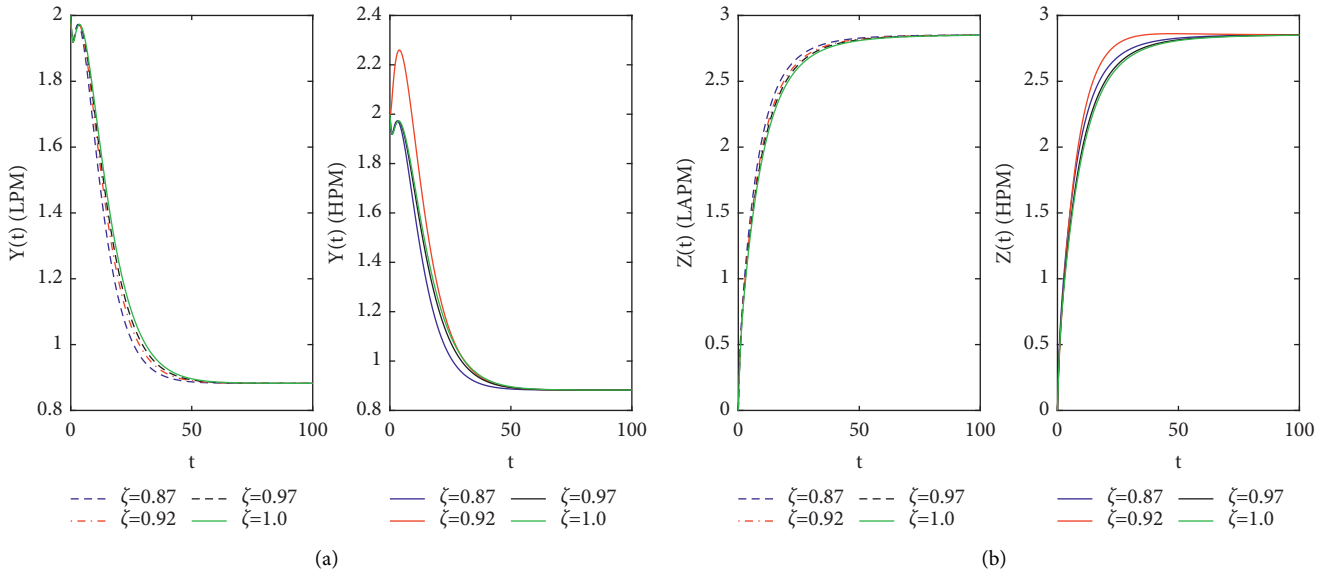

Figure 3: Comparison of LADM and HPM for the series solution of $(\mathbb{Y}(t), \mathbb{Z}(t))$ for various arbitrary orders of the considered model (2). (a) Comparison of LADM and HPM for the series solution of Y(t) for various arbitrary orders. (b) Comparison of LADM and HPM for the series solution of Z(t) for various arbitrary orders.

$$\begin{aligned}
\mathbb{W}(t) &= 6 - 5.654737025t^{0.7} + 2.8759942t^{1.4} - 1.324229934t^{2.1} + \ldots,\\
\mathbb{X}(t) &= 3 - 4.765353842t^{0.7} - 2.654389698t^{1.4} + 0.654351204t^{2.1} \ldots,\\
\mathbb{Y}(t) &= 2 + 0.05502737025t^{0.7} + 0.8473079812t^{1.4} - 0.4321037668t^{2.1} + \ldots,\\
\mathbb{Z}(t) &= 0.098769077782t^{1.4} - 0.98767203392t^{2.1} + \ldots,
\end{aligned} \tag{25}$$

and for $\zeta = 0.4$, the approximate solution for (23) is

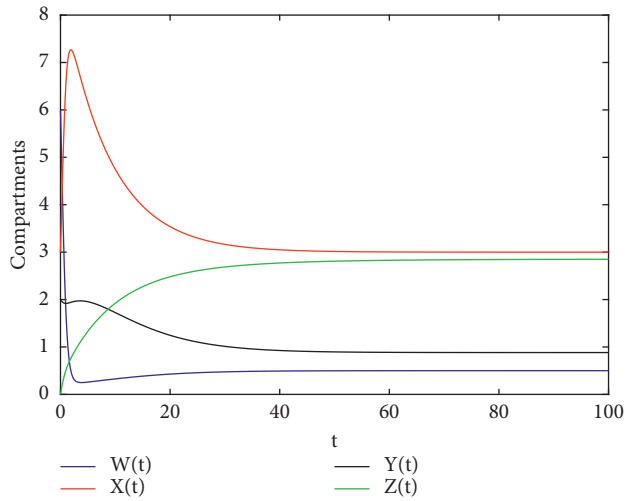

Figure 4: Graphical representation of the series solution for all the quantities of the considered model (2) with $\zeta = 1$.

$$\begin{aligned}
\mathbb{W}(t) &= 6 - 5.765495834t^{0.5} + 2.645t^{1.0} - 2.8763389788t^{1.5} \ldots, \\
\mathbb{X}(t) &= 3 - 4.987430418t^{0.5} - 3.343t^{1.0} + 2.765458202t^{1.5} \ldots, \\
\mathbb{Y}(t) &= 2 + 0.32421895835t^{0.5} + 2.2345t^{1.0} - 0.7643392382t^{1.5} + \ldots, \\
\mathbb{Z}(t) &= 0.098t^{1.0} - 0.764062165752t^{1.5} + \ldots.
\end{aligned} \tag{26}$$

For the verification of our semianalytical solution by both methods, we provide numerical simulations for problem (2). Our simulation pertains to the qualitative point analysis, and the parameters are considered through a biological feasibility approach. We take parameter numerical value and then different initial class sizes for each of the compartment, namely, susceptible $\mathbb{W}(t)$, acutely infectious $\mathbb{X}(t)$, chronic carries, $\mathbb{Y}(t)$, and recovered $\mathbb{Z}(t)$, from Table 2. Figure 1(a) shows a a quick decline in the starting in the quantity of susceptible class at at different fractional orders. The occurred decline took much more time at low nonnatural order and very slow at high noninteger order. We observe that, as the arbitrary order values increased, the curve of simulation goes, converging to the order 1. Besides this, after few days, the said individuals show low growth and then show converging towards stability to the equilibrium point. Figure 1(b) represents the acute infectious class, $\mathbb{X}(t)$ increases for some beginning days at various fractional orders. Beside that, the curve declines and stay stable through all arbitrary orders and converges to an integer order. In Figure 1(c), one may see the chronical infectious cases. $\mathbb{Y}(t)$ decreases at the starting of few days and then moves up to the maximum value of 1.5 at different noninteger order as no treatment and precautionary measures are done. But after keeping the precautions, the infectious case declines to 0.9 and then their after show stability and convergency. From Figure 1(d) we see that the recovery class goes up to 2.7 at the starting at various fractional orders and by keeping precautions and treatment the recovered class also stabilized.

Next, we have provided the comparison of different agents of the considered model by both the methods of LADM and HPM, as given from Figures 2(a)–3(b). Figure 4 represents the comparison of various agents at $\zeta = 1$.

6. Conclusions

The current investigation is the development of the four compartmental fractional-order SARS-CoV-2 model with regard to the Caputo fractional-order operative of Caputo having a singular kernel. The analysis for the series type solution of the proposed problem has been successfully achieved by two methods, one is the Laplace transform along with the Adomian polynomial (LADM) for a nonlinear term and the other one is the homotopy perturbation method (HPM). The semianalytical type solution has been obtained by both the methods which are comparable with each other. The numerical simulation for a few terms has been plotted using the available data given in Table 1 for four different values of ζ. We also compare few fractional-order values with that of integer 1, and as increasing the fractional-order value, we achieved the behavior of order 1. A complete spectrum for all compartments has established, and we can use other fractional values between 0 and 1. As a result, we say that fractional-order analysis provides better results than those of the integer-order problems.

Data Availability

Data are available upon the request by email and according to the type of collaboration.

Conflicts of Interest

The author declares no conflicts of interest.

Acknowledgments

The author expresses his appreciation to the Deanship of Scientific Research at King Saud University for funding this work through research group no. RG-1437-017.

References

[1] A. Din, Y. Li, T. Khan, and G. Zaman, "Mathematical analysis of spread and control of the novel corona virus (SARS-CoV-2) in China," *Chaos, Solitons & Fractals*, vol. 141, Article ID 110286, 2020.

[2] Y. Li and A. Din, "Levy noise impact on a stochastic hepatitis B epidemic model under real statistical data and its Fractal-fractional Atangana-Baleanu order model," *Physica Scripta*, 2021.

[3] M. Wang and J. Qi, *A Deterministic Epidemic Model for the Emergence of SARS-CoV-2 in China*, medRxiv, 2020.

[4] A. J. Kucharski, T. W. Russell, C. Diamond et al., "Early dynamics of transmission and control of SARS-CoV-2: a mathematical modelling study," *The Lancet Infectious Diseases*, vol. 20, no. 5, pp. 553–558, 2020.

[5] A. R. Tuite, D. N. Fisman, and A. L. Greer, "Mathematical modelling of SARS-CoV-2 transmission and mitigation strategies in the population of Ontario, Canada," *Canadian Medical Association Journal*, vol. 192, no. 19, pp. E497–E505, 2020.

[6] A. Din and Y. Li, "The extinction and persistence of a stochastic model of drinking alcohol," *Results in Physics*, vol. 28, Article ID 104649, 2021.

[7] M. Goyal, H. M. Baskonus, and A. Prakash, "An efficient technique for a time fractional model of lassa hemorrhagic fever spreading in pregnant women," *European Physical Journal Plus*, vol. 134, no. 481, pp. 1–10, 2019.

[8] A. Din, Y. Li, F. M. Khan, Z. U. Khan, and P. Liu, "On analysis of fractional order mathematical model of hepatitis b using atangana-baleanu caputo (abc) derivative," *Fractals*, Article ID 2240017, 2021.

[9] W. Gao, P. Veeresha, D. G. Prakasha, H. M. Baskonus, and G. Yel, "New approach for the model describing the deathly disease in pregnant women using Mittag-Leffler function," *Chaos, Solitons & Fractals*, vol. 134, Article ID 109696, 2020.

[10] I. Podlubny, *Fractional Differential Equations, Mathematics in Science and Engineering*, Academic Press, Cambridge, MA, USA, 1999.

[11] R. Hilfer, *Applications of Fractional Calculus in Physics*, World Scientific, Singapore, 2000.

[12] Y. A. Rossikhin and M. V. Shitikova, "Applications of fractional calculus to dynamic problems of linear and nonlinear hereditary mechanics of solids," *Applied Mechanics Reviews*, vol. 50, no. 1, pp. 15–67, 1997.

[13] D. Baleanu, S. M. Aydogn, H. Mohammadi, and S. Rezapour, "On modelling of epidemic childhood diseases with the Caputo-Fabrizio derivative by using the Laplace Adomian decomposition method," *Alexandria Engineering Journal*, vol. 59, no. 5, pp. 3029–3039, 2020.

[14] S. M. Aydogan, D. Baleanu, H. Mohammadi, and S. Rezapour, "On the mathematical model of Rabies by using the fractional Caputo-Fabrizio derivative," *Advances in Difference Equations*, vol. 1, pp. 1–21, 2020.

[15] S. Rezapour, H. Mohammadi, and M. E. Samei, "SEIR epidemic model for SARS-CoV-2 transmission by Caputo derivative of fractional order," *Advances in Difference Equations*, vol. 1, pp. 1–19, 2020.

[16] I. Ullah, S. Ahmad, M. u. Rahman, and M. Arfan, "Investigation of fractional order tuberculosis (TB) model via Caputo derivative," *Chaos, Solitons & Fractals*, vol. 142, Article ID 110479, 2021.

[17] A. A. Kilbas, H. Srivastava, and J. Trujillo, *Theory and Application of Fractional Differential Equations*, Elseveir, Amsterdam, Netherlands, North Holland Mathematics Studies, 1996.

[18] K. S. Miller and B. Ross, *An Introduction to the Fractional Calculus and Fractional Differential Equations*, Wiley, Hoboken, NJ, USA, 1993.

[19] F. Haq, M. Shahzad, S. Wahab, and G. Rahman, "Numerical analysis of fractional order model of HIV-1 infection of CD4+ T-cells," *Discrete Dynamics in Nature and Society*, vol. 2017, Article ID 4057089, 7 pages, 2017.

[20] J.-H. He, "The homotopy perturbation method for nonlinear oscillators with discontinuities," *Applied Mathematics and Computation*, vol. 151, no. 1, pp. 287–292, 2004.

[21] Y. Liu, Z. Li, and Y. Zhang, "Homotopy perturbation method to fractional biological population equation," *Fractional Differential Calculus*, vol. 1, no. 1, pp. 117–124, 2011.

[22] A. Kadem and D. Baleanu, "Homotopy perturbation method for the coupled fractional Lotka-Volterra equations," *Romanian Journal of Physics*, vol. 56, pp. 332–338, 2011.

[23] A. A. Kilbas, H. M. Srivastava, and J. J. Trujillo, *Theory and Applications of Fractional Differential Equations, North-Holland Mathematics Studies*, Elsevier, Amsterdam, Netherlands, 2006.

[24] F. Liu and K. Burrage, "Novel techniques in parameter estimation for fractional dynamical models arising from biological systems," *Computers & Mathematics with Applications*, vol. 62, no. 3, pp. 822–833, 2011.

[25] F. C. Meral, T. J. Royston, and R. Magin, "Fractional calculus in viscoelasticity: an experimental study," *Communications in Nonlinear Science and Numerical Simulation*, vol. 15, no. 4, pp. 939–945, 2010.

[26] C. S. Goodrich, "Existence and uniqueness of solutions to a fractional difference equation with nonlocal conditions," *Computers & Mathematics with Applications*, vol. 61, no. 2, pp. 191–202, 2011.

[27] B. Ahmad and J. J. Nieto, "Existence results for a coupled system of nonlinear fractional differential equations with three-point boundary conditions," *Computers & Mathematics with Applications*, vol. 58, no. 9, pp. 1838–1843, 2009.

[28] Y. Chen and H.-L. An, "Numerical solutions of coupled Burgers equations with time- and space-fractional derivatives," *Applied Mathematics and Computation*, vol. 200, no. 1, pp. 87–95, 2008.

[29] C.-z. Bai and J.-x. Fang, "The existence of a positive solution for a singular coupled system of nonlinear fractional differential equations," *Applied Mathematics and Computation*, vol. 150, no. 3, pp. 611–621, 2004.

[30] A. Atangana and D. Baleanu, "New fractional derivatives with non-local and non- singular kernel: theory and application to heat transfer model," *Thermal Science*, vol. 20, no. 2, pp. 763–769, 2016.

Hindawi
Journal of Function Spaces
Volume 2021, Article ID 9358496, 12 pages
https://doi.org/10.1155/2021/9358496

Research Article

Mixture of Lindley and Lognormal Distributions: Properties, Estimation, and Application

A. S. Al-Moisheer

Department of Mathematics, College of Science, Jouf University, P.O. Box 848, Sakaka 72351, Saudi Arabia

Correspondence should be addressed to A. S. Al-Moisheer; asalmoisheer@ju.edu.sa

Received 26 June 2021; Revised 23 July 2021; Accepted 29 September 2021; Published 29 December 2021

Academic Editor: Badr Saad. T. Alkaltani

Finite mixture models provide a flexible tool for handling heterogeneous data. This paper introduces a new mixture model which is the mixture of Lindley and lognormal distributions (MLLND). First, the model is formulated, and some of its statistical properties are studied. Next, maximum likelihood estimation of the parameters of the model is considered, and the performance of the estimators of the parameters of the proposed models is evaluated via simulation. Also, the flexibility of the proposed mixture distribution is demonstrated by showing its superiority to fit a well-known real data set of 128 bladder cancer patients compared to several mixture and nonmixture distributions. The Kolmogorov Smirnov test and some information criteria are used to compare the fitted models to the real dataset. Finally, the results are verified using several graphical methods.

1. Introduction

In most reliability applications, data is modeled by a single parametric distribution. However, in many situations, a population can be divided into a number of subpopulations each representing a different type of failure. Finite mixture models play an important role in modeling such heterogeneous data. Applications of mixture models are especially in clustering and classification, see, for example, Everitt and Hand [1], McLachlan and Peel [2], McLachlan and Basford [3], Titterington et al. [4], Lindsay [5], McLachlan and Krishnan [6], Al-Moisheer et al. [7, 8], and Al-Moisheer [9, 10]. In this paper, we will introduce a finite mixture of Lindley and lognormal distributions (MLLND). The motivation of suggesting this mixture comes from the importance of its component distributions. The one-parameter Lindley distribution was introduced by Lindley [11, 12], and then Ghitany et al. [13] illustrated its importance in lifetesting and reliability applications. With regards to one component lognormal distribution, it has found important applications in a wide variety of fields; (see, Kim and Yum [14] and Lin et al. [15]). In the literature, work has been done on mixture models having the Lindley distribution as one of its components, see, for example, Al-Moisheer et al. (Al-Moisheer et al. [16], Al-Moisheer et al. [17]) for the mixture of two one-parameter Lindley distribution and the mixture of Lindley and inverse Weibull distributions, respectively. Also, Daghestani et al. [18] considered the mixture of Lindley and Weibull distributions. In this paper, we will introduce a new mixture distribution, namely, the finite mixture of Lindley and lognormal distribution (MLLND). This paper is organized as follows. In Section 2, we obtain the new model and derive some of its properties. In Sections 3 and 4, we derive the probability density function of the order statistics and the equations required to obtain the maximum likelihood estimation of the model parameters. In Section 5, the flexibility of the proposed model is illustrated by showing its ability to provide the best fit for a well-known real data set compared to six competitive models. Finally, In Section 6, we draw a conclusion.

2. Model Formulation and Some Properties

The MLLND has the following probability density function (pdf)

$$f(x;\Theta) = p_1 f_1(x;\Theta_1) + p_2 f_2(x;\Theta_2),\ 0 < p_1, p_2 < 1,\ p_1 + p_2 = 1,\ x \geq 0, \tag{1}$$

whereas the pdf of the Lindley component is given by

$$f_1(x;\Theta_1) = \frac{\theta^2}{\theta+1}(1+x)e^{-\theta x},\ x \geq 0,\ \theta > 0. \tag{2}$$

The pdf of the lognormal component is given by

$$f_2(x;\Theta_2) = \frac{1}{\sqrt{2\pi}\sigma x} e^{-\frac{1}{2}\left(\frac{\log x-\mu}{\sigma}\right)^2},\ x \geq 0,\ -\infty < \mu < \infty,\ \sigma > 0, \tag{3}$$

$\Theta = (p_1, \theta, \mu, \sigma)$, $\Theta_1 = (\theta)$, and $\Theta_2 = (\mu, \sigma)$.

Evidently, the cumulative distribution function (cdf) of the MLLND is given by

$$F(x;\Theta) = p_1 F_1(x;\Theta_1) + p_2 F_2(x;\Theta_2), \tag{4}$$

where

$$F_1(x;\Theta_1) = 1 - \frac{\theta+1+\theta x}{\theta+1}e^{-\theta x},\ x \geq 0,\ \theta > 0,$$
$$F_2(x;\Theta_2) = \Phi\left(\frac{\log x-\mu}{\sigma}\right),\ x \geq 0,\ -\infty < \mu < \infty,\ \sigma > 0, \tag{5}$$

with $\Phi(.)$ referring to the cdf of the standard normal distribution.

Ghitany et al. [13] and Shanker et al. [19] displayed some properties of the LD in (2), while properties of the LND in (3) were given, for example, by Crow and Shimizu [20] and Johnson et al. [21]. In this section, we introduce some properties of the MLLND by mixing the results of the LD and LND.

2.1. Mean and Variance. The mean of the MLLND in (1) is simply given by

$$E(X) = p_1\left[\frac{\theta+2}{\theta(\theta+1)}\right] + p_2 e^{\mu+\frac{\sigma^2}{2}},\ \text{for } x \geq 0,\ \theta, \sigma > 0,\ -\infty < \mu < \infty, \tag{6}$$

while the variance is given by

$$Var(X) = \frac{p_1}{\theta^2(\theta+1)}[2(\theta+3) - p_1(\theta+2)\theta] + p_2 e^{2\mu+\sigma^2}\left[e^{\sigma^2} - p_2\right] - 2p_1p_2\left(\frac{\theta+2}{\theta(\theta+1)}\right)e^{\mu+\frac{\sigma^2}{2}},$$
$$\text{for } x \geq 0,\ \theta, \sigma > 0,\ -\infty < \mu < \infty. \tag{7}$$

Also, the rth moments of the MLLND is given by

$$E(X^r) = \frac{p_1(\theta+r+1)\Gamma(r+1)}{\theta^r(\theta+1)} + p_2 e^{r\mu+\frac{r^2\sigma^2}{2}},\ \text{for } r = 1, 2, 3, \cdots. \tag{8}$$

2.2. Mode and Median. It can be shown that the equations for obtaining the modes and median of the MLLND, respectively, are

$$p_1\frac{\theta^2 e^{-\theta x}}{\theta+1}[1-\theta(1+x)] - p_2\frac{1}{\sqrt{2\pi}\sigma^3 x^2}e^{-\frac{1}{2}\left(\frac{\log x-\mu}{\sigma}\right)^2}\left[\sigma^2 + (\log x - \mu)\right] = 0, \tag{9}$$

and

$$p_1\left(1 - \frac{(\theta+1+\theta x)e^{-\theta x}}{\theta+1}\right) + p_2\Phi\left(\frac{\log x-\mu}{\sigma}\right) = 0.5. \tag{10}$$

Figure 1(a) shows the pdf of the MLLND unimodal case at the choice of parameters $\Theta = (p_1 = 0.5, \theta = 0.95, \mu = 0.25, \sigma = 0.25)$ with the values of mode and median (1.1623, 1.2712), respectively. Also, Figure 1(b) shows the shape of the pdf in the MLLND bimodal case at the choice of parameters $\Theta = (p_1 = 0.5, \theta = 2.95, \mu = 0.85, \sigma = 0.25)$ with the values of mode and median ((1.4370, 2.1430), 1.4542), respectively. For plotting the pdf of the LD and LND in *R*, we use the function dlindley() and dlnorm(), respectively. The package rootSolve() in *R* is used for modes and median of the MLLND.

2.3. Reliability and Failure Rate Functions. The reliability function of the MLLND is given by

$$R(x) = p_1\left[\frac{\theta+1+\theta x}{\theta+1}e^{-\theta x}\right] + p_2\left[1 - \Phi\left(\frac{\log x-\mu}{\sigma}\right)\right],\ x \geq 0. \tag{11}$$

By using (3) and (4), the hazard rate function (HRF) of the MLLND is given by

$$r(x) = \frac{p_1\left(\theta^2/\theta+1\right)(1+x)e^{-\theta x} + p_2\left(1/\sqrt{2\pi}\sigma x\right)e^{-1/2(\log x-\mu/\sigma)^2}}{p_1\left((\theta+1+\theta x/\theta+1)e^{-\theta x}\right) + p_2(1-\Phi(\log x-\mu/\sigma))},\ x \geq 0, \tag{12}$$

which can be written by using the result in AL-Hussaini and Sultan [22], as

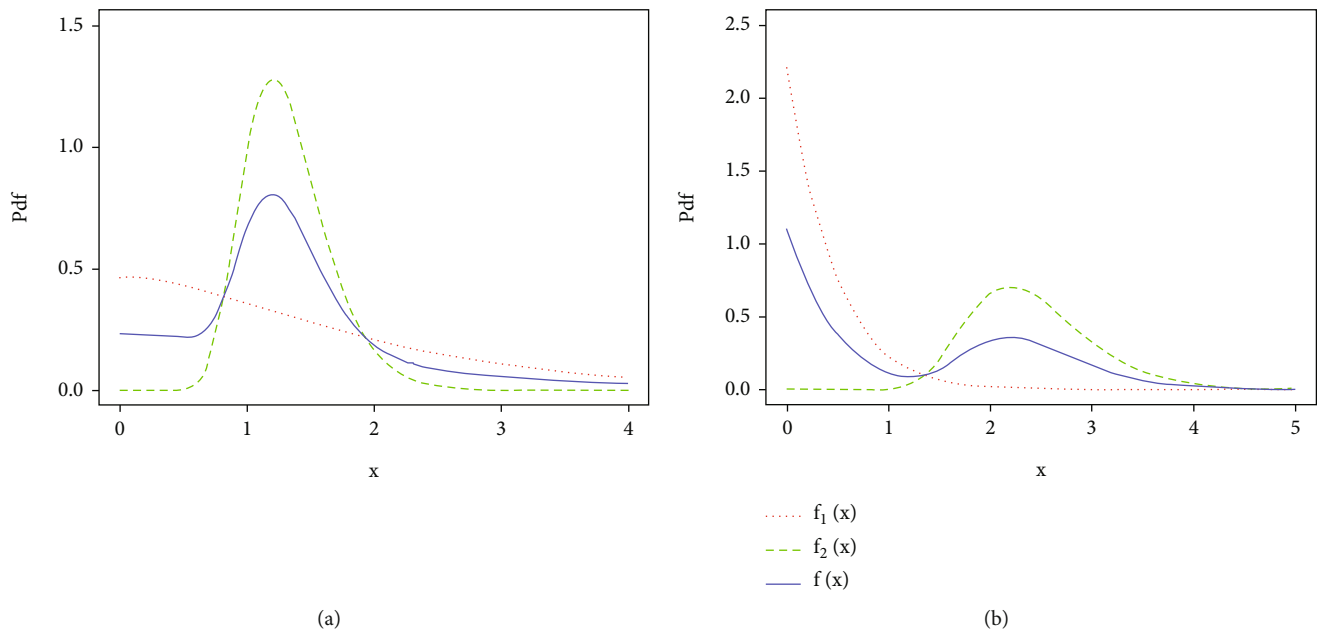

Figure 1: pdf plot of MLLND with (a) $\Theta = (p_1 = 0.5, \theta = 0.95, \mu = 0.25, \sigma = 0.25)$ (b) $\Theta = (p_1 = 0.5, \theta = 2.95, \mu = 0.85, \sigma = 0.25)$.

$$r(x) = h(x)\, r_1(x) + (1 - h(x)) r_2(x), \tag{13}$$

where

$$h(x) = \frac{1}{1 + (p_2 R_2(x)/p_1 R_1(x))}, r_i(x) = \frac{f_i(x)}{R_i(x)}, i = 1, 2, R_1(x) = \left(\frac{\theta + 1 + \theta x}{\theta + 1} e^{-\theta x}\right) \text{and } R_2(x) = 1 - \Phi\left(\frac{\log x - \mu}{\sigma}\right). \tag{14}$$

The HRF of the MLLND in (12) achieves the following limits.

Lemma 1.

$$\lim_{x \longrightarrow 0} r(x) = \frac{p_1 \theta^2}{\theta + 1}, \tag{15}$$

$$\lim_{x \longrightarrow \infty} r(x) = 0. \tag{16}$$

Proof. To prove the first part of the limits, using the equation (13), we get

$$\lim_{x \longrightarrow 0} h(x) = p_1, \text{and } \lim_{x \longrightarrow 0} (1 - h(x)) = p_2. \tag{17}$$

□

Then, we have

$$\lim_{x \longrightarrow 0} r_1(x) = \frac{p_1 \theta^2}{\theta + 1}, \text{and } \lim_{x \longrightarrow 0} r_2(x) = 0, \tag{18}$$

and thus (15) is proved.

Also, to prove (16),

$$\lim_{x \longrightarrow \infty} r(x) = \lim_{x \longrightarrow \infty} \frac{f(x)}{1 - F(x)} = -\lim_{x \longrightarrow \infty} \frac{f'(x)}{f(x)}, \left(f'(x) = \frac{df(x)}{dx}\right), \tag{19}$$

$$\text{where, } f'(x) = p_1 f'_1(x) + p_2 f'_2(x). \tag{20}$$

It follows from (19) and (20) that

$$\lim_{x \longrightarrow \infty} r(x) = -\lim_{x \longrightarrow \infty} \frac{p_1 f'_1(x) + p_2 f'_2(x)}{p_1 f_1(x) + p_2 f_2(x)}. \tag{21}$$

It follows that

$$\lim_{x \longrightarrow \infty} r(x) = 0. \tag{22}$$

For more details, see Sultan [23], Sultan and Al-Moisheer [24], and Al-Moisheer et al. (Al-Moisheer et al. [16]).

2.4. Skewness, Kurtosis, and the Coefficient of Variation. The coefficient of skewness (Sk), the coefficient of kurtosis (Ku), and the coefficient of variation (Cv) of the MLLND distribution are given by, respectively,

$$Sk = \frac{E(X^3) - 3\mu\sigma^2 - \mu^3}{\sigma^3}, = \left(\frac{6p_1(\theta + 4)}{\theta^3(\theta + 1)}\right) - \left(\frac{p_1(\theta + 2)}{\theta(\theta + 1)} + p_2 e^{\mu + \frac{\sigma^2}{2}}\right)^3 + p_2 e^{3\mu + \frac{9\sigma^2}{2}} - 3\left(\frac{2p_1(\theta + 3)}{\theta^2(\theta + 1)} - \left(\frac{p_1(\theta + 2)}{\theta(\theta + 1)} + p_2 e^{\mu + \frac{\sigma^2}{2}}\right)^2 + p_2 e^{2(\mu + \sigma^2)}\right) \cdot \left(\frac{p_1(\theta + 2)}{\theta(\theta + 1)} + p_2 e^{\mu + \frac{\sigma^2}{2}}\right) / \left(\frac{2p_1(\theta + 3)}{\theta^2(\theta + 1)} - \left(\frac{p_1(\theta + 2)}{\theta(\theta + 1)} + p_2 e^{\mu + \frac{\sigma^2}{2}}\right)^2 + p_2 e^{2(\mu + \sigma^2)}\right)^{\frac{3}{2}},$$

Table 1: Results of the mean, standard deviation, coefficient of variation, skewness, and kurtosis for the MLLND at the choice ($p_1 = 0.5\,; \theta = 0.1\,; \sigma = 3$).

μ	Mean	Stand.Dev.	Cv	Sk	Ku
1	124.013	15574.6	125.589	1.03165×10^6	8.62356×10^{15}
2	334.237	42336.1	126.665	1.03165×10^6	8.62354×10^{15}
3	905.688	115081	127.065	1.03165×10^6	8.62353×10^{15}
4	2459.05	312824	127.213	1.03165×10^6	8.62353×10^{15}
5	6681.53	850343	127.268	1.03165×10^6	8.62353×10^{15}
6	18159.4	2.31147×10^6	127.288	1.03165×10^6	8.62353×10^{15}
7	49359.6	6.28324×10^6	127.295	1.03165×10^6	8.62353×10^{15}
8	134170	1.70796×10^7	127.298	1.03165×10^6	8.62353×10^{15}
9	364710	4.64272×10^7	127.299	1.03165×10^6	8.62353×10^{15}
10	991381	1.26202×10^8	127.299	1.03165×10^6	8.62353×10^{15}

Table 2: Results of the mean, standard deviation, coefficient of variation, skewness, and kurtosis for the MLLND at the choice ($p_1 = 0.5\,; \theta = 0.5\,; \sigma = 3$).

μ	Mean	Stand.Dev.	Cv	Sk	Ku
1	131.891	15574.5	118.086	1.03166×10^6	8.62368×10^{15}
2	342.116	42336.0	123.747	1.03165×10^6	8.62359×10^{15}
3	913.567	115081	125.969	1.03165×10^6	8.62355×10^{15}
4	2466.93	312824	126.807	1.03165×10^6	8.62354×10^{15}
5	6689.41	850343	127.118	1.03165×10^6	8.62353×10^{15}
6	18167.3	2.31147×10^6	127.233	1.03165×10^6	8.62353×10^{15}
7	49367.4	6.28324×10^6	127.275	1.03165×10^6	8.62353×10^{15}
8	134178	1.70796×10^7	127.290	1.03165×10^6	8.62353×10^{15}
9	364718	4.64272×10^7	127.296	1.03165×10^6	8.62353×10^{15}
10	991389	1.26202×10^8	127.298	1.03165×10^6	8.62353×10^{15}

$$
\begin{aligned}
Ku = \frac{E\left(X^4\right) - 4\mu E\left(X^3\right) + 6\mu^2\sigma^2 + 3\mu^4}{\sigma^4}, &= \frac{24p_1(\theta+5)}{\theta^4(\theta+1)} \\
&- 4\left(\frac{6p_1(\theta+4)}{\theta^3(\theta+1)} + p_2 e^{3\mu+\frac{9\sigma^2}{2}}\right)\left(\frac{p_1(\theta+2)}{\theta(\theta+1)} + p_2 e^{\mu+\frac{\sigma^2}{2}}\right) \\
&+ 3\left(\frac{p_1(\theta+2)}{\theta(\theta+1)} + p_2 e^{\mu+\frac{\sigma^2}{2}}\right)^4 + p_2 e^{4\mu+8\sigma^2} \\
&+ 6\left(\frac{p_1(\theta+2)}{\theta(\theta+1)} + p_2 e^{\mu+\frac{\sigma^2}{2}}\right)^2 \left(\frac{2p_1(\theta+3)}{\theta^2(\theta+1)}\right. \\
&\left. - \left(\frac{p_1(\theta+2)}{\theta(\theta+1)} + p_2 e^{\mu+\frac{\sigma^2}{2}}\right)^2 + p_2 e^{2\left(\mu+\sigma^2\right)}\right) \Big/ \left(\frac{2p_1(\theta+3)}{\theta^2(\theta+1)}\right. \\
&\left. - \left(\frac{p_1(\theta+2)}{\theta(\theta+1)} + p_2 e^{\mu+\frac{\sigma^2}{2}}\right)^2 + p_2 e^{2\left(\mu+\sigma^2\right)}\right)^2,
\end{aligned}
\tag{23}
$$

$$
Cv = \frac{\sigma}{\mu} = \frac{\sqrt{\left(2p_1(\theta+3)/\theta^2(\theta+1) - \left(\left(p_1(\theta+2)/\theta(\theta+1)\right) + p_2 e^{\mu+(\sigma^2/2)}\right)^2 + p_2 e^{2(\mu+\sigma^2)}\right)}}{\left(\left(p_1(\theta+2)/\theta(\theta+1)\right) + p_2 e^{\mu+(\sigma^2/2)}\right)}.
\tag{24}
$$

Some values of the mean, standard deviation, coefficient of variation, coefficient skewness, and coefficient kurtosis for the MLLND distributions are obtained for the two choices of the parameter θ and different values of the parameter μ. From the results which are presented in Tables 1 and 2, we note that as μ increases, both the mean and the standard deviation increase, whereas the values of the other measures remain fairly stable.

3. Order Statistics

Let $X_1, X_2, \cdots, X_m$ be a random sample of size m selected from a distribution with pdf $f(x)$ and cdf $F(x)$, and also let $X_{1:m} < X_{2:m} < \cdots < X_{m:m}$ be the corresponding order statistics. The pdf of the rth order statistics that say $X_{r:m}$ is given by

$$f_{r:m}(x) = \frac{m!}{(r-1)!(m-r)!}[F(x)]^{r-1}[1-F(x)]^{m-r}f(x), -\infty < x < \infty, \tag{25}$$

and the corresponding cdf is given by

$$\begin{aligned} F_{(r:m)}(x) &= \sum_{j=r}^{m}\binom{m}{j}F^{j}(x)[1-F(x)]^{m-j} \\ &= \sum_{j=r}^{m}\sum_{k=0}^{m-j}\binom{m}{j}\binom{m-j}{k}(-1)^{k}F^{j+k}(x). \end{aligned} \tag{26}$$

Therefore, using (25) and (26), the pdf and cdf of the rth order statistics, are, respectively, given by

$$f_{r:m}(x,\theta,\sigma) = \frac{m!\left(\left(p_1\theta^2(x+1)e^{-\theta x}/\theta+1\right)+\left(p_2e^{-1/2(\log x-\mu/\sigma)^2}/\sqrt{2\pi}\sigma x\right)\right)W}{\Gamma(j)\Gamma(m-j+1)}, \tag{27}$$

where

$$W = \left(\frac{p_2}{2}\ \text{erf}\ c\left(\frac{\mu-\log(x)}{\sqrt{2}\sigma}\right)+p_1\left(1-\frac{e^{-\theta x}(\theta+\theta x+1)}{\theta+1}\right)\right)^{j-1}\times\left(-\frac{p_2}{2}\ \text{erf}\ c\left(\frac{\mu-\log(x)}{\sqrt{2}\sigma}\right)+p_1\left(\frac{e^{-\theta x}(\theta+\theta x+1)}{\theta+1}-1\right)+1\right)^{m-j}, \tag{28}$$

$$F_{r:m}(x,\theta,\sigma) = \frac{m!\delta_{j-m}\left((p_2/2)\ \text{erf}\ c\left(\mu-\log(x)/\sqrt{2}\sigma\right)+p_1\left(1-e^{-\theta x}(\theta+\theta x+1)/\theta+1\right)\right)^{j+1}}{(j+1)\Gamma(j)\Gamma(m-j+1)}. \tag{29}$$

Accordingly, the density functions of the minimum and maximum order statistics, respectively, are given by

$$\begin{aligned} f_{1:m}(x) = m\Bigg(&\frac{p_1\theta^2(x+1)e^{-\theta x}}{\theta+1}+\frac{p_2e^{-1/2(\log x-\mu/\sigma)^2}}{\sqrt{2\pi}\sigma x}\Bigg), \\ &\times\left(-\frac{p_2}{2}\text{erfc}\left(\frac{\mu-\log(x)}{\sqrt{2}\sigma}\right)\right. \\ &\left.+p_1\left(-\left(1-\frac{e^{-\theta x}(\theta+\theta x+1)}{\theta+1}\right)\right)+1\right)^{m+1}, \end{aligned} \tag{30}$$

$$\begin{aligned} f_{m:m}(x) = m\Bigg(&\frac{p_1\theta^2(x+1)e^{-\theta x}}{\theta+1}+\frac{p_2e^{-1/2(\log x-\mu/\sigma)^2}}{\sqrt{2\pi}\sigma x}\Bigg), \\ &\times\left(\frac{p_2}{2}\ \text{erf}\ c\left(\frac{\mu-\log(x)}{\sqrt{2}\sigma}\right)\right. \\ &\left.+p_1\left(1-\frac{e^{-\theta x}(\theta+\theta x+1)}{\theta+1}\right)\right)^{m-1}. \end{aligned} \tag{31}$$

4. Maximum Likelihood Estimation

The likelihood function (LF) for the MLLND in (1) is given by

$$L(\Theta) = \prod_{j=1}^{n}\left[p_1f_1\left(x_j;\Theta_1\right)+p_2f_2\left(x_j;\Theta_2\right)\right], \tag{32}$$

where $\Theta_1=(\theta)$ and $\Theta_2=(\mu,\sigma)$. By differentiating the log LF with respect to the model parameters $\Theta=(p_1,\theta,\mu,\sigma)$, respectively, we get the following equations

$$\begin{aligned} \sum_{j=1}^{n}\omega\left(x_j;\Theta\right) = 0,\ &\sum_{j=1}^{n}p_1\psi_1\left(x_j;\Theta\right)\eta_1\left(x_j;\Theta\right) \\ &= 0,\ \sum_{j=1}^{n}p_2\phi_1\left(x_j;\Theta\right)\eta_2\left(x_j;\Theta\right) \\ &= 0,\ \sum_{j=1}^{n}p_2\phi_2\left(x_j;\Theta\right)\eta_2\left(x_j;\Theta\right) = 0, \end{aligned} \tag{33}$$

where $\omega(x_j;\Theta)$, $\psi_1(x_j;\Theta)$, $\eta_1(x_j;\Theta)$, $\eta_2(x_j;\Theta)$, $\phi_1(x_j;\Theta)$, and $\phi_2(x_j;\Theta)$ are as follows:

$$\begin{aligned} \omega\left(x_j;\Theta\right) &= \frac{f_1\left(x_j;\Theta_1\right)-f_2\left(x_j;\Theta_2\right)}{f\left(x_j;\Theta\right)}, \\ \psi_1\left(x_j;\Theta\right) &= 2\theta^{-1}-x_j-1, \\ \eta_1\left(x_j;\Theta\right) &= \frac{f_1\left(x_j;\Theta_1\right)}{f\left(x_j;\Theta\right)}, \\ \eta_2\left(x_j;\Theta\right) &= \frac{f_2\left(x_j;\Theta_2\right)}{f\left(x_j;\Theta\right)}, \\ \phi_1\left(x_j;\Theta\right) &= \frac{\left(\log x_j-\mu\right)}{\sigma^2},\ \phi_2\left(x_j;\Theta\right) = \left(\log x_j-\mu\right)^2\sigma^{-3}-\sigma^{-1}, \end{aligned} \tag{34}$$

Table 3: MLEs for the MLLND parameters with their averages, biases, MSEs, and CIs.

$\Theta = (p_1, \theta, \mu, \sigma)$		n	$p\wedge_1$	$\theta\wedge$	$\mu\wedge$	$\sigma\wedge$
(0.50, 0.95, 0.25, 0.25)	Aveg.	30	0.42098178	1.3880892	0.26007314	0.26373918
	Bias		-0.0790180	0.4380890	0.01007314	0.01373918
	MSE		0.04314494	2.4538343	0.01261492	0.01984133
	90%CIs		(0.06875, 0.71539)	(0.63975, 4.21360)	(0.09383, 0.43337)	(0.09522, 0.49725)
	95%CIs		(0.02500, 0.76579)	(0.57416, 7.27137)	(0.05603, 0.47826)	(0.06583, 0.57054)
	Aveg.	50	0.45201752	1.1532198	0.256110576	0.256695006
	Bias		-0.04798248	0.2032198	0.006110576	0.006695006
	MSE		0.02578189	1.0242892	0.006485839	0.009521935
	90%CIs		(0.16097, 0.68077)	(0.71706, 1.71599)	(0.12595, 0.38932)	(0.12420, 0.43820)
	95%CIs		(0.09463, 0.72194)	(0.66882, 3.49642)	(0.09611, 0.41885)	(0.10079, 0.49013)
	Aveg.	75	0.47460679	1.02075786	0.253259473	0.252181908
	Bias		-0.02539321	0.07075786	0.003259473	0.002181908
	MSE		0.01564727	0.28849904	0.00414685	0.0054144
	90%CIs		(0.26408, 0.66297)	(0.76299, 1.25958)	(0.14861, 0.35969)	(0.14830, 0.38325)
	95%CIs		(0.19820, 0.69821)	(0.72714,1.46520)	(0.12957,0.38270)	(0.12761,0.42832)
	Aveg.	100	0.47989155	0.98821225	0.252882986	0.251725793
	Bias		-0.02010845	0.03821225	0.002882986	0.001725793
	MSE		0.01101642	0.13257566	0.002925308	0.003657510
	90%CIs		(0.30911, 0.64102)	(0.79201, 1.18252)	(0.16472, 0.34125)	(0.16431, 0.35621)
	95%CIs		(0.26617, 0.67108)	(0.76341, 1.26408)	(0.14856, 0.36121)	(0.14669, 0.38801)
(0.50, 2.95, 0.85, 0.25)	Aveg.	30	0.51085594	3.1659382	0.854910354	0.244567051
	Bias		0.01085594	0.2159382	0.004910354	-0.00543290
	MSE		0.01287378	1.3430948	0.051054250	0.032862658
	90%CIs		(0.33493, 0.69426)	(1.65368, 5.12052)	(0.71319, 0.98390)	(0.13525, 0.33944)
	95%CIs		(0.30361, 0.73304)	(1.44724, 5.71634)	(0.67448, 1.01376)	(0.11017, 0.33944)
	Aveg.	50	0.507576054	3.0707105	0.852470382	0.240278966
	Bias		0.007576054	0.1207105	0.002470382	-0.00972100
	MSE		0.007065907	0.6709617	0.010009987	0.004340029
	90%CIs		(0.37350, 0.64665)	(1.89865, 4.48536)	(0.74975, 0.95241)	(0.16456, 0.31975)
	95%CIs		(0.35033, 0.67656)	(1.71581, 4.85850)	(0.72685, 0.97424)	(0.14466, 0.33891)
	Aveg.	75	0.505553756	3.02406667	0.8505206847	0.24284061
	Bias		0.005553756	0.07406667	0.0005206847	-0.00715939
	MSE		0.004523098	0.40053500	0.002560209	0.002114857
	90%CIs		(0.39807, 0.61738)	(1.94383, 4.39174)	(0.77062, 0.93072)	(0.18319, 0.30590)
	95%CIs		(0.37909, 0.63999)	(2.08437, 4.12198)	(0.75182, 0.94835)	(0.17228, 0.32117)
	Aveg.	100	0.502508608	2.99851936	0.8507297408	0.24475867
	Bias		0.002508608	0.04851936	0.0007297408	-0.0052413
	MSE		0.003210267	0.27651139	0.001779217	0.00108009
	90%CIs		(0.41022, 0.59639)	(2.20464, 3.91893)	(0.78248, 0.91894)	(0.19393, 0.29928)
	95%CIs		(0.39236, 0.61599)	(2.08727, 4.15153)	(0.76705, 0.93227)	(0.18413, 0.31123)

Table 4: Results for fitting the MLLND comparing with their components and others models.

Models	MLEs (Std.Error)	Loglikelihood	AIC	BIC	KS	p value
MLLND	$p\wedge_1 = 0.16733$ (0.0525)	-399.423	806.8461	818.2542	0.0344	0.9981
	$\theta\wedge = 1.8819$ (0.7011)					
	$\mu\wedge = 1.9453$ (0.1119)					
	$\sigma\wedge = 0.8455$ (0.0852)					
MTLD	$p\wedge_1 = 0.2022$ (0.1150)	-402.4761	810.9522	819.5083	0.0704	0.5495
	$\theta\wedge_1 = 0.0912$ (0.0264)					
	$\theta\wedge_2 = 0.3239$ (0.0483)					
MLIWD	$p\wedge_1 = 0.2374$ (0.0701)	-399.8651	807.7303	819.1384	0.0428	0.9730
	$\theta\wedge = 1.2975$ (0.4920)					
	$\alpha\wedge = 0.1804$ (0.0221)					
	$\beta\wedge = 1.5473$ (0.1528)					
MTWD	$p\wedge_1 = 0.9554$ (0.0438)	-401.2711	812.5422	826.8023	0.0584	0.7746
	$\alpha\wedge_1 = 8.8542$ (1.0315)					
	$\alpha\wedge_2 = 0.4747$ (0.2526)					
	$\beta\wedge_1 = 0.9751$ (0.0811)					
	$\beta\wedge_2 = 2.5650$ (1.9307)					
MIWWD	$p\wedge_1 = 0.7344$ (0.0680)	-398.7583	807.5166	821.7768	0.0439	0.9655
	$\alpha\wedge_1 = 0.1879$ (0.0166)					
	$\alpha\wedge_2 = 1.7452$ (0.5879)					
	$\beta\wedge_1 = 1.5208$ (0.1446)					
	$\beta\wedge_2 = 0.8896$ (0.1764)					
LND	$\mu = 1.5111\wedge$ (0.1133)	-406.8025	817.6050	823.3091	0.0998	0.1556
	$\sigma = 1.2818\wedge$ (0.0801)					
LD	$\theta = 0.2129\wedge$ (0.0134)	-417.9239	837.8477	840.6997	0.1335	0.0207

and $f(x_j;\Theta)$, $f_1(x_j;\Theta_1)$, and $f_2(x_j;\Theta_2)$ are as in $(1, 2, 3)$, respectively. The MLEs of the parameters can be obtained by solving systems of nonlinear Eqs. given in (33) using the package nleqslv() in *R*.

The numerical results are obtained in Table 3 for two different combinations of the parameters. The first one corresponds to a unimodal distribution ,whereas the second choice is for bimodal distribution.

In each case, the averages of the MLEs, biases, mean squared errors (MSE), and the lower and upper limits of the 95% nd 90% confidence intervals (CIs) for the parameters are computed at different sample sizes.

It is clear from Table 3 that the MSE decreases as the sample size increases for all estimates parameters. Furthermore, the values of the bias decrease. Also, as the sample size increases, the width of the confidence intervals (CIs) for the parameters decreases. The number of replications of the simulation results is taken to 10000.

5. Application

The flexibility of the proposed model is illustrated by applying it on a real data set given in Shanker et al. [25]. It represents the remission times (in months) of sample size $n = 128$ bladder cancer patients as reported in Lee and Wang [26]. This data was previously analyzed by Daghestani et al. [18], who compared their proposed model, mixture of Lindley and Weibull distribution MLWD to two other models; mixture of two one- parameter Lindley distribution MTLD and mixture of two Weibull distribution MTWD. They showed that their model provides the best fit as it has the lowest values of the KS statistic and AIC criterion and the highest p value.

In this paper, we compared our proposed model with six other models including the three models given in Daghestani et al. [18] and there other models, namely, the mixture of Lindley inverse Weibull distributions (MLIWD), mixture of inverse Weibull and Weibull distributions (MIWWD), one component Lindley distribution, and one component lognormal distribution. All the seven models are fitted to the real data. The results are listed in Table 4. Table 4 shows the MLEs of the parameters of the seven models with their standard errors and values of the KS statistic which is used to assess the similarity between the actual data and the fitted distributions. In the *R* software, the packages (MASS) and (fitdistrplus) are used to calculate the values of KS statistics and their corresponding *R* values for the seven distributions. The loglikelihood function and some criteria that measure the quality of the fitted models such as AIC and BIC criteria are computed. Table 5 gives the results of the variance

Table 5: CIs real data of bladder cancer patients for the MLLND and others models.

Models	Variance-covariance matrix	Parameters	Confidence level 95% Lower	95% Upper	90% Lower	90% Upper
MLLND	$\begin{bmatrix} 0.002769817 & -0.02377380 & 0.003083012 & -0.002329422 - 0.023773805 \\ 0.49176060 & -0.040758408 & 0.0275291510.003083012 & -0.04075841 \\ 0.012532830 & -0.004612044 - 0.002329422 & 0.02752915 & -0.004612044 \\ 0.007266494 & & & \end{bmatrix}$	$p\wedge_1$	0.0642	0.2704	0.0808	0.2538
		$\theta\wedge$	0.5076	3.2562	0.7285	3.0352
		$\mu\wedge$	1.7259	2.1647	1.7611	2.1294
		$\sigma\wedge$	0.6784	1.0127	0.7052	0.9858
MTLD	$\begin{bmatrix} 0.013234095 & 0.0025007524 & 0.00444309000.002500752 \\ 0.0006987247 & 0.00087883810.004443090 & 0.0008788381 \\ 0.0023397156 & & \end{bmatrix}$	$p\wedge_1$	-0.023	0.4277	0.130	0.3914
		$\theta\wedge_1$	0.0394	0.1430	0.0478	0.1347
		$\theta\wedge_2$	0.229	0.4187	0.2444	0.4035
MLIWD	$\begin{bmatrix} 0.004920991 & -0.026698250 & -0.0010711278 & 0.004868889 - 0.026698250 \\ 0.242100512 & 0.0079738493 & -0.034270165 - 0.001071128 & 0.007973849 \\ 0.0004890109 & -0.0011123350.004868889 & -0.034270165 & -0.0011123352 \\ 0.023372212 & & & \end{bmatrix}$	$p\wedge_1$	0.1000	0.3749	0.1221	0.3528
		$\theta\wedge$	0.331	2.2619	0.4882	2.1068
		$\alpha\wedge$	0.1371	0.2237	0.1440	0.2168
		$\beta\wedge$	1.2477	1.8470	1.2959	1.7988
MTWD	$\begin{bmatrix} 0.001923592 & -0.02215016 & -0.005512600 & -0.001879567 & 0.04563591 - 0.022150161 \\ 1.06419567 & 0.066782566 & 0.044848532 & -0.61971134 - 0.005512600 & 0.06678257 \\ 0.063829872 & 0.004559112 & -0.24653248 - 0.001879567 & 0.04484853 & 0.004559112 \\ 0.006593381 & -0.051259900.045635907 & -0.61971134 & -0.246532478 & -0.051259904 \\ 3.72766949 & & & & \end{bmatrix}$	$p\wedge_1$	0.8694	1.0413	0.8832	1.0275
		$\alpha\wedge_1$	6.8323	10.876	7.1574	10.551
		$\alpha\wedge_2$	-0.020	0.9698	0.0591	0.8902
		$\beta\wedge_1$	0.8159	1.1342	0.8415	1.1086
		$\beta\wedge_2$	-1.219	6.3491	-0.610	5.7407
MIWWD	$\begin{bmatrix} 0.0046242796 & 3.494765e-04 & 0.025746042 & -2.986093e-03 & 0.00686686310.0003494765 \\ 2.762975e-04 & 0.002350313 & -3.977995e-05 & 0.00039934530.0257460424 & 2.350313e-03 \\ 0.345648000 & -2.312262e-02 & 0.0740712470 - 0.0029860928 & -3.977995e-05 & -0.023122624 \\ 2.091868e-02 & -0.00572836730.0068668631 & 3.993453e-04 & 0.074071247 & -5.728367e-03 \\ 0.0311504072 & & & & \end{bmatrix}$	$p\wedge_1$	0.6011	0.8677	0.6225	0.8462
		$\alpha\wedge_1$	0.1553	0.2204	0.1605	0.2152
		$\alpha\wedge_2$	0.5929	2.8975	0.7782	2.7122
		$\beta\wedge_1$	1.2373	1.8043	1.2829	1.7587
		$\beta\wedge_2$	0.5436	1.2355	0.5993	1.1799
LND	$\begin{bmatrix} 1.283697e-02 & 2.541429e-062.541429e-06 \\ 6.417786e-03 & \end{bmatrix}$	$\mu\wedge$	1.2890	1.7331	1.3247	1.6974
		$\sigma\wedge$	1.1248	1.4388	1.1500	1.4136
LD	$[0.0001798515]$	$\theta\wedge$	0.1866	0.2392	0.1908	0.2349

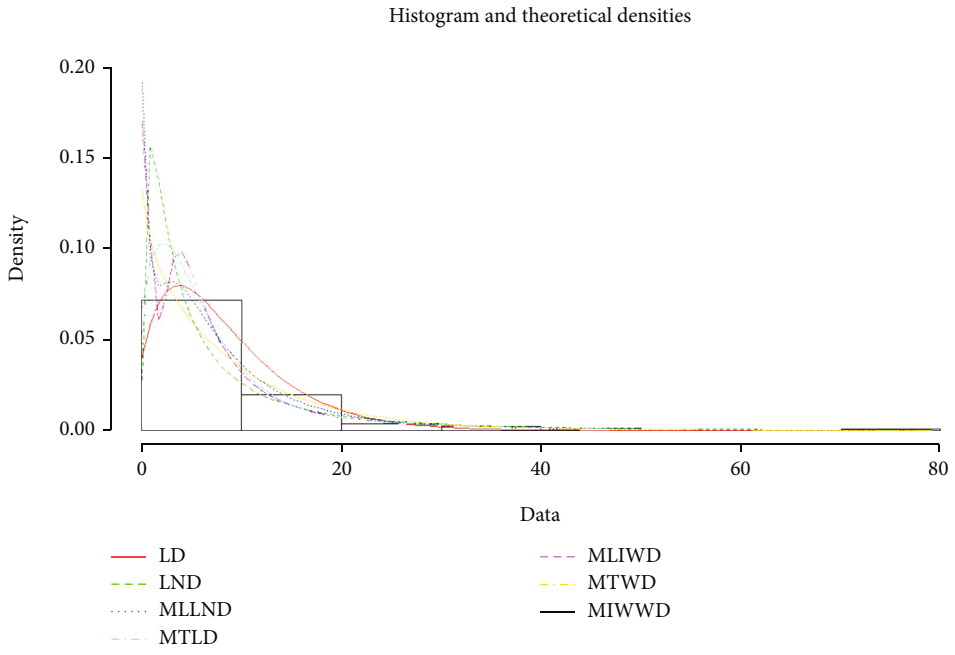

Figure 2: Comparison of different pdfs of the data application.

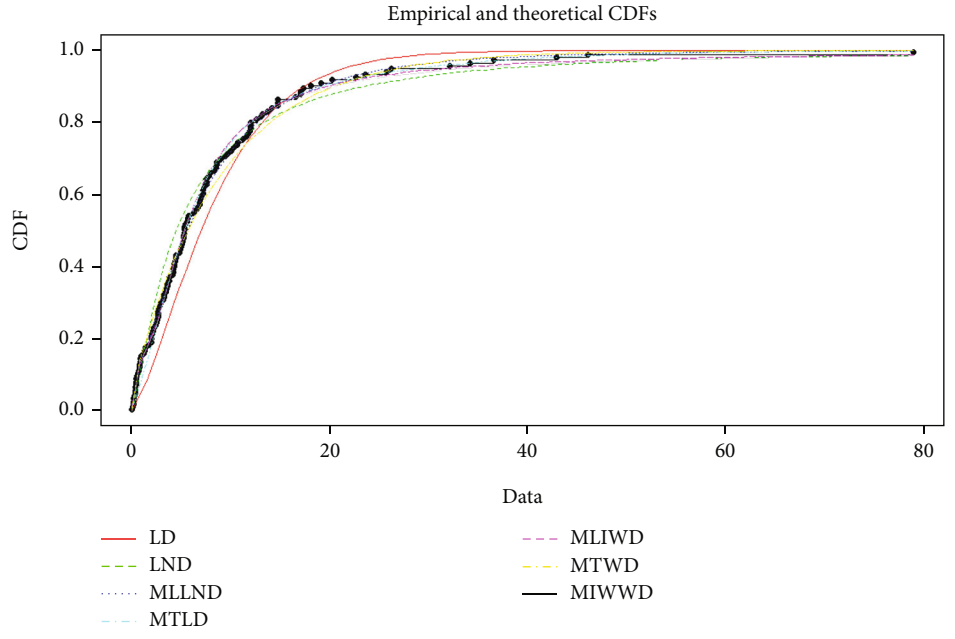

Figure 3: Comparison of different CDFs of the data application.

covariance matrices for the competitive models calculated by the function vcov() in *R* which depends on the package fitdist(). Lower and upper limits of the 95% nd 90% confidence intervals (CIs) for the parameters of the different distributions are also provided. Figure 2 displays the plots of the pdfs of the seven fitted models superimposed on the histogram of the real data set by using the function denscomp() in *R*. The figure shows that the MLLND provides a very good fit for these data compared to other mixtures and one component models. Figure 3 shows the comparisons of the plots of the theoretical cdfs of the fitted distributions to the empirical cdf of the data using the function cdfcomp() in *R*. Again, it is clear that the cdf of the MLLND is closer to the empirical distribution than any other model. Figures 4 and 5 show the pp plots and qq plots for the real data to those of the compared models using the functions ppcomp() and qqcomp(), respectively, in *R*. The plots show the adequency of the proposed model to fit the real data compared to other models.

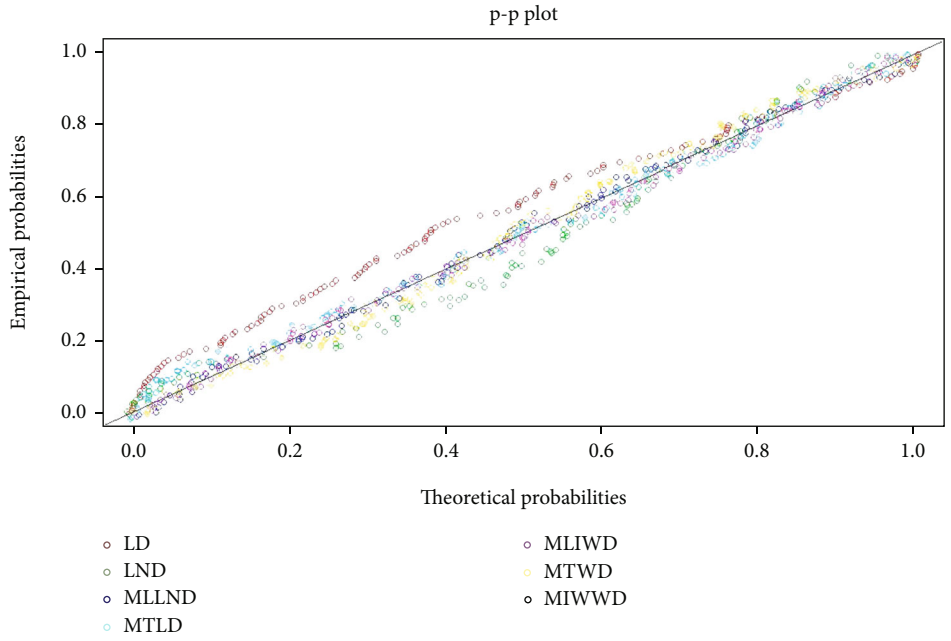

Figure 4: Comparison of different pp plots of the data application.

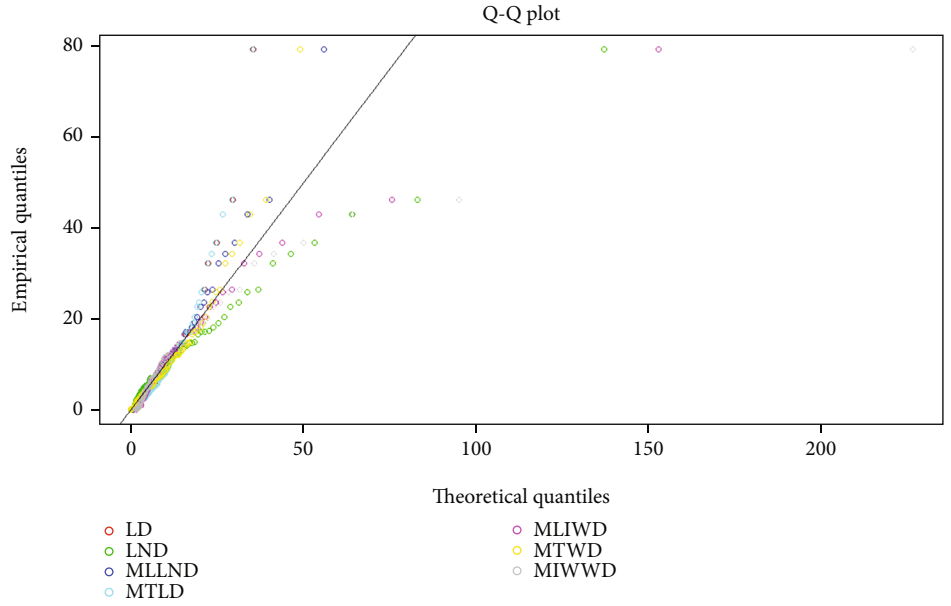

Figure 5: Comparison of different qq plots of the data application.

In short, all the above figures indicate that the MLLND is the perfect fit for the real data set compared to all the competitive models.

6. Concluding Remarks

This paper introduces a new mixture model which is the MLLND to handle heterogeneous data. This model was proposed due to the importance of each of the Lindley and lognormal distributions and their great applications, and so it was expected that mixing these two distributions together would lead to a more flexible model than its components distributions. Some properties of the MLLND were obtained such as the expectation, the mean, variance, the mode (s), median, reliability function, HRF, skewness, kurtosis, and coefficient of variation. The pdf for the minimum and maximum order statistics of the MLLND is presented. Maximum likelihood estimation of the parameters of the model was discussed and estimated via simulation with number of replications 10000 runs. The main objective of this paper was to illustrate the applicability of the proposed distribution compared to six competitive distributions. This was achieved by showing the ability of the model to fit a well-known real data set better than the compared models.

This was done by using the formal test like K-S statistic as well as information criteria and also through graphical procedures such as plots of theoretical and empirical cdfs, pp plots, and qq plots.

Abbreviations

MLLND: Mixture of Lindley and lognormal distributions
MTLD: Mixture of two Lindley distributions
MLIWD: Mixture of Lindley inverse Weibull distributions; mixture of two Weibull distributions (MTWD)
MIWWD: Mixture of inverse Weibull Weibull distributions
LD: One component of Lindley distribution
LND: One component from lognormal distribution
MLEs: Maximum likelihood estimates
LF: Likelihood function
pdf: Probability density function
cdf: Cumulative distribution function
HRF: Hazard rate function
Sk: Coefficient of skewness
Ku: Coefficient of kurtosis
Cv: Coefficient of variation
CIs: Confidence intervals
AIC: Akaike information criterion
KS: Kolmogorov-Smirnov
ECDF: Empirical cumulative distribution function
pp: Probability plot
qq plot: Quantile quantile plot
Std.: Error: standard error
BIC: Bayesian information criterion.

Data Availability

The data used to support the findings of this study have been deposited in the Shanker et al. [26] repository ([doi:10 .15406/bbij.2016.03.00061]).

Conflicts of Interest

The author declares that there is no conflict of interests regarding the publication of this paper.

References

[1] B. S. Everitt and D. J. Hand, *Finite Mixture Distributions*, Chapman & Hall, London, England, 1981.

[2] G. McLachlan and D. Peel, *Finite Mixture Models*, John Wiley & Sons, New York, 2000.

[3] G. J. McLachlan and K. E. Basford, *Mixture Models: Applications to Clustering*, Marcel Dekker, New York, 1988.

[4] D. M. Titterington, A. F. M. Smith, and U. E. Makov, *Statistical Analysis of Finite Mixture Distributions*, John Wiley & Sons, Chichester, England. w Jersey, 1985.

[5] B. G. Lindsay, *Mixture Models: Theory, Geometry and Applications*, The Institute of Mathematical Statistics, Hayward, CA, 1995.

[6] G. J. McLachlan and T. Krishnan, *The EM Algorithm and Extensions*, John Wiley & Sons, New York, 1997.

[7] A. S. Al-Moisheer, K. S. Sultan, and M. A. Al-Shehri, "A Mixture of Inverse Weibull and Inverse Burr Distributions: Properties, Estimation, and Fitting," *Mathematical Problems in Engineering*, vol. 2017, Article ID 7824323, 11 pages, 2017.

[8] A. S. Al-Moisheer, R. M. Alotaibi, G. A. Alomani, and H. Rezk, "Bivariate mixture of inverse Weibull distribution: properties and estimation," *Mathematical Problems in Engineering*, vol. 2020, Article ID 5234601, 12 pages, 2020.

[9] A. S. Al-Moisheer, "Homogeneity tests for Burr III mixture model," *Journal of Computational and Theoretical Nanoscience*, vol. 15, no. 8, pp. 2515–2520, 2018.

[10] A. S. Al-Moisheer, "Sequential test for a mixture of finite exponential distribution," *Journal of Mathematics*, vol. 2021, Article ID 6625853, 10 pages, 2021.

[11] D. V. Lindley, "Fiducial distributions and Bayes' theorem," *Journal of the Royal Statistical Society: Series B*, vol. 20, no. 1, pp. 102–107, 1958.

[12] D. V. Lindley, "Approximate Bayesian methods," *Trabajos de Estadistica Y de Investigacion Operativa*, vol. 31, no. 1, pp. 223–245, 1980.

[13] M. E. Ghitany, B. Atieh, and S. Nadarajah, "Lindley distribution and its application," *Mathematics and Computers in Simulation*, vol. 78, no. 4, pp. 493–506, 2008.

[14] J. S. Kim and B. J. Yum, "Selection between Weibull and lognormal distributions: a comparative simulation study," *Computational Statistics & Data Analysis*, vol. 53, no. 2, pp. 477–485, 2008.

[15] C. T. Lin, S. J. S. Wu, and N. Balakrishnan, "Planning life tests with progressively Type-I interval censored data from the lognormal distribution," *Journal of Statistical Planning and Inference*, vol. 139, no. 1, pp. 54–61, 2009.

[16] A. S. Al-Moisheer, A. F. Daghestani, and K. S. Sultan, "Mixture of two one-parameter Lindley distributions: properties and estimation," *Journal Of Statistical Theory And Practice*, vol. 15, no. 1, 2021.

[17] A. S. Al-Moisheer, A. F. Daghestani, and K. S. Sultan, "Mixture of lindley and inverse Weibull distributions: properties and estimation," *WSEAS Transactions on Mathematics*, vol. 20, pp. 134–143, 2021.

[18] A. F. Daghestani, K. S. Sultan, and A. S. Al-Moisheer, "Mixture of lindley and Weibull distributions: properties and estimation," *Journal of Statistics Applications & Probability*, vol. 10, no. 2, pp. 301–313, 2021.

[19] R. Shanker, S. Sharma, and R. Shanker, "A two-parameter Lindley distribution for modeling waiting and survival times data," *Applied Mathematics*, vol. 4, no. 2, pp. 363–368, 2013.

[20] E. L. Crow and K. Shimizu, Eds., *The Lognormal Distribution*, Marcel Dekker, New York, 1988.

[21] N. L. Johnson, S. Kotz, and N. Balakrishnan, *Continuous Univariate Distributions, Vol. 1*, John Wiley & Sons, New York, 2nd edition, 1994.

[22] E. K. Al-Hussaini and K. S. Sultan, "Reliability and hazard based on finite mixture models," in *Handbook of Statistics-Vol. 20*, N. Balakrishnan and C. R. Rao, Eds., pp. 139–183, Elsevier, Amsterdam, 2001.

[23] K. S. Sultan, *Mixtures of lognormal distributions, [Ph.D. thesis]*, University of Assiut, Egypt, 1991.

[24] K. S. Sultan and A. S. Al-Moisheer, "Mixture of Inverse Weibull and Lognormal Distributions: Properties, Estimation, and Illustration," *Mathematical problems in Engineering*, vol. 2015, Article ID 526786, 8 pages, 2015.

[25] R. Shanker, H. Fesshaye, and S. Selvaraj, "On modeling of life-time data using one parameter Akash, Lindley and exponential distributions," *Biometrics & Biostatistics International Journal*, vol. 3, no. 2, 2016.

[26] E. T. Lee and J. W. Wang, *Statistical Methods for Survival Data Analysis*, John Wiley & Sons, Incorporated, Hoboken, New Jersey, 2003.

Hindawi
Journal of Function Spaces
Volume 2021, Article ID 1148618, 12 pages
https://doi.org/10.1155/2021/1148618

Research Article

Modelling to Engineering Data Using a New Class of Continuous Models

I. Elbatal and Naif Alotaibi

Department of Mathematics and Statistics-College of Science,
Imam Mohammad Ibn Saud Islamic University (IMSIU), Saudi Arabia

Correspondence should be addressed to I. Elbatal; iielbatal@imamu.edu.sa

Received 6 October 2021; Accepted 30 October 2021; Published 24 November 2021

Academic Editor: Badr Saad. T. Alkaltani

In this paper, a new flexible generator of continuous lifespan models referred to as the Topp-Leone Weibull G (TLWG) family is developed and studied. Several mathematical characteristics have been investigated. The new hazard rate of the new model can be "monotonically increasing," "monotonically decreasing," "bathtub," and "**J** shape." The Farlie Gumbel Morgenstern (FGM) and the modified FGM (MFGM) families and Clayton Copula (CCO) are used to describe and display simple type Copula. We discuss the estimation of the model parameters by the maximum likelihood (MLL) estimations. Simulations are carried out to show the consistency and efficiency of parameter estimates, and finally, real data sets are used to demonstrate the flexibility and potential usefulness of the proposed family of algorithms by using the TLW exponential model as example of the new suggested family.

1. Introduction and Motivation

There has already been a great emphasis on building more flexible distributions in the recent past. To simulate real-life data in various practical disciplines, including finance, engineering, medical sciences, biological research, environmental studies, and insurance, over the last few decades, a variety of G families of distributions has been constructed and researched. We have generated numerous kinds of distributions by generalizing G families. With these new families, at least one shape parameter is merged with the baseline one, allowing for greater versatility, for instance, the generalized transmuted exponentiated G [1], Weibull (W) G (WG) [2], the Burr type X-G by [3], Type II half logistic G [4], exponentiated transmuted G by [5], a new compound G family [6], the beta W G by [7], the generalized odd W G [8], the transmuted W G by [9], a new W G [10], TL G [11], a special generalized mixture class of probabilistic models [12], sine Topp-Leone G [13], Type 2 power Topp-Leone G [14], a new version of Power Topp-Leone G [15], and Type 2 generalized Topp-Leone G [16], among others.

According to [11], the cumulative distribution function (CDF) of the TL G (TLG) class could well be found with

$$F_\alpha(z) = \left[1 - \bar{G}^2_{\underline{\Phi}}(z)\right]^\alpha = G^\alpha_{\underline{\Phi}}(z)\left[2 - G_{\underline{\Phi}}(z)\right]^\alpha, \quad (1)$$

where $G_{\underline{\Phi}}(z)$ refers to the CDF of the baseline model, and the corresponding density function (PDF) of (1) can be derived as

$$f_\alpha(z) = 2\alpha g_{\underline{\Phi}}(z)\left[1 - \bar{G}^2_{\underline{\Phi}}(z)\right]^{\alpha-1}\bar{G}_{\underline{\Phi}}(z), \quad (2)$$

where $G_{\underline{\Phi}}(z) = dG_{\underline{\Phi}}(z)/dz$ refers to the PDF of the baseline model. According to [2], the WG family's CDF may be computed via

$$G_{\underline{\Phi}}(z) = G_\beta(z) = 1 - \exp\left[-O_{\underline{\Phi}}(z)^\beta\right], \quad (3)$$

where $O_{\underline{\Phi}}(z) = G_{\underline{\Phi}}(z)/\bar{G}_{\underline{\Phi}}(z)$ and $\bar{G}_{\underline{\Phi}}(z) = 1 - G_{\underline{\Phi}}(z)$. Then,

Table 1: Special cases.

Baseline	New model	Corresponding CDF
E	*TLWE*	$\left\{1-\exp\left[-2(\exp(\theta z)-1)^{\beta}\right]\right\}^{\alpha}$
W	*TLWW*	$\left[1-\exp\left(-2\left\{\exp\left[(\theta z)^{b}\right]-1\right\}^{\beta}\right)\right]^{\alpha}$
Lx	*TLWLx*	$\left(1-\exp\left\{-2\left[\left[1+\left(\frac{z}{b}\right)\right]^{\theta}-1\right]^{\beta}\right\}\right)^{\alpha}$
BX	*TLWBX*	$\left\{1-\exp\left[-2\left(\left\{1-\exp\left[-\left(\frac{z}{\theta}\right)^{2}\right]\right\}^{-b}-1\right)^{-\beta}\right]\right\}^{\alpha}$
LL	*TLWLL*	$\left\{1-\exp\left[-2\left(\frac{z}{\theta}\right)^{b\beta}\right]\right\}^{\alpha}$
L	*TLWL*	$\left(1-\exp\left\{-2\left[\left(\frac{1+\theta+\theta z}{1+\theta}\right)^{-1}-1\right]^{\beta}\right\}\right)^{\alpha}$

using (3) and (1), the CDF of the TL W G (TLWG) class may indeed be expressed via

$$F_{\alpha,\beta,\underline{\Phi}}(z)=\left\{1-\exp\left[-2O_{\underline{\Phi}}(z)^{\beta}\right]\right\}^{\alpha}. \tag{4}$$

The corresponding PDF is

$$f_{\alpha,\beta,\underline{\Phi}}(z)=2\alpha\beta g_{\underline{\Phi}}(z)\exp\left[-2O_{\underline{\Phi}}(z)^{\beta}\right]\frac{G_{\underline{\Phi}}(z)^{\beta-1}}{\bar{G}_{\underline{\Phi}}(z)^{\beta+1}}\left\{1-\exp\left[-2O_{\underline{\Phi}}(z)^{\beta}\right]\right\}^{\alpha-1}. \tag{5}$$

The hazard rate function (HRF) can be easily derived using $h_{\alpha,\beta,\underline{\Phi}}(z)=f_{\alpha,\beta,\underline{\Phi}}(z)/[1-F_{\alpha,\beta,\underline{\Phi}}(z)]$. The function $h_{\alpha,\beta,\underline{\Phi}}(z)$ is called the failure rate of $F_{\alpha,\beta,\underline{\Phi}}(z)$ and often referred to as the rate function or the intensity function or failure rate or instantaneous failure rate; in actuarial mathematics, it is named the "force of mortality," and in demographic disciplines, it is called the "mortality rate." It represents the failure intensity of an x-year-old equipment. It denotes the likelihood of an operational item failing in the next time period or the likelihood of a failure in a tiny unit interval of time $(z, z+\Delta z]$ given that no failure has occurred in $[0, z]$ and satisfies $h_{\alpha,\beta,\underline{\Phi}}(z)>0$ and $\int_0^{\infty}h_{\alpha,\beta,\underline{\Phi}}(z)dx=0$. The HRF is critical because it intuitively translates as the level of risk associated with an object that has lived to time x. In life (death) tables, $h_{\alpha,\beta,\underline{\Phi}}(z)$ is approximated by the probability that a certain individual of age x will die during the next year. Some notions of aging refer to the HR such as $h'_{\alpha,\beta,\underline{\Phi}}(z)>0$ means positive aging, $h'_{\alpha,\beta,\underline{\Phi}}(z)=0$ means no aging, and $h'_{\alpha,\beta,\underline{\Phi}}(z)<0$ means negative aging. The idea of aging in statistical lifetime and reliability analysis does not imply that the unit grows older in the sense of time. Rather, it is a concept associated with residual life.

2. Important Expansions

Take a look at the binomial series expansion provided as

$$\left(1-\frac{a_1}{a_2}\right)^{a_3-1}=\sum_{l=0}^{\infty}(-1)^{l}\binom{a_3-1}{l}\left(\frac{a_1}{a_2}\right)^{l}\Bigg|_{(b>0\text{ and }|a_1/a_2|<1)}. \tag{6}$$

Then, the PDF in (5) can be expressed as

$$f_{\alpha,\beta,\underline{\Phi}}(z)=2\alpha\beta g_{\underline{\Phi}}(z)\frac{G_{\underline{\Phi}}(z)^{\beta-1}}{\bar{G}_{\underline{\Phi}}(z)^{1+\beta}}\sum_{l=0}^{\infty}(-1)^{l}\binom{\alpha-1}{l}\underbrace{\exp\left[-2(1+l)O_{\underline{\Phi}}(z)^{\beta}\right]}_{A(z,\beta,\underline{\Phi})}. \tag{7}$$

Applying the power series expansion to $A(z)$, we have

$$\mathrm{A}(\mathrm{z},\beta,\underline{\Phi})=\sum_{\mathrm{l}=0}^{\infty}\frac{1}{\mathrm{l}!}[-2(1+\mathrm{l})]^{\mathrm{l}}\mathrm{O}_{\underline{\Phi}}(\mathrm{z})^{\beta\mathrm{l}}, \tag{8}$$

where $O_{\underline{\Phi}}(z)^{\beta d}=G_{\underline{\Phi}}(z)^{\beta d}/\bar{G}_{\underline{\Phi}}(z)^{\beta d}$. Then,

$$f_{\alpha,\beta,\underline{\Phi}}(z)=2\alpha\beta\sum_{l,d=0}^{\infty}\frac{1}{d!}(-1)^{l+d}[2(1+l)]^{d}\binom{\alpha-1}{l}g_{\underline{\Phi}}(z)\frac{G_{\underline{\Phi}}(z)^{(1+d)\beta-1}}{\bar{G}_{\underline{\Phi}}(z)^{(1+d)\beta+1}}, \tag{9}$$

but $\bar{G}_{\underline{\Phi}}(z)^{-(1+d)\beta-1}=\sum_{k=0}^{\infty}\binom{\beta(d+1)+1}{k}G_{\underline{\Phi}}(z)^{k}$. Then, the $f_{\alpha,\beta,\underline{\Phi}}(z)$ can be written as

$$f_{\alpha,\beta,\underline{\Phi}}(z)=\sum_{l,d,k=0}^{\infty}v_{(l,d,k)}\,h_{\beta^{*}}(z)\Bigg|_{(\beta^{*}=\beta(1+d)+k)}, \tag{10}$$

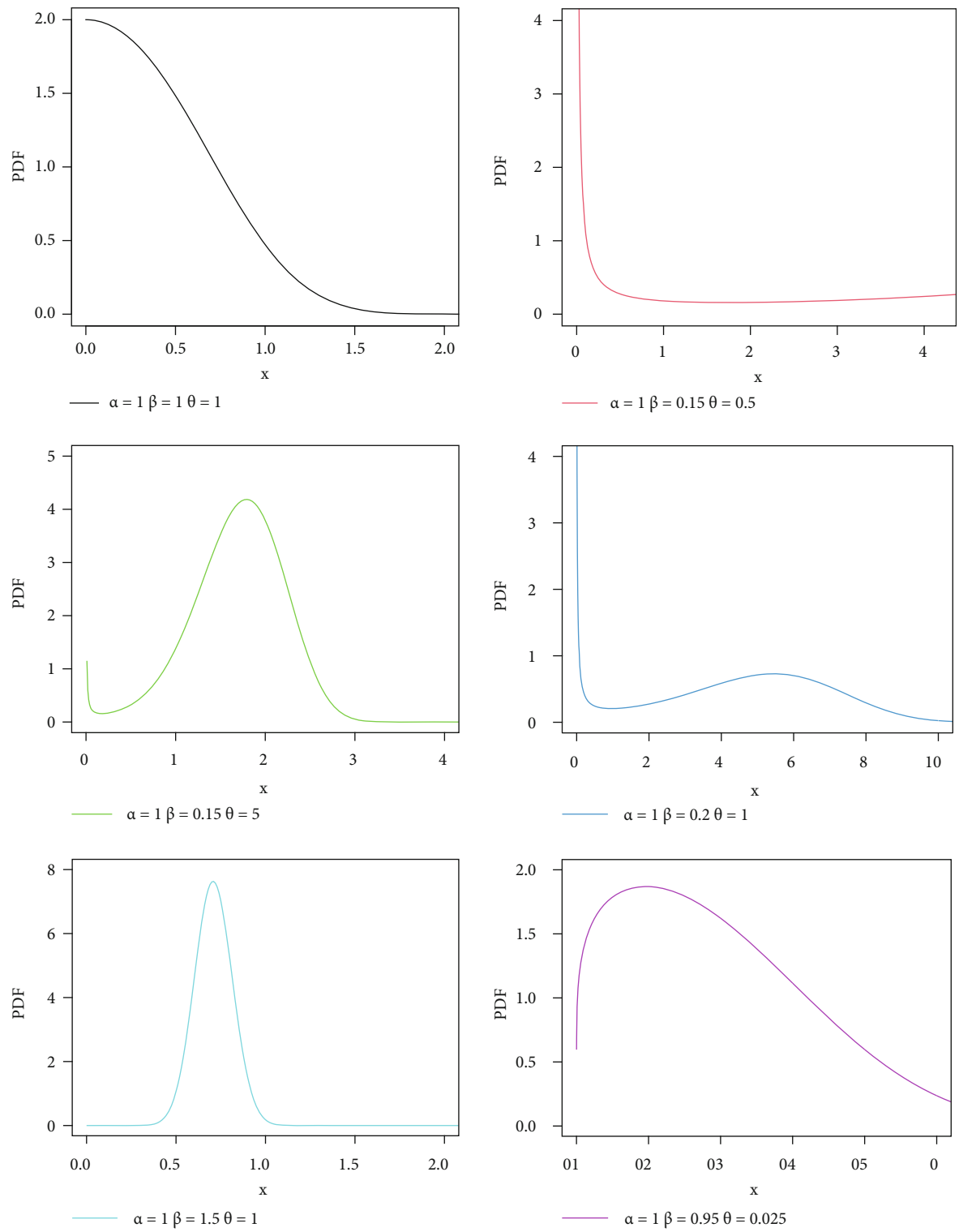

Figure 1: Plots illustrating the PDF of the TLWE model.

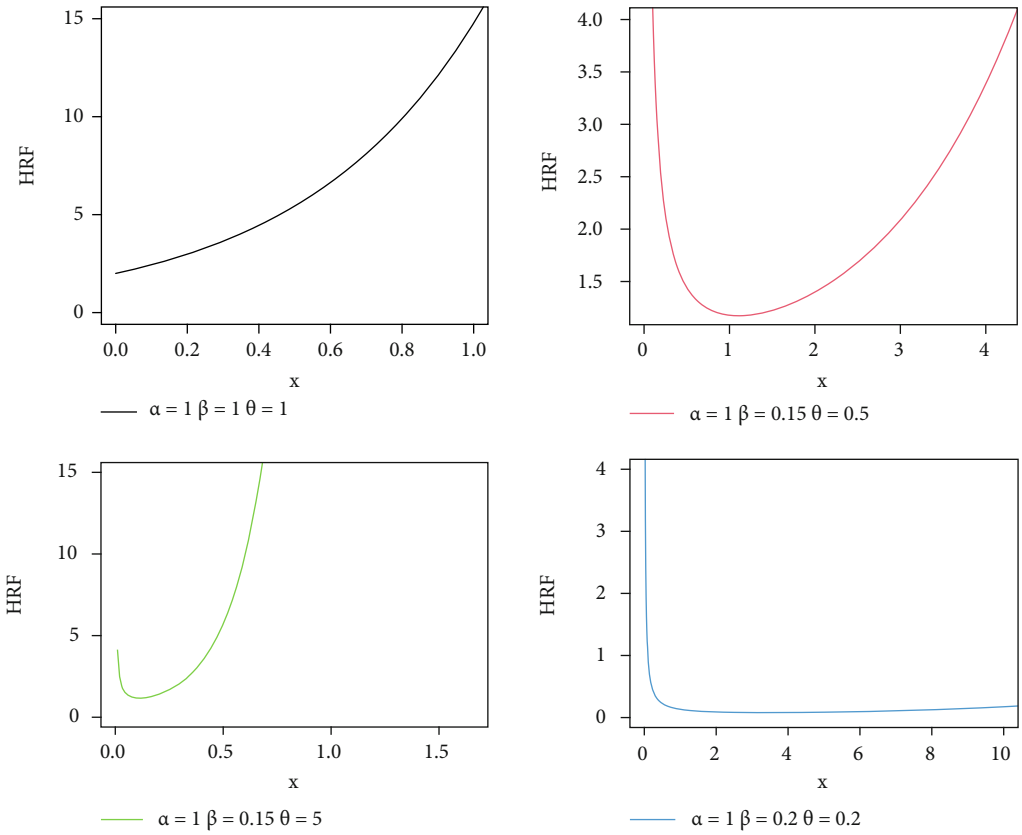

Figure 2: HRF graphs for the TLWE model.

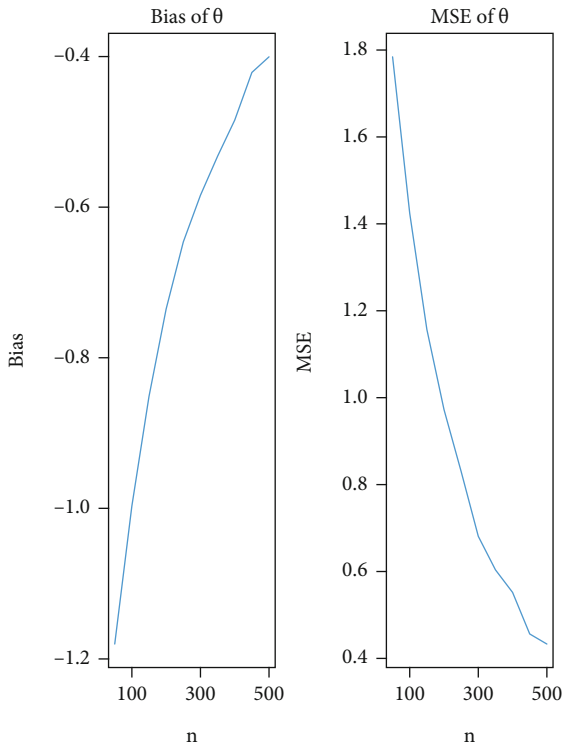

Figure 3: Biases and MSEs for the parameter α.

where

$$v_{(l,d,k)} = 2\alpha\beta \sum_{l,d,k=0}^{\infty} (-1)^{l+d} \binom{\alpha-1}{l} \binom{\beta(d+1)+1}{k} \frac{[2(l+1)]^d}{d!\beta^*}, \tag{11}$$

and $h_{\beta^*}(z) = \beta^* g_{\underline{\Phi}}(z) G_{\underline{\Phi}}(z)^{\beta^*-1}$ depicts the PDF of the exponentiated G (ExG) distribution with parameter β^*.

3. Copula

3.1. Via FGM Family. Starting with the joint CDF for the FGM family of random variables (RVrs) (Z_1, Z_2) where $F_\lambda(u,w)|_{(|\lambda|\le 1)} = uw(1+\lambda\bar{u}\bar{w})$, let

$$\begin{aligned} u &= F_{\alpha_1,\beta_1,\underline{\Phi}}(z_1) = \left\{1 - \exp\left[-2O_{\underline{\Phi}}(z_1)^{\beta_1}\right]\right\}^{\alpha_1}, \\ w &= F_{\alpha_2,\beta_2,\underline{\Phi}}(z_2) = \left\{1 - \exp\left[-2O_{\underline{\Phi}}(z_2)^{\beta_2}\right]\right\}^{\alpha_2}, \end{aligned} \tag{12}$$

where $O_{\underline{\Phi}}(z_1) = G_{\underline{\Phi}}(z_1)/\bar{G}_{\underline{\Phi}}(z_1)$ and $O_{\underline{\Phi}}(z_2) = G_{\underline{\Phi}}(z_2)/\bar{G}_{\underline{\Phi}}(z_2)$; then, we have a $(5+\underline{\Phi})$ dimension parameter family

$$\begin{aligned} F_\lambda(z_1,z_2) = {} & \left\{1 - \exp\left[-2O_{\underline{\Phi}}(z_1)^{\beta_1}\right]\right\}^{\alpha_1} \left\{1 - \exp\left[-2O_{\underline{\Phi}}(z_2)^{\beta_2}\right]\right\}^{\alpha_2} \\ & \times \left\{1 + \begin{bmatrix} \lambda\left(1 - \left\{1 - \exp\left[-2O_{\underline{\Phi}}(z_1)^{\beta_1}\right]\right\}^{\alpha_1}\right) \\ \times \left(1 - \left\{1 - \exp\left[-2O_{\underline{\Phi}}(z_2)^{\beta_2}\right]\right\}^{\alpha_2}\right) \end{bmatrix}\right\}. \end{aligned} \tag{13}$$

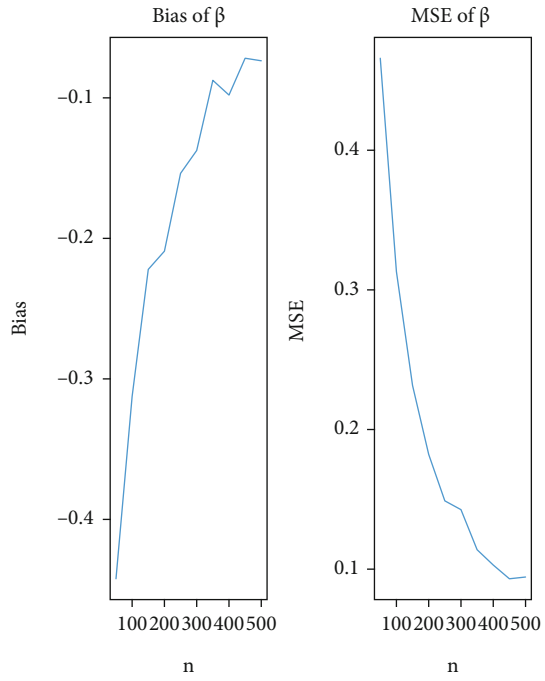

Figure 4: Biases and MSEs for the parameter β.

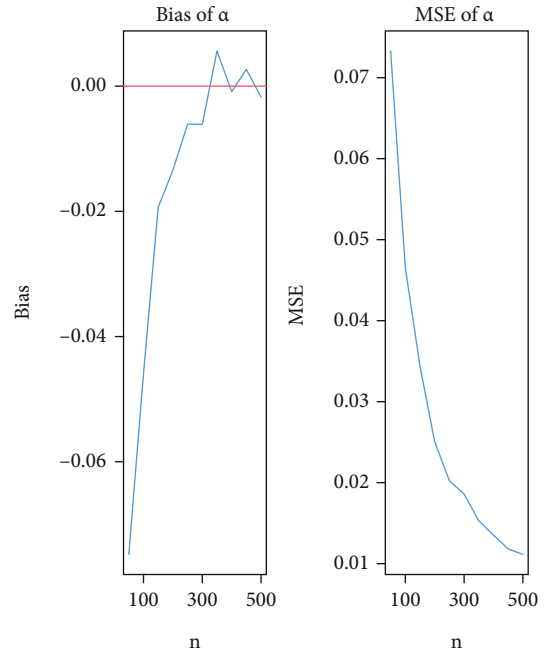

Figure 5: Biases and MSEs for the parameter θ.

3.2. Via MFGM Copula. As an example, take the MFGM Copula (see [17–22])

$$C_\tau(u,v)|_{\tau\in[-1,1]} = uv[1+\tau\Phi(u)\Psi(v)] = uv+\tau\dot{\Phi}(u)\dot{\Psi}(v), \tag{14}$$

where $\dot{\Phi}(u) = u\Phi(u)$ and $\dot{\Psi}(v) = v\Psi(v)$. Where $\Phi(u)$ and $\Psi(v)$ are two absolutely continuous CDFs on $(0,1)$ where $\Phi(0) = \Psi(0) = \Phi(1) = \Psi(1) = 0$, let

$$\begin{aligned}\varepsilon &= \ln f\left\{\frac{\partial\dot{\Phi}(u)}{\partial u|_{C_1}}\right\} < 0, \beta = \sup\left\{\frac{\partial\dot{\Phi}(u)}{\partial u|_{C_1}}\right\} < 0,\\ \xi &= \ln f\left\{\frac{\partial\dot{\Psi}(v)}{\partial v|_{C_2}}\right\} > 0, \eta = \sup\left\{\frac{\partial\dot{\Psi}(v)}{\partial v|_{C_2}}\right\} > 0.\end{aligned} \tag{15}$$

Then, $mln(\varepsilon\beta, \xi\eta) \geq 1$, where $\partial\dot{\Phi}(u)/\partial u = \Phi(u) + (u\partial\Phi(u)/\partial u)$,

$$\begin{aligned}C_1 &= \left\{u \mid u\in(0,1), \frac{\partial\dot{\Phi}(u)}{\partial u} \text{ exists}\right\},\\ C_2 &= \left\{v \mid v\in(0,1), \frac{\partial\dot{\Psi}(v)}{\partial v} \text{ exists}\right\}.\end{aligned} \tag{16}$$

Type I MFGM:
Consider $\Phi(u)$ and $\Psi(v)$ as defined above, then

$$\begin{aligned}C_\tau(u,v) = \tau\left[\dot{\Phi}(u)\dot{\Psi}(v)\right] + \left(\left\{1-\exp\left[-2O_{\underline{\Phi}}(u)^{\beta_1}\right]\right\}^{\alpha_1}\right.\\ \left.\times\left\{1-\exp\left[-2O_{\underline{\Phi}}(v)^{\beta_2}\right]\right\}^{\alpha_2}\right),\end{aligned} \tag{17}$$

where

$$\begin{aligned}\dot{\Phi}(u) &= u\left(1-\left\{1-\exp\left[-2O_{\underline{\Phi}}(u)^{\beta_1}\right]\right\}^{\alpha_1}\right),\\ \dot{\Psi}(v) &= v\left(1-\left\{1-\exp\left[-2O_{\underline{\Phi}}(v)^{\beta_2}\right]\right\}^{\alpha_2}\right).\end{aligned} \tag{18}$$

Type II MFGM:
Let

$$\begin{aligned}\Phi(u)|_{(\tau_1>0)} &= u^{\tau_1}(1-u)^{1-\tau_1},\\ \Psi(v)|_{(\tau_2>0)} &= v^{\tau_2}(1-v)^{1-\tau_2}.\end{aligned} \tag{19}$$

Then, the corresponding bivariate Copula can be derived directly from

$$C_{\tau,\tau_1,\tau_2}(u,v) = uv\left[1+\tau u^{\tau_1}v^{\tau_2}(1-u)^{1-\tau_1}(1-v)^{1-\tau_2}\right]. \tag{20}$$

Type III MFGM:
The CDF of the bivariate Type **III** MFGM model can be derived from

$$C_\tau(u,w) = uF^{-1}(w) + wF^{-1}(u) - F^{-1}(u)F^{-1}(w), \tag{21}$$

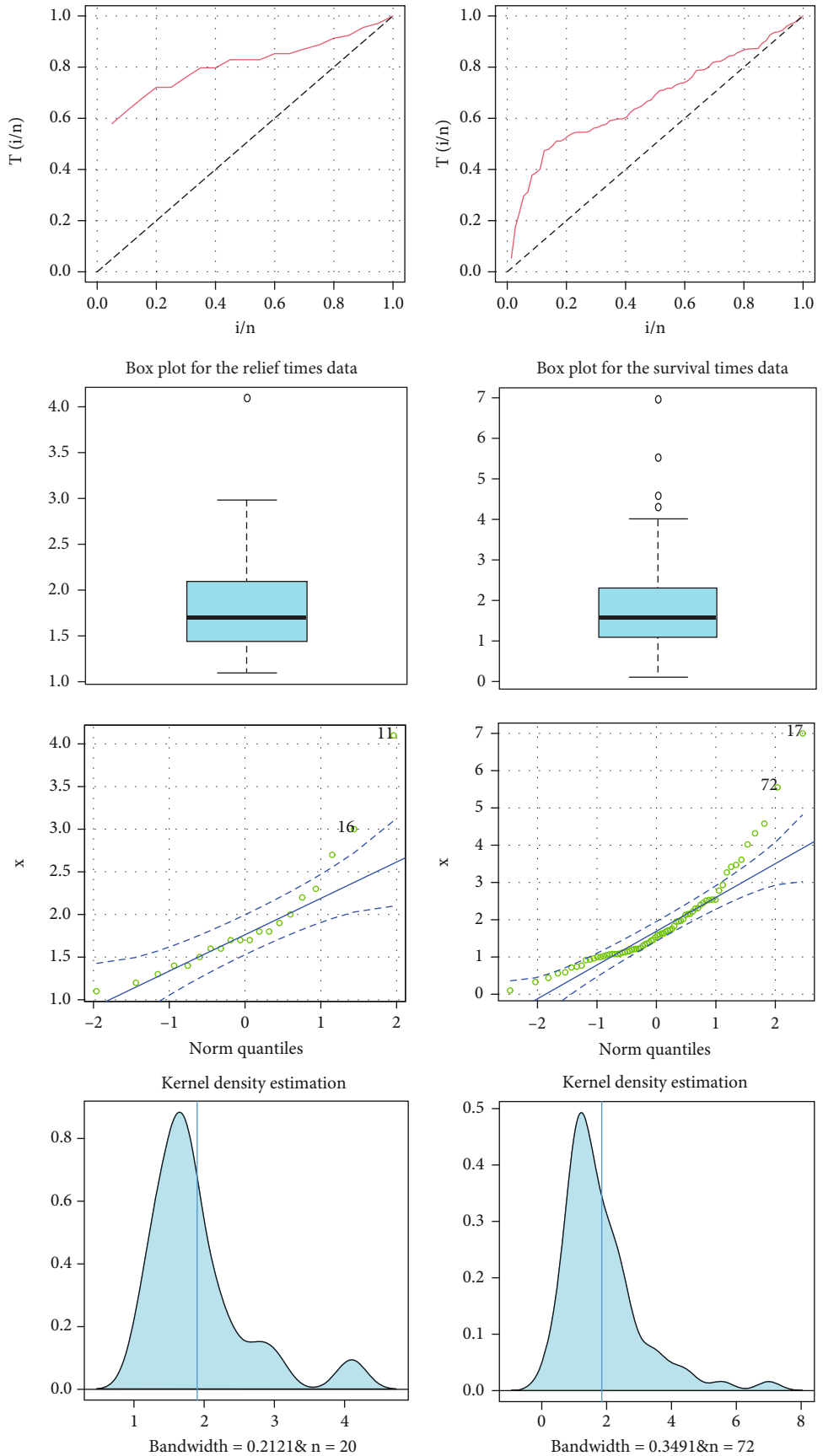

Figure 6: TTT plots, box plots, Q-Q plots, and KDE for the two real data sets.

Table 2: MLLEs, SErs, and C.I. (in parentheses) values for the relief time data.

Models	Estimates, SEs, and C.I.s
$E(\theta)$	0.5261 (0.1172) (0.3, 0.8)
ME(θ)	0.950 (0.150) (0.7, 1.2)
LBHE(θ)	0.5263 (0.118) (0.4, 0.6)
OLE(θ)	0.6044 (0.0535) (0.5, 0.7)
BrXE(a, θ)	1.1635, 0.321 (0.33), (0.03) (0.5, 1.8), (0.26,0.4)
MOE(α, θ)	54.47, 2.32 (35.58), (0.37) (0, 124.2), (1.58, 3.0)
TLWE(α, β, θ)	8.03, 1.58, 3.15 (4.22), (1.01), (0.025) (0, 16.5), (0, 3.6), (3.1, 3.2)
BE(α, β, θ)	81.633, 0.542, 3.514 (120.41), (0.327), (1.410) (0, 317.63), (0, 1.18), (0.75, 6.3)
KwE(α, β, θ)	83.756, 0.568, 3.330 (42.361), (0.326), (1.188) (0.7, 167), (0, 1.2), (1.00, 5.7)
GMOE(λ, α, θ)	0.519, 89.462, 3.169 (0.256), (66.278), (0.77) (0.02, 1.02), (0, 219.4), (1.66, 4.7)
KwMOE($\alpha, \beta, \lambda, \theta$)	8.868, 34.826, 0.299, 4.899 (9.15), (22.31), (0.24), (3.18) (10.9, 46.8), (0, 78.6), (0, 0.76), (0, 11)
MOKwE($\alpha, \beta, \lambda, \theta$)	0.133, 33.232, 0.571, 1.669 (0.332), (57.84), (0.72), (1.81) (0, 0.8), (0, 146.6), (0, 2), (0, 5.2)

Table 3: MLLEs, SErs, and C.I. (in parentheses) values for the survival time data.

Models	Estimates, SEs, and C.I.s
$E(b)$	0.540 (0.063) (0.4, 0.7)
OLE(θ)	0.38145 (0.021) (0.3, 0.4)
ME(θ)	0.9250 (0.080) (0.62, 1.08)
LBHE(θ)	0.542 (0.06) (0.41, 0.68)
BrXE(a, θ)	0.480, 0.2060 (0.061), (0.012) (0.4, 0.5), (0.18, 0.23)
MOE(α, θ)	8.780, 1.380 (3.555), (0.193) (1.81,15.74), (1.0,1.80)
TLWE(α, β, θ)	3.225, 1.55, 0.018 (0.85), (0.25), (0.059) (1.5, 4.9), (1, 2), (0, 0.136)
GMOE(λ, α, θ)	0.179, 47.635, 4.470 (0.07), (44.901), (1.327) (0.04, 0.3), (0, 14), (2, 7)
KwE(a, β, θ)	3.3039, 1.101, 1.038 (1.120), (0.763), (0.615) (1.12, 5.53), (0, 2.62), (0, 2.24)
MOKE($\alpha, \beta, \lambda, \theta$)	0.008, 2.716, 1.986, 0.099 (0.002), 1.316), (0.784), (0.048) (0.004,0.010), (0.14, 5), (0.4, 4), (0, 0.2)

where

$$F^{-1}(u) = G^{-1}\left\{\frac{\left[-1/2\log\left(1-u^{1/\alpha_1}\right)\right]^{1/\beta_1}}{1+\left[-1/2\log\left(1-u^{1/\alpha_1}\right)\right]^{1/\beta_1}}\right\},$$
$$F^{-1}(w) = G^{-1}\left\{\frac{\left[-1/2\log\left(1-u^{1/\alpha_2}\right)\right]^{1/\beta_2}}{1+\left[-1/2\log\left(1-u^{1/\alpha_2}\right)\right]^{1/\beta_2}}\right\}. \tag{22}$$

3.3. Via CCO. The CCO is a weighted variant of the CCO, which has the following form:

$$C(u, w) = \left[u^{-\tau} + v^{-\tau} - 1\right]^{-\tau^{-1}}. \tag{23}$$

Then, setting

$$u = u_{\alpha_1,\beta_1,\underline{\Phi}}(z_1) = \left\{1 - \exp\left[-2O_{\underline{\Phi}}(z)^{\beta_1}\right]\right\}^{\alpha_1},$$
$$w = w_{\alpha_2,\beta_2,\underline{\Phi}}(z_2) = \left\{1 - \exp\left[-2O_{\underline{\Phi}}(y)^{\beta_2}\right]\right\}^{\alpha_2}, \tag{24}$$

Table 4: Statistic for the relief time data.

Models	(D2), D1	C_1	C_2	C_3, C_4, C_5, C_6
E	(0.004), 0.4	4.60	0.96	68.0, 68.7, 67.9, 68.0
KwE	(0.86), 0.14	0.45	0.07	42.0, 44.8, 43.3, 42.3
BrXE	(0.17), 0.25	1.33	0.24	48.1, 50.1, 49.0, 48.5
MOE	(0.55), 0.18	0.80	0.14	43.5, 45.5, 44.2, 43.9
GMOE	(0.78), 0.15	0.51	0.08	42.8, 45.7, 44.3, 43.3
KMOE	(0.86), 0.15	1.08	0.19	43.0, 46.8, 45.6, 43.6
MOKE	(0.87), 0.14	0.60	0.11	41.6, 45.5, 44.3, 42.3
OLE	(<0.1%), 0.9	1.30	0.22	49.1, 50.1, 49.3, 49.3
BE	(0.80), 0.16	0.70	0.12	43.5, 46.5, 44.9, 44.0
ME	(0.07), 0.32	2.76	0.53	54.3, 55.3, 54.5, 54.5
LBHE	(<0.1%), 0.4	0.62	0.11	67.7, 68.7, 67.9, 67.8
TLWE	(0.952), 0.10	0.36	0.040	41.35, 41.14, 41.39, 40.15

Table 5: Statistic for the survival time data.

Models	(D2), D1	C_1	C_2	C_3, C_4, C_5, C_6
E	(0.060), 0.27	6.53	1.25	234.6, 236.9, 234.7, 235.5
MOKE	(0.440), 0.10	0.79	0.12	209.4, 218.6, 210.0, 213.0
OLE	(<0.1%), 0.49	1.94	0.33	229.1, 231.4, 229.2, 230.0
ME	(0.130), 0.14	1.52	0.25	210.4, 212.7, 210.5, 211.3
LBHE	(<0.1%), 0.28	0.79	0.19	235.0, 237.0, 235.0, 236.0
GMOE	(0.811), 0.09	1.02	0.16	210.5, 217.4, 211.0, 213.2
KwE	(0.500), 0.09	0.74	0.11	209.4, 216.2, 209.8, 212.1
BrXE	(0.002), 0.22	2.90	0.52	235.3, 239.9, 235.5, 237.1
MOE	(0.430), 0.10	1.20	0.17	210.4, 215.0, 210.5, 212.2
TLWE	(0.770), 0.066	0.75	0.12	208.6, 212.2, 207.6, 210.2

where

$$\mathrm{O}_{\underline{\Phi}}(\mathrm{y}) = \frac{\mathrm{G}_{\underline{\Phi}}(\mathrm{y})}{\bar{\mathrm{G}}_{\underline{\Phi}}(\mathrm{y})}. \tag{25}$$

Then,

$$H(z,y) = \left(\left\{1-\exp\left[-2O_{\underline{\Phi}}(z)^{\beta_1}\right]\right\}^{-\tau\alpha_1} + \left\{1-\exp\left[-2O_{\underline{\Phi}}(y)^{\beta_2}\right]\right\}^{-\tau\alpha_2} - 1\right)^{-\tau^{-1}}. \tag{26}$$

A simple d-dimensional expansion of the above will be as follows:

$$H(z_1, z_2, \cdots, z_d) = \left(\sum_{l=1}^{d}\left\{1-\exp\left[-2O_{\underline{\Phi}}(z_l)^{\beta_l}\right]\right\}^{-\tau\alpha_l} + 1 - d\right)^{-\tau^{-1}}. \tag{27}$$

Recently, many new articles are allocated to study some of these types, see [23, 24].

4. Structural Properties of the TLWG Family

4.1. Quantile Function. The TLWG quantile function (QuF), say $z = Q(u)$, might be obtained by filliping (4); we have

$$z = Q(u) = G^{-1}\left\{\frac{\left[-1/2\log\left(1-u^{1/\alpha}\right)\right]^{1/\beta}}{1+\left[-1/2\log\left(1-u^{1/\alpha}\right)\right]^{1/\beta}}\right\}. \tag{28}$$

We can easily generate z by taking u as a uniform RVr in $(0,1)$.

4.2. Moments. The r^{th} moment (MO) of TLWG could be acquired in the prescribed sequence:

$$\mu_r^{/} = \int_0^{\infty} z^r f(z)dz = \sum_{l,d,k=0}^{\infty} v_{(l,d,k)}\, I_{(0,\infty)}(\beta^*), \tag{29}$$

where $I_{(0,\infty)}(\beta^*) = \int_0^{\infty} z^r h_{\beta^*}(z)dz$ is the r^{th} moment of the ExG model using parameter β^*.

4.3. Conditional Moments. The s^{th} lower and upper incomplete MOs (ICMOs) of Z characterized features $\upsilon_s(t) = E(Z^s|_{(Z<t)}) = \int_0^t z^s f(z)dz$ and $\zeta_s(t) = E(Z^s|_{(Z>t)}) = \int_t^{\infty} z^s f(z)dz$, respectively, for just about every real $s>0$. The s^{th} lower ICMO of TLWG is

$$\upsilon_s(t) = \int_0^t z^s f(z)dz = \sum_{l,d,k=0}^{\infty} v_{(l,d,k)}\, I_{(0,t)}(\beta^*, s, t), \tag{30}$$

where $I_{(0,t)}(\beta^*, s, t) = \int_0^t z^s h_{\beta^*}(z)dz$ is the s^{th} lower ICMO of ExG model with exponential parameter β^*. Similarly, the s^{th} upper ICMO of TLWG is

$$\zeta_s(t) = \int_t^{\infty} z^s f(z)dz = \sum_{l,d,k=0}^{\infty} v_{(l,d,k)}\, I_{(t,\infty)}(\beta^*, s, t), \tag{31}$$

where $I_{(t,\infty)}(\beta^*, s, t) = \int_t^{\infty} z^s h_{\beta^*}(z)dz$ is the s^{th} upper ICM of ExG model with exponential parameter β^*.

4.4. Bonferroni and Lorenz Curves. A positive RVr Z is described by the following Lorenz curve

$$L(p) = \frac{1}{\mu}\int_q^{\infty} z f(z)dz = \frac{1}{\mu}\sum_{l,d,k=0}^{\infty} v_{(l,d,k)} I_{(q,\infty)}(\beta^*, 1, q), \tag{32}$$

where $q = G^{-1}(p)$. Also, the Bonferroni curve is defined by

$$B(p) = \frac{1}{p\mu}\int_q^{\infty} z f(z)dz = \sum_{l,d,k=0}^{\infty} v_{(l,d,k)} I_{(q,\infty)}(\beta^*, 1, q). \tag{33}$$

There are numerous uses for the Bonferroni curve in economics to analyze income and poverty, as well as dependability, medical, and insurance areas.

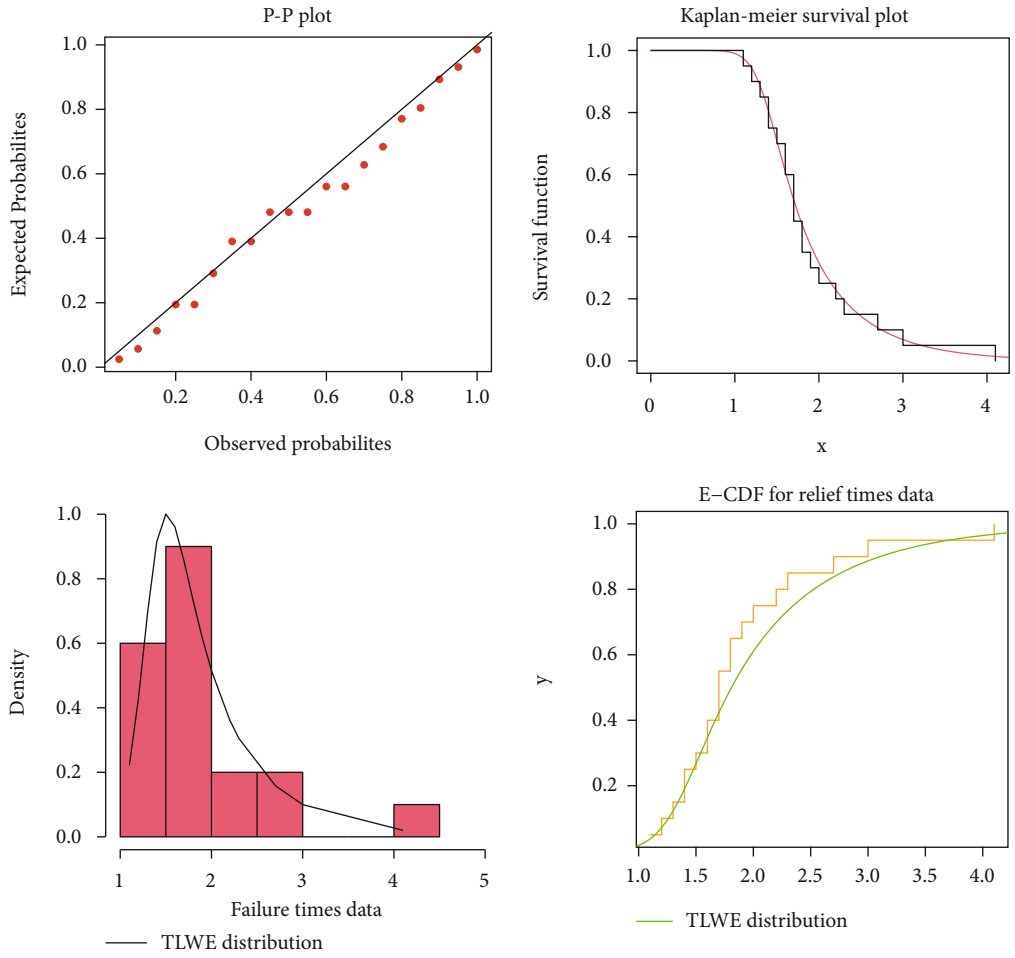

Figure 7: P-P, KMS plot, FPDF, and FCDF for the 1st data.

5. Special Cases

In this part, we will look at various TLWG family-specific situations. We provide six TLWG family special models equivalent to the baseline exponential (E), Weibull (W), Lomax (Lx), Burr-X (BX), log-logistic (LL), and Lindley (L) distributions. The odd ratio $O_{\underline{\Phi}}(z)$ of these baseline models along with the new models are listed in Table 1.

The above-mentioned PDF parameters are all positive actual numbers. Figure 1 shows graphs of the PDF of the TLWE model. Figure 2 depicts the TLWE model's HRF graphs. According to Figure 1, the new PDF can have a variety of useful forms. According to Figure 2, the new HRF can be increasing ($\alpha = \beta = \theta = 1$), bathtub ($\alpha = 1, \beta = 0.15, \theta = 0.5$), **J** shape ($\alpha = 1, \beta = 0.15, \theta = 5$), and decreasing ($\alpha = 1, \beta = 0.2, \theta = 2$).

6. Maximum Likelihood (MLL) Estimation

Suppose $z_1, \cdots, z_n$ be an n^{th} random sample from the TLWG class provided via (5). Take $\underline{P} = (\alpha, \beta, \underline{\delta})^T$ become the vector of parameters. The total log-likelihood (LLL) function for $\underline{P}$ is

$$L_n(\underline{P}) = n \log(2\beta\alpha) + \sum_{l=1}^{n} \log g_{\underline{\Phi}}(z_l) + (\beta - 1) \sum_{l=1}^{n} \log G_{\underline{\Phi}}(z_l) - (\beta + 1) \sum_{l=1}^{n} \log \bar{G}_{\underline{\Phi}}(z_l) - 2 \sum_{l=1}^{n} \left[O_{\underline{\Phi}}(z_l)\right]^{\beta} + (\alpha - 1) \sum_{l=1}^{n} \log\left(1 - \exp\left\{-2\left[O_{\underline{\Phi}}(z_l)\right]^{\beta}\right\}\right), \tag{34}$$

where $O_{\underline{\Phi}}(z_l) = G_{\underline{\Phi}}(z_l)/\bar{G}_{\underline{\Phi}}(z_l)$. The LLL can really be optimized immediately employing SAS software or the R-language, or implicitly through solving nonlinear LL formulas acquired through differentiating (34). The score function's related components $U_n(\psi) = (\partial L_n(\underline{P})/\partial\alpha, \partial L_n(\underline{P})/\partial\beta, \partial L_n(\underline{P})/\partial\underline{\Phi})^T$ are

$$\frac{\partial L_n(\underline{P})}{\partial \alpha} = \frac{n}{\alpha} + \sum_{l=1}^{n} \log\left(1 - \exp\left\{-2\left[O_{\underline{\Phi}}(z_l)\right]^{\beta}\right\}\right),$$

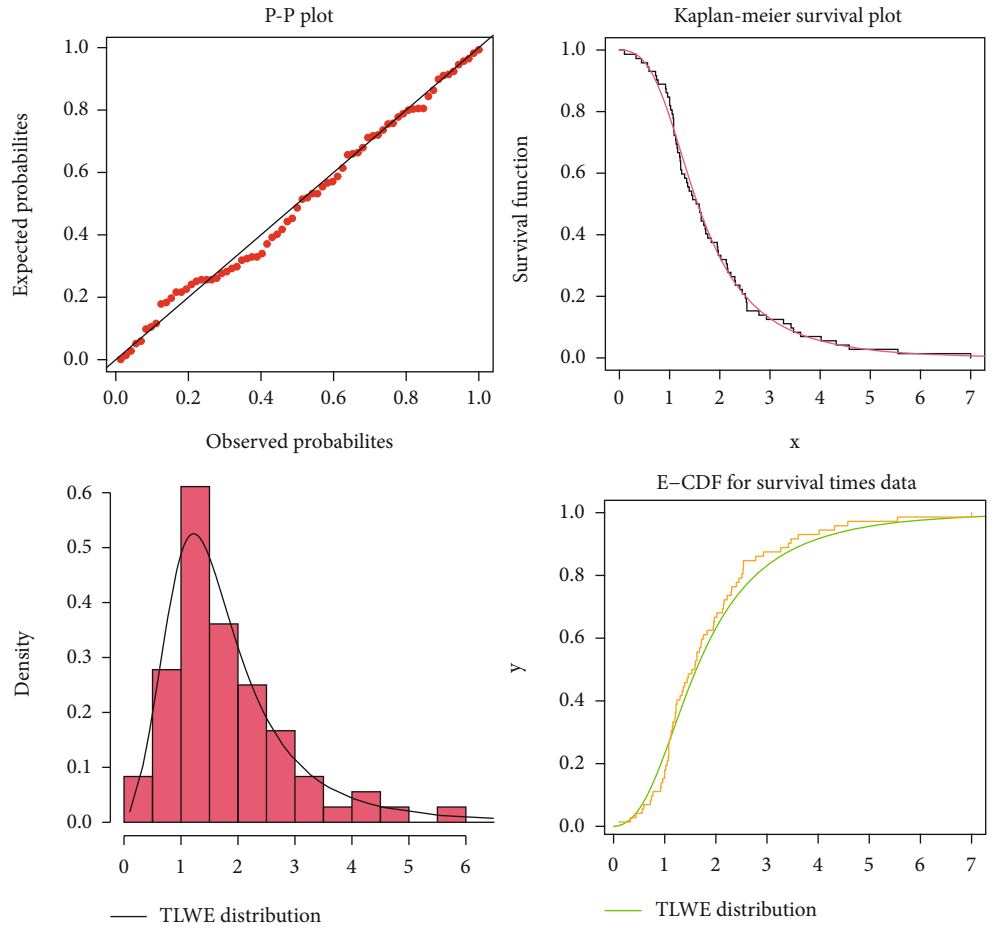

Figure 8: P-P, KMS plot, FPDF, and FCDF for the 2nd data.

$$\frac{\partial L_n(\underline{P})}{\partial \beta} = \frac{n}{\beta}\sum_{l=1}^{n}\log G_{\underline{\Phi}}(z_l) - \sum_{l=1}^{n}\log \bar{G}_{\underline{\Phi}}(z_l) - 2\sum_{l=1}^{n}\left[O_{\underline{\Phi}}(z_l)\right]^{\beta}\log\left[O_{\underline{\Phi}}(z_l)\right] + 2(\alpha-1)\sum_{l=1}^{n}\frac{\log\left[O_{\underline{\Phi}}(z_l)\right]\left[O_{\underline{\Phi}}(z_l)\right]^{\beta}\exp\left\{-2\left[O_{\underline{\Phi}}(z_l)\right]^{\beta}\right\}}{1-\exp\left\{-2\left[O_{\underline{\Phi}}(z_l)\right]^{\beta}\right\}},$$

$$\frac{\partial L_n(\underline{P})}{\partial \underline{\Phi}_k} = \sum_{l=1}^{n}\frac{\partial G_{\underline{\Phi}}(z_l)/\partial \underline{\Phi}_k}{G_{\underline{\Phi}}(z_l)} + (\beta-1)\sum_{l=1}^{n}\frac{\partial G_{\underline{\Phi}}(z_l)/\partial \underline{\Phi}_k}{G_{\underline{\Phi}}(z_l)} + (\beta+1)\sum_{l=1}^{n}\frac{\partial G_{\underline{\Phi}}(z_l)/\partial \underline{\Phi}_k}{\bar{G}_{\underline{\Phi}}(z_l)} - 2\sum_{l=1}^{n}O_{\underline{\Phi}}(z_l)\partial G_{\underline{\Phi}}(z_l)/\partial \underline{\Phi}_k + 2(\alpha-1)\sum_{l=1}^{n}\frac{\exp\left\{-2\left[O_{\underline{\Phi}}(z_l)\right]^{\beta}\right\}O_{\underline{\Phi}}(z_l)\partial G_{\underline{\Phi}}(z_l)/\partial \underline{\Phi}_k}{1-\exp\left\{-2\left[O_{\underline{\Phi}}(z_l)\right]^{\beta}\right\}}, \tag{35}$$

where $\underline{\delta}_k$ is the kth member of the parameter vector δ. The MLL estimation (MLLE) of $\underline{P}$ is achieved through solving the nonlinear equations $U_n(\underline{P}) = 0$.

7. Graphical Simulations

(i) We could perform numerical simulations to visually analyze the finite sample performance of the MLLEs utilizing biases (Bs) and mean squared errors (MSEs). For the assessment, the basic procedure had been used

(ii) Generate $N = 1000$ samples of size $n|_{(n=50,100,\cdots,500)}$ from the TLWE model using (7)

(iii) Compute the MLLEs for $N = 1000$ samples

(iv) Compute the standard errors (SErs) of the MLLEs for the 1000 samples

(v) Compute the Bs and MSErs given for $\underline{P} = \alpha, \beta, \theta$

The biases (left boxes) and MSEs (right windows) for the parameters are shown in Figures 3–5. The plots on the left demonstrate how the three biases grow with large sample n , while the graphs on the right platform how the three MSEs change with n. The zero biases are depicted by the broken line as shown in Figure 1. From Figures 3–5, the biases with each parameter are typically negative and eventually drop to 0 as n tends to infinity the MSEs with each parameter decrease to 0 as tends to infinity.

8. Modelling

Inside this part, we look at two real-world data sets to show how adaptable the TLWE model is. The first data set (1.1, 1.4, 1.3, 1.7, 1.9, 1.8, 1.6, 2.2, 1.7, 2.7, 4.1, 1.8, 1.5, 1.2, 1.4, 3, 1.7, 2.3, 1.6, and 2) (see [25]) is known as the "failure times data," and it comprises lifetime data on "relief times" (in minutes) of analgesic-using individuals. In the second data set, [26] investigated and reported the "survival times" in days for 72 guinea pigs infected with virulent tubercle bacilli (0.1, 0.33, 0.44, 0.56, 0.59, 0.72, 0.74, 0.77, 0.92, 0.93, 0.96, 1, 1, 1.02, 1.05, 1.07, 07, 1.08, 1.08, 1.08, 1.09, 1.12, 1.13, 1.15, 1.16, 1.2, 1.21, 1.22, 1.22, 1.24, 1.3, 1.34, 1.36, 1.39, 1.44, 1.46, 1.53, 1.59, 1.6, 1.63, 1.63, 1.68, 1.71, 1.72, 1.76, 1.83, 1.95, 1.96, 1.97, 2.02, 2.13, 2.15, 2.16, 2.22, 2.3, 2.31, 2.4, 2.45, 2.51, 2.53, 2.54, 2.54, 2.78, 2.93, 3.27, 3.42, 3.47, 3.61, 4.02, 4.32, 4.58, and 5.55). Figure 6 shows the total time in the test (TTT) plot for determining the form of the empirical HRFs (first row). To explore the extreme observations, the box plot is sketched in Figure 6 (second row). To ensure that the normality state is maintained, the Q-Q plot is reported in Figure 6 (third row). Kernel density estimation (KDE) may be used to investigate the initial form of real-world data, and it is seen within Figure 6 (fourth row). According to Figure 6 (first row), we note that the HRF is "asymmetric monotonically increasing" for the two data sets. Based on Figure 6 (second row), we note that some extreme observations were spotted. Based on Figure 6 (third row), we see that the normality does not exist. Based on Figure 6 (fourth row), it is noted that the nonparametric Kernel densities are asymmetric.

We will compare the TLWE distribution's fits to various competing models, particularly exponential (E), odd Lindley E (OLE), Marshall-Olkin (MO) E (MOE), Moment E (MomE), the logarithmic Burr-Hatke E (LBHE), generalized MOE (GMOE), beta E (BE), MO Kumaraswamy E (MOKwE), Kumaraswamy E (KwE), and Kumaraswamy MOE (KwMOE). See the PDFs of the competitive models in [27, 28].

We discuss the Anderson-Darling (C_1) and the Cramér-Von Mises (C_2) statistics, as well as the Kolmogorov-Smirnov (D1) statistic as well as its associated P value (D2). Moreover, we consider some other goodness-of-fit measures including the Akaike-Information-Criterion (IC) (C_3), Bayesian IC (C_4), Consistent-Akaike-IC (C_5), and Hannan-Quinn IC (C_6); Table 2 gives the MLLEs, SEs, and confidence interval (C.I.) values for the relief time data. Table 3 gives the MLLEs, SErs, and C.I. values for the survival time data. Table 4 illustrates the C_1, C_2, C_3, C_4, C_5, C_6, D1, and D2 for the relief time data. Table 5 refers to the C_1, C_2, C_3, C_4, C_5, C_6, D1, and D2 for the survival time data. Figure 7 gives the P-P plot, Kaplan-Meier survival (KMS) plot, fitted PDF (FPDF), and FCDF for the 1st data. Figure 8 offers the P-P plot, KMS plot, fitted PDF (FPDF), and FCDF for the 2nd data.

The TLWE model is much better than many common competitive models such as the exponential (standard version), MOE, OLE, LBHE, MomE, GMOE, KwE, MOKwE, and KwMOE models. As a result, the new lifespan model offers a practical alternate to all these models. For both data sets, we can see from Figures 7 and 8 that the TLWE model fits the two real data sets well.

9. Discussion and Concluding Remarks

We described and explored the TLWG family, a novel generator of continuous lifespan distributions, in this work. Statistical attributes of the family are offered, such as density function expansion, moments, incomplete moments, mean deviation, and Bonferroni and Lorenz curves. The new HRF might be described as "monotonically rising," "bathtub," "J shape," or "monotonically declining." FGM and MFGM families and CCO are often used to describe and visualize Copula of the basic kind. Regarding estimating model parameters, we glance at the MLL methodology. We conducted simulated studies to examine the limited sample behavior of MLL estimations utilizing graphs, biases, and mean squared errors. Two applications to actual data sets demonstrate the relevance and versatility of the intended family.

As a future work, we can apply many new useful goodness-of-fit tests for right-censored validation such as the Nikulin-Rao-Robson goodness-of-fit test, modified Nikulin-Rao-Robson goodness-of-fit test, Bagdonavicius-Nikulin goodness-of-fit test, and modified Bagdonavicius-Nikulin goodness-of-fit test. However, some bivariate versions could be studied in more details.

Data Availability

If you would like to get the quantitative data set utilized to conduct the investigation described in the publication, please notify the person author.

Conflicts of Interest

The authors declare no conflict of interest.

Acknowledgments

The authors extend their appreciation to the Deanship of Scientific Research at Imam Mohammad Ibn Saud Islamic University for funding this work through Research Group no. RG-21-09-08.

References

[1] H. M. Yousof, A. Z. Afify, M. Alizadeh, N. S. Butt, G. G. Hamedani, and M. M. Ali, "The transmuted exponentiated generalized-G family of distributions," *Pakistan Journal of Statistics and Operation Research*, vol. 11, no. 4, pp. 441–464, 2015.

[2] M. Bourguignon, R. B. Silva, and G. M. Cordeiro, "The Weibull–G family of probability distributions," *Journal of Data Science*, vol. 12, no. 1, pp. 53–68, 2014.

[3] H. M. Yousof, A. Z. Afify, G. G. Hamedani, and G. Aryal, "The Burr X generator of distributions for lifetime data," *Journal of Statistical Theory and Applications*, vol. 16, no. 3, pp. 1–19, 2017.

[4] A. H. Soliman, M. Elgarhy, and M. Shakil, "Type II half logistic family of distributions with applications," *Pakistan Journal of Statistics and Operation Research*, vol. 13, no. 2, pp. 245–264, 2017.

[5] F. Merovci, M. Alizadeh, H. M. Yousof, and G. G. Hamedani, "The exponentiated transmuted-G family of distributions: theory and applications," *Communications in Statistics-Theory and Methods*, vol. 46, no. 21, pp. 10800–10822, 2017.

[6] M. El-Morshedy, F. S. Alshammari, Y. S. Hamed, M. S. Eliwa, and H. M. Yousof, "A new family of continuous probability distributions," *Entropy*, vol. 23, no. 2, p. 194, 2021.

[7] H. M. Yousof, M. Rasekhi, A. Z. Afify, M. Alizadeh, I. Ghosh, and G. G. Hamedani, "The beta Weibull-G family of distributions: theory, characterizations and applications," *Pakistan Journal of Statistics*, vol. 33, pp. 95–116, 2017.

[8] M. C. Korkmaz, M. Alizadeh, H. M. Yousof, and N. S. Butt, "The generalized odd Weibull generated family of distributions: statistical properties and applications," *Pakistan Journal of Statistics and Operation Research*, vol. 14, no. 3, pp. 541–556, 2018.

[9] M. Alizadeh, M. Rasekhi, H. M. Yousof, and G. G. Hamedani, "The transmuted Weibull G family of distributions," *Hacettepe Journal of Mathematics and Statistics*, vol. 47, no. 6, pp. 1–20, 2017.

[10] H. M. Yousof, M. Majumder, S. M. A. Jahanshahi, M. Masoom Ali, and G. G. Hamedani, "A new Weibull class of distributions: theory, characterizations and applications," *Journal of Statistical Research of Iran*, vol. 15, no. 1, pp. 45–82, 2018.

[11] S. Rezaei, B. B. Sadr, M. Alizadeh, and S. Nadarajah, "Topp-Leone generated family of distributions: properties and applications," *Communications in Statistics-Theory and Methods*, vol. 46, no. 6, pp. 2893–2909, 2017.

[12] C. Chesneau and H. M. Yousof, "On a special generalized mixture class of probabilistic models," *Journal of Nonlinear Modeling and Analysis*, vol. 3, no. 1, pp. 71–92, 2021.

[13] A. A. Al-Babtain, I. Elbatal, C. Chesneau, and M. Elgarhy, "Sine Topp-Leone-G family of distributions: theory and applications," *Open Physics*, vol. 18, no. 1, pp. 574–593, 2020.

[14] R. A. Bantan, F. Jamal, C. Chesneau, and M. Elgarhy, "Type II power Topp–Leone generated family of distributions with statistical inference and applications," *Symmetry*, vol. 12, no. 1, 2020.

[15] R. A. Bantan, F. Jamal, C. Chesneau, and M. Elgarhy, "A new power Topp–Leone generated family of distributions with applications," *Entropy*, vol. 21, no. 12, 2019.

[16] A. S. Hassan, M. Elgarhy, and Z. Ahmad, "Type II generalized Topp–Leone family of distributions: properties and applications," *Journal of Data Science*, vol. 17, no. 4, pp. 638–659, 2019.

[17] D. J. G. Farlie, "The performance of some correlation coefficients for a general bivariate distribution," *Biometrika*, vol. 47, no. 3-4, pp. 307–323, 1960.

[18] E. J. Gumbel, "Bivariate logistic distributions," *Journal of the American Statistical Association*, vol. 56, no. 294, pp. 335–349, 1961.

[19] E. J. Gumbel, "Bivariate exponential distributions," *Journal of the American Statistical Association*, vol. 55, no. 292, pp. 698–707, 1960.

[20] D. Morgenstern, "Einfache beispiele zweidimensionaler verteilungen," *Mitteilingsblatt fur Mathematische Statistik*, vol. 8, pp. 234-235, 1956.

[21] J. A. Rodriguez-Lallena and M. Ubeda-Flores, "A new class of bivariate copulas," *Statistics and Probability Letters*, vol. 66, no. 3, pp. 315–325, 2004.

[22] N. Balakrishna and C. D. Lai, "Construction of bivariate distributions," *Springer Science & Business Media*, 2009.

[23] E. S. A. El-Sherpieny, H. Z. Muhammed, and E. M. Almetwally, "Bivariate Weibull-G family based on copula function: properties, Bayesian and non-Bayesian estimation and applications," *Statistics, Optimization & Information Computing*, vol. x, 31 pages, 2021.

[24] E. S. A. El-Sherpieny, E. M. Almetwally, and H. Z. Muhammed, "Bayesian and non-bayesian estimation for the parameter of bivariate generalized Rayleigh distribution based on Clayton copula under progressive type-II censoring with random removal," *Sankhya A*, pp. 1–38, 2021.

[25] T. Bjerkedal, "Acquisition of resistance in guinea pigs infected with different doses of virulent tubercle bacilli," *American Journal of Hygiene*, vol. 72, pp. 130–148, 1960.

[26] J. Gross and V. A. Clark, "Survival distributions: reliability applications in the biometrical sciences," John Wiley, New York, USA, 1975.

[27] H. Elgohari, M. Ibrahim, and H. M. Yousof, "A new probability distribution for modeling failure and service times: properties, copulas and various estimation methods," *Statistics, Optimization & Information Computing*, vol. 9, no. 3, pp. 555–586, 2021.

[28] M. Ibrahim, E. A. EA, and H. M. Yousof, "A new distribution for modeling lifetime data with different methods of estimation and censored regression modeling," *Statistics, Optimization & Information Computing*, vol. 8, no. 2, pp. 610–630, 2020.

Hindawi
Journal of Function Spaces
Volume 2021, Article ID 5207152, 13 pages
https://doi.org/10.1155/2021/5207152

Research Article

Global Stability for Novel Complicated SIR Epidemic Models with the Nonlinear Recovery Rate and Transfer from Being Infectious to Being Susceptible to Analyze the Transmission of COVID-19

Fehaid Salem Alshammari and F. Talay Akyildiz

Department of Mathematics and Statistics, Faculty of Science, Imam Mohammad Ibn Saud Islamic University, Riyadh, Saudi Arabia

Correspondence should be addressed to Fehaid Salem Alshammari; falshammari@imamu.edu.sa

Received 29 July 2021; Accepted 22 September 2021; Published 21 October 2021

Academic Editor: Pranay Goswami

Epidemiological models play pivotal roles in predicting, anticipating, understanding, and controlling present and future epidemics. The dynamics of infectious diseases is complex, and therefore, researchers need to consider more complicated mathematical models. In this paper, we first describe the dynamics of a complex SIR epidemic model with nonstandard nonlinear incidence and recovery rates. In this model, we consider the rate at which individuals lose immunity. Rigorous mathematical results have been established from the point of view of stability and bifurcation. The basic reproduction number (R_0) is determined. We then apply LaSalle's invariance principle and Lyapunov's direct method to prove that the disease-free equilibrium is globally asymptotically stable when $R_0 < 1$. The model has a unique endemic equilibrium when $R_0 > 1$. A nonlinear Lyapunov function is used together with LaSalle's invariance principle to show that the endemic equilibrium is globally asymptotically stable under some conditions. Further, for the case when $R_0 = 1$, we analyze the model and show a backward bifurcation under certain conditions. In the second part of this paper, we analyze a modified SIR model with a vaccination term, which must be a function of time. We show that the modified model agrees well with COVID-19 data in Saudi Arabia. We then investigate different future scenarios. Simulation results suggest that a two-pronged strategy is crucial to control the COVID-19 pandemic in Saudi Arabia.

1. Introduction

There is a long and rich history of mathematical modeling of epidemiology. Most often, compartmental deterministic models are used for modeling the spread of infectious diseases [1–3]. In these models, a population of susceptible individuals evolves into other categories representing different stages of infection. Among many epidemiological models which had been used for infectious disease, SIR types of models have received more attention. In 1927, Kermack and McKendrick were the first to develop the susceptible-infective-recovered (SIR) model, where the total population is divided into three classes: susceptible, infective, and recovered [4]. After that, variant of SIR compartmental models were developed, some of them outlined in [5–8]. Here, we consider a complex SIR epidemic model with nonstandard nonlinear incidence and recovery rates. We also consider in our model the rate of losing immunity, which has not been considered before.

In classic SIR epidemic models, the bilinear incident rate $\beta IS/N$ (where $N(t) = S(t) + I(t) + R(t)$ is the number of total populations, parameter β is the infection transmission rate, and $S(t), I(t)$, and $R(t)$ represent the number of susceptible and infected and recovered individuals at time (t). Also, a linear recovery rate μI (μ is the per capita recovery rate) is often used. These classic models do not have bistability

and periodicity in their solution which is not realistic, especially for COVID-19. Their dynamics basically depend on the basic reproducing number R_0; the disease will be eliminated if $R_0 < 1$; otherwise, the disease persists [9]. However, in reality, many infectious diseases show multiple peaks and/or periodic oscillations during the outbreak. The monotone incident rate term $f(I)S$ (which describes the mechanism of disease transmission) does not capture the "psychological" or behavioral change and crowding effect of infected individuals. Therefore, we use the following general incidence rate:

$$f(I)S = \frac{\beta I^q S}{1 + kI^p}, \tag{1}$$

where $k > 0$ measures the psychological or inhibitory effect and q and p are constants. This type of incidence rate was first considered by Liu et al. [10]. This incidence rate was used by many other scholars [11, 12]. In the rest of the paper, we use the incidence rate term (1) with $q = 1$.

Determining the treatment rate is not an easy task and many factors are involved in this process. The main factor is the number of health workforce that includes physicians, nurses, pharmacists, and other health care workers (HCW). The facilities of the hospital such as medical equipment and apparatus, the availability of the intensive care unit, and the number of the hospital beds and medicines are the other significant factors which are necessary and essential for safe and effective avoiding, diagnosis, and treatment of illness [13, 14]. In this work, we follow the work of Shan and Zhu [15] and use the following nonlinear treatment function

$$\mu(b, I) = \left(\mu_0 + (\mu_1 - \mu_0)\frac{b}{b + I}\right), \tag{2}$$

where $\mu_0, \mu_1(\mu_1 > \mu_0)$ are the minimum and maximum per capita recovery rates, respectively. Parameter b is considered as a measure of available hospital resources.

We need herd immunity to eradicate the COVID-19 pandemic from the human population. This could be achieved either by previous infection or by vaccination. Several pharmacological companies declared high efficacy rates of their vaccine products [16, 17]. In Saudi Arabia, the Ministry of Health launched a vaccine campaign through a mobile application, which is called "Sehaty," that provides registration for COVID-19 vaccination, and vaccination centers were established in different cities around the country. The campaign was launched offering both the Pfizer-BioNTech and AstraZeneca's COVID-19 vaccines. They aim to provide free vaccination to all citizens and residents until getting herd immunity [18]. Hence, it is extremely important to create public awareness on the importance of vaccination. In this paper, we develop a mathematical model to show the effectiveness of vaccination in reducing the infection rates in Saudi Arabia.

The organization of this paper is as follows: the model framework is given in Section 2, the existence of equilibria and global stability of disease-free and endemic equilibria is studied in Section 3. In Section 4, we study the backward bifurcation. Section 5 is devoted to the modification of the model that was previously defined in Section 2. In Section 6, we summarize our results and provide a short discussion on possible extensions of our model with a possibility of additional vaccinated component.

2. Model Framework

In this section, we describe the mathematical formulation of an SIR epidemic model, where the total population size of individuals is represented by $N(t)$. The total population size is subdivided into three different classes, namely, $S(t)$: susceptible, $I(t)$: infected, and $R(t)$: removed or recovered individuals. We consider that the (viruses) parasites of the diseases are transmitted to the susceptible populations by the direct contact with the infected populations.

We assume that the total recruitment at any time t is $"A"$ and all the new recruited populations go to the susceptible class. We consider that $\beta \geq 0$, which is the disease transmission rate and the incidence rate to be $\beta IS/1 + kI$, where k is the half-saturation constant for which the susceptible population decreases. The population of susceptible people is decreased by the natural death rate d, and the recovery population goes to the susceptible class at a rate δ (the recovered individuals could become susceptible again due to lose of immunity). Hence, the governing equation can be modeled as

$$\frac{dS}{dt} = A - \frac{\beta IS}{1 + kI} - dS + \delta R. \tag{3}$$

The infected population is decreased by the natural death rate d and the disease death rate γ. The medical treatments, determining how well the diseases are controlled, are normally expressed as constant recovery rates. There are several suggested functions to describe the treatment term. In this paper, we follow the work of Shan and Zhu [15], where they defined the recovery rate as a function of b, the number of hospital beds, and the number of infectives I. Thus, the time rate of change for this can be represented by the following equation:

$$\frac{dI}{dt} = \frac{\beta IS}{1 + kI} - \left(\mu_0 + (\mu_1 - \mu_0)\frac{b}{b + I}\right)I - (d + \gamma)I. \tag{4}$$

The recovered population is increased by the recovery rate as in above and decreased by the natural death rate d and the susceptibility of recovered individuals δ. The time rate of change for the population of recovered individuals can be represented by the following equation:

$$\frac{dR}{dt} = \left(\mu_0 + (\mu_1 - \mu_0)\frac{b}{b + I}\right)I - (d + \delta)R. \tag{5}$$

All parameters involved in equations (3)–(5) are nonnegative. Equations (3)–(5) can be written in the combined form as follows:

$$\frac{dS}{dt} = A - \frac{\beta IS}{1+kI} - dS + \delta R, \tag{6}$$

$$\frac{dI}{dt} = \frac{\beta IS}{1+kI} - \left(\mu_0 + (\mu_1 - \mu_0)\frac{b}{b+I}\right)I - (d+\gamma)I, \tag{7}$$

$$\frac{dR}{dt} = \left(\mu_0 + (\mu_1 - \mu_0)\frac{b}{b+I}\right)I - (d+\delta)R, \tag{8}$$

subject to initial conditions

$$S(0) = S_0 \geq 0, \tag{9}$$

$$I(0) = I_0 \geq 0, \tag{10}$$

$$R(0) = R_0 \geq 0. \tag{11}$$

For systems (6)–(9), the cone $\mathscr{R}^{3+}$ is positively invariant. The C^1 smoothness of the right side of systems (6)–(9) implies local existence and uniqueness of solutions with the initial values in $\mathscr{R}^{3+}$.

It is not difficult to show that every solution of (6)–(9) with nonnegative initial conditions remains nonnegative. If we add up the three equations of systems (6)–(8), we get

$$\frac{d(S+I+R)}{dt} = A - d(S+I+R) - \gamma I \leq A - d(S+I+R), \tag{12}$$

which implies that the set

$$\Omega = \left\{(S,I,R) \in \mathscr{R}^{3+} : S \geq 0, I \geq, R \geq 0, S+I+R \leq \frac{A}{d}\right\} \tag{13}$$

is positively invariant and an attractive set for (6)–(9); hence, all solutions in the first octant approach enter or stay inside the set defined above and also bounded and, hence, globally exist. Thus, the initial value problem of systems (6)–(9) is mathematically well posed and epidemiologically reasonable.

Because of total population $N(t) = S(t) + I(t) + R(t)$ is regulated by the disease, the system cannot be reduced to the lower dimension; hence, we need to analyze systems (6)–(9) in the three-dimensional phase space.

3. Basic Reproduction Number

The basic reproduction number is denoted by R_0, and it is defined as the number of newly infected individuals caused by a single infection. We now find the basic reproduction number of systems (6)–(9) using the next-generation matrix method developed by Driessche and Watmough [19]. Let us write systems (6)–(9) as follows:

$$\dot{x}_i = \mathscr{F}_i(x) - \mathscr{V}_i(x), i = 1, \cdots, 3, \tag{14}$$

where

$$x_i = (I, S, R)^T,$$

$$\mathscr{F}_i = \begin{pmatrix} \frac{\beta S}{1+kI} \\ 0 \\ 0 \end{pmatrix},$$

$$\mathscr{V}_i = \left(\left(\mu_0 + (\mu_1 - \mu_0)\frac{b}{b+I}\right)I + (d+\gamma)I - A + dS - \delta R + \frac{\beta S}{1+kI} - \left(\mu_0 + (\mu_1 - \mu_0)\frac{b}{b+I}\right)I + (d+\delta)R\right). \tag{15}$$

We denote the disease-free equilibrium of models (6)–(9) by E_0, where

$$E_0^* = \left(0, \frac{A}{d}, 0\right). \tag{16}$$

Now, the Jacobian matrixes of $\mathscr{F}_i$ and $\mathscr{V}_i$ at E_0 are given as

$$F = J(\mathscr{F}_i) = \begin{pmatrix} \frac{\beta A}{d} & 0 \\ 0 & 0 \end{pmatrix}, \quad J(\mathscr{V}_i) = \begin{pmatrix} V & 0 \\ M_1 & M_2 \end{pmatrix}, \tag{17}$$

where

$$V = \begin{pmatrix} d+\gamma+\mu_1 & 0 \\ \frac{\beta A}{d} & d \end{pmatrix}. \tag{18}$$

The basic reproduction number R_0 of system (14) is defined by the spectral radius of the matrix $\rho(FV^{-1})$ (see Driessche and Watmough [19]) and it is given by $R_0 = \beta A/(d(d+\gamma+\mu_1))$.

4. Existence and Types of Equilibria

4.1. Existence of Equilibria. We have already established the existence of the disease-free equilibrium $E_0 = (A/d, 0, 0)$ for systems (6)–(9) for all values of parameters. For any endemic equilibrium $E^* = (S, I, R)$, its coordinates satisfy

$$R = \frac{1}{d+\delta}\left(\mu_0 + (\mu_1 - \mu_0)\frac{b}{b+I}\right)I. \tag{19}$$

Substituting this into the first equation in (6)–(9) and solving for S, we obtain

$$S = \frac{A + (\delta/(d+\delta))(\mu_0 + (\mu_1 - \mu_0)(b/(b+I)))}{((\beta IS/(1+kI)) + d)}. \quad (20)$$

The variable I should be the positive root of the following quadratic equation

$$f(I) = \mathscr{A}I^2 + \mathscr{C}I + \mathscr{D}, \quad (21)$$

where

$$\mathscr{A} = \frac{d^3k + (\gamma + \beta + \delta k + k\mu_0)d^2 + (\gamma\beta + \gamma\delta k + \beta\delta + \beta\mu_0 + \delta k\mu_0)d + \gamma\beta\delta}{d(\gamma + d + \mu_1)},$$

$$\mathscr{C} = \frac{\begin{array}{c}(bk+1)d^3 + (\gamma bk + b\beta + bk\delta + bk\mu_1 + \delta + \mu_0 + \gamma)d^2 + \\ (\gamma b\delta\beta + kb\delta\mu + \gamma b\beta + b\beta\delta + b\beta\delta + b\beta\mu_1 + k\mu_0 + \gamma\delta - A\beta)d + \gamma b\beta\delta - \delta\beta A\end{array}}{d(\gamma + d + \mu_1)}, \quad (22)$$

and

$$\mathscr{D} = \frac{b(d+\delta)}{d(\gamma + d + \mu_1)}(1 - R_0). \quad (23)$$

Equation $f(I) = 0$ may have two roots if $\Delta_0 > 0$, which are

$$I_1 = \frac{-\mathscr{C} - \sqrt{\Delta_0}}{2\mathscr{A}}, \qquad I_1 = \frac{-\mathscr{C} + \sqrt{\Delta_0}}{2\mathscr{A}}, \quad (24)$$

where $\Delta_0 = \mathscr{C}^2 - 4\mathscr{A}\mathscr{D}$.

If $I > 0$, we see from (19) and (20) that $S > 0$ and $R > 0$, respectively.

We study the existence of equilibria in the following three cases:

$$R_0 > 1. \quad (25)$$

In this case, $\mathscr{D} > 0$; since $\mathscr{A} > 0$, we have $I_1 < 0$ and $I_2 > 0$, so systems (6)–(9) have a unique endemic equilibrium $E_2 = (S(I_2), I_2, R(I_2))$.

$$R_0 = 1. \quad (26)$$

In this case, $I_1 = -(\mathscr{C}/\mathscr{A})$ and $I_2 = 0$; if $\mathscr{C} < 0$, then, systems (6)–(9) have a unique endemic equilibrium $E_1 = (S(I_1), I_1, R(I_1))$.

$$R_0 < 1. \quad (27)$$

In this case, if $\mathscr{C} > 0$, there is no endemic equilibrium; if $\mathscr{C} < 0$ and $\Delta_0 > 0$, we have two endemic equilibria $E_1 = (S(I_1), I_1, R(I_1))$ and $E_2 = (S(I_2), I_2, R(I_2))$. If $\Delta_0 = 0$, then, we have one root multiplicity 2. We summarize the result in the following theorem.

Theorem 1. *For systems (6)–(9),*

(1) The disease-free equilibrium exists

(2) If $R_0 > 1$, there exists a unique endemic equilibrium E_2

(3) If $R_0 = 1$, there exists a unique endemic equilibrium E_1 provided that $\mathscr{C} < 0$; otherwise, there is no endemic equilibrium

(4) If $R_0 < 1$ and if $\mathscr{C} > 0$, there is no endemic equilibrium; if $\mathscr{C} < 0$ and $\Delta_0 > 0$, the system has two endemic equilibria E_1 and E_2; if $\mathscr{C} < 0$ and $\Delta_0 = 0$, the system has two equilibria coalesce into E^*

Theorem 2. *For systems (6)–(9), the disease-free equilibrium $E_0 = (A/d, 0, 0)$ is*

(i) $R_0 < 1$: an attracting node

(ii) $R_0 > 1$:a hyperbolic saddle

(iii) $R_0 = 1$: and $b > d^2((\mu_1 - \mu_0)d + (\mu_1 - \mu_0)\delta)/\beta(A(d + k)(dk + \beta) - \delta\mu_1 d)$: a saddle-node of codimension 1

$b < (d^2((\mu_1 - \mu_0)d + (\mu_1 - \mu_0)\delta))/(\beta(A(d+k)(dk+\beta) - \delta\mu_1 d))$ is a saddle-node of codimension 1; $b = (d^2((\mu_1 - \mu_0)d + (\mu_1 - \mu_0)\delta))/(\beta(A(d+k)(dk+\beta) - \delta\mu_1 d))$ is an attracting semihyperbolic node of codimension 2.

Proof. The Jacobian matrix $J(E_0)$ for systems (6)–(9) is given by

$$J(E_0) = \begin{pmatrix} -d & -\frac{\beta A}{d} & \delta \\ 0 & \frac{\beta A}{d} - \mu_1 - \gamma & 0 \\ 0 & \mu_1 & -d - \delta \end{pmatrix}. \quad (28)$$

The eigenvalues are obtained from this.

$$\lambda_1 = -d, \qquad \lambda_2 = -d - \delta, \qquad \lambda_3 = \frac{A\beta - \gamma d - d^2 - d\mu_1}{d}. \quad (29)$$

Since $R_0 < 1$, λ_3 is negative, because $\lambda_3 = (\gamma d + d^2 + d\mu_1)/d(R_0 - 1)$; hence, all eigenvalues are negative. Thus, if $R_0 < 1$, E_0 is an attracting node, and if $R_0 > 1$, then, E_0 is a hyperbolic saddle. If $R_0 = 1$, the third eigenvalue is zero. In order to determine the type of E_0, we first transform the disease-free equilibrium point E_0 to the origin. We use $\tilde{S} =$

$S - A/d$; then, using the Taylor expansion as in [15], we get

$$\frac{d\tilde{S}}{dt} = \delta R(t) - d\tilde{S}(t) + \frac{\beta A I(t)}{d} + O\left(\left|\tilde{S}, I, R\right|^3\right), \tag{30}$$

$$\frac{dI}{dt} = -\left(\frac{\beta A k}{d} + \frac{-\mu_1 + \mu_0}{b}\right) I^2 + O\left(\left|\tilde{S}, I, R\right|^3\right), \tag{31}$$

$$\frac{dR}{dt} = -(d+\delta)R + \mu_1 I(t) + O\left(\left|\tilde{S}, I, R\right|^3\right), \tag{32}$$

Using eigenvectors, we find following transform:

$$I(t) = X(t),$$

$$\tilde{S}(t) = \frac{(-(\delta\mu_1/(d+\delta)) + (\beta A/d))I(t) + Y(t) - (\delta d/((d+\delta)(2d+\delta)))Z(t)}{d},$$

$$R(t) = \frac{Z(t) - \mu_1 I(t)}{d+\delta}. \tag{33}$$

Thus, using these variables in (30), we obtain

$$\frac{dX}{dt} = -\left(\frac{\beta A k}{d} + \frac{-\mu_1 + \mu_0}{b} + \frac{\beta(-(\delta\mu_1/(d+\delta)) + (\beta A/d))}{d}\right) X^2 + XO(|Y, Z|) + O\left(|Y, Z|^2, |X, Y, Z|^3\right), \tag{34}$$

$$\frac{dY}{dt} = -dY + O\left(|X, Y, Z|^2\right), \tag{35}$$

$$\frac{dZ}{dt} = -(d+\delta)Z + O\left(|X, Y, Z|^2\right). \tag{36}$$

It is unnecessary to calculate the center manifold if $b \neq (d^2((\mu_1 - \mu_0)d + (\mu_1 - \mu_0)\delta))/(\beta(A(d+k)(dk+\beta) - \delta\mu_1 d))$, and E_0 is a saddle node. If $b = (d^2((\mu_1 - \mu_0)d + (\mu_1 - \mu_0)\delta))/(\beta(A(d+k)(dk+\beta) - \delta\mu_1 d))$, then, from the central manifold theorem for systems (6)–(9), we obtain

$$\frac{dX}{dt} = -\left[\frac{\beta A k}{d} + \frac{\beta(-(\delta\mu_1/(d+\delta)) + (\beta A/d))}{d} + \frac{\delta d(-\mu_1 + \mu_0)}{b(2d+\delta)} + \frac{\delta\mu_1}{d+\delta} - \frac{\beta A k}{d}\right] X^3 + O\left(|X|^4\right), \tag{37}$$

$$\frac{dY}{dt} = -dY + O\left(|X, Y, Z|^2\right), \tag{38}$$

$$\frac{dZ}{dt} = -(d+\delta)Z + O\left(|X, Y, Z|^2\right). \tag{39}$$

Hence, E_0 is a semihyperbolic attracting node.□ □

From Theorem 1, one can see that for the existence of endemic equilibrium, $\beta A < d(d + \gamma + \mu_1)$ is a necessary condition. If $< d(d + \gamma + \mu_1)$, E_2 is the unique equilibrium point and we have the following theorem.

Theorem 3. *For the system (4)-(7), if $< d(d + \gamma + \mu_1)$, the disease-free equilibrium $E_0 = (A/d, 0, 0)$ is globally asymptotically stable.*

Proof. Consider the Lyapunov function $V = I$ in R^{3+} with the Liapunov derivative

$$\begin{aligned} V' &= \frac{\beta I S}{1+kI} - \left(\mu_0 + (\mu_1 - \mu_0)\frac{b}{b+I}\right) I - (d+\gamma) I \\ &\leq \left[\beta S - \left(\mu_0 + (\mu_1 - \mu_0)\frac{b}{b+I}\right) - (d+\gamma)\right] I \\ &\leq \lim_{S \longrightarrow \frac{A}{d}, I \longrightarrow 0} \left[\beta S - \left(\mu_0 + (\mu_1 - \mu_0)\frac{b}{b+I}\right) - (d+\gamma)\right] I \\ &\leq \left[\frac{\beta A}{d} - (\mu_1 + d + \gamma)\right] \lim_{I \longrightarrow 0} I \leq (\mu_1 + d + \gamma)[R_0 - 1] \lim_{I \longrightarrow 0} I. \end{aligned} \tag{40}$$

The Lyapunov–Lasalle theorem implies that solutions in Ω approach the largest positively invariant subset of set $V' = 0$, i.e., plane $I = 0$. In this plane, $S \longrightarrow A/d$ and $R \longrightarrow 0$ as $t \longrightarrow \infty$. Thus, all solutions in plane $I = 0$ go to the disease-free equilibrium E_0. Therefore, E_0 is globally asymptotically stable.□ □

Theorem 4. *A sufficient condition for the endemic equilibrium E_2 to be locally asymptotically stable is $R_0 > 1$*

Proof. In this case, the Jacobian matrix has the following form:

$$J = \begin{pmatrix} \frac{-\beta I^*}{1+I^*k} - d & \Sigma & \delta \\ \frac{\beta I^*}{1+I^*k} & -\Sigma + \Xi - d - \gamma & 0 \\ 0 & -\Xi & -d - \delta \end{pmatrix}, \tag{41}$$

where $\Sigma = (-\beta S^*/(1 + I^*k)) + (\beta k I^* S^*/((1 + I^*k)^2))$ and $\Xi = ((\mu_1 - \mu_0)b)/(b + I^*)((I^*/(b + I^*)) - 1) - \mu_0$. The characteristic equation for the above Jacobian around its endemic equilibrium E_2 is

$$x^3 + C_1 x^2 + C_2 x + C_3 = 0, \tag{42}$$

where C_1, C_2, and C_3 are too long to reproduce here. We have observed that C_1, C_2, and C_3 are positive and $C_1 C_2 > C_3$; hence, the Routh–Hurwitz criterion is satisfied, so systems (6)–(9) are locally asymptotically stable for $R_0 > 1$.□ □

Theorem 5. *The epidemic models (4)–(7) at E_2 are globally asymptotically stable if $R_0 > 1$.*

Proof. We consider the Lyapunov function given by

$$L = \int_{S^*}^{S} \left(1 - \frac{S^*}{z}\right) dz + \int_{I^*}^{I} \left(1 - \frac{I^*}{z}\right) dz + \int_{R^*}^{S} \left(1 - \frac{R^*}{z}\right) dz. \tag{43}$$

Taking the derivative, we have

$$\begin{aligned}
\dot{L} &= \left(1 - \frac{S^*}{S}\right)\frac{dS}{dt} + \left(1 - \frac{I^*}{I}\right)\frac{dI}{dt} + \left(1 - \frac{R^*}{R}\right)\frac{dR}{dt} \\
&= \left(1 - \frac{S^*}{S}\right)\left(A - \frac{\beta IS}{1+kI} - dS + \delta R\right) + \left(1 - \frac{I^*}{I}\right) \\
&\quad \cdot \left(\frac{\beta IS}{1+kI} - \left(\mu_0 + (\mu_1 - \mu_0)\frac{b}{b+I}\right)I - (d+\gamma)I\right) \\
&\quad + \left(1 - \frac{R^*}{R}\right)\left(\left(\mu_0 + (\mu_1 - \mu_0)\frac{b}{b+I}\right)I - (d+\delta)R\right) \\
&= \left(1 - \frac{S^*}{S}\right)\left(\frac{\beta I^* S^*}{1+kI^*} + dS^* + \delta R^* - \frac{\beta IS}{1+kI} - dS - \delta R\right) \\
&\quad + \left(1 - \frac{I^*}{I}\right)\left(\frac{\beta IS}{1+kI} - \left(\mu_0 + (\mu_1 - \mu_0)\frac{b}{b+I}\right)I\right. \\
&\quad - (d+\gamma)I - \frac{\beta I^* S^*}{1+kI^*} + \left(\mu_0 + (\mu_1 - \mu_0)\frac{b}{b+I^*}\right)I^* \\
&\quad \left. + (d+\gamma)I^*\right) + \left(1 - \frac{R^*}{R}\right)\left(\left(\mu_0 + (\mu_1 - \mu_0)\frac{b}{b+I}\right)I\right. \\
&\quad \left. - (d+\delta)R - \left(\mu_0 + (\mu_1 - \mu_0)\frac{b}{b+I^*}\right)I^* + (d+\delta)R^*\right),
\end{aligned}$$

$$\begin{aligned}
\dot{L} &= \left(1 - \frac{S^*}{S}\right)\left(\frac{1}{(1+kI^*)(1+kI)}\left[(\beta I^* S)\left(\frac{S^*}{S} - \frac{I}{I^*}\right)\right.\right. \\
&\quad \left.\left. + k\beta I^* I S^*\left(1 - \frac{S}{S^*}\right)\right] + \delta R^*\left(1 - \frac{R}{R^*}\right) + dS^*\left(1 - \frac{S}{S^*}\right)\right) \\
&\quad + \left(1 - \frac{I^*}{I}\right)\left(\frac{-1}{(1+kI^*)(1+kI)}\left[(\beta I^* S)\left(\frac{S^*}{S} - \frac{I}{I^*}\right)\right.\right. \\
&\quad \left.\left. + k\beta I^* I S^*\left(1 - \frac{S}{S^*}\right)\right] + \frac{b^2 I^*}{(b+I^*)(b+I)}\left(1 - \frac{I}{I^*}\right)\right. \\
&\quad \left. + (\mu_0 + d + \gamma)I^*\left(1 - \frac{I}{I^*}\right)\right) + \left(1 - \frac{R^*}{R}\right) \\
&\quad \cdot \left(\left(d+\delta\right)R^*\left(1 - \frac{R}{R^*}\right) - \frac{b^2 I^*}{(b+I^*)(b+I)}\right. \\
&\quad \left. \cdot \left(1 - \frac{I}{I^*}\right) - (\mu_0 + d + \gamma)I^*\left(1 - \frac{I}{I^*}\right)\right),
\end{aligned}$$

$$\begin{aligned}
\dot{L} &= \left(1 - \frac{S^*}{S}\right)k\beta I^* I S^*\left(1 - \frac{S}{S^*}\right) + \left(1 - \frac{I^*}{I}\right) \\
&\quad \cdot \left(\frac{b^2 I^*}{(b+I^*)(b+I)}\left(1 - \frac{I}{I^*}\right) + (\mu_0 + d + \gamma)I^*\left(1 - \frac{I}{I^*}\right)\right) \\
&\quad + \left(1 - \frac{R^*}{R}\right)(d+\delta)R^*\left(1 - \frac{R}{R^*}\right) + \left(1 - \frac{R^*}{R}\right) \\
&\quad \cdot \left(\delta R^*\left(1 - \frac{S^*}{S}\right) - \frac{b^2 I^*}{(b+I^*)(b+I)}\left(1 - \frac{I}{I^*}\right)\right. \\
&\quad \left. - (\mu_0 + d + \gamma)I^*\left(1 - \frac{I}{I^*}\right)\right) + \left(1 - \frac{I^*}{I}\right) \\
&\quad \cdot \left(\frac{-1}{(1+kI^*)(1+kI)}\left[(\beta I^* S)\left(\frac{S^*}{S} - \frac{I}{I^*}\right)\right.\right. \\
&\quad \left.\left. + k\beta I^* I S^*\left(1 - \frac{S}{S^*}\right)\right]\right) \\
&\quad + \frac{1}{(1+kI^*)(1+kI)}\beta I^* S\left(\frac{S^*}{S} - \frac{I}{I^*}\right)\left(1 - \frac{S^*}{S}\right),
\end{aligned} \tag{44}$$

if

$$\begin{aligned}
&\left(1 - \frac{R^*}{R}\right)\left(1 - \frac{S^*}{S}\right) < 0, \\
&\left(1 - \frac{R^*}{R}\right)\left(1 - \frac{I}{I^*}\right) > 0, \\
&\left(1 - \frac{I^*}{I}\right)\left(\frac{-1}{(1+kI^*)(1+kI)}\right. \\
&\quad \left. \cdot \left[(\beta I^* S)\left(\frac{S^*}{S} - \frac{I}{I^*}\right) + k\beta I^* I S^*\left(1 - \frac{S}{S^*}\right)\right]\right) \\
&\quad + \frac{1}{(1+kI^*)(1+kI)}\beta I^* S\left(\frac{S^*}{S} - \frac{I}{I^*}\right)\left(1 - \frac{S^*}{S}\right) < 0.
\end{aligned} \tag{45}$$

Then, we have

$$\dot{L} < 0, \tag{46}$$

Hence, the theorem is proved.□ □

Theorem 6. *For systems (6)–(9), consider R_0 as the bifurcation parameter. Then, we have, when $R_0 = 1$, systems (6)–(9) which undergo forward bifurcation if $b > (d^2((\mu_1 - \mu_0)d + (\mu_1 - \mu_0)\delta))/(\beta(A(d+k)(dk+\beta) - \delta\mu_1 d))$; systems (6)–(9) undergo backward bifurcation if $b < (d^2((\mu_1 - \mu_0)d + (\mu_1 - \mu_0)\delta))/(\beta(A(d+k)(dk+\beta) - \delta\mu_1 d))$; systems (6)–(9) undergo pitchfork bifurcation if $b = (d^2((\mu_1 - \mu_0)d + (\mu_1 - \mu_0)\delta))/(\beta(A(d+k)(dk+\beta) - \delta\mu_1 d))$.*

Proof. Since R_0 is a function of the parameters β, γ, δ, d, and μ_1, without loss of generality, we can choose μ_1 as the bifurcation parameter.

Let $\mu_1 = (\beta A/d) - d - \gamma + \varepsilon$, we substitute this into (6)–(9); we note that if $\varepsilon = 0$, then, it reduces to $\mathscr{R}_0 = 1$. We then use Taylor expansion at E_0; diagonalizing the linear part, we then apply the center manifold theorem for the parameter ε. We found that

$$\begin{aligned}
\frac{dX}{dt} &= -\left(\varepsilon + O(\varepsilon^2)\right)X - \left(\frac{\beta Ak}{d} + \frac{-\Pi + \mu_0}{b}\right. \\
&\quad \left. + \frac{\beta(-(\delta\Pi/d + \delta) + (\beta A/d))}{d} + O(\varepsilon)\right)X^2 + O(X^3),
\end{aligned} \tag{47}$$

where $\Pi = (\beta A/d - d - \gamma)$. Denoting the right-hand side of (47) as $\Gamma(\varepsilon, X)$, we have

$$\begin{aligned}
\Gamma(0,0) &= 0, \\
\frac{\partial}{\partial\varepsilon}\Gamma(0,0) &= 0, \\
\frac{\partial}{\partial X}\Gamma(0,0) &= 0, \\
\frac{\partial^2}{\partial X\partial\varepsilon}\Gamma(0,0) &= -1,
\end{aligned}$$

$$\frac{\partial^2}{\partial X^2}\Gamma(0,0) = -\left(\frac{\beta Ak}{d} + \frac{-\Pi + \mu_0}{b} + \frac{\beta(-(\delta\Pi/d + \delta) + (\beta A/d))}{d}\right) = -\left(\frac{\beta \mathrm{A}k}{d} + \frac{-\mu_1 + \mu_0}{b} + \frac{\beta(-(\delta\mu_1/d + \delta) + (\beta A/d))}{d}\right). \tag{48}$$

Therefore, the system has transcritical bifurcation if

$$\mathrm{b} \neq \frac{d^2((\mu_1 - \mu_0)d + (\mu_1 - \mu_0)\delta)}{\beta(A(d+k)(dk+\beta) - \delta\mu_1 d)}. \tag{49}$$

If $b = (d^2((\mu_1 - \mu_0)d + (\mu_1 - \mu_0)\delta))/(\beta(A(d+k)(dk+\beta) - \delta\mu_1 d))$, using the center manifold theory, as the above, from (6)–(9), we obtain

$$\frac{dX}{dt} = -\left(\varepsilon + O\left(\varepsilon^2\right)\right)X + O(\varepsilon)X^2 - \left[\frac{\beta Ak}{d} + \frac{\beta(-(\delta\Pi/(d+\delta)) + (\beta A/d))}{d} + \frac{\delta d(-\Pi + \mu_0)}{b(2d+\delta)} + \frac{\delta\Pi}{d+\delta} - \frac{\beta Ak}{d} + O(\varepsilon)\right]X^3 + O\left(|X|^4\right). \tag{50}$$

Again, denoting the right-hand side of (50) as $\Gamma(\varepsilon, X)$, we have

$$\Gamma(0,0) = 0,$$
$$\frac{\partial}{\partial\varepsilon}\Gamma(0,0) = 0,$$
$$\frac{\partial}{\partial X}\Gamma(0,0) = 0,$$
$$\frac{\partial^2}{\partial X\partial\varepsilon}\Gamma(0,0) = -1,$$
$$\frac{\partial^2}{\partial X^2}\Gamma(0,0) = 0,$$

$$\frac{\partial^3}{\partial X^3}\Gamma(0,0) = -\left(\frac{\beta Ak}{d} + \frac{\beta(-(\delta\Pi/d + \delta) + (\beta A/d))}{d} + \frac{\delta d(-\Pi + \mu_0)}{b(2d+\delta)} + \frac{\delta\Pi}{d+\delta} - \frac{\beta Ak}{d}\right) = -\left(\frac{\beta Ak}{d} + \frac{\beta(-(\delta\Pi/d + \delta) + (\beta A/d))}{d} + \frac{\delta d(-\Pi + \mu_0)}{b(2d+\delta)} + \frac{\delta\Pi}{d+\delta} - \frac{\beta Ak}{d}\right). \tag{51}$$

It is clear that systems (6)–(9) have pitchfork bifurcation if $b = (d^2((\mu_1 - \mu_0)d + (\mu_1 - \mu_0)\delta))/(\beta(A(d+k)(dk+\beta) - \delta\mu_1 d))$ when $R_0 = 1$ [20]. We note that If $\varepsilon = 0$, the system related with equation (47) and the system related with equation (50) reduce to the systems in equations (34) and (37), respectively.

Since R_0 is a function of μ_1, also b and k, we choose μ_1 as the bifurcation parameter. In Theorem 1, there are two endemic equilibria provided that if $R_0 < 1$, $\mathscr{C} < 0$, and $\Delta_0 > 0$ and if $\mathscr{C} < 0$ and $\Delta_0 = 0$, then, there are two equilibria coalesce.

The basic reproducing number $R_0 = 1$ defines a straight line P_0 in the (μ_1, b) plane

$$P_0 : \mu_1 = \frac{A\beta - \gamma d - d^2}{d}, \tag{52}$$

$\mathscr{C}$=0 defines one branch of hyperbola $P_{\mathscr{C}}$ (see Figure 1):

$$P_{\mathscr{C}} : b = H_{\mathscr{C}}(\mu_1) = \frac{\left(A\beta - \gamma d - d^2 - d\mu_0\right)(d+k)}{d^3k + ((\gamma + \delta + \mu_1)k + \beta)d^2 + (\delta(\gamma + \mu_1)k + \beta(\gamma + \delta + \mu_1))d + \gamma\beta\delta}. \tag{53}$$

The branch of $P_{\mathscr{C}}$ has an intersection with P_0 at point K, where $\mathrm{K} = ((A\beta - \gamma d - d^2)/d, (d^2((\mu_1 - \mu_0)d + (\mu_1 - \mu_0)\delta))/(\beta(A(d+k)(dk+\beta) - \delta\mu_1 d)))$. We also have $(dH_{\mathscr{C}}(\mu_1))/d\mu_1 < 0$ and $(d^2H_{\mathscr{C}}(\mu_1))/d\mu_1^2 > 0$, so $H_{\mathscr{C}}(\mu_1)$ is decreasing and a convex function of μ_1.

Now, let

$$P_0^+ = \left\{(\mu_1, b) : \mu_1 = \frac{A\beta - \gamma d - d^2}{d}, b > \frac{d^2((\mu_1 - \mu_0)d + (\mu_1 - \mu_0)\delta)}{\beta(A(d+k)(dk+\beta) - \delta\mu_1 d)}\right\},$$

$$P_0^- = \left\{(\mu_1, b) : \mu_1 = \frac{A\beta - \gamma d - d^2}{d}, b < \frac{d^2((\mu_1 - \mu_0)d + (\mu_1 - \mu_0)\delta)}{\beta(A(d+k)(dk+\beta) - \delta\mu_1 d)}\right\}. \tag{54}$$

Then, $P_0 = P_0^+ \cup P_0^- \cup K$, where P_0^+ and P_0^- are the parts of P_0 which are separated by K. Now, we consider the curve defined by $\Delta_0(\mu_1, b) = 0$ and we indicate these curves as $P_\Delta^\pm$; solving for b from $\Delta_0(\mu_1, b) = 0$, we got

$$P_\Delta^\pm : \mathrm{b} = f_\Delta^\pm(\mu_1). \tag{55}$$

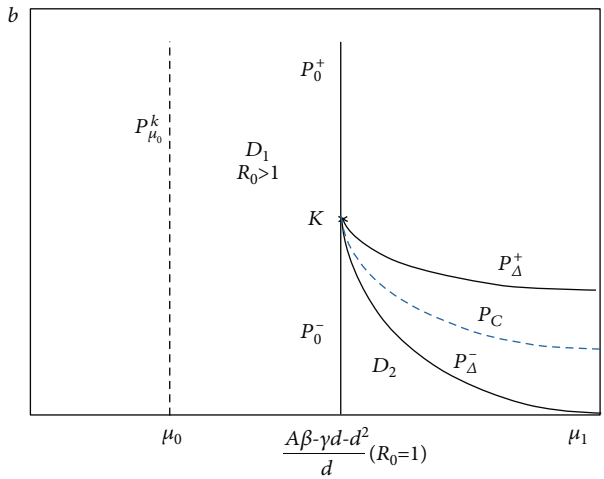

Figure 1: For fixed k, the bifurcation curves in the (μ_1, b) plane when $A\beta > d\mu_0 + \gamma d + d^2$. In D_1 region $R_0 > 1$, where there exists a unique endemic equilibrium. There are two endemic equilibria in D_2. Two equilibria coalesce and a saddle-node bifurcation occurs on P_Δ^- . The forward bifurcation occurs on P_0^- and backward bifurcation occurs on P_0^+. There is no endemic equilibrium in the first region.

We found that $f_\Delta^+((A\beta - \gamma d - d^2)/d) = f_\Delta^-((A\beta - \gamma d - d^2)/d)$ and straightforward calculations lead to

$$f_\Delta^-(\mu_1) < H_{\mathscr{C}}(\mu_1) < f_\Delta^+(\mu_1), \quad \mu_1 \in \left(\frac{A\beta - \gamma d - d^2}{d}, \infty\right). \tag{56}$$

Furthermore, we have found that

$$\begin{aligned} &\frac{df_\Delta^\pm(\mu_1)}{d\mu_1} < 0, \quad \mu_1 \in \left(\frac{A\beta - \gamma d - d^2}{d}, \infty\right) \text{ and } \lim_{\mu_1 \longrightarrow \infty} f_\Delta^-(\mu_1) \longrightarrow 0. \\ &\frac{d^2 f_\Delta^\pm(\mu_1)}{d\mu_1^2} > 0, \quad \mu_1 \in \left(\frac{A\beta - \gamma d - d^2}{d}, \infty\right) \text{ and } \lim_{\mu_1 \longrightarrow \infty} f_\Delta^-(\mu_1) \longrightarrow 0. \end{aligned} \tag{57}$$

Hence, $f_\Delta^\pm(\mu_1)$ and $H_{\mathscr{C}}(\mu_1)$ are decreasing and they are convex functions of μ_1.

Based on the above discussion and Theorem 1, for fix k, we define

$$\begin{aligned} D_0 &= \left\{(b, \mu_1): b > f_\Delta^-(\mu_1), \mu_1 > \frac{A\beta - \gamma d - d^2}{d}\right\}, \\ D_1 &= \left\{(b, \mu_1): b > 0, \mu_0 < \mu_1 < \frac{A\beta - \gamma d - d^2}{d}\right\}, \\ D_2 &= \left\{(b, \mu_1): 0 < b < f_\Delta^-(\mu_1), \mu_1 > \frac{A\beta - \gamma d - d^2}{d}\right\}. \end{aligned} \tag{58}$$

In Figure 1, we see that there is one endemic equilibrium in region D_1 and two equilibria in region D_2. The system of equations (6)–(9) undergoes saddle-node bifurcation on the curve P_Δ^-. The forward bifurcation occurs on P_Δ^- and we have backward bifurcation, which occurs on P_Δ^-. The pitchfork bifurcation occurs when transversally passing through curve P_0 at point K. The mathematical system of equations (6)–(9) has a semihyperbolic node of codimension 2 at point K. The similar discussion can be done for fixed b and varying value of k to show the backward bifurcation. This part is omitted since the analysis is the same as before.□ □

5. Further Development of the Model, Numerical Results, and Discussion

We numerically show that equilibrium point $E_2(S^*, I^*, R^*)$ is locally and globally asymptotically stable. For the parameters in Table 1, $R_0 = 6.9307$, the endemic equilibrium E_2 exists at $E_2(S^*, I^*, R^*) = (243.9075, 2.455, 1.6707)$. Figure 2 provides that Theorem 1 is satisfied, i.e., E_2 is locally asymptotically stable where initial conditions $S(0) = 150$, $I(0) = 50$, and $R(0) = 20$ are used. In Figure 2, we could see that solutions approach to $E_2(S^*, I^*, R^*) = (243.9075, 2.455, 1.6707)$. Furthermore, in Figure 3, we use the parameters in Table 1 to show that the endemic equilibrium $E_2(S^*, I^*, R^*) = (243.9075, 2.455, 1.6707)$ is globally asymptotically stable because the solutions of S, I, and R converge to the same E_2 independently from the initial values of S, I, and R.

We further simulate the inhibition effect due to the behavioral change of susceptible population when the number of infected individuals increases. We use parameter values given in Table 1 with $k = 0, 0.2, 1, 2$, and 4. Figure 4 shows different levels of the inhibition effect: low, moderate, and significant. The results are depicted in Figure 5, which shows that moderate and significant inhibition considerably reduces the number of infected individuals (I).

We now consider a modification of the model defined in equations (6)–(9). We define a new term, which is the vaccination ratio v, and incorporate this term into our existing model. The modified model is shown in Figure 6

We assume that the vaccination rate is constant, but in general, v is a function of susceptible, infected, and recovered individuals. Using the idea from [21], we can further modify the defined model in (6)–(9) to be

$$\frac{dS}{dt} = A - \frac{\beta IS}{1 + kI} - (d + vp_s)S + \delta R, \tag{59}$$

$$\frac{dI}{dt} = \frac{\beta IS}{1 + kI} - \left(\mu_0 + (\mu_1 - \mu_0)\frac{b}{b + I}\right)I - (d + \gamma + \gamma vp_i)I, \tag{60}$$

$$\frac{dR}{dt} = vp_s S + \left(\mu_0 + (\mu_1 - \mu_0)\frac{b}{b + I}\right)I + \gamma vp_i I - (d + \delta)R, \tag{61}$$

Table 1: Random parameters used in the numerical simulations in Figures 2 and 3.

Parameter	Value	Dimension
A	1.75	Individual/time
β	0.01	1/(individual × time)
k	2	1/individual
d	0.005	1/time
μ_0	0.2	1/time
μ_1	0.3	1/time
b	0.2	Individual
γ	0.2	1/time
α	0.3	1/time

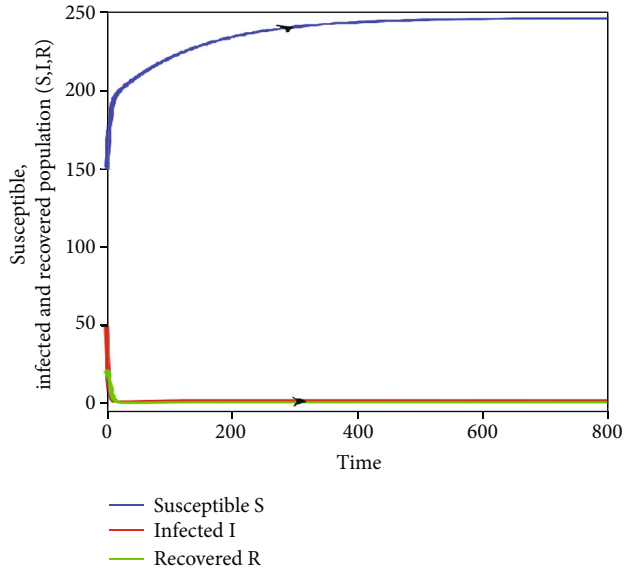

Figure 2: Susceptible (S), infected (I), and recovered (R) individuals as functions of time.

subject to initial conditions

$$S(0) = S_0 \geq 0, \tag{62}$$

$$I(0) = I_0 \geq 0, \tag{63}$$

$$R(0) = R_0 \geq 0, \tag{64}$$

where v is the vaccination rate of the population, p_s represents the vaccine efficacy for the suspected, and p_i is the effectiveness of the vaccination in infected individuals. We could analyze systems (59)–(62) as we did for the original system; therefore, there is no need to duplicate the same analysis here. We apply the modified model to describe COVID-19 scenarios in Saudi Arabia. The total population of Saudi Arabia is 35575027. The total reported cases in Saudi Arabia on April 1, 2021, are 390007, and the active cases are 5452. The Saudi government has provided

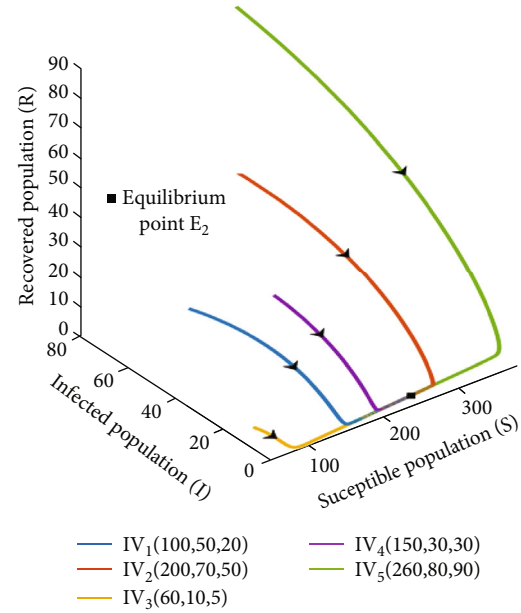

Figure 3: Global stability of endemic equilibrium E_2 for different initial values.

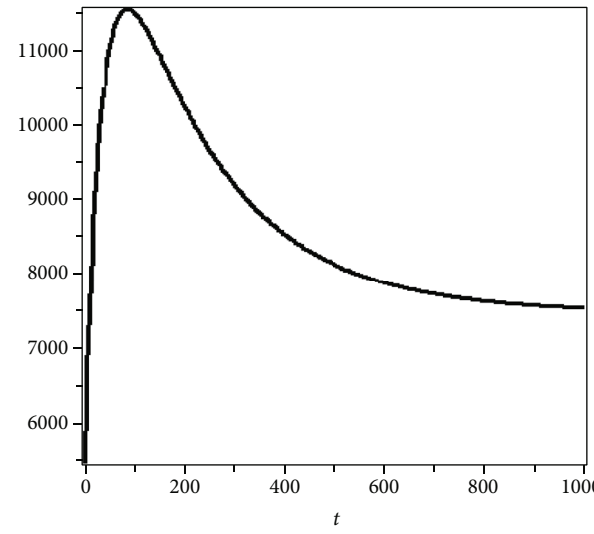

Figure 4: Prediction of model (46–49) for a long time, $\beta = 2.79.1\ 0^{-7}$ and $R_0 = 1.108$.

4571478 doses of vaccine until April 1, 2021, and 3818608 people of the population are considered to be immune. It is clear from the model that we can derive the reproducing number easily as we explained above using $R_0 = \beta A/((d + v\ p_s)(d + \gamma + \mu_1 + \gamma v p_i))$. We now try to simulate Saudi Arabia cases, where $p_i = 0.5, p_S = 0.95$, $\gamma = 0.28, v = 0.00233$, and $R_0 = 1.108$. We use the least square method to fit the other parameters. Figure 5 shows the model predictions in comparison with real COVID-19 data of Saudi Arabia for infected individuals. The model predicts current cases nicely, but the model prediction in the future cannot be accurate (see Figure 4 after 1000 days). Furthermore, we know from

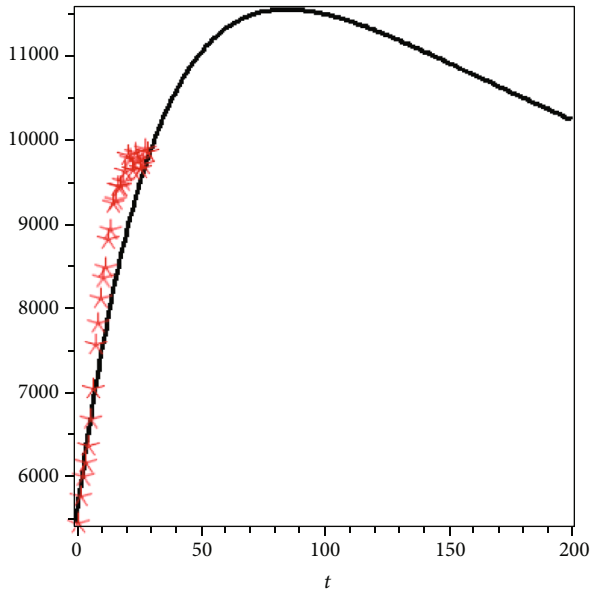

Figure 5: Comparing the prediction of model (46–49 (black line) with real data of Saudi Arabia (red asterisks) for $\beta = 2.79.10^{-7}$ and $R_0 = 1.108$.

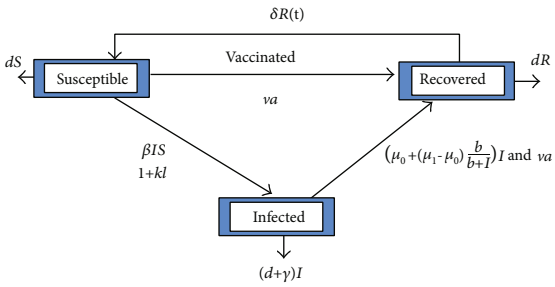

Figure 6: Schematic diagram of the modified model. The arrows represent a progression from one compartment to the next and death rates.

other transmitted diseases that vaccination together with some simple restrictions on the society could control the spread of transmitted diseases. This fact tells us that the current model must be modified as we do below.

It is well known that the coefficients β, μ_0, and μ_1 are functions of time in general. But these functions can be written using empirical assumptions by using constant parameters, where empirical relations depend on disease control measures, such as social distancing, partial closure, and tracing of suspected people. In this report, we model these functions as

$$\begin{aligned} \beta(t) &= \beta_0 m_1(t), \\ \mu_0(t) &= \mu_0 m_2(t), \\ \mu_1(t) &= \mu_1 m_3(t). \end{aligned} \tag{65}$$

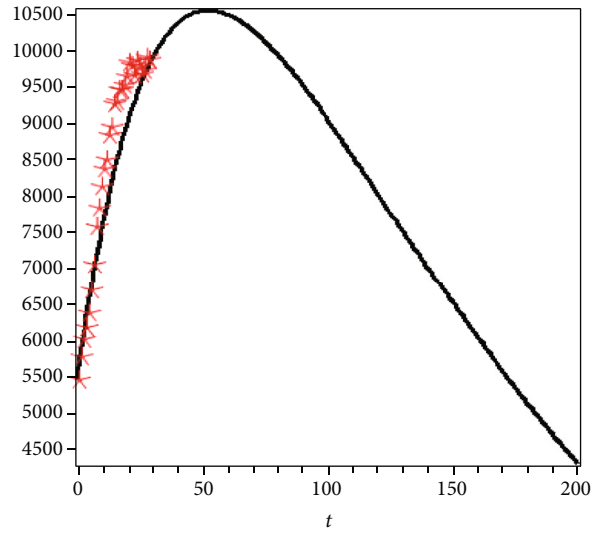

Figure 7: Compared the prediction of model (53–55) (black line) with real data of Saudi Arabia (red asterisks) for $v = 75000$ individual/per day and $\beta_0 = 4.10^{-7}$, i.e., $R_0 \leq 1.311$.

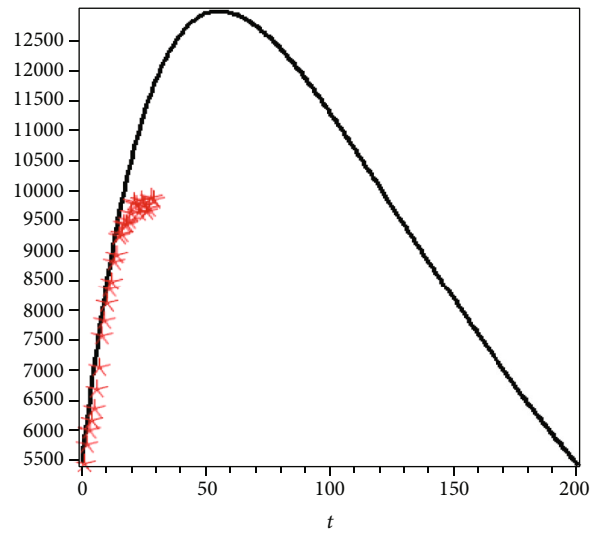

Figure 8: Compared the prediction of model (53–55) (black line) with real data of Saudi Arabia (red asterisks) for $v = 75000$ individual/per day and $\beta_0 = 5.10^{-7}$, i.e., $R_0 \leq 1.64$.

In general, the form of the $m_i(t)$ can be considered as in the work of [22, 23] as

$$m_i(t) = \begin{cases} (m_0 - m_1)\exp\left(k_1(t - t_0)\right) + m_1 \; t \in [t_0, \lambda_1], \\ \left(m_{\lambda_1} - m_2\right)\exp\left(k_2(t - \lambda_1)\right) + m_2 \; t \in (\lambda_1, \lambda_2], \\ -- \\ -- \\ \left(m_{\lambda_{p-1}} - m_p\right)\exp\left(k_p\left(t - \lambda_{p-1}\right)\right) + m_p \; t \in \left(\lambda_{p-1}, \infty\right), \end{cases} \tag{66}$$

where m_i measures the intensity of the control measures, k_i has a dimension 1/day and simulates the efficiency of the

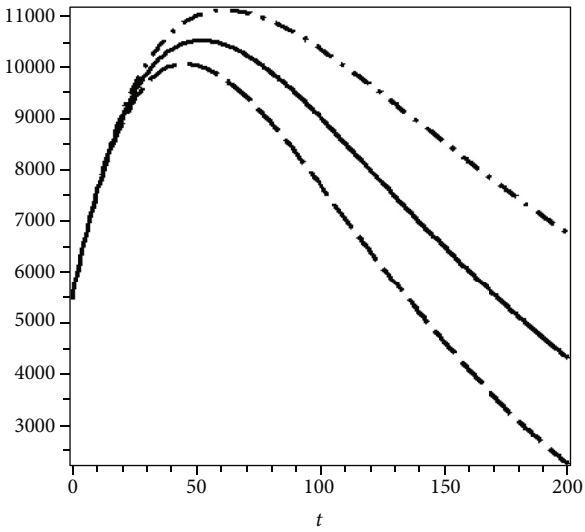

Figure 9: The effect of the number of vaccination on the infected individuals (dashed line, $v = 100000$, continuous line $v = 75000$, dashed-dotted line, $v = 50000$).

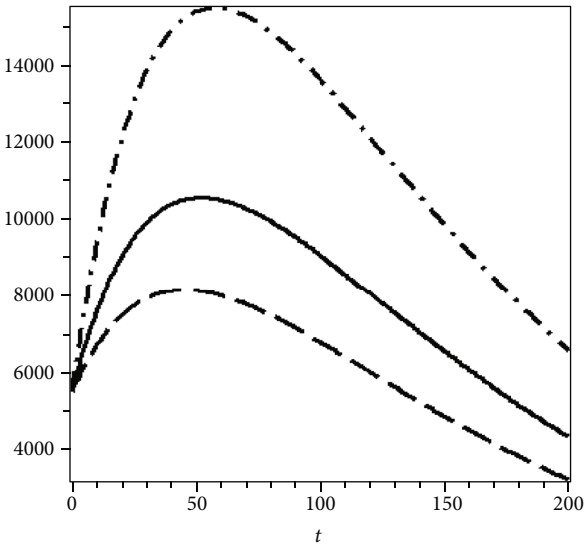

Figure 10: The effect of the reproducing number on the infected individuals (dashed line, $R_0 \leq 0.98$, continuous line $R_0 \leq 1.311$, and dashed-dotted line $R_0 \leq 1.96$.

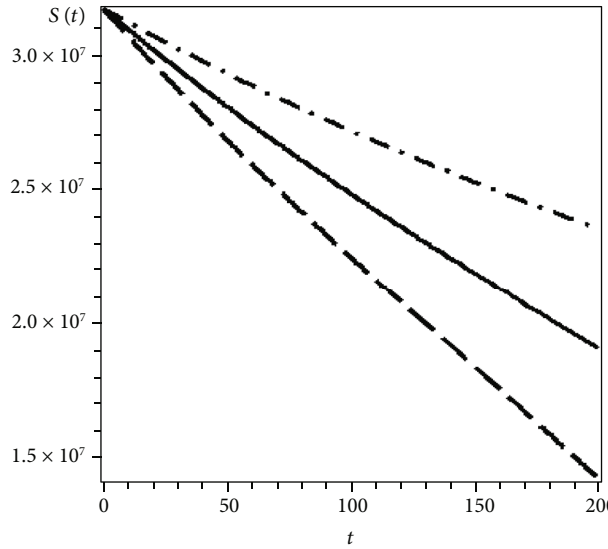

Figure 11: The effect of vaccination on the suspected individuals (dashed line, $v = 100000$, continuous line $v = 75000$, and dashed-dotted line, $v = 50000$) for $\beta_0 = 4.10^{-7}$.

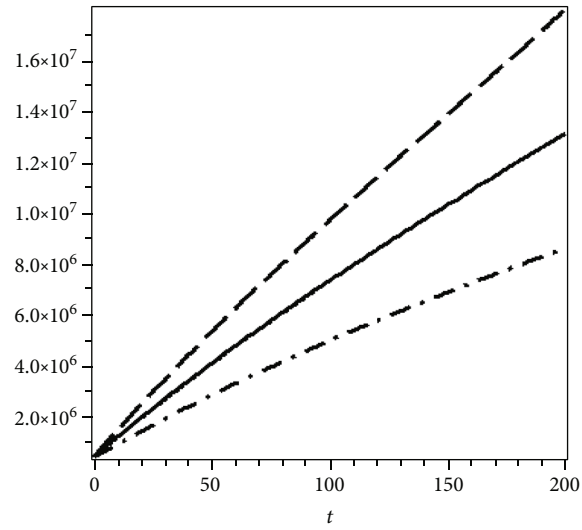

Figure 12: The effect of vaccination on recovered individuals (dashed line, $v = 100000$, continuous line $v = 75000$, dashed-dotted line, $v = 50000$) for $\beta_0 = 4.10^{-7}$.

control measures, and λ_i represents the number of days for each implemented control strategy. The vaccination rate is also a function of time and can be assumed to equal the following equation

$$v(t) = \frac{V}{\mathrm{N} + \text{number of } NBX\text{day} - NDX\text{day} - VX\text{day}}, \quad (67)$$

where V is the number of vaccinations per day, the denominator is the total population × the number of new born per day – new death per day– the number of vaccinations per day. The values of λ_i, m_i, and k_i are not fixed; they are different for each country. In this study, we use data from Saudi Arabia. Under the above discussion, our model can be written as

$$\begin{aligned}
\frac{dS}{dt} &= A - \beta_0 m_1(t)\frac{\mathrm{IS}}{1+kI} - (d + v(t)p_s)S + \delta R,\\
\frac{dI}{dt} &= \beta_0 m_1(t)\frac{\mathrm{IS}}{1+kI} + -(\mu_0 m_2(t) + (\mu_1 m_3(t)\\
&\quad - \mu_0 m_2(t))\frac{b}{b+I})I - (d + \gamma + \alpha t v(t))I,\\
\frac{dR}{dt} &= \left(\mu_0 m_2(t) + (\mu_1 m_3(t) - \mu_0 m_2(t))\frac{b}{b+I}\right)I\\
&\quad - (d+\delta)R + \alpha t v(t) I.
\end{aligned} \quad (68)$$

Table 2: Random parameters used in the numerical simulations for the real data of Saudi Arabia.

Parameter	Value	Dimension
Population of Saudi Arabia = N	35575027	Individual
$A = nN/365$	1252	Individual/time
k	[0, 2]	1/individual
d	$3.6593.10^{-5}$	1/time
μ_0	0.0002	1/time
μ_1	0.15	1/time
b	100	Individual
γ	0.0028	1/time
β_0	0.0000004	1/(individual × time)

Increasing the number of vaccinations per day reduces the reproducing number. Figure 7 shows the total infected individuals, where the continuous black line is the model prediction and symbol red asterisk represents the real data of Saudi Arabia (WHO) for the number of vaccinations $\nu = 75000$ individual/day and $R_0 \leq 1.311$. We now increase the reproducing number up to $R_0 \leq 1.64$, where we increase the transmission rate of infection from 4.10^{-7} to 5.10^{-7}. Model prediction of the current infected individuals against the real data of Saudi Arabia is shown in Figure 8. We see that the prediction agrees with real data even for the first month unlike the results in Figure 7. The prediction of the model is not a feasible region of real data; from here, we can conclude that the reproducing number of disease for Saudi Arabia is around 1.311. We now consider 50000 vaccinations per day and then consider 1000000 vaccinations per day to show the effect of vaccination as in Figure 9 for $\beta_0 = 4.10^{-7}$, where the dashed line represents 100000 vaccinations per day, while the continuous line represents 75000 vaccinations per day and the dashed-dotted line represents 50000 vaccinations per day. We see that increasing the number of vaccinations per day decreases the number of infected individuals as we expected. We also observe from Figure 10 that we could certainly control the spread of COVID-19 after 200 days for more than 75000 vaccinations per day. Next, we show the effect of the reproducing number on the number of infected individuals. Figure 10 shows the effect of the reproducing number on infected individuals. The dashed line, black line, and dashed-dotted line represent the reproducing number $R_0 \leq 0.98$, 1.311, and 1.96, respectively, for fixed vaccinations $\nu = 75000$. Now, we check the effect of vaccination and reproducing number on the suspected and recovered individuals. Figure 11 shows the effect of vaccination on the suspected population for $\beta_0 = 4.10^{-7}$. It is clear that increasing the number of vaccinations reduces the number of suspected individuals. Finally, Figure 12 shows the effect of the vaccination on the recovered population. We find that increasing the number of vaccination increases the number of recovered individuals.

6. Conclusions

In this paper, we established a new model with nonstandard nonlinear incidence and recovery rates formulated to consider the impact of available resources of public health, in particular the number of hospital beds and rate of losing immunity. We used Lyapunov's direct method to show global asymptotic stability of the disease-free equilibrium when $R_0 < 1$ and global asymptotic stability of the endemic equilibria when $R_0 > 1$. We also solved the system numerically, which confirms our theoretical results.

Vaccination is an effective method to prevent individuals from contracting transmitted diseases like flu and cholera. In the second part of this paper, we included a vaccination term and found that the modified model agrees well with the real data of Saudi Arabia.

In a forthcoming study, we will study a system with an additional vaccinated component such as

$$\begin{aligned} \frac{dV}{dt} &= f(V, S, I, R), \\ \frac{dS}{dt} &= g(V, S, I, R), \\ \frac{dI}{dt} &= h(V, S, I, R), \\ \frac{dR}{dt} &= z(V, S, I, R). \end{aligned} \tag{69}$$

We will compare the prediction of this system with our newly defined system in this paper.

Data Availability

The authors confirm that the data supporting the findings of this study are available within the article and/or its supplementary materials.

Conflicts of Interest

The authors declare that they have no competing interests.

Authors' Contributions

Fehaid Salem Alshammari did the conceptualization, methodology, numerical simulations, and writing of the original

draft. F. Talay Akyildiz did the conceptualization, methodology, numerical simulations, and writing of the original draft.

Acknowledgments

This research was supported by the Deanship of Scientific Research, Imam Mohammad Ibn Saud Islamic University (IMSIU), Saudi Arabia, Grant no. 21-13-18-004.

References

[1] F. Brauer and C. Castillo-Chávez, *Mathematical Models in Population Biology and Epidemiology*, Springer-Verlag, New York, 2001.

[2] V. Capasso, *Mathematical Structures of Epidemic Systems*, Springer Verlag, Berlin, 2nd edition, 2008.

[3] O. Diekmann, H. Heesterbeek, and T. Britton, *Mathematical Tools for Understanding Infectious Disease Dynamics*, Princeton University Press, Princeton, 2013.

[4] W. O. Kermack and A. G. McKendrick, "A contribution to the mathematical theory of epidemics," *Proceedings of the Royal Society of London A*, vol. 115, pp. 700–721, 1927.

[5] F. Rao, P. S. Mandal, and Y. Kang, "Complicated endemics of an SIRS model with a generalized incidence under preventive vaccination and treatment controls," *Applied Mathematical Modelling*, vol. 67, pp. 38–61, 2019.

[6] S. S. Alzaid, B. S. T. Alkahtani, S. Sharma, and R. S. Dubey, "Numerical solution of fractional model of HIV-1 infection in framework of different fractional derivatives," *Journal of Function Spaces*, vol. 2021, Article ID 6642957, 10 pages, 2021.

[7] M. A. Almuqrin, P. Goswami, S. Sharma, I. Khan, R. S. Dubey, and A. Khan, "Fractional model of Ebola virus in population of bats in frame of Atangana- Baleanu fractional derivative," *Results in Physics*, vol. 26, article 104295, 2021.

[8] H. M. Srivastava, R. Shanker Dubey, and M. Jain, "A study of the fractional-order mathematical model of diabetes and its resulting complications," *Mathematical Methods in Applied Sciences*, vol. 42, no. 13, pp. 4570–4583, 2019.

[9] P. Samui, J. Mondal, and S. Khajanchi, "A mathematical model for COVID-19 transmission dynamics with a case study of India," *Chaos, Solitons & Fractals*, vol. 140, article 110173, 2020.

[10] W. Liu, S. Levin, and Y. Iwasa, "Influence of nonlinear incidence rates upon the behavior of SIRS epidemiological models," *Journal of Mathematical Biology*, vol. 23, no. 2, pp. 187–204, 1986.

[11] Y. Cai, Y. Kang, and W. Wang, "A stochastic SIRS epidemic model with nonlinear incidence rate," *Applied Mathematics and Computation*, vol. 305, pp. 221–240, 2017.

[12] M. Alexander and S. Moghadas, "Periodicity in an epidemic model with a generalized non-linear incidence," *Mathematical Biosciences*, vol. 189, no. 1, pp. 75–96, 2004.

[13] World Health Organization, *World Health Statistics 2005–2011*.

[14] H. Zhu, S. Campbell, and G. Wolkowicz, "Bifurcation analysis of a predator–prey system with nonmonotonic functional response," *SIAM Journal on Applied Mathematics*, vol. 63, pp. 636–682, 2003.

[15] C. Shan and H. Zhu, "Bifurcations and complex dynamics of an SIR model with the impact of the number of hospital beds," *Journal of Difference Equations*, vol. 257, no. 5, pp. 1662–1688, 2014.

[16] https://www.astrazeneca.com/media-centre/covid-19-media.html.

[17] The Centre for Disease Control and Prevention (CDC), "COVID-19 vaccination," February 2021, https://www.cdc.gov/coronavirus/2019-ncov/vaccines/index.html.

[18] Ministry of Health (MOH), "COVID-19 vaccines," February 2021, https://covid19awareness.sa/en/archives/.

[19] P. Van den Driessche and J. Watmough, "Reproduction numbers and sub-threshold endemic equilibria for compartmental models of disease transmission," *Mathematical Biosciences*, vol. 180, no. 1-2, pp. 29–48, 2002.

[20] S. Wiggins, *Introduction to Applied Nonlinear Dynamical Systems and Chaos, Second Edition, Texts in Applied Mathematics*, vol. 2, Springer-Verlag, New York, 2003.

[21] B. H. Foy, B. Wahl, K. Mehta, S. Shet, G. I. Menon, and C. Britto, "Comparing COVID-19 vaccine allocation strategies in India: a mathematical modelling study," *International Journal of Infectious Diseases*, vol. 103, pp. 431–438, 2021.

[22] B. Ivorra, M. R. Ferrández, M. Vela-Pérez, and A. M. Ramos, "Mathematical modeling of the spread of the coronavirus disease 2019 (COVID-19) taking into account the undetected infections. The case of China," *Communications in Nonlinear Science and Numerical Simulation*, vol. 88, article 105303, 2020.

[23] A. M. Ramos, M. R. Ferrández, M. Vela-Pérez, A. B. Kubik, and B. Ivorra, "A simple but complex enough θ-SIR type model to be used with COVID-19 real data. Application to the case of Italy," *Physica D*, vol. 421, article 132839, 2021.

Hindawi
Journal of Function Spaces
Volume 2021, Article ID 8331731, 11 pages
https://doi.org/10.1155/2021/8331731

Research Article

On Impulsive Boundary Value Problem with Riemann-Liouville Fractional Order Derivative

Zareen A. Khan,[1] **Rozi Gul**,[2] **and Kamal Shah**[2,3]

[1]*College of Science, Mathematical Sciences, Princess Nourah bint Abdulrahman University, Riyadh, Saudi Arabia*
[2]*Department of Mathematics, University of Malakand, Chakdara Dir (Lower), Khyber Pakhtunkhawa, Pakistan*
[3]*Department of Mathematics and General Sciences, Prince Sultan University, Riyadh, Saudi Arabia*

Correspondence should be addressed to Zareen A. Khan; zakhan@pnu.edu.sa

Received 17 June 2021; Revised 4 August 2021; Accepted 27 August 2021; Published 30 September 2021

Academic Editor: Badr Saad. T. Alkaltani

Our manuscript is devoted to investigating a class of impulsive boundary value problems under the concept of the Riemann-Liouville fractional order derivative. The subject problem is of implicit type. We develop some adequate conditions for the existence and puniness of a solution to the proposed problem. For our required results, we utilize the classical fixed point theorems from Banach and Scheafer. It is to be noted that the impulsive boundary value problem under the fractional order derivative of the Riemann-Liouville type has been very rarely considered in literature. Finally, to demonstrate the obtained results, we provide some pertinent examples.

1. Introduction

The fractional order differential equations (abbreviated as FODEs) are the generalization of the ordinary differential equations of the integer order. In the 17th century (1665), the great mathematicians Newton, Leibnitz and L'Hospital introduced for the first time the idea of fractional order differential equations (FODEs). Later on, in 1823, another mathematician by the name of Lacroix, introduced the fractional derivative [1] of simple power function. Furthermore, this area has been studied by many researchers because it has significant applications in various fields of science and technology in mathematical modeling of different fields of Science and Technology. For instance, some phenomena including the diffusion process [2], some chemical processes of electrochemistry [3], infectious disease in biology [4], signal and image processing [5], dynamic processes [6], and systems control theory [7] can be excellently described by using FODEs instead of the ordinary derivative. For further applications of FODEs, we refer to [8–13] and the references therein.

On the other hand, an interesting and important branch recently got warm attention known as impulsive differential equations (IDEs). In recent times, the said area has been increasingly used to model many physical and social phenomena in social sciences in a very interesting way. Currently in the said area, significant contribution has been done by various researchers like Simeonov and Bainov [14], Benchohra et al. [15], Lakshmikantham et al. [16], and Samoilenko and Perestyuk [17]. Benchohra and Slimani [18] has initiated the study of FODEs under impulsive conditions by using fractional derivatives of the Caputo and Riemann-Liouville type with order $\alpha \in (0, 1)$. In addition, some applications of IDEs have been studied in various scientific disciplines such as biology, geography, engineering, dynamics, physics, geology, and management sciences. In terms of the important applications of IDEs, due to important applications of IDEs this field has a lot of significance and concentration (see [19–22]). For general research and significance, we refer some more important publications [23–26]. Many researchers have recently studied nonlinear FODEs with different kinds of boundary and initial conditions. Boundary value problems have significant applications in various fields of dynamics and fluid mechanics as well as engineering disciplines. Here, it is

remarkable that problems under integral boundary conditions have some important applications in fluid mechanics, chemical engineering, thermoelasticity, flow of groundwater, population dynamics, and more (see [27–29]). Furthermore, we also refer some significance of FODEs under integral boundary conditions as discussed in [27–31].

Recently, due to increasing applications of FODEs to model real world problems more comprehensively, researchers are taking keen interest to investigate different areas of fractional calculus. In particular, the use of FODEs in mathematical modeling of infectious diseases and other biological phenomena have got more attention. Various researchers have studied the fractional predator-prey pathogen model, the n-predator-prey model with herd behavior, etc. (see [32–34]). Further, there is also modeling of the interaction between tumor growth and the immune system, edge-detecting techniques, an infectious diesease on a pre-predator model, etc., (we refer to [35–40]).

As stated earlier, the area devoted to IDEs with a fractional order has many applications. These differential equations can be modeled to those evolutionary processes which are subjected to abrupt changes in their states. Recently, some authors have used IDEs for the mathematical modeling of certain biological events. It is remarkable that impulsive differential equations are using in mathematical models which give rise to some important dual-layered impulsive systems. The said systems will open new doors in the future to develop a general mathematical theory for the said systems. For instance, the author of [41] has obtained very interesting results in this regard for various kinds of biological models of infectious diseases. Here, we remark that a very basic and important qualitative problem in the investigation of IDEs with a fractional order concerns the existence theory of solutions. For these purposes, researchers have used the classical fixed point theory and some tools of nonlinear analysis. For instance, in [42], the authors have applied fixed point results to develop the corresponding existence theory of solutions by using the Caputo derivative of the fractional order. In the same line, in [43], the authors have used the Picard-type analysis to investigate the stochastic-type IDEs of a fractional order by using the Caputo operator. In all these papers, the Caputo operator has been increasingly used. It is to be noted that the fractional order derivative of the Riemann-Liouville type has been very rarely used in IDEs.

Authors [44] have established existence theory for fractional order IDEs with initial conditions by using the fixed point theory. The authors in [45] investigated the following problem of IDEs under the fractional order derivative of the Riemann-Liouville type as

$$\begin{cases} {}^{RL}\mathbf{D}^{\alpha_k} r(z) = f(z, r(z)), \quad z \in [0,T], z \neq z_m, 1 < \alpha_m \leq 2, z \in \mathcal{J}, z \neq z_m, \\ \Delta r(z_m) = \psi_m(r(z_m)), \quad m = 1,2,3,\cdots,q, \\ \Delta^* r(z_m) = \psi_m^*(r(z_m)), \quad m = 1,2,3,\cdots,q, \\ r(0) = 0, \quad \mathbf{D}^{\alpha_0 - 1} r(0) = \beta, \end{cases} \tag{1}$$

where $\beta \in \mathcal{R}$ and $f : [0,T] \times \mathcal{R} \longrightarrow \mathcal{R}$ is a continuous function. They developed sufficient conditions for the existence of at least one solution to the considered problem by using a fixed point approach.

Motivated from the said work given in (1), we are interested in studying a class of nonlinear implicit fractional order IDEs under the Riemann-Liouville derivative with the Riemann-Liouville-type integral boundary conditions as

$$\begin{cases} {}^{RL}\mathbf{D}^{\alpha_k} r(z) = f\left(z, r(z), \quad {}^{RL}\mathbf{D}^{\alpha} r(z)\right), 1 < \alpha \leq 2, z \in \mathcal{J}, z \neq z_m, \\ \Delta r(z_m) = \psi_m(r(z_m)), \quad m = 1,2,3,\cdots,q, \\ \Delta^* r(z_m) = \psi_m^*(r(z_m)), \quad m = 1,2,3,\cdots,q, \\ I^{1-\alpha} r(0) = 0, \quad I^{2-\alpha} r(1) = 0, \end{cases} \tag{2}$$

where ${}^{RL}\mathbf{D}$ is denoted as the Riemann-Liouville fractional order derivative, $\mathcal{J} = [0,1]$, $f : \mathcal{J} \times \mathcal{R} \times \mathcal{R} \longrightarrow \mathcal{R}$ is a continuous function. Furthermore, $\psi_m, \psi_m^* : \mathcal{R} \longrightarrow \mathcal{R}$ are continuous functions for $m = 1,2,\cdots,q$ and $\Delta r(z_m) = I_{z_m}^{1-\alpha} r(z_m^+) - I_{z_m}^{1-\alpha} r(z_m^-)$, $\Delta^* r(z_m) = I_{z_m}^{2-\alpha} r(z_m^+) - I_{z_m}^{2-\alpha} r(z_m^-)$ with $r(z_m^+) = \lim_{h \longrightarrow 0^+} r(z_m + h)$, $r(z_m^-) = \lim_{h \longrightarrow 0^-} r(z_m + h)$, $m = 1,2,. \cdots, q$, for $0 = z_0 < z_1 < z_2 \cdots < z_{q+1} = 1$. And also, where $I^{1-\alpha}$, $I^{2-\alpha}$ are denoted as the Riemann-Liouville integral of fractional order $1-\alpha < 0$, $2-\alpha > 0$ on $\mathcal{J}$, respectively. To establish the required results, we utilize the Scheafer fixed point theorem to investigate sufficient conditions for the existence of at least one solution to the problem under consideration (2). Furthermore, the criterion of uniqueness is derived by using the Banach contraction theorem. For the demonstration of our results, we provide some concrete examples.

2. Preliminaries

In this section, we provide some important results, basic definitions, and lemmas from the literature of fractional calculus [1, 3, 10, 11], which are needed in this manuscript.

Let $\mathcal{J} = [0,1]$, $\mathcal{J}_0 = (z_0, z_1]$, and $\mathcal{J}_m = (z_m, z_{m+1}]$ for $m = 1,2,3 \cdots q$. Suppose that $PC(\mathcal{J}, \mathcal{R}) = \{r : \mathcal{J} \longrightarrow \mathcal{R}; r \in \mathcal{C}((z_m, z_{m+1}], \mathcal{R}), m = 0,1,2,\cdots,q+1\}$ and $r(z_m^+)$ and $r(z_m^-)$ exist with $r(z_m^-) = \{r(z_m), m = 1,2,\cdots,q\}$. Note that $PC(\mathcal{J}, \mathcal{R})$ is a Banach space of piece-wise continuous function with norm $\|r\| = \sup_{z \in \mathcal{J}} |r(z)|$.

Definition 1. The integral of the Riemann-Liouville fractional order $\beta > 0$ of a continuous function $f : (0,\infty) \longrightarrow \mathcal{R}$ is defined by

$$\mathbf{I}^{\beta} f(z) = \int_0^z \frac{(z-s)^{\beta-1}}{\Gamma(\beta)} f(s) ds, \quad z \in (0,1). \tag{3}$$

Therefore, the right side is point-wise defined on $(0, \infty)$, where Γ is the symbol of gamma function defined as $\Gamma(\beta) = \int_0^{\infty} e^{-s} s^{\beta-1} ds$.

Definition 2. The derivative of the Riemann-Liouville fractional order $\beta > 0$, of a continuous function $f \in C[0,1] \cap L[0,1]$, $b > 0$ is defined by

$$ {}^{RL}\mathbf{D}^{\beta} f(z) = \left(\frac{d}{dz}\right)^{n} \int_0^z \frac{(z-s)^{n-\beta-1}}{\Gamma(n-\beta)} f(s)ds, \quad n-1 < \beta < n, z \in (0,1), \tag{4} $$

where $n = [\beta] + 1$, $[\beta]$ represent the whole part of the real number β; therefore, the right side is point-wise defined on $(0, \infty)$.

Definition 3. If the function $f : (c,d) \longrightarrow \mathscr{R}$ is at least n -times differentiable, then the Caputo fractional derivative of order $\beta > 0$ is defined as

$$ {}^{C}\mathbf{D}_c^{\beta} f(z) = \int_c^z \frac{(z-s)^{n-\beta-1}}{\Gamma(n-\beta)} f^n(s)ds, \quad n-1 < \beta < n, z \in (c,d), \tag{5} $$

where $n = [\beta] + 1$.

Lemma 4 [11]. *Suppose $\beta > 0$, and $r \in C(b,d) \cap L(b,d)$. Then, FODE*

$$ {}^{RL}\mathbf{D}^{\beta} r(z) = 0, \tag{6} $$

has a unique solution given by

$$ r(z) = d_1(z-b)^{\beta-1} + d_2(z-b)^{\beta-2} + \cdots + d_n(z-b)^{\beta-n}, \tag{7} $$

where $d_i \in \mathscr{R}$, $i = 1, 2, \cdots, n$, and $n-1 < \beta < n$.

Lemma 5 [11]. *In particular, $\beta > 0$ and $r \in C[0,1] \cap L[0,1]$. We have*

$$ I^{\beta}\mathbf{D}^{\beta} r(z) = r(z) + a_1 z^{\beta-1} + a_2 z^{\beta-2} + \cdots + a_n z^{\beta-n}, \tag{8} $$

where $a_k \in \mathscr{R}$, $k = 1, 2, \cdots, n$, and $n-1 < \beta < n$.

3. Main Works

To convert our considered problem in to an impulsive fractional integral equation, the given Lemma is provided.

Lemma 6. *The solution of the given linear IDE of the fractional order with the Riemann-Liouville derivative*

$$ \begin{cases} {}^{RL}\mathbf{D}^{\alpha} r(z) = \sigma(z), & 1 < \alpha \le 2, z \in \mathscr{J}, z \ne z_m, \\ \Delta r(z_m) = \psi_m(r(z_m)), & m = 1, 2, 3, \cdots, q, \\ \Delta^{*} r(z_m) = \psi_m^{*}(r(z_m)), & m = 1, 2, 3, \cdots q, \\ I^{1-\alpha} r(0) = 0, \quad I^{2-\alpha} r(1) = 0, \end{cases} \tag{9} $$

is given by

$$ r(z) = \begin{cases} \displaystyle\int_0^z \frac{(z-s)^{\alpha-1}}{\Gamma(\alpha)}\sigma(s)ds + z_m \left[\int_{z_m}^1 (1-s)^2\sigma(s)ds + \left((1-z_m)\left(\int_0^{z_m}(z_m-s)\sigma(s)ds - \psi_m(r(z_m))\right)\right)\right. \\ \qquad \left. + \left(\int_0^{z_m}(z_m-s)^2\sigma(s)ds - \psi_m^{*}(r(z_m))\right)\right] z^{\alpha-2}, z \epsilon [0, z_1], \\ \displaystyle\int_{z_m}^z \frac{(z-s)^{\alpha-1}}{\Gamma(\alpha)}\sigma(s)ds - \left[\left((z-z_m)^{\alpha-1} + \left((z-z_m)^{\alpha-1} + z_m(z-z_m)^{\alpha-2}\right)\right)(1-z_m)\right] \\ \qquad \times \left(\int_{z_{m-1}}^{z_m}(z_m-s)\sigma(s)ds - \psi_m(r(z_m))\right) - \left[(z-z_m)^{\alpha-2} + \left((z-z_m)^{\alpha-1} + z_m(z-z_m)^{\alpha-2}\right)\right] \\ \times \left(\displaystyle\int_{z_{m-1}}^{z_m}(z_m-s)^2\sigma(s)ds - \psi_m^{*}(r(z_m))\right) - \left((z-z_m)^{\alpha-1} + z_m(z-z_m)^{\alpha-2}\right)\left(\int_{z_m}^1 (1-s)^2\sigma(s)ds\right), z \epsilon (z_m, z_{m+1}]. \end{cases} \tag{10} $$

Proof. Suppose $r(z)$ is a solution to Problem (9); then, taking the Riemann-Liouville integral on both sides to using Lemma 5, there exist some constants $c_0, c_1 \in \mathscr{R}$ such that

$$ r(z) = \int_0^z \frac{(z-s)^{\alpha-1}}{\Gamma(\alpha)}\sigma(s)ds - c_0 z^{\alpha-1} - c_1 z^{\alpha-2}, \quad z \in [0, z_1]. \tag{11} $$

Again taking the Riemann-Liouville integral to using Lemma (9), for some constant $d_0, d_1 \in \mathscr{R}$, we have

$$ r(z) = \int_{z_1}^z \frac{(z-s)^{\alpha-1}}{\Gamma(\alpha)}\sigma(s)ds - d_0(z-z_1)^{\alpha-1} - d_1(z-z_1)^{\alpha-2}, \quad z \in (z_1, z_2]. \tag{12} $$

Now, by using the impulsive conditions, we have $\Delta r(z_1) = I_{z_1}^{1-\alpha} r(z_1^{+}) - I_{z_1}^{1-\alpha} r(z_1^{-}) = \psi_1(r(z_1))$ and $\Delta^{*} r(z_1) = I_{z_1}^{2-\alpha} r(z_1^{+}) - I_{z_1}^{2-\alpha} r(z_1^{-}) = \psi_1^{*}(r(z_1))$, and we find that

$$ -d_0 = \int_0^{z_1}(z_1-s)\sigma(s)ds - c_0 - c_1 z_1^{-1} + \psi_1(r(z_1)), $$

$$ -d_1 = \int_0^{z_1}(z_1-s)^2\sigma(s)ds - c_0 z_1 - c_1 + \psi_1^{*}(r(z_1)). \tag{13} $$

Thus, putting the values in (12), we have

$$\begin{aligned} r(z) = {} & \int_{z_1}^{z} \frac{(z-s)^{\alpha-1}}{\Gamma(\alpha)}\sigma(s)ds - (z-z_1)^{\alpha-1} \\ & \cdot \left(\int_0^{z_1}(z_1-s)\sigma(s)ds - \psi_1(r(z_1))\right) - (z-z_1)^{\alpha-2} \\ & \cdot \left(\int_0^{z_1}(z_1-s)^2\sigma(s)ds - \psi_1^*(r(z_1))\right) \\ & - c_0\left\{(z-z_1)^{\alpha-1} + z_1(z-z_1)^{\alpha-2}\right\} \\ & - c_1\left\{z_1^{-1}(z-z_1)^{\alpha-1} + (z-z_1)^{\alpha-2}\right\}, \quad z \in (z_1, z_2]. \end{aligned} \tag{14}$$

The above process can be repeated in this way until we obtain the solution $r(z)$ for $z \in (z_m, z_{m+1}]$ as

$$\begin{aligned} r(z) = {} & \int_{z_m}^{z} \frac{(z-s)^{\alpha-1}}{\Gamma(\alpha)}\sigma(s)ds - (z-z_m)^{\alpha-1} \\ & \cdot \left(\int_{z_{m-1}}^{z_m}(z_m-s)\sigma(s)ds - \psi_m(r(z_m))\right) - (z-z_m)^{\alpha-2} \\ & \cdot \left(\int_{z_{m-1}}^{z_m}(z_m-s)^2\sigma(s)ds - \psi_m^*(r(z_m))\right) \\ & - c_0\left\{(z-z_m)^{\alpha-1} + z_m(z-z_m)^{\alpha-2}\right\} \\ & - c_1\left\{z_m^{-1}(z-z_m)^{\alpha-1} + (z-z_m)^{\alpha-2}\right\}, \quad z \in (z_m, z_{m+1}]. \end{aligned} \tag{15}$$

Now, applying boundary condition $I^{1-\alpha}r(0) = 0$ and $I^{2-\alpha}r(1) = 0$ to get the values of constant c_0 and c_1, we have

$$\begin{aligned} & c_0 = 0, \\ & c_1 = z_m\int_{z_m}^{1}(1-s)^2\sigma(s)ds - z_m(1-z_m) \\ & \quad \cdot \left(\int_0^{z_m}(z_m-s)\sigma(s)ds - \psi_m(r(z_m))\right) \\ & \quad - z_m\left(\int_0^{z_m}(z_m-s)^2\sigma(s)ds - \psi_m^*(r(z_m))\right). \end{aligned} \tag{16}$$

The values of c_0, c_1 putting in (11) and (15), one can obtain (10). On the contrary, suppose $r(z)$ is a solution of the impulsive fractional integral equation (10). Following the direct calculation, we see that (10) satisfies the problem (9). □

For simplification, we use the following notations:

$$\sigma_1 = \sup_{z\in[0,1]}\left|(z-z_m)^{\alpha-1} + \left\{(z-z_m)^{\alpha-1} + z_m(z-z_m)^{\alpha-2}\right\}(1-z_m)\right|,$$

$$\sigma_2 = \sup_{z\in[0,1]}\left|(z-z_m)^{\alpha-2} + \left\{(z-z_m)^{\alpha-1} + z_m(z-z_m)^{\alpha-2}\right\}\right|,$$

$$\sigma_3 = \sup_{z\in[0,1]}\left|(z-z_m)^{\alpha-1} + z_m(z-z_m)^{\alpha-2}\right|. \tag{17}$$

For the existence and uniqueness of the solution, we use some fixed point theorems. To transform the considered Problem (2) to a fixed point problem, we need to define the operator by $M : PC(\mathcal{J}, \mathcal{R}) \longrightarrow PC(\mathcal{J}, \mathcal{R})$ as

$$\begin{aligned} Mr(z) = {} & \int_{z_m}^{z} \frac{(z-s)^{\alpha-1}}{\Gamma(\alpha)}\sigma(s)ds - \left[\left((z-z_m)^{\alpha-1}\right.\right. \\ & \left.\left. + \left((z-z_m)^{\alpha-1} + z_m(z-z_m)^{\alpha-2}\right)\right)(1-z_m)\right] \\ & \times \left(\int_{z_{m-1}}^{z_m}(z_m-s)\sigma(s)ds - \psi_m(r(z_m))\right) \\ & - \left[(z-z_m)^{\alpha-2} + \left((z-z_m)^{\alpha-1} + z_m(z-z_m)^{\alpha-2}\right)\right] \\ & \times \left(\int_{z_{m-1}}^{z_m}(z_m-s)^2\sigma(s)ds - \psi_m^*(r(z_m))\right) \\ & - \left((z-z_m)^{\alpha-1} + z_m(z-z_m)^{\alpha-2}\right)\left(\int_{z_m}^{1}(1-s)^2\sigma(s)ds\right). \end{aligned} \tag{18}$$

By using Lemma 6 with $r(z) = f(z, r(z), {}^{RL}\mathbf{D}^{\alpha}r(z))$, Problem (2) is reduced to a fixed point problem $Mr(z) = r(z)$, where the operator M is given by (18). Therefore, Problem (2) has a solution if and only if operator M has a fixed point, where $\tau(z) = f(z, r(z), \tau(z))$ and $\tau(z) = {}^{RL}\mathbf{D}^{\alpha}r(z)$. The following hypotheses are satisfied:

(H_1) The function $f : \mathcal{J} \times \mathcal{R} \times \mathcal{R} \longrightarrow \mathcal{R}$ is continuous

(H_2) There exist some constants $K^* > 0$ and $0 < L^* < 1$, such that

$$\begin{aligned} & |f(z, r(z), \tau(z)) - f(z, \bar{r}(z), \bar{\tau}(z))| \\ & \quad \le K^*|r(z) - \bar{r}(z)| + L^*|\tau(z) - \bar{\tau}(z)|, \end{aligned} \tag{19}$$

for any $r, \bar{r} \in PC(\mathcal{J}, \mathcal{R})$, $\tau, \bar{\tau} \in \mathcal{R}$, and $z \in \mathcal{J}$.

(H_3) There exists a constant $N_1^* > 0$, such that

$$|\psi_m(r(z)) - \psi_m(\bar{r}(z))| \le N_1^*|r(z) - \bar{r}(z)|, \tag{20}$$

for each $r, \bar{r} \in PC(\mathcal{J}, \mathcal{R})$ and $m = 1, 2, 3, \cdots, q$.

(H_4) There exists a constant $N_2^* > 0$, such that

$$|\psi_m^*(r(z)) - \psi_m^*(\bar{r}(z))| \le N_2^*|r(z) - \bar{r}(z)|, \tag{21}$$

for every $r, \bar{r} \in PC(\mathcal{J}, \mathcal{R})$ and $m = 1, 2, 3, \cdots, q$.

We use Banach fixed point theorem to prove that problem (2) has unique solution.

Theorem 7. *Under hypotheses (H_1)–(H_4) and if the following condition holds*

$$\left[\frac{K^*}{1-L^*}\left(\frac{1}{\Gamma(\alpha+1)}+\frac{\sigma_1}{2}+\frac{\sigma_2}{3}+\frac{\sigma_3}{3}\right)+(\sigma_1 N_1^*+\sigma_2 N_2^*)\right]<1, \tag{22}$$

then, there exists a unique solution for Problem (2) on $\mathscr{J}$.

Proof. Let $r,\bar{r}\in PC(\mathscr{J},\mathscr{R})$ for some $z\in\mathscr{J}$, we have

$$\begin{aligned}
&|Mr(z)-M\bar{r}(z)|\\
&\le\int_{z_m}^{z}\frac{(z-s)^{\alpha-1}}{\Gamma(\alpha)}|f(s,r(s),\tau(s))-f(s,\bar{r}(s),\bar{\tau}(s))|ds\\
&\quad+\left|(z-z_m)^{\alpha-1}+\left\{(z-z_m)^{\alpha-1}+z_m(z-z_m)^{\alpha-2}\right\}(1-z_m)\right|\\
&\quad\times\left(\int_{z_{m-1}}^{z_m}(z_m-s)|f(s,r(s),\tau(s))-f(s,\bar{r}(s),\bar{\tau}(s))|ds\right.\\
&\quad\left.+|\psi_m(r(z))-\psi_m(\bar{r}(z))|\right)+\left|(z-z_m)^{\alpha-2}\right.\\
&\quad\left.+\left\{(z-z_m)^{\alpha-1}+z_m(z-z_m)^{\alpha-2}\right\}\right|\\
&\quad\times\left(\int_{z_{m-1}}^{z_m}(z_m-s)^2|f(s,r(s),\tau(s))-f(s,\bar{r}(s),\bar{\tau}(s))|ds\right.\\
&\quad\left.+|\psi_m^*(r(z))-\psi_m^*(\bar{r}(z))|\right)+\left|(z-z_m)^{\alpha-1}+z_m(z-z_m)^{\alpha-2}\right|\\
&\quad\times\left(\int_{z_m}^{1}(1-s)^2|f(s,r(s),\tau(s))-f(s,\bar{r}(s),\bar{\tau}(s))|ds\right),
\end{aligned}\tag{23}$$

which further gives

$$\begin{aligned}
&|Mr(z)-M\bar{r}(z)|\\
&\le\int_{z_m}^{z}\frac{(z-s)^{\alpha-1}}{\Gamma(\alpha)}|\tau(s)-\bar{\tau}(s)|ds+|(z-z_m)^{\alpha-1}\\
&\quad+\left\{(z-z_m)^{\alpha-1}+z_m(z-z_m)^{\alpha-2}\right\}(1-z_m)|\\
&\quad\times\left(\int_{z_{m-1}}^{z_m}(z_m-s)|\tau(s)-\bar{\tau}(s)|+|\psi_m(r(z))-\psi_m(\bar{r}(z))|\right)\\
&\quad+\left|(z-z_m)^{\alpha-2}+\left\{(z-z_m)^{\alpha-1}+z_m(z-z_m)^{\alpha-2}\right\}\right|\\
&\quad\times\left(\int_{z_{m-1}}^{z_m}(z_m-s)^2|\tau(s)-\bar{\tau}(s)|ds+|\psi_m^*(r(z))-\psi_m^*(\bar{r}(z))|\right)\\
&\quad+\left|(z-z_m)^{\alpha-1}+z_m(z-z_m)^{\alpha-2}\right|\left(\int_{z_m}^{1}(1-s)^2|\tau(s)-\bar{\tau}(s)|ds\right),
\end{aligned}\tag{24}$$

where $\tau,\bar{\tau}\in\mathscr{C}(\mathscr{J},\mathscr{R})$ are given by

$$\begin{aligned}
\tau(z)&=f(z,r(z),\tau(z)),\\
\bar{\tau}(z)&=f(z,\bar{r}(z),\bar{\tau}(z)).
\end{aligned}\tag{25}$$

By using hypothesis (H_2), we have

$$\begin{aligned}
|\tau(z)-\bar{\tau}(z)|&=|f(z,r(z),\tau(z))-f(z,\bar{r}(z),\bar{\tau}(z))|\\
&\le K^*|r(z)-\bar{r}(z)|+L^*|\tau(z)-\bar{\tau}(z)|.
\end{aligned}\tag{26}$$

Repeating this process, we get

$$|\tau(z)-\bar{\tau}(z)|\le\frac{K^*}{1-L^*}|r(z)-\bar{r}(z)|. \tag{27}$$

Therefore, for every $z\in\mathscr{J}$ and from (24), using hypothesis (H_3), (H_4), and (27), one has

$$\begin{aligned}
&|Mr(z)-M\bar{r}(z)|\\
&\le\frac{K^*}{1-L^*}\int_{z_m}^{z}\frac{(z-s)^{\alpha-1}}{\Gamma(\alpha)}|r(s)-\bar{r}(s)|ds+|(z-z_m)^{\alpha-1}\\
&\quad+\left\{(z-z_m)^{\alpha-1}+z_m(z-z_m)^{\alpha-2}\right\}(1-z_m)|\\
&\quad\times\left(\frac{K^*}{1-L^*}\int_{z_{m-1}}^{z_m}(z_m-s)|r(s)-\bar{r}(s)|ds+N_1^*|r(z)-\bar{r}(z)|\right)\\
&\quad+\left|(z-z_m)^{\alpha-2}+\left\{(z-z_m)^{\alpha-1}+z_m(z-z_m)^{\alpha-2}\right\}\right|\\
&\quad\times\left(\frac{K^*}{1-L^*}\int_{z_{m-1}}^{z_m}(z_m-s)^2|r(s)-\bar{r}(s)|ds+N_2^*|r(z)-\bar{r}(z)|\right)\\
&\quad+\left|(z-z_m)^{\alpha-1}+z_m(z-z_m)^{\alpha-2}\right|\frac{K^*}{1-L^*}\\
&\quad\times\left(\int_{z_m}^{1}(1-s)^2|r(s)-\bar{r}(s)|ds\right).
\end{aligned}\tag{28}$$

Upon further simplification, (29) yields

$$\begin{aligned}
&\|Mr-M\bar{r}\|\\
&\le\frac{K^*}{1-L^*}\frac{(z-z_m)^{\alpha}}{\Gamma(\alpha+1)}\|r-\bar{r}\|+\sigma_1\left(\frac{K^*}{1-L^*}\frac{(z_m-z_{m-1})^2}{2}\|r-\bar{r}\|\right.\\
&\quad\left.+N_1^*\|r-\bar{r}\|\right)+\sigma_2\left(\frac{K^*}{1-L^*}\frac{(z_m-z_{m-1})^3}{3}\|r-\bar{r}\|+N_2^*\|r-\bar{r}\|\right)\\
&\quad+\sigma_3\frac{K^*}{1-L^*}\left(\frac{(1-z_m)^3}{3}\|r-\bar{r}\|\right).
\end{aligned}\tag{29}$$

Hence, from (29), we have

$$\begin{aligned}
&\|Mr-M\bar{r}\|\\
&\le\left[\frac{K^*}{1-L^*}\left(\frac{1}{\Gamma(\alpha+1)}+\frac{\sigma_1}{2}+\frac{\sigma_2}{3}+\frac{\sigma_3}{3}\right)+(\sigma_1N_1^*+\sigma_2N_2^*)\right]\\
&\quad\times\|r-\bar{r}\|.
\end{aligned}\tag{30}$$

By (22), operator M is a contraction. Thus, according to Banach's contraction principle, operator M has a unique fixed point which is the unique solution to Problem (2). □

Next, we will prove that Problem (2) has at least one solution for this, and we use Schaefer's fixed point theorem. Let the given hypotheses hold true:

(H_5) There exist $x, y, h \in PC(\mathcal{J}, \mathcal{R})$, with

$$\begin{aligned} x^* &= \sup_{z\in[0,1]} x(z), \\ y^* &= \sup_{z\in[0,1]} y(z), \\ h^* &= \sup_{z\in[0,1]} |h(z)| < 1, \end{aligned} \tag{31}$$

such that

$$|f(z, r(z), \tau(z))| \le x(z) + y(z)|r(z)| + h(z)|\tau(z)|, \tag{32}$$

for $z \in \mathcal{J}$, $r \in PC(\mathcal{J}, \mathcal{R})$, and $\tau \in \mathrm{R}$.

(H_6) The function $\psi_m : PC(\mathcal{J}, \mathcal{R}) \longrightarrow \mathcal{R}$ is continuous, and there exist constants $A_1^*, B_1^* > 0$ such that

$$|\psi_m(r(z))| \le A_1^*|r(z)| + B_1^*, \tag{33}$$

for every $r \in PC(\mathcal{J}, \mathcal{R})$, $m = 1, \cdots, q$.

(H_7) The function $\psi_m^* : PC(\mathcal{J}, \mathcal{R}) \longrightarrow \mathcal{R}$ is continuous, and there exist constants $A_2^*, B_2^* > 0$ such that

$$|\psi_m^*(r(z))| \le A_2^*|r(z)| + B_2^*, \tag{34}$$

for every $r \in PC(\mathcal{J}, \mathcal{R})$, $m = 1, \cdots, q$.

Theorem 8. *If the hypotheses (H_1), (H_2), (H_5)-(H_7) are satisfied, then Problem (2) has at least one solution.*

Proof. The proof is performed in several steps.

(Step 1) The operator M is continuous

Assume $\{r_n\}$ be a sequence such that $r_n \longrightarrow r$ on $PC(\mathcal{J}, \mathcal{R})$.

For $z \in \mathcal{J}$, we have

$$\begin{aligned} &|Mr_n(z) - Mr(z)| \\ &\le \int_{z_m}^{z} \frac{(z-s)^{\alpha-1}}{\Gamma(\alpha)} |\tau_n(s) - \tau(s)|ds + |(z - z_m)^{\alpha-1} \\ &\quad + \left\{(z - z_m)^{\alpha-1} + z_m(z - z_m)^{\alpha-2}\right\}(1 - z_m)| \\ &\quad \times \left(\int_{z_{m-1}}^{z_m} (z_m - s)|\tau_n(s) - \tau(s)|ds + |\psi_m(r_n(z)) - \psi_m(r(z))|\right) \\ &\quad + \left|(z - z_m)^{\alpha-2} + \left\{(z - z_m)^{\alpha-1} + z_m(z - z_m)^{\alpha-2}\right\}\right| \\ &\quad \times \left(\int_{z_{m-1}}^{z_m} (z_m - s)^2|\tau_n(s) - \tau(s)|ds + |\psi_m^*(r_n(z)) - \psi_m^*(r(z))|\right) \\ &\quad + \left|(z - z_m)^{\alpha-1} + z_m(z - z_m)^{\alpha-2}\right|\left(\int_{z_m}^{1} (1 - s)^2|\tau_n(s) - \tau(s)|ds\right), \end{aligned} \tag{35}$$

where $\tau_n(z), \tau(z) \in PC(\mathcal{J}, \mathcal{R})$ are given by

$$\begin{aligned} \tau_n(z) &= f(z, r_n(z), \tau_n(z)), \\ \tau(z) &= f(z, r(z), \tau(z)). \end{aligned} \tag{36}$$

Now, from assumption (H_2), we have

$$\begin{aligned} |\tau_n(z) - \tau(z)| &= |f(z, r_n(z), \tau_n(z)) - f(z, r(z), \tau(z))| \\ &\le K^*\|r_n - r\| + L^*|\tau_n(z) - \tau(z)|. \end{aligned} \tag{37}$$

Repeating this process, we get

$$|\tau_n(z) - \tau(z)| \le \frac{K^*}{1 - L^*}\|r_n - r\|. \tag{38}$$

Since $r_n \longrightarrow r$, $\tau_n(z) \longrightarrow \tau(z)$ as $n \longrightarrow \infty$ for every $z \in \mathcal{J}$. We know that every convergent sequence is bounded, so for this, let $\zeta > 0$ such that for every $z \in \mathcal{J}$, we have $|\tau_n(z)| \le \zeta$ and $|\tau(z)| \le \zeta$. Then, we have

$$\begin{aligned} (z-s)^{\alpha-1}|\tau_n(z) - \tau(z)| &\le (z-s)^{\alpha-1}[|\tau_n(z)| + |\tau(z)|] \\ &\le 2\zeta(z-s)^{\alpha-1}, \\ (z_m-s)^{\alpha-1}|\tau_n(z) - \tau(z)| &\le (z_m-s)^{\alpha-1}[|\tau_n(z)| + |\tau(z)|] \\ &\le 2\zeta(z_m-s)^{\alpha-1}, \end{aligned} \tag{39}$$

for every $z \in \mathcal{J}$; the function $s \longrightarrow 2\zeta(z-s)^{\alpha-1}$ and $s \longrightarrow 2\zeta(z_m-s)^{\alpha-1}$ are integrable on $[0, 1]$, upon the use of these facts and the Lebesque-dominated convergence theorem in (35). After using assumptions (H_5)-(H_7), we see that

$$|Mr_n(z) - Mr(z)| \longrightarrow 0, \quad \text{as } n \longrightarrow \infty, \tag{40}$$

and hence, we have

$$\|Mr_n - Mr\| \longrightarrow 0, \quad n \longrightarrow \infty. \tag{41}$$

Therefore, operator M is continuous.

(Step 2) The operator M assigns bounded sets to bounded sets on $PC(\mathcal{J}, \mathcal{R})$. Just prove it for any $\xi^* > 0$, there exists a positive constant E^*, such that for every $r \in D = \{r \in PC(\mathcal{J}, \mathcal{R}), \|r\| \le \xi^*\}$, we have $\|Mr\| \le E^*$. To derive this result for each $z \in \mathcal{J}$, one has

$$
\begin{aligned}
&|Mr(z)| \\
&\leq \int_{z_m}^{z} \frac{(z-s)^{\alpha-1}}{\Gamma(\alpha)} |\tau(s)|ds + |(z-z_m)^{\alpha-1} \\
&\quad + \left\{(z-z_m)^{\alpha-1} + z_m(z-z_m)^{\alpha-2}\right\}(1-z_m)| \\
&\quad \times \left(\int_{z_{m-1}}^{z_m} (z_m-s)|\tau(s)|ds + |\psi_m(r(z_m))|\right) \\
&\quad + \left|(z-z_m)^{\alpha-2} + \left\{(z-z_m)^{\alpha-1} + z_m(z-z_m)^{\alpha-2}\right\}\right| \\
&\quad \times \left(\int_{z_{m-1}}^{z_m} (z_m-s)^2|\tau(s)|ds + |\psi_m^*(r(z_m))|\right) \\
&\quad + \left|(z-z_m)^{\alpha-1} + z_m(z-z_m)^{\alpha-2}\right| \left(\int_{z_m}^{1} (1-s)^2|\tau(s)|ds\right),
\end{aligned} \tag{42}
$$

where $\tau(z) \in \mathscr{C}(\mathscr{J}, \mathscr{R})$ is given by

$$
\tau(z) = f(z, r(z), \tau(z)). \tag{43}
$$

By hypothesis (H_5) and for every $z \in \mathscr{J}$, we have

$$
\begin{aligned}
|\tau(z)| = |f(z, r(z), \tau(z))| &\leq x(z) + y(z)|r(z)| + h(z)|\tau(z)| \\
&\leq x(z) + y(z)\|r\| + h(z)|\tau(z)| \\
&\leq x(z) + y(z)\xi^* + h(z)|\tau(z)| \leq x^* + y^*\xi^* + h^*|\tau(z)|.
\end{aligned} \tag{44}
$$

Thus, we have

$$
|\tau(z)| \leq \frac{x^* + y^*\xi^*}{1-h^*} \coloneqq R^*. \tag{45}
$$

Therefore, from (42) by using (45), one has

$$
\begin{aligned}
|Mr(z)| \leq{}& \frac{R^*}{\Gamma(\alpha+1)} + \frac{\sigma_1 R^*}{2} + A_1^*\xi^* + B_1^* + \frac{\sigma_2 R^*}{3} \\
&+ A_2^*\xi^* + B_2^* + \frac{\sigma_3 R^*}{3}.
\end{aligned} \tag{46}
$$

Hence, one has

$$
\begin{aligned}
\|Mr\| &\leq \left[R^*\left(\frac{1}{\Gamma(\alpha+1)} + \frac{\sigma_1}{2} + \frac{\sigma_2}{3} + \frac{\sigma_3}{3}\right) + (A_1^* + A_2^*)\xi^* + B_1^* + B_2^*\right] \\
&\coloneqq E^*,
\end{aligned}
$$

$$
\|Mr\| \leq E^*. \tag{47}
$$

Therefore, the operator M is bounded.

(Step 3) The operator M assigns bounded sets to equicontinuous sets of $PC(\mathscr{J}, \mathscr{R})$. Let $z_1,\ z_2 \in \mathscr{J}$, and $z_1 < z_2$. D is a bounded set as in Step 2, and let $r \in D$; then, we have

$$
\begin{aligned}
&|Mr(z_2) - Mr(z_1)| \\
&\leq \left|\int_{z_m}^{z_2} \frac{(z_2-s)^{\alpha-1}}{\Gamma(\alpha)}\tau(s)ds - \int_{z_m}^{z_1} \frac{(z_1-s)^{\alpha-1}}{\Gamma(\alpha)}\tau(s)ds\right| \\
&\quad + \left|\left[(z_2-z_m)^{\alpha-1} + \left\{(z_2-z_m)^{\alpha-1} + z_m(z_2-z_m)^{\alpha-2}\right\}(1-z_m)\right]\right. \\
&\quad \left. - \left[(z_1-z_m)^{\alpha-1} + \left\{(z_1-z_m)^{\alpha-1} + z_m(z_1-z_m)^{\alpha-2}\right\}(1-z_m)\right]\right| \\
&\quad \times \left(\int_{z_{m-1}}^{z_m} (z_m-s)|\tau(s)|ds + |\psi_m(r(z_m))|\right) \\
&\quad + \left|\left[(z_2-z_m)^{\alpha-2} + \left\{(z_2-z_m)^{\alpha-1} + z_m(z_2-z_m)^{\alpha-2}\right\}\right]\right. \\
&\quad \left. - \left[(z_1-z_m)^{\alpha-2} + \left\{(z_1-z_m)^{\alpha-1} + z_m(z_1-z_m)^{\alpha-2}\right\}\right]\right| \\
&\quad \times \left(\int_{z_{m-1}}^{z_m} (z_m-s)^2|\tau(s)|ds + |\psi_m^*(r(z_m))|\right) \\
&\quad + \left|\left[(z_2-z_m)^{\alpha-1} + z_m(z_2-z_m)^{\alpha-2}\right]\right. \\
&\quad \left. - \left[(z_1-z_m)^{\alpha-1} + z_m(z_1-z_m)^{\alpha-2}\right]\right| \left(\int_{z_m}^{1} (1-s)^2|\tau(s)|ds\right).
\end{aligned} \tag{48}
$$

Using (45) and hypotheses (H_6) and (H_7) in (48), we obtain

$$
\begin{aligned}
&|Mr(z_2) - Mr(z_1)| \\
&\leq \frac{R^*}{\Gamma(\alpha+1)}\left((z_2-z_m)^{\alpha} - (z_1-z_m)^{\alpha}\right) \\
&\quad + \left[\frac{R^*(z_m-z_{m-1})^2}{2} + A_1^*\xi^* + B_1^*\right] \\
&\quad \times \left((z_2-z_m)^{\alpha-1} - (z_1-z_m)^{\alpha-1}\right)z_m \\
&\quad + \left[\frac{R^*(z_m-z_{m-1})^2}{2} + A_1^*\xi^* + B_1^*\right] \\
&\quad \times \left((z_2-z_m)^{\alpha-2} - (z_1-z_m)^{\alpha-2}\right)z_m(1-z_m) \\
&\quad + \left[\frac{R^*(z_m-z_{m-1})^3}{3} + A_2^*\xi^* + B_2^*\right] \\
&\quad \times \left((z_2-z_m)^{\alpha-2} - (z_1-z_m)^{\alpha-2}\right)(1+z_m) \\
&\quad + \left[\frac{R^*(z_m-z_{m-1})^3}{3} + A_2^*\xi^* + B_2^*\right] \\
&\quad \times \left((z_2-z_m)^{\alpha-1} - (z_1-z_m)^{\alpha-1}\right) + \left[\frac{R^*(1-z_m)^3}{3}\right] \\
&\quad \times \left((z_2-z_m)^{\alpha-1} - (z_1-z_m)^{\alpha-1}\right) + \left[\frac{R^*(1-z_m)^3}{3}\right] \\
&\quad \times \left((z_2-z_m)^{\alpha-2} - (z_1-z_m)^{\alpha-2}\right)(z_m).
\end{aligned} \tag{49}
$$

Clearly, in the inequality (49), the right hand side tends to zero as $z_1 \longrightarrow z_2$. Hence, $|Mr(z_2) - Mr(z_1)| \longrightarrow 0$ as $z_1 \longrightarrow z_2$. As a consequence of the passage from Step 1 to Step 3 combined with the Arzellá-Ascolli theorem, we

conclude that $M : PC(\mathcal{J}, \mathcal{R}) \longrightarrow PC(\mathcal{J}, \mathcal{R})$ is completely continuous.

(Step 4) In the last step, we need to show that the set $F = \{r(z) \in PC(\mathcal{J}, \mathcal{R})\colon r(z) = \mu M(r(z)), \text{for some } 0 < \mu < 1\}$ is bounded. Let $r \in F$; then, $r(z) = \mu M(r(z))$ for some $0 < i < 1$. Therefore, for every $z \in \mathcal{J}$, we have

$$\begin{aligned} r(z) &= \mu M(r(z)) \\ &= \mu \int_{z_m}^{z} \frac{(z-s)^{\alpha-1}}{\Gamma(\alpha)} \tau(s) ds \\ &\quad - \mu\left[\left((z-z_m)^{\alpha-1} + \left((z-z_m)^{\alpha-1} + z_m(z-z_m)^{\alpha-2}\right)\right)(1-z_m)\right] \\ &\quad \times \left(\int_{z_{m-1}}^{z_m} (z_m - s)\tau(s) ds - \psi_m(r(z_m))\right) \\ &\quad - \mu\left[(z-z_m)^{\alpha-2} + \left((z-z_m)^{\alpha-1} + z_m(z-z_m)^{\alpha-2}\right)\right] \\ &\quad \times \left(\int_{z_{m-1}}^{z_m} (z_m - s)^2 \tau(s) ds - \psi_m^*(r(z_m))\right) \\ &\quad - \mu\left((z-z_m)^{\alpha-1} + z_m(z-z_m)^{\alpha-2}\right)\left(\int_{z_m}^{1} (1-s)^2 \tau(s) ds\right). \end{aligned} \tag{50}$$

Now, we have

$$\begin{aligned} |r(z)| &= \mu |M(r(z))| \\ &\le \int_{z_m}^{z} \frac{(z-s)^{\alpha-1}}{\Gamma(\alpha)} |\tau(s)| ds + |(z-z_m)^{\alpha-1} \\ &\quad + \left\{(z-z_m)^{\alpha-1} + z_m(z-z_m)^{\alpha-2}\right\}(1-z_m)| \\ &\quad \times \left(\int_{z_{m-1}}^{z_m} (z_m - s)|\tau(s)| ds + |\psi_m(r(z_m))|\right) \\ &\quad + \left|(z-z_m)^{\alpha-2} + \left\{(z-z_m)^{\alpha-1} + z_m(z-z_m)^{\alpha-2}\right\}\right| \\ &\quad \times \left(\int_{z_{m-1}}^{z_m} (z_m - s)^2 |\tau(s)| ds + |\psi_m^*(r(z_m))|\right) \\ &\quad + \left|(z-z_m)^{\alpha-1} + z_m(z-z_m)^{\alpha-2}\right|\left(\int_{z_m}^{1} (1-s)^2 \mid \tau(s) \mid ds\right). \end{aligned} \tag{51}$$

Using (45) and hypotheses (H_6) and (H_7) in (51), we get

$$\begin{aligned} |r(z)| \le{}& \frac{R^*}{\Gamma(\alpha+1)} + \frac{\sigma_1 R^*}{2} + A_1^* \xi^* + B_1^* + \frac{\sigma_2 R^*}{3} \\ &+ A_2^* \xi^* + B_2^* + \frac{\sigma_3 R^*}{3}. \end{aligned} \tag{52}$$

Hence, one has from where

$$\begin{aligned} \|r\| &\le \left[R^*\left(\frac{1}{\Gamma(\alpha+1)} + \frac{\sigma_1}{2} + \frac{\sigma_2}{3} + \frac{\sigma_3}{3}\right) + (A_1^* + A_2^*)\xi^* + B_1^* + B_2^*\right] \\ &:= Z^*, \\ \|r\| &\le Z^*. \end{aligned} \tag{53}$$

Hence, the given set F is bounded as a result of the Schaefer fixed point theorem, and we conclude that operator M has at least one fixed point. Hence, the corresponding Problem (2) has at least one solution. □

4. Examples

Here, we provide two pertinent examples to verify the previous results.

Example 1. Consider the following IDE under the Riemann-Liouville-type integral boundary condition and the Riemann-Liouville fractional order derivative

$$\begin{cases} {}^{RL}\mathbf{D}^{\alpha} r(z) = \dfrac{z + \cos\left(r(z)\right) + \cos\left({}^{RL}\mathbf{D}^{\alpha} r(z)\right)}{90 + z^2}, \quad 1 < \alpha \le 2, z \in [0,1], z \ne \dfrac{1}{5}, \\ \Delta r\left(\dfrac{1}{5}\right) = \psi_1\left(r\left(\dfrac{1}{5}\right)\right) = \dfrac{\sin\left(r(1/5)\right)}{30}, \\ \Delta^* r\left(\dfrac{1}{5}\right) = \psi_1^*\left(r\left(\dfrac{1}{5}\right)\right) = \dfrac{e^{-r(1/5)}}{15}, \\ I^{1-\alpha} r(0) = 0, I^{2-\alpha} r(1) = 0. \end{cases} \tag{54}$$

where $\alpha = (1/2)$, we set

$$\begin{aligned} f(z, r(z), \tau(z)) = \frac{z + \cos\left(r(z)\right) + \cos\left(\tau(z)\right)}{90 + z^2}, \quad r(z) \in PC(\mathcal{J}, \mathcal{R}), \\ \tau(z) \in \mathcal{R}, \text{and } z \in [0,1]. \end{aligned} \tag{55}$$

Clearly f is a jointly continuous function.

Now for every $r(z),\ \bar{r}(z) \in PC(\mathcal{J}, \mathcal{R}),\ \tau(z),\ \bar{\tau}(z) \in \mathcal{R}$, and $z \in [0,1]$, we have

$$\begin{aligned} &|f(z, r(z), \tau(z)) - f(z, \bar{r}(z), \bar{\tau}(z))| \\ &\quad = \left|\frac{z + \cos\left(r(z)\right) + \cos\left(\tau(z)\right)}{90 + z^2} - \frac{z + \cos\left(\bar{r}(z)\right) + \cos\left(\bar{\tau}(z)\right)}{90 + z^2}\right| \\ &\quad = \left|\frac{\cos\left(r(z)\right) - \cos\left(\bar{r}(z)\right) + \cos\left(\tau(z)\right) - \cos\left(\bar{\tau}(z)\right)}{90 + z^2}\right| \\ &\quad \le \left|\frac{\cos\left(r(z)\right) - \cos\left(\bar{r}(z)\right)}{90 + z^2}\right| + \left|\frac{\cos\left(\tau(z)\right) - \cos\left(\bar{\tau}(z)\right)}{90 + z^2}\right|, \end{aligned}$$

$$|f(z, r(z), \tau(z)) - f(z, \bar{r}(z), \bar{\tau}(z))| \le \frac{1}{90}\left(|r - \bar{r}| + |\tau - \bar{\tau}|\right). \tag{56}$$

Which satisfies hypothesis (H_2) with $K^* = L^* = (1/90)$. Now, we set

$$\Delta r\left(\frac{1}{5}\right) = \psi_1\left(r\left(\frac{1}{5}\right)\right) = \frac{\sin\left(r(1/5)\right)}{30}, \quad r \in PC(\mathcal{J}, \mathcal{R}). \tag{57}$$

Then, for $r(z), \bar{r}(z) \in PC(\mathcal{J}, \mathcal{R})$, we have

$$\begin{aligned}&\left|\psi_1\left(r\left(\frac{1}{5}\right)\right) - \psi_1\left(r\left(\frac{1}{5}\right)\right)\right| \\ &= \left|\frac{\sin\left(r(1/5)\right)}{30} - \frac{\sin\left(\bar{r}(1/5)\right)}{30}\right| \leq \frac{1}{30}|r - \bar{r}|.\end{aligned} \tag{58}$$

Therefore, with $N_1^* = (1/30)$, hypothesis (H_3) is satisfied. Next, we set

$$\Delta^* r\left(\frac{1}{5}\right) = \psi_1^*\left(r\left(\frac{1}{5}\right)\right) = \frac{e^{-(r(1/5))}}{15}, \quad r \in PC(\mathcal{J}, \mathcal{R}). \tag{59}$$

Then, for $r(z), \bar{r}(z) \in PC(\mathcal{J}, \mathcal{R})$, we have

$$\left|\psi_1^*\left(r\left(\frac{1}{5}\right)\right) - \psi_1^*\left(r\left(\frac{1}{5}\right)\right)\right| = \left|\frac{e^{-(r(1/5))}}{15} - \frac{e^{-(\bar{r}((1/5)))}}{15}\right| \leq \frac{1}{15}|r - \bar{r}|. \tag{60}$$

Thus, with $N_2^* = (1/15)$, hypothesis (H_4) is satisfied. Further, we need to satisfy the given condition of Theorem 7, by

$$\begin{aligned}&\left[\frac{K^*}{1 - L^*}\left(\frac{1}{\Gamma(\alpha+1)} + \frac{\sigma_1}{2} + \frac{\sigma_2}{3} + \frac{\sigma_3}{3}\right) + (\sigma_1 N_1^* + \sigma_2 N_2^*)\right] \\ &= \frac{1}{90}\left[\left(\frac{1}{\Gamma(\alpha+1)} + \frac{35}{20} + \frac{55}{30} + \frac{28}{30}\right) + \frac{35}{300} + \frac{55}{150}\right] < 1.\end{aligned} \tag{61}$$

Therefore, all the hypotheses and conditions of Theorem 7 are satisfied. Therefore, the considered problem (54) has a unique solution on $\mathcal{J}$.

Example 2. Consider another example of IDE under the Riemann-Liouville-type integral boundary condition and the Riemann-Liouville fractional order derivative:

$$\begin{cases} {}^{RL}\mathbf{D}^{\alpha} r(z) = \dfrac{e^{-z} + e^{-2z}\sin\left(\sqrt{r(z)}\right) + \sin\left(\sqrt{{}^{RL}\mathbf{D}^{\alpha} r(z)}\right)}{35 + z^3}, \quad 1 < \alpha \leq 2, z \in [0,1], z \neq \dfrac{1}{7}, \\ \Delta r\left(\dfrac{1}{7}\right) = \psi_1\left(r\left(\dfrac{1}{7}\right)\right) = \dfrac{\tan\left(r(1/7)\right)}{25 + \tan\left(r(1/7)\right)}, \\ \Delta^* r\left(\dfrac{1}{7}\right) = \psi_1^*\left(r\left(\dfrac{1}{7}\right)\right) = \dfrac{e^{r(z)}}{55 + 30e^{r(z)}}, \\ I^{1-\alpha} r(0) = 0, I^{2-\alpha} r(1) = 0. \end{cases} \tag{62}$$

where $\alpha = (3/2)$ and ${}^{RL}\mathbf{D}^{\alpha} r(z) = \tau(z)$. We set

$$\begin{aligned}f(z, r(z), \tau(z)) &= \frac{e^{-z} + e^{-2z}\sin\left(\sqrt{r(z)}\right) + \sin\left(\sqrt{\tau(z)}\right)}{35 + z^3}, \\ &r(z) \in PC(\mathcal{J}, \mathcal{R}),\ \tau(z) \in \mathcal{R}, z \in [0,1].\end{aligned} \tag{63}$$

Clearly f is a jointly continuous function.

Now for every $r(z),\ \bar{r}(z) \in PC(\mathcal{J}, \mathcal{R}),\ \tau(z),\ \bar{\tau}(z) \in \mathcal{R}$, and $z \in [0,1]$, we have

$$\begin{aligned}&|f(z, r(z), \tau(z)) - f(z, \bar{r}(z), \bar{\tau}(z))| \\ &= \left|\frac{e^{-z} + e^{-2z}\sin\left(\sqrt{r(z)}\right) + \sin\left(\sqrt{\tau(z)}\right)}{35 + z^3}\right. \\ &\quad \left. - \frac{e^{-z} + e^{-2z}\sin\left(\sqrt{\bar{r}(z)}\right) + \sin\left(\sqrt{\bar{\tau}(z)}\right)}{35 + z^3}\right| \\ &\leq \left|\frac{e^{-2z}\left\{\sin\left(\sqrt{r(z)}\right) - \sin\left(\sqrt{\bar{r}(z)}\right)\right\}}{35 + z^3}\right| \\ &\quad + \left|\frac{\sin\left(\sqrt{\tau(z)}\right) - \sin\left(\sqrt{\bar{\tau}(z)}\right)}{35 + z^3}\right| \\ &\leq \frac{e^{-2z}}{35 + z^3}\left|\sqrt{r(z)} - \sqrt{\bar{r}(z)}\right| + \frac{1}{35 + z^3}\left|\sqrt{\tau(z)} - \sqrt{\bar{\tau}(z)}\right|,\end{aligned}$$

$$|f(z, r(z), \tau(z)) - f(z, \bar{r}(z), \bar{\tau}(z))| \leq \frac{1}{35}(|r - \bar{r}| + |\tau - \bar{\tau}|). \tag{64}$$

This satisfies hypothesis (H_2), with $K^* = L^* = (1/35)$.

Now, another hypotheses for every $r(z) \in PC(\mathcal{J}, \mathcal{R})$, $\tau(z) \in \mathcal{R}$, and $z \in [0, 1]$, we have

$$\begin{aligned} &|f(z, r(z), \tau(z))| \\ &= \left| \frac{e^{-z} + e^{-2z} \sin\left(\sqrt{r(z)}\right) + \sin\left(\sqrt{\tau(z)}\right)}{35 + z^3} \right| \\ &\leq \frac{e^{-z}}{35 + z^3} + \frac{e^{-2z}}{35 + z^3} \left|\sqrt{r(z)}\right| + \frac{1}{35 + z^3} \left|\sqrt{\tau(z)}\right| \\ &\leq \frac{e^{-z}}{35 + z^3} + \frac{e^{-2z}}{35 + z^3} |r(z)| + \frac{1}{35 + z^3} |\tau(z)|. \end{aligned} \tag{65}$$

Thus, hypothesis (H_5) is satisfied with $x(z) = (e^{-z}/35 + z^3)$, $y(z) = (e^{-2z}/35 + z^3)$, and $h(z) = (1/35 + z^3)$. Now, we set

$$\Delta r\left(\frac{1}{7}\right) = \psi_1\left(r\left(\frac{1}{7}\right)\right) = \frac{\tan\left(r(1/7)\right)}{25 + \tan\left(r(1/7)\right)}, \quad r \in PC(\mathcal{J}, \mathcal{R}). \tag{66}$$

Then, for every $r \in PC(\mathcal{J}, \mathcal{R})$, we have

$$\left|\psi_1\left(r\left(\frac{1}{7}\right)\right)\right| = \left|\frac{\tan\left(r(1/7)\right)}{25 + \tan\left(r(1/7)\right)}\right|, \quad \leq \frac{1}{25}|r| + 1. \tag{67}$$

Therefore, hypothesis (H_6) is satisfied with $A_1^* = (1/25)$ and $B_1^* = 1$. Next, we set

$$\Delta^* r\left(\frac{1}{7}\right) = \psi_1^*\left(r\left(\frac{1}{7}\right)\right) = \frac{e^{(r(1/7))}}{55 + 30e^{(r(1/7))}}, \quad r \in PC(\mathcal{J}, \mathcal{R}). \tag{68}$$

Then, for every $r \in PC(\mathcal{J}, \mathcal{R})$, we have

$$\left|\psi_1^*\left(r\left(\frac{1}{7}\right)\right)\right| = \left|\frac{e^{(r(1/7))}}{55 + 30e^{(r(1/7))}}\right|, \quad \leq \frac{1}{55}|r| + \frac{1}{30}. \tag{69}$$

Thus, hypothesis (H_7) is satisfied with $A_2^* = (1/55)$ and $B_2^* = (1/30)$. Therefore, all of the hypotheses of Theorem 8 are satisfied, and therefore, the considered problem (62) has at least one solution on $\mathcal{J}$.

5. Conclusion

IDEs of the fractional order have received proper attention due to their important applications in various fields of applied sciences. In the past, most studies have been done using the Caputo-type fractional derivatives to handle IDEs. In very few papers, investigating IDEs of the fractional order was done using the Riemann-Liouville derivative. Therefore, we have established successfully some important results devoted to the existence theory of a solution to the considered nonlinear implicit IDE with the Riemann-Liouville-type integral boundary conditions under the Riemann-Liouville fractional order derivative. The corresponding results for the existence and uniqueness of the solution have been archived by utilizing the classical Schiefer and Banach contraction fixed point theorems. For the demonstration of our results, we have enriched the paper by providing two pertinent examples.

Data Availability

Data used to support the findings of this study are included within the article.

Conflicts of Interest

No conflict of interest exist.

Authors' Contributions

Equal contribution has been done by all the authors.

Acknowledgments

This research was funded by the Deanship of Scientific Research at Princess Nourah bint Abdulrahman University through the Fast-track Research Funding Program to support publication in the top journal (Grant No: 42.FTTJ-87).

References

[1] J. T. Machado, V. Kiryakova, and F. Mainardi, "Recent history of fractional calculus," *Communications in Nonlinear Science and Numerical Simulation*, vol. 16, no. 3, pp. 1140–1153, 2011.

[2] R. Metzler and J. Klafter, "Boundary value problems for fractional diffusion equations," *Physica A: Statistical Mechanics and its Applications*, vol. 278, no. 1-2, pp. 107–125, 2000.

[3] K. B. Oldham, "Fractional differential equations in electrochemistry," *Advances in Engineering Software*, vol. 41, no. 1, pp. 9–12, 2010.

[4] F. A. Rihan, "Numerical modeling of fractional-order biological systems," *Abstract and Applied Analysis*, vol. 2013, Article ID 816803, 11 pages, 2013.

[5] J. Sabatier, O. P. Agrawal, and J. A. T. Machado, *Advances in Fractional Calculus*, Springer, Dordrecht, 2007.

[6] V. E. Tarasov, *Fractional Dynamics: Application of Fractional Calculus to Dynamics of Particles*, Fields and Media, Springer, Heidelberg, Higher Education Press, Beijing, 2010.

[7] B. M. Vintagre, I. Podlybni, A. Hernandez, and V. Feliu, "Some approximations of fractional order operators used in control theory and applications," *Fractional Calculus Applied Analysis*, vol. 3, no. 3, pp. 231–248, 2000.

[8] G. A. Anastassiou, "On right fractional calculus," *Chaos, Solitons and Fractals*, vol. 42, no. 1, pp. 365–376, 2009.

[9] D. Baleanu, Z. B. Güvenc, and J. A. T. Machado, *New Trends in Nanotechnology and Fractional Calculus Applications*, Springer, New York, 2010.

[10] E. Hiffer, *Application of Fractional Calculus in Physics*, Word Scientific, Singapore, 2000.

[11] A. A. Kilbas, H. M. Srivasta, and J. J. Trujilllo, *Theory and Application of Fractional Differential Equations*, North-Holland Mathematics Studies, North-Holand, Amsterdam, 2006.

[12] M. D. Ortigueira, *Fractional Calculus for Scientists and Engineers*, Springer, Dordrecht, Lecture Notes in Electrical Engineering edition, 2011.

[13] I. Podlubny, *Fractional Differential Equations*, Academic Press, San Diego, 1999.

[14] D. D. Bajnov and P. S. Simeonov, *Systems with Impulse Efect. Stability, Theory and Applications*, Ellis Horwood Series in Mathematics and Its Applications, Ellis Horwood Limited; New York etc.: Halsted Press, Chichester, 1989.

[15] M. Benchohra, J. Henderson, and V. Ntouyas, *Impulsive Diferential Equations and Inclusions*, Contemporary Mathematics and Its Applications, Hindawi Publishing Corporation, New York, 2006.

[16] V. Lakshmikantham, D. D. Bainov, and P. S. Simeonov, *Theory of Impulsive Differential Equations*, Series in Modern Applied Mathematics, World Scientific, Singapore etc., 1989.

[17] A. M. Samoilenko and N. A. Perestyuk, *Impulsive Diferential Equations*, World Scientifc Series on Nonlinear Science. Series A: Monographs and Treatises, World Scientifc Publishing Co., Inc., River Edge, New Jersey, 1995, (Translated from the Russian).

[18] M. Benchohra and B. A. Slimani, "Impulsive fractional diferential equations," (submitted).

[19] A. Ali, F. Rabiei, and K. Shah, "On Ulam's type stability for a class of impulsive fractional differential equations with nonlinear integral boundary conditions," *The Journal of Nonlinear Sciences and Applications*, vol. 10, no. 9, pp. 4760–4775, 2017.

[20] Y. V. Rogovchenko, "Impulsive evolution systems: main results and new trends," *Dynamics of Continuous, Discrete and Impulsive Systems series*, vol. 3, no. 1, pp. 57–88, 1997.

[21] K. Shah, K. Ali, and S. Bushnaq, "Hyers-Ulam stability analysis to implicit Cauchy problem of fractional differential equations with impulsive conditions," *Mathematical Methods in the Applied Sciences*, vol. 41, pp. 1–15, 2018.

[22] K. Shah, H. Khalil, and R. A. Khan, "Investigation of positive solution to a coupled system of impulsive boundary value problems for nonlinear fractional order differential equations," *Chaos, Solitons and Fractals*, vol. 77, pp. 240–246, 2015.

[23] J. X. Sun, *Nonlinear Functional Analysis and Its Application*, Science Press, Beijing, 2008.

[24] G. Wang, L. Zhang, and G. Song, "Extremal solutions for the first order impulsive functional differential equations with upper and lower solutions in reversed order," *Journal of Computational and Applied Mathematics*, vol. 235, no. 1, pp. 325–333, 2010.

[25] S. T. Zavalishchin and A. N. Sesekin, *Dynamic Impulse Systems. Theory and Applications*, Kluwer Academic, Dordrecht, 1997.

[26] X. Zhang, P. Agarwal, Z. Liu, and H. Peng, "The general solution for impulsive differential equations with Riemann-Liouville fractional-order $q \in (1, 2)$," *Open Mathematics*, vol. 13, no. 1, pp. 908–923, 2015.

[27] R. P. Agarwal, M. Benchohra, and S. Hamani, "Boundary value problems for fractional differential equations," *Georgian Mathematical Journal*, vol. 16, no. 3, pp. 401–411, 2009.

[28] A. Cabada and G. Wang, "Positive solutions of nonlinear fractional differential equations with integral boundary value conditions," *Journal of Mathematical Analysis and Applications*, vol. 389, no. 1, pp. 403–411, 2012.

[29] B. Ahmad and J. J. Nieto, "Existence results for nonlinear boundary value problems of fractional integrodifferential equations with integral boundary conditions," *Boundary Value Problems*, vol. 2009, Article ID 708576, 11 pages, 2009.

[30] B. Ahmad, J. J. Nieto, and A. Alsaedi, "Existence and uniqueness of solutions for nonlinear fractional differential equations with non-separated type integral boundary conditions," *Acta Mathematica Scientia*, vol. 31, no. 6, pp. 2122–2130, 2011.

[31] B. Ahmad and S. Sivasundaram, "Existence of solutions for impulsive integral boundary value problems of fractional order," *Nonlinear Analysis: Hybrid Systems*, vol. 4, no. 1, pp. 134–141, 2010.

[32] W. M. Ahmad and R. el-Khazali, "Fractional-order dynamical models of love," *Chaos, Solitons & Fractals*, vol. 33, no. 4, pp. 1367–1375, 2007.

[33] K. Adolfsson, M. Enelund, and P. Olsson, "On the fractional order model of viscoelasticity," *Mechanics of Time-dependent Materials*, vol. 9, no. 1, pp. 15–34, 2005.

[34] E. Ahmed, A. Hashish, and F. A. Rihan, "On fractional order cancer model," *Journal of Fractional Calculus and Applications*, vol. 3, no. 2, pp. 1–6, 2012.

[35] X. Yang, X. Jiang, and J. Kang, "Parameter identification for fractional fractal diffusion model based on experimental data," *Chaos: An Interdisciplinary Journal of Nonlinear Science*, vol. 29, no. 8, p. 083134, 2019.

[36] C. Cattani, H. M. Srivastava, and X.-J. Yang, *Fractional Dynamics*, De Gruyter Open Poland, 2016.

[37] M. A. Dokuyucu and H. Dutta, "A fractional order model for Ebola virus with the new Caputo fractional derivative without singular kernel," *Chaos, Solitons & Fractals*, vol. 134, p. 109717, 2020.

[38] M. Arfan, H. Alrabaiah, M. U. Rahman et al., "Investigation of fractal-fractional order model of COVID-19 in Pakistan under Atangana-Baleanu Caputo (ABC) derivative," *Results in Physics*, vol. 24, p. 104046, 2021.

[39] A. Atangana, A. Akgül, and K. M. Owolabi, "Analysis of fractal fractional differential equations," *Alexandria Engineering Journal*, vol. 59, no. 3, pp. 1117–1134, 2020.

[40] A. Atangana, M. A. Khan, and Fatmawati, "Modeling and analysis of competition model of bank data with fractal-fractional Caputo-Fabrizio operator," *Alexandria Engineering Journal*, vol. 59, no. 4, pp. 1985–1998, 2020.

[41] R. Miron, "Impulsive differential equations with applications to infectious diseases, doctoral dissertation," Université d'Ottawa/University of Ottawa, Canada, 2014.

[42] Asma, A. Ali, K. Shah, and F. Jarad, "Ulam-Hyers stability analysis to a class of nonlinear implicit impulsive fractional differential equations with three point boundary conditions," *Advances in Difference Equations*, vol. 2019, no. 1, Article ID 7, 2019.

[43] D. Yang and J. R. Wang, "Non-instantaneous impulsive fractional-order implicit differential equations with random effects," *Stochastic Analysis and Applications*, vol. 35, no. 4, pp. 719–741, 2017.

[44] Q. Chen, A. Debbouche, Z. Luo, and J. R. Wang, "Impulsive fractional differential equations with Riemann-Liouville derivative and iterative learning control," *Chaos, Solitons & Fractals*, vol. 102, pp. 111–118, 2017.

[45] W. Yukunthorn, S. K. Ntouyas, and J. Tariboon, "Impulsive multiorders Riemann-Liouville fractional differential equations," *Discrete Dynamics in Nature and Society*, vol. 2015, Article ID 603893, 9 pages, 2015.

Hindawi
Journal of Function Spaces
Volume 2021, Article ID 6069201, 17 pages
https://doi.org/10.1155/2021/6069201

Research Article

Further Developments of Bessel Functions via Conformable Calculus with Applications

Mahmoud Abul-Ez,[1] **Mohra Zayed**,[2] **and Ali Youssef**[1]

[1]*Mathematics Department, Faculty of Science, Sohag University, Sohag 82524, Egypt*
[2]*Mathematics Department, College of Science, King Khalid University, Abha, Saudi Arabia*

Correspondence should be addressed to Mohra Zayed; mzayed@kku.edu.sa

Received 9 June 2021; Revised 1 August 2021; Accepted 26 August 2021; Published 27 September 2021

Academic Editor: Badr Saad. T. Alkaltani

The theory of Bessel functions is a rich subject due to its essential role in providing solutions for differential equations associated with many applications. As fractional calculus has become an efficient and successful tool for analyzing various mathematical and physical problems, the so-called fractional Bessel functions were introduced and studied from different viewpoints. This paper is primarily devoted to the study of developing two aspects. The starting point is to present a fractional Laplace transform via conformable fractional-order Bessel functions (CFBFs). We establish several important formulas of the fractional Laplace Integral operator acting on the CFBFs of the first kind. With this in hand, we discuss the solutions of a generalized class of fractional kinetic equations associated with the CFBFs in view of our proposed fractional Laplace transform. Next, we derive an orthogonality relation of the CFBFs, which enables us to study an expansion of any analytic functions by means of CFBFs and to propose truncated CFBFs. A new approximate formula of conformable fractional derivative based on CFBFs is provided. Furthermore, we describe a useful scheme involving the collocation method to solve some conformable fractional linear (nonlinear) multiorder differential equations. Accordingly, several practical test problems are treated to illustrate the validity and utility of the proposed techniques and examine their approximate and exact solutions. The obtained solutions of some fractional differential equations improve the analog ones provided by various authors using different techniques. The provided algorithm may be beneficial to enrich the Bessel function theory via fractional calculus.

1. Introduction

The theory of special functions is a critical branch of modern mathematical analysis. During the past three decades, several new classes of special functions have been proposed as solutions of fractional differential equations (FDEs). No other special functions have received such detailed treatment in readily available treatises as Bessel functions. The investigation of such functions is an important problem in fractional calculus, which has earned much attention as real-life problems can be analyzed well. Fractional calculus appears in many branches of science, such as medicine, material sciences, electromagnetics, and fluid mechanics (see [1–4]). Many applications have been performed through FDEs, and their solution techniques could be found, for example, in [5–11].

We trace the existing efforts regarding fractional order derivatives. Several definitions of the fractional order derivative have been introduced by many famous authors, such as Euler, Fourier, Letnikov, Laurent, Grünwald-Letnikov, Caputo, and Riemann-Liouville. Other definitions have also been provided by Kilbas et al. and Miller and Ross in [3, 10]. The most popular definitions considered frequently in the literature are derivatives by Riemann-Liouville, Caputo, and Grünwald-Letnikov. Interestingly, each definition of the arbitrary order derivative captures only a few properties of the classical integral derivative. However, a few drawbacks exist; for instance, $\mathscr{D}_a^{\alpha}(1) = 0$ does not fulfill the Riemann-Liouville definition. In Caputo's definition, $f(x)$ is assumed to be differentiable; otherwise, one cannot use such a definition. Moreover, Liouville's theorem in the fractional setting does not hold. Therefore, it is clear that all definitions of

fractional derivatives seem deficient regarding certain mathematical properties, such as the rules of product, quotient, and chain. For more details concerning other properties of these fractional order derivatives, see, for example, [4] and the references therein.

Due to the mentioned arguments, a new definition of the fractional order derivative is needed to achieve suitable mathematical properties. Khalil et al. [12] introduced a well-extended definition of the noninteger order derivative called the conformable fractional derivative (CFD). This definition is formulated as follows:

Definition 1 (see [12]). For the initial real value a, the conformable fractional derivative $\mathscr{D}_a^\alpha f(x)$ of a real function $f : [a, \infty) \longrightarrow \mathbb{R}, \alpha \in (0, 1]$ is defined by the following:

$$\mathscr{D}_a^\alpha f(x) = \lim_{h \longrightarrow 0} \frac{f\left(x + h(x-a)^{1-\alpha}\right) - f(x)}{h}, \quad \text{for all } x > a. \tag{1}$$

The initial value a can be zero, and if the limit exists, then $f(x)$ is called α-differentiable.

Along with the CFD's Definition 1, if $f(x)$ is differentiable, then $\mathscr{D}^\alpha f(x) = x^{1-\alpha} f'(x)$ (see [12]). Moreover, if Definition 1 holds for $\alpha = 0$, we obtain $\mathscr{D}^0 f(x) = f(x)$. Additionally, we have $\mathscr{D}^0 f(x) = x f'(x)$; hence, $x = f(x)/f'(x)$, which indicates that x relies on some functions; it is unreasonable. Therefore, the CFD definition [12] does not need to hold for zero order. For the conformable fractional integral, we state the following definition as given in the following [12]:

Definition 2 (see [12]). Let $f : [0, \infty) \longrightarrow \mathbb{R}$. Then, for any $\beta \in (0, 1]$, the conformable fractional integral $I_\beta f(x)$ of order β of f is defined as follows:

$$I_\beta f(x) = \int_0^x t^{\beta-1} f(t) dt. \tag{2}$$

Definition 1 depends entirely on the basic limit like the classical order derivative. Furthermore, Definition 1 fulfills various classical properties, such as the mean value theorem and the product, quotient, and chain rules. Moreover, this definition is provided with the Leibniz rule, in which other fractional derivatives can not achieve (see [13]). Growing attention has been paid to explore the conformable derivatives due to the enormous number of their meaningful applications in many fields of science. Abul-Ez et al. [14] introduced a comprehensive study on the conformable fractional Legendre polynomials. They presented the shifted conformable fractional Legendre polynomials and described an applicable scheme using the collocation method to solve some fractional differential equations (FDEs) in the sense of conformable derivative. Recently, the conformable fractional Gauss hypergeometric function and a class of conformable fractional differential equations through that function were treated in [15]. Further interesting ideas on the conformable derivative can be found in the work by [16–23].

Note that some authors have demonstrated that the conformable derivative is not the same as a fractional order derivative, but it is a first-order derivative multiplied by an additional factor (see for example [23]). Hence, Definition 1 seems to be a natural extension of the conventional order derivative to noninteger order loosing memory effect. In addition, a new approach for finding fractional operators was introduced by Antagan and Baleanu [24] with a nonsingular Mittag-Leffler kernel with a memory effect.

Returning to the purpose of the present work, we observe that Bessel functions are playing a significant role in investigating the solution of important differential equations (for example, see [25]). The theory of Bessel functions is usually used when solving problems related to information theory, nuclear physics, radiophysics, and hydrodynamics. Recently, as in [26–30], a resurgence of interest has occurred in the study of Bessel functions in the framework of fractional calculus theory. Along with the work in [26, 27], we employ conformable fractional order Bessel functions (CFBFs) to solve problems of a fractional nature. The study of a Bessel function of half-integer order led to discovering another interesting class of orthogonal polynomials called the Bessel polynomials. Many authors have used these polynomials. For example, Yüzbaşi et al. [31] solved linear integral, differential, and integro-differential equations, while Parand et al. [32] applied Bessel functions to solve nonlinear Lane-Emden equations. In [33], fractional optimal control problems were solved using the Bessel collocation method.

The present work proposes an approach to approximating the solution for some important linear and nonlinear FDEs in the conformable sense. The paper is designed with two objectives. The first is to establish some interesting properties of fractional Laplace-type integrals of functions via CFBFs. Then, we use the obtained results to establish the possible solutions of conformable fractional kinetic equations through CFBFs. The second objective is concerned with developing applications of the fundamental process of the proposed approach in terms of CFBFs. To achieve that, we derive an orthogonality relation, expand functions in terms of the truncated CFBFs, and effectively formulate a scheme involving the collocation method which employed to provide solutions of certain types of linear and nonlinear CFBEs.

The structure of this paper is organized as follows. The needed concepts and features of CFD are collected in Section 2. Next, Section 3 establishes useful properties of Laplace transforms in the sense of CFBFs, with some applications to solve a new type of conformable fractional kinetic equations. Section 4 is divided into four subsections. Section 4.1 provides essential results on orthogonality relations. A brief study on an expansion of any analytic function employing CFBFs is the subject of Section 4.2. In Section 4.3, we construct an algorithm for solving various kinds of problems using CFBFs through the collocation method. Section 4.4 presents the concepts that have been developed through previous subsections to solve some linear and nonlinear conformable fractional differential equations (CFDEs), including the nonlinear Riccati FDE. Concluding remarks are provided in Section 5.

2. Preliminaries and Basic Concepts

The Bessel equation is a special case of the Sturm-Liouville problem, and it can be written as [34]

$$x^2y'' + xy' + \left(x^2 - n^2\right)y = 0. \tag{3}$$

In view of formula (1), the authors of [26] solved the following conformable fractional Bessel equation:

$$x^{2\alpha}\mathscr{D}^\alpha\mathscr{D}^\alpha y + \alpha x^\alpha \mathscr{D}^\alpha y + \alpha^2\left(x^{2\alpha} - n^2\right)y = 0, \tag{4}$$

around the regular singular point $x = 0$, and introduced the CFBFs of the first kind $J_n^\alpha(x)$ as its solution such that

$$J_n^\alpha(x) = \sum_{\kappa=0}^{\infty} \frac{(-1)^\kappa}{\kappa!\Gamma(n+\kappa+1)}\left(\frac{x^\alpha}{2}\right)^{n+2\kappa}. \tag{5}$$

Moreover, they investigated in [26] some of its recurrence relations from which we may mention

$$\begin{aligned}
\mathscr{D}^\alpha[x^{\alpha n}J_n^\alpha(x)] &= \alpha x^{\alpha n}J_{n-1}^\alpha(x),\\
\mathscr{D}^\alpha[x^{-\alpha n}J_n^\alpha(x)] &= -\alpha x^{-\alpha n}J_{n+1}^\alpha(x),\\
\mathscr{D}^\alpha[J_n^\alpha(x)] &= \alpha J_{n-1}^\alpha(x) - \frac{\alpha n}{x^\alpha}J_n^\alpha(x),\\
\mathscr{D}^\alpha[J_n^\alpha(x)] &= \frac{\alpha n}{x^\alpha}J_n^\alpha(x) - \alpha J_{n+1}^\alpha(x),
\end{aligned} \tag{6}$$

In the following, we are about to recall some essential definitions and results which are needed in the sequel.

Definition 3. The Gauss hypergeometric function ${}_2F_1(a, b; c; x)$ is defined by (see [35])

$${}_2F_1(a, b; c; x) = \sum_{n=0}^{\infty}\frac{(a)_n(b)_n}{(c)_n}\frac{x^n}{n!}, \quad |x| < 1 \tag{7}$$

where $(\delta)_n$ stands for the familiar Pochhammar symbol which can be written in terms of Gamma function as

$$(\delta)_n = \frac{\Gamma(\delta+n)}{\Gamma(\delta)} = \delta(\delta+1)(\delta+2),\cdots,(\delta+n-1),\ n\in\mathbb{N},\ (\delta)_0 = 1 \tag{8}$$

Definition 4 (see [36]). The function ${}_p\psi_q(x)$ where p and q refer to its numerators and denominators, respectively, is called the Fox-Wright function, and it can be defined by the formula

$${}_p\psi_q(x) = {}_p\psi_q\left(\begin{matrix}(a_i,\mu_i)_{1,p}\\(b_j,\nu_j)_{1,q}\end{matrix};x\right) = \sum_{n=0}^{\infty}\frac{\prod_{i=1}^{p}\Gamma(a_i+n\mu_i)}{\prod_{j=1}^{q}\Gamma\left(b_j+n\nu_j\right)}\frac{x^n}{n!}, \tag{9}$$

such that $\sum_{j=1}^{q}\nu_j - \sum_{i=1}^{p}\mu_i > -1$, where $a_i, b_j \in \mathbb{R}(i = 1, 2, \cdots, p; j = 1, 2, \cdots, q)$.

In particular, when $\mu_i = \nu_j = 1$ in Definition 4, then the function ${}_p\psi_q(x)$ immediately reduced to the generalized hypergeometric function ${}_pF_q$ (see [35]). Abdeljawad [16] defined the fractional Laplace transform in the conformable sense as follows:

Definition 5 (see [16]). For a real valued function $f : [0,\infty) \longrightarrow \mathbb{R}$, the conformable fractional Laplace transform of noninteger order $\alpha, \alpha \in (0, 1]$ is given by

$$L_\alpha[f(t)] = F_\alpha(s) = \int_0^\infty e^{-s(t^\alpha/\alpha)}f(t)d_\alpha t = \int_0^\infty e^{-s(t^\alpha/\alpha)}f(t)t^{\alpha-1}dt. \tag{10}$$

The inverse fractional Laplace transform is the transformation of a fractional Laplace transform into a function of time. If $L_\alpha[f(t)] = F_\alpha(s)$, then $f(t)$ is the inverse fractional Laplace transform of $F_\alpha(s)$, and it can be written as

$$L_\alpha^{-1}[F_\alpha(s)] = f(t). \tag{11}$$

Remark 6. If $\alpha = 1$, then (10) is the classical definition of the Laplace transform of integer order.

Furthermore, the author in [16] gave the following interesting results.

Lemma 7 [16]. *For a real valued function $f : [0,\infty) \longrightarrow \mathbb{R}$ satisfying $L_\alpha[f(t)] = F_\alpha(s), \alpha \in (0, 1]$, the following relations hold true:*

(1) $F_\alpha(s) = L[f(\alpha t)^{1/\alpha}]$, *where* $L[f(t)] = \int_0^\infty e^{-st}f(t)dt$

(2) $L_\alpha[1] = 1/s,\ s > 0$

(3) $L_\alpha[t^p] = \alpha^{p/\alpha}((\Gamma(1+(p/\alpha)))/(s^{1+(p/\alpha)})),\ s > 0$

(4) $L_\alpha[e^{k(t^\alpha/\alpha)}] = 1/(s-k)$

3. Fractional Laplace Transform of the CFBFs

In this section, we derive some new interesting fractional Laplace-type integrals of functions involving CFBFs. Then, as an application, we are going to employ the obtained results in order to find the possible solutions of the fractional kinetic equations in the conformable sense associated with CFBFs.

3.1. Fractional Laplace Integral Formulas

Theorem 8. *Let $J_n^\alpha(x)$, $\alpha \in (0, 1]$ be the CFBFs; then,*

$$L_\alpha\{J_n^\alpha(t)\} = \frac{\alpha^n}{2^n s^{n+1}}\,{}_2F_1\left(\frac{n+1}{2}, \frac{n}{2}+1; n+1; \frac{-\alpha^2}{s^2}\right). \tag{12}$$

Proof. Owing to the definition of CFBFs (5) and applying the conformable fractional Laplace transform operator of order $\alpha \in (0, 1]$ as stated in Lemma 7, we have

$$L_\alpha\{J_n^\alpha(t)\} = \sum_{\kappa=0}^{\infty} \frac{(-1)^\kappa}{\kappa!\Gamma(n+\kappa+1)2^{n+2\kappa}} L_\alpha\left\{t^{\alpha(n+2\kappa)}\right\}. \tag{13}$$

According to (3) of Lemma 7, one can see

$$\begin{aligned} L_\alpha\{J_n^\alpha(t)\} &= \sum_{\kappa=0}^{\infty} \frac{(-1)^\kappa}{\kappa!\Gamma(n+\kappa+1)2^{n+2\kappa}} \frac{\alpha^{n+2\kappa}\Gamma(n+2\kappa+1)}{s^{n+2\kappa+1}} \\ &= \frac{\alpha^n}{2^n s^{n+1}} \sum_{\kappa=0}^{\infty} \frac{\Gamma(n+2\kappa+1)}{\kappa!\Gamma(n+\kappa+1)2^{2\kappa}} \left[\frac{-\alpha^2}{s^2}\right]^\kappa \\ &= \frac{\alpha^n}{2^n s^{n+1}} \sum_{\kappa=0}^{\infty} \frac{(n+1)_{2\kappa}}{\kappa!(n+1)_\kappa 2^{2\kappa}} \left[\frac{-\alpha^2}{s^2}\right]^\kappa. \end{aligned} \tag{14}$$

Using the identity $(n+1)_{2\kappa} = 2^{2\kappa}((n+1)/2)_\kappa((n/2)+1)_\kappa$, we obtain

$$L_\alpha\{J_n^\alpha(t)\} = \frac{\alpha^n}{2^n s^{n+1}} \sum_{\kappa=0}^{\infty} \frac{((n+1)/2)_\kappa((n/2)+1)_\kappa}{\kappa!(n+1)_\kappa} \left[\frac{-\alpha^2}{s^2}\right]^\kappa. \tag{15}$$

Therefore, the result is established. □

Now, consider the Fox-Wright function ${}_1\Psi_1$ defined in (9) to deduce the following important results.

Theorem 9. *Let $J_n^\alpha(x), \alpha \in (0, 1]$ be the CFBFs. Then, the following relation is satisfied:*

$$L_\alpha\{J_n^\alpha(a^\mu t^\mu)\} = \frac{(\alpha a)^{\mu n}}{2^n s^{\mu n+1}} {}_1\psi_1\left(\begin{matrix}(\mu n+1, 2\mu)\\(n+1, 1)\end{matrix}; \frac{(\alpha a)^{2\mu}}{4s^{2\mu}}\right). \tag{16}$$

Proof. By combining (5) and (10), we get

$$\begin{aligned} L_\alpha\{J_n^\alpha(a^\mu t^\mu)\} &= L_\alpha\left\{\sum_{\kappa=0}^{\infty} \frac{(-1)^\kappa}{\kappa!\Gamma(n+\kappa+1)} \left(\frac{a^\mu t^{\mu\alpha}}{2}\right)^{(n+2\kappa)}\right\} \\ &= \sum_{\kappa=0}^{\infty} \frac{(-1)^\kappa a^{\mu(n+2\kappa)}}{\kappa!\Gamma(n+\kappa+1)2^{n+2\kappa}} L_\alpha\left\{t^{\alpha\mu(n+2\kappa)}\right\}. \end{aligned} \tag{17}$$

Due to (3) of Lemma 7, it follows that

$$\begin{aligned} L_\alpha\{J_n^\alpha(a^\mu t^\mu)\} &= \sum_{\kappa=0}^{\infty} \frac{(-1)^\kappa a^{\mu(n+2\kappa)}}{\kappa!\Gamma(n+\kappa+1)2^{n+2\kappa}} \cdot \frac{\alpha^{\mu(n+2\kappa)}\Gamma(\mu n+2\mu\kappa+1)}{s^{\mu n+2\mu\kappa+1}} \\ &= \frac{\alpha^{\mu n} a^{\mu n}}{2^n s^{\mu n+1}} \sum_{\kappa=0}^{\infty} \frac{\Gamma(\mu n+2\mu\kappa+1)}{\kappa!\Gamma(n+\kappa+1)} \left[\frac{-(\alpha a)^{2\mu}}{4s^{2\mu}}\right]^\kappa \\ &= \frac{(\alpha a)^{\mu n}}{2^n s^{\mu n+1}} {}_1\psi_1\left(\begin{matrix}(\mu n+1, 2\mu)\\(n+1, 1)\end{matrix}; \frac{-(\alpha a)^{2\mu}}{4s^{2\mu}}\right), \end{aligned} \tag{18}$$

as required. □

Theorem 10. *Let $J_n^\alpha(x), \alpha \in (0, 1]$ be the CFBFs. Then,*

$$L_\alpha\left\{t^{\alpha(\mu-1)} J_n^\alpha(t)\right\} = \frac{(\alpha)^{n+\mu}}{2^n s^{n+\mu}} {}_1\psi_1\left(\begin{matrix}(n+\mu, 2)\\(n+1, 1)\end{matrix}; \frac{-\alpha^2}{4s^2}\right). \tag{19}$$

Proof. As proceeded in the proof of Theorem 8 then, relying on Equation (5) and Lemma 7, we conclude that

$$\begin{aligned} L_\alpha\left\{t^{\alpha(\mu-1)} J_n^\alpha(t)\right\} &= \sum_{\kappa=0}^{\infty} \frac{(-1)^\kappa}{\kappa!\Gamma(n+\kappa+1)2^{n+2\kappa}} L_\alpha\left\{t^{\alpha(n+2\kappa+\mu-1)}\right\} \\ &= \sum_{\kappa=0}^{\infty} \frac{(-1)^\kappa}{\kappa!\Gamma(n+\kappa+1)2^{n+2\kappa}} \cdot \frac{\alpha^{(n+2\kappa+\mu)}\Gamma(n+2\kappa+\mu)}{s^{(n+2\kappa+\mu)}} \\ &= \frac{\alpha^{n+\mu}}{2^n s^{n+\mu}} \sum_{\kappa=0}^{\infty} \frac{\Gamma(n+2\kappa+\mu)}{\Gamma(n+\kappa+1)\kappa!} \left(\frac{-\alpha^2}{4s^2}\right)^\kappa. \end{aligned} \tag{20}$$

□

Theorem 11. *Let $J_n^\alpha(x), \alpha \in (0, 1]$ be the CFBFs. Then, the following identity holds:*

$$L_\alpha\left\{t^{\alpha(\mu-1)} J_n^\alpha\left(\frac{1}{t}\right)\right\} = \frac{(\alpha)^{\mu-n}}{2^n s^{\mu-n}} {}_1\psi_1\left(\begin{matrix}(\mu-n, -2)\\(n+1, 1)\end{matrix}; \frac{-s^2}{4\alpha^2}\right). \tag{21}$$

Proof. The reduction of (5) and (10) yields

$$\begin{aligned} L_\alpha\left\{t^{\alpha(\mu-1)}J_n^\alpha\left(\frac{1}{t}\right)\right\} &= \sum_{\kappa=0}^{\infty}\frac{(-1)^\kappa}{\kappa!\Gamma(n+\kappa+1)2^{n+2\kappa}}L_\alpha\left\{t^{\alpha(\mu-n-2\kappa-1)}\right\} \\ &= \sum_{\kappa=0}^{\infty}\frac{(-1)^\kappa}{\kappa!\Gamma(n+\kappa+1)2^{n+2\kappa}} \\ &\quad\cdot\frac{\alpha^{(\mu-n-2\kappa)}\Gamma(\mu-n-2\kappa)}{s^{(\mu-n-2\kappa)}} \\ &= \frac{\alpha^{\mu-n}}{2^n s^{\mu-n}}\sum_{\kappa=0}^{\infty}\frac{\Gamma(\mu-n-2\kappa)}{\Gamma(n+\kappa+1)\kappa!}\left(\frac{-s^2}{4\alpha^2}\right)^\kappa, \end{aligned} \tag{22}$$

which ends the proof. □

The above obtained results provide the necessary tools which enable us to carry out the following interesting study.

3.2. Fractional Kinetic Equations Associated with the CFBFs and Their Solutions via Fractional Laplace Transform. One of the most important equations in mathematical physics and natural sciences is the kinetic equation, which describes the continuity of motion of substances. Therefore, many researchers investigated extensions and generalizations of this equation in the context of various fractional calculus operators. For such type of work, we refer for example to [37, 38]. We begin by briefly reviewing these previous efforts; then, we introduce our extended form of the fractional kinetic differential equation associated with the CFBFs. Assuming that $\mathcal{N}(t)$ denotes an arbitrary reaction which depends on time, d refers to the destruction rate, and p is the production rate on $\mathcal{N}$, Haubold and Mathai [37] characterized the FDE of the quantities $\mathcal{N}(t)$, d and p, by the formula

$$\frac{d\mathcal{N}}{dt} = -d(\mathcal{N}_t) + p(\mathcal{N}_t), \tag{23}$$

where $\mathcal{N}_t(t^*) = \mathcal{N}(t-t^*)$ for $t^* > 0$. In the case where spatial fluctuation or inhomogeneities in the quantity $\mathcal{N}(t)$ is neglected, the authors in [37] handled the following equation:

$$\frac{d\mathcal{N}_i}{dt} = -c_i\mathcal{N}_i(t), \tag{24}$$

where the primary condition $\mathcal{N}_i(t=0) = \mathcal{N}_0$ gives the number density of species i at time $t = 0$ and constant $c_i > 0$. Equation (24) is known as the standard kinetic equation. Alternatively, if the index i is neglected, then, by integrating the standard kinetic Equation (24), one can get

$$\mathcal{N}(t) - \mathcal{N}_0 = c_0\mathscr{D}^{-1}\mathcal{N}(t), \tag{25}$$

where ${}_0\mathscr{D}^{-1}$ is the standard integral operator. Equation Equation (25) has been extended to the fractional setting in the form (see [37]).

$$\mathcal{N}(t) - \mathcal{N}_0 = c_0\mathscr{D}^{-\nu}\mathcal{N}(t), \tag{26}$$

where ${}_0\mathscr{D}^{-\nu}$ denotes the standard fractional integral operator in Riemann-Liouville sense (see [10, 39]).

Now, consider the conformable fractional kinetic equation in the form:

$$\mathcal{N}(t) - \mathcal{N}_0 = cI_\alpha(\mathcal{N}(t)), \tag{27}$$

where $I_\alpha(\cdot)$ is the conformable fractional integral of order $\nu \in (0,1]$ in the frame of Definition 2. Accordingly, we develop here a new type of generalization of the fractional kinetic differential equation in the conformable sense involving the fractional-order Bessel function in view of a fractional Laplace transform.

Remark 12. The solutions we are going to conclude for the conformable fractional kinetic equations will be determined through the generalized Mittag-Leffler function $E_{\mu,\nu}(x)$ [36], which is defined as

$$E_{\mu,\nu}(x) = \sum_{n=0}^{\infty}\frac{x^n}{\Gamma(\mu n+\nu)}, \quad \mu,\nu > 0. \tag{28}$$

Theorem 13. *For $d > 0$ and $\alpha \in (0,1]$, the following conformable fractional equation*

$$\mathcal{N}(t) - \mathcal{N}_0\{J_n^\alpha(t)\} = -d^\alpha I_\alpha(\mathcal{N}(t)) \tag{29}$$

has a solution in the form

$$\begin{aligned} \mathcal{N}(t) = \mathcal{N}_0\sum_{\kappa=0}^{\infty}\frac{(-1)^\kappa\Gamma(n+2\kappa+1)}{\kappa!\Gamma(n+\kappa+1)}\left(\frac{t^\alpha}{2}\right)^{n+2\kappa} \\ \cdot E_{(1,n+2\kappa+1)}\left(\frac{-d^\alpha t^\alpha}{\alpha}\right). \end{aligned} \tag{30}$$

Proof. Following Abdeljawad [16], then, in virtue of $I_\alpha(f(t))$, we have

$$L_\alpha\{I_\alpha(f(t))\} = \frac{F_\alpha(s)}{s}, \tag{31}$$

where $F_\alpha(s) = L_\alpha\{f(t)\}$ defined in (10) and I_α is the conformable fractional integral operator (2). Acting by the conformable fractional Laplace transform on both sides of Equation (30) implies that

$$L_\alpha\{\mathcal{N}(t)\} - \mathcal{N}_0L_\alpha\{J_n^\alpha(t)\} = -d^\alpha L_\alpha\{I_\alpha(\mathcal{N}(t))\}. \tag{32}$$

Combining Equation (5) and Equation (31) leads to

$$\begin{aligned} \mathcal{N}_\alpha(s) - \mathcal{N}_0\sum_{\kappa=0}^{\infty}\frac{(-1)^\kappa}{\kappa!\Gamma(n+\kappa+1)2^{n+2\kappa}}L_\alpha\left\{t^{\alpha(n+2\kappa)}\right\} \\ = -d^\alpha\frac{\mathcal{N}_\alpha(s)}{s}, \end{aligned} \tag{33}$$

$$\mathcal{N}_\alpha(s)\left(1+\frac{d^\alpha}{s}\right)=\mathcal{N}_0\sum_{\kappa=0}^{\infty}\frac{(-1)^\kappa}{\kappa!\Gamma(n+\kappa+1)2^{n+2\kappa}}\cdot\int_0^\infty e^{-s(t^\alpha/\alpha)}t^{\alpha(n+2\kappa)}d_\alpha t. \tag{34}$$

Considering Equation (10) with (34), we obtain

$$\mathcal{N}_\alpha(s)\left(1+\frac{d^\alpha}{s}\right)=\mathcal{N}_0\sum_{\kappa=0}^{\infty}\frac{(-1)^\kappa\alpha^{(n+2\kappa)}}{\kappa!\Gamma(n+\kappa+1)2^{n+2\kappa}}\frac{\Gamma(n+2\kappa+1)}{s^{n+2\kappa+1}}. \tag{35}$$

Therefore,

$$\begin{aligned}\mathcal{N}_\alpha(s)&=\mathcal{N}_0\sum_{\kappa=0}^{\infty}\frac{(-1)^\kappa\alpha^{(n+2\kappa)}\Gamma(n+2\kappa+1)}{\kappa!\Gamma(n+\kappa+1)2^{n+2\kappa}}\frac{1}{s^{n+2\kappa+1}}\left(1+\frac{d^\alpha}{s}\right)^{-1}\\&=\mathcal{N}_0\sum_{\kappa=0}^{\infty}\frac{(-1)^k\alpha^{(n+2\kappa)}\Gamma(n+2\kappa+1)}{\kappa!\Gamma(n+\kappa+1)2^{n+2\kappa}}\cdot\frac{1}{s^{n+2\kappa+1}}\sum_{i=0}^{\infty}\frac{(1)_i(-d^\alpha/s)^i}{i!}\\&=\mathcal{N}_0\sum_{\kappa=0}^{\infty}\frac{(-1)^\kappa\alpha^{(n+2k)}\Gamma(n+2\kappa+1)}{\kappa!\Gamma(n+\kappa+1)2^{n+2\kappa}}\sum_{i=0}^{\infty}\frac{(-1)^id^{\alpha i}}{s^{n+2\kappa+i+1}}.\end{aligned} \tag{36}$$

With the aid of the inverse Laplace transform (10), it follows that

$$\begin{aligned}\mathcal{N}(t)&=\mathcal{N}_0\sum_{\kappa=0}^{\infty}\frac{(-1)^\kappa\alpha^{(n+2\kappa)}\Gamma(n+2\kappa+1)}{\kappa!\Gamma(n+\kappa+1)2^{n+2\kappa}}\cdot\sum_{i=0}^{\infty}\frac{(-1)^id^{\alpha i}t^{\alpha(n+2\kappa+i)}}{\alpha^{n+2\kappa+i}\Gamma(n+2\kappa+i+1)}\\&=\mathcal{N}_0\sum_{\kappa=0}^{\infty}\frac{(-1)^\kappa\Gamma(n+2\kappa+1)}{k!\Gamma(n+\kappa+1)}\left(\frac{t^\alpha}{2}\right)^{n+2\kappa}\cdot\sum_{i=0}^{\infty}\frac{1}{\Gamma(n+2\kappa+i+1)}\left(\frac{-d^\alpha t^\alpha}{\alpha}\right)^i\\&=\mathcal{N}_0\sum_{\kappa=0}^{\infty}\frac{(-1)^\kappa\Gamma(n+2\kappa+1)}{\kappa!\Gamma(n+\kappa+1)}\left(\frac{t^\alpha}{2}\right)^{n+2\kappa}\cdot E_{(1,n+2\kappa+1)}\left(\frac{-d^\alpha t^\alpha}{\alpha}\right).\end{aligned} \tag{37}$$

□

Theorem 14. *The solution of the following conformable fractional equation*

$$\mathcal{N}(t)-\mathcal{N}_0\{J_n^\alpha(d^\mu t^\mu)\}=-d^{\alpha\mu}I_\alpha(\mathcal{N}(t)),\quad \text{for } d,\mu>0,\alpha\in(0,1], \tag{38}$$

is given by

$$\mathcal{N}(t)=\mathcal{N}_0\sum_{\kappa=0}^{\infty}\frac{(-1)^\kappa\Gamma(n\mu+2\mu\kappa+1)}{\kappa!\Gamma(n+\kappa+1)}\left(\frac{d^{\alpha\mu}t^{\alpha\mu}}{2}\right)^{n+2\kappa}\cdot E_{(1,n\mu+2\mu\kappa+1)}\left(\frac{-d^\alpha\mu t^\alpha}{\alpha}\right). \tag{39}$$

Proof. Operating the conformable fractional Laplace transform on both sides of Equation (38), we get

$$L_\alpha\{\mathcal{N}(t)\}-\mathcal{N}_0L_\alpha\{J_n^\alpha(d^\mu t^\mu)\}=-d^{\alpha\mu}L_\alpha\{I_\alpha((t))\}. \tag{40}$$

In view of Equations (5) and (31), we obtain

$$\begin{aligned}&\mathcal{N}_\alpha(s)+d^{\alpha\mu}\frac{\mathcal{N}_\alpha(s)}{s}\\&=N_0\sum_{\kappa=0}^{\infty}\frac{(-1)^\kappa d^{\mu\alpha(n+2\kappa)}}{\kappa!\Gamma(n+\kappa+1)2^{n+2\kappa}}L_\alpha\left\{t^{\alpha\mu(n+2\kappa)}\right\}.\end{aligned} \tag{41}$$

Hence, using (3) of Lemma 7 implies

$$\mathcal{N}_\alpha(s)\left(1+\frac{d^{\alpha\mu}}{s}\right)=\mathcal{N}_0\sum_{\kappa=0}^{\infty}\frac{(-1)^\kappa d^{\mu\alpha(n+2\kappa)}}{\kappa!\Gamma(n+\kappa+1)2^{n+2\kappa}}\cdot\frac{\alpha^{\mu(n+2\kappa)}\Gamma(n\mu+2\mu\kappa+1)}{s^{n\mu+2\mu\kappa+1}}, \tag{42}$$

from which one can obtain

$$\begin{aligned}\mathcal{N}_\alpha(s)&=\mathcal{N}_0\sum_{\kappa=0}^{\infty}\frac{(-1)^\kappa d^{\mu\alpha(n+2\kappa)}\alpha^{\mu(n+2\kappa)}\Gamma(n\mu+2\mu\kappa+1)}{\kappa!\Gamma(n+\kappa+1)2^{n+2\kappa}}\cdot\frac{1}{s^{n\mu+2\mu\kappa+1}}\sum_{i=0}^{\infty}\frac{(-1)^id^{\alpha i}\mu^i}{s^i}.\end{aligned} \tag{43}$$

Therefore,

$$\begin{aligned}\mathcal{N}_\alpha(s)&=\mathcal{N}_0\sum_{\kappa=0}^{\infty}\frac{(-1)^\kappa d^{\mu\alpha(n+2\kappa)}\alpha^{\mu(n+2\kappa)}\Gamma(n\mu+2\mu\kappa+1)}{\kappa!\Gamma(n+\kappa+1)2^{n+2\kappa}}\cdot\sum_{i=0}^{\infty}(-1)^id^{\alpha i}\mu^i\frac{1}{s^{n\mu+2\mu\kappa+i+1}}.\end{aligned} \tag{44}$$

In view of the inverse fractional Laplace transform (10), it follows that

$$\mathcal{N}(t) = \mathcal{N}_0 \sum_{\kappa=0}^{\infty} \frac{(-1)^{\kappa} d^{\mu\alpha(n+2\kappa)} \Gamma(n\mu + 2\mu\kappa + 1)}{\kappa! \Gamma(n+\kappa+1) 2^{n+2\kappa}} t^{\alpha(n\mu+2\mu\kappa)} \cdot \sum_{i=0}^{\infty} \frac{1}{\Gamma(n\mu + 2\mu\kappa + i + 1)} \left[\frac{-d^{\alpha}\mu t^{\alpha}}{\alpha}\right]^{i} = \mathcal{N}_0 \sum_{\kappa=0}^{\infty} \frac{(-1)^{\kappa} \Gamma(n\mu + 2\mu\kappa + 1)}{\kappa! \Gamma(n+\kappa+1)} \left[\frac{d^{\mu\alpha} t^{\alpha\mu}}{2}\right]^{n+2\kappa} \cdot E_{(1,\mu n+2\mu\kappa+1)}\left(\frac{-d^{\alpha}\mu t^{\alpha}}{\alpha}\right). \tag{45}$$

Thus, the result is established. □

4. Orthogonality of the CFBFs

Understanding the orthogonality relation of the CFBFs is mandatory to compute coefficients of series whose terms include the CFBFs. These series represent solutions of the FDEs as we will encounter in the application part of this section. Along with [40] and in view of the CFD definition (1), we introduce the following interesting results on orthogonality which will be useful in the current study.

4.1. An Orthogonal Relation of the CFBFs

Theorem 15. *The orthogonality relation of the CFBFs $J_n^{\alpha}(x)$ is deduced over $[0, b]$ with respect to the weight function $w(x) = x^{2\alpha-1}$ by the following:*

$$\int_0^b x^{2\alpha-1} J_n^{\alpha}(\lambda_s x) J_n^{\alpha}(\lambda_r x) dx = \frac{b^{2\alpha}}{2\alpha} [J_{n+1}^{\alpha}(\lambda_s b)]^2 \delta_{\lambda_s\lambda_r}, \quad \alpha \in (0, 1], \tag{46}$$

where $\delta_{\lambda_s\lambda_r}$ is the familiar Kronker delta function and λ_s, λ_r are distinct roots of $J_n^{\alpha}(x) = 0$.

Proof. Since $J_n^{\alpha}(x)$ is a solution of the CFBE (4), it follows that $y = J_n^{\alpha}(\lambda_s x)$ which satisfies the more general equation

$$x^{2\alpha} \mathscr{D}^{\alpha} \mathscr{D}^{\alpha} y(x) + \alpha x^{\alpha} \mathscr{D}^{\alpha} y(x) + \alpha^2 \left(x^{2\alpha} \lambda_s^{2\alpha} - n^2\right) y(x) = 0. \tag{47}$$

It is convenient to reformulate (47) in the following way:

$$x^{\alpha} \mathscr{D}^{\alpha} (x^{\alpha} \mathscr{D}^{\alpha} y(x)) + \alpha^2 \left(x^{2\alpha} \lambda_s^{2\alpha} - n^2\right) y(x) = 0. \tag{48}$$

Consequently, $J_n^{\alpha}(\lambda_s x)$ and $J_n^{\alpha}(\lambda_r x)$ satisfy the following CFDEs, respectively:

$$x^{\alpha} \mathscr{D}^{\alpha} (x^{\alpha} \mathscr{D}^{\alpha} J_n^{\alpha}(\lambda_s x)) + \alpha^2 \left(x^{2\alpha} \lambda_s^{2\alpha} - n^2\right) J_n^{\alpha}(\lambda_s x) = 0, \tag{49}$$

$$x^{\alpha} \mathscr{D}^{\alpha} (x^{\alpha} \mathscr{D}^{\alpha} J_n^{\alpha}(\lambda_r x)) + \alpha^2 \left(x^{2\alpha} \lambda_r^{2\alpha} - n^2\right) J_n^{\alpha}(\lambda_r x) = 0. \tag{50}$$

Multiplying (49) by $x^{-\alpha} J_n^{\alpha}(\lambda_r x)$ and (50) by $x^{-\alpha} J_n^{\alpha}(\lambda_s x)$ and then subtracting the resulting equations produce

$$\left(\lambda_s^{2\alpha} - \lambda_r^{2\alpha}\right) x^{\alpha} J_n^{\alpha}(\lambda_s x) J_n^{\alpha}(\lambda_r x) = J_n^{\alpha}(\lambda_s x) \mathscr{D}^{\alpha} [x^{\alpha} \mathscr{D}^{\alpha} J_n^{\alpha}(\lambda_r x)] - J_n^{\alpha}(\lambda_r x) \mathscr{D}^{\alpha} [x^{\alpha} \mathscr{D}^{\alpha} J_n^{\alpha}(\lambda_s x)]. \tag{51}$$

In view of the conformable fractional integral formula (2) over $[0, b]$, we obtain

$$\left(\lambda_s^{2\alpha} - \lambda_r^{2\alpha}\right) \int_0^b x^{\alpha} J_n^{\alpha}(\lambda_s x) J_n^{\alpha}(\lambda_r x) d_{\alpha} x = \int_0^b J_n^{\alpha}(\lambda_s x) \mathscr{D}^{\alpha} [x^{\alpha} \mathscr{D}^{\alpha} J_n^{\alpha}(\lambda_r x)] d_{\alpha} x - \int_0^b J_n^{\alpha}(\lambda_r x) \mathscr{D}^{\alpha} [x^{\alpha} \mathscr{D}^{\alpha} J_n^{\alpha}(\lambda_s x)] d_{\alpha} x. \tag{52}$$

By performing integration by parts [16] on the right-hand side divided by the factor $(\lambda_s^{2\alpha} - \lambda_r^{2\alpha})$, one can conclude that

$$\int_0^b x^{\alpha} J_n^{\alpha}(\lambda_s x) J_n^{\alpha}(\lambda_r x) d_{\alpha} x = \frac{x^{\alpha}}{\left(\lambda_s^{2\alpha} - \lambda_r^{2\alpha}\right)} [J_n^{\alpha}(\lambda_s x) \mathscr{D}^{\alpha} J_n^{\alpha}(\lambda_r x) - J_n^{\alpha}(\lambda_r x) \mathscr{D}^{\alpha} J_n^{\alpha}(\lambda_s x)]_0^b. \tag{53}$$

Hence, according to the values of λ_s and λ_r, we consider the following two cases:

(i) If $\lambda_s \neq \lambda_r$ and by hypothesis $J_n^{\alpha}(\lambda_s) = J_n^{\alpha}(\lambda_r) = 0$, then the right-hand side of (53) vanishes

(ii) If $\lambda_s = \lambda_r$, then the resulting integral

$$I = \int_0^b x^{\alpha} [J_n^{\alpha}(\lambda_s x)]^2 d_{\alpha} x = \int_0^b x^{2\alpha-1} [J_n^{\alpha}(\lambda_s x)]^2 dx \tag{54}$$

creates an interest to look at. In order to deduce its value, we take the limit of (53) as $\lambda_r \longrightarrow \lambda_s$. As the right-hand side in (53) approaches the indeterminate form 0/0 in the limit, we apply L'Hopital's rule, which leads to

$$I = \frac{x^{\alpha}}{2\alpha\lambda_s^{\alpha}} \left[\mathscr{D}_{\lambda_s}^{\alpha} J_n^{\alpha}(\lambda_s x) \mathscr{D}_x^{\alpha} J_n^{\alpha}(\lambda_s x) - J_n^{\alpha}(\lambda_s x) \mathscr{D}_{\lambda_s}^{\alpha} \mathscr{D}_x^{\alpha} J_n^{\alpha}(\lambda_s x)\right]_0^b \tag{55}$$

Now, using the following recurrence relations of CFBFs [26]

$$\mathscr{D}_{\lambda_s}^{\alpha} J_n^{\alpha}(\lambda_s x) = \frac{n}{x^{\alpha}} J_n^{\alpha}(\lambda_s x) - \lambda_s^{\alpha} J_{n+1}^{\alpha}(\lambda_s x), \quad \mathscr{D}_x^{\alpha} J_n^{\alpha}(\lambda_s x) = \frac{n}{\lambda_s^{\alpha}} J_n^{\alpha}(\lambda_s x) - x^{\alpha} J_{n+1}^{\alpha}(\lambda_s x), \tag{56}$$

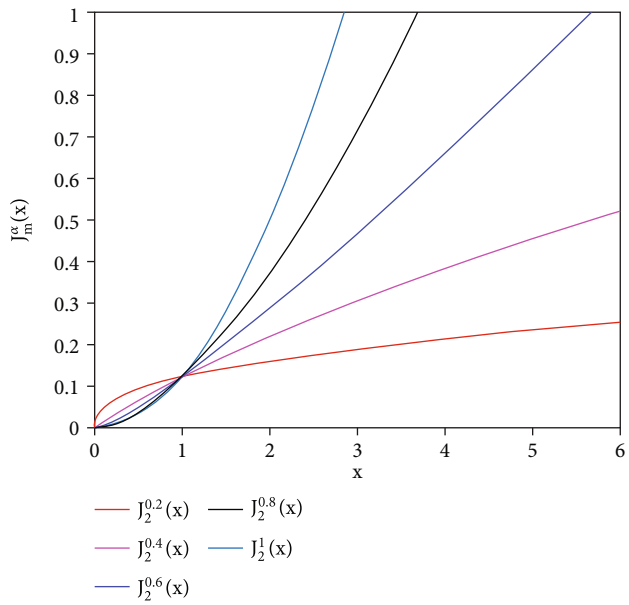

FIGURE 1: Graph of CFBFs with $\mathscr{M} = 2$, $m = 2$ and various values of $\alpha = 0.2,0.4,0.6,0.8,1$.

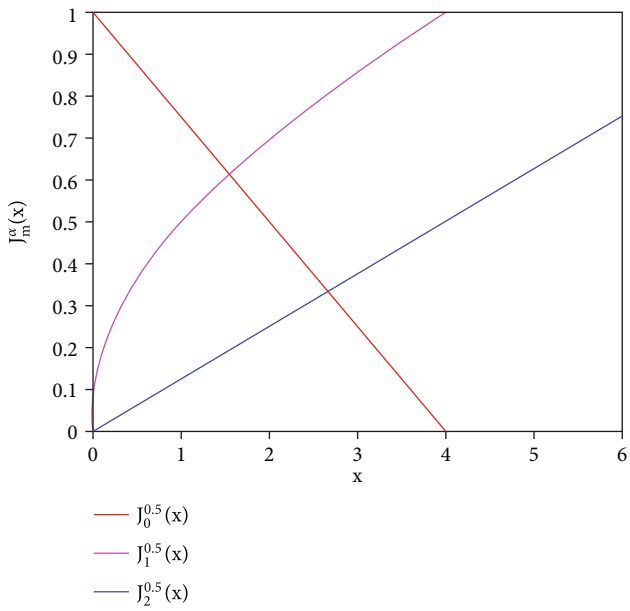

FIGURE 2: Graph of CFBFs with $\mathscr{M} = 2$, $\alpha = 0.5$ and various values of $m = 0, 1, 2$.

it follows that

$$I = \left[\frac{n^2}{2\alpha\lambda_s^{2\alpha}}[J_n^\alpha(\lambda_s x)]^2 + \frac{x^{2\alpha}}{2\alpha}[J_{n+1}^\alpha(\lambda_s x)]^2 - \frac{nx^\alpha}{2\alpha\lambda_s^\alpha}J_n^\alpha(\lambda_s x)J_{n+1}^\alpha(\lambda_s x)\right]_0^b = \frac{b^{2\alpha}}{2\alpha}[J_{n+1}^\alpha(\lambda_s b)]^2. \quad (57)$$

□

As a special case of Theorem 15, the following result can be easily verified.

Corollary 16. *The CFBFs $J_n^\alpha(x)$ are orthogonal over $[0, 1]$ with respect to the weight function $w(x) = x^{2\alpha-1}$ and*

$$\int_0^1 x^{2\alpha-1}J_n^\alpha(\lambda_s x)J_n^\alpha(\lambda_r x)dx = \frac{1}{2\alpha}[J_{n+1}^\alpha(\lambda_s)]^2\delta_{\lambda_s\lambda_r}. \quad (58)$$

The results obtained in the current Section 4.1 treated the topic of orthogonal polynomials which pave the way to discuss a function representation via a series of the CFBFs.

4.2. Expansion of Functions via CFBFs. The classical theory of expressing analytic functions as expansions in terms of an arbitrary set of orthogonal polynomials can be described as the backbone of many topics in analysis. It was originated by several authors to whom we may mention Boas and Buck [41], Faber [42], and Whittaker and Gattegno [43] and later on in higher dimension by Abul-Ez et al. [29, 30, 44–46]. In the usual classical calculus, we found that not all functions have the Taylor power series representation around specific points, but this is not the case in the theory of conformable fractional calculus. This fact has been shown by Abdeljawad [16], where he also proposed the expansion of the fractional power series for an infinity α-differentiable function through the fractional Taylor series. The expansion of a given real function in a series of Bessel functions is extremely useful in determining the solution of certain FDEs involving radial symmetry [40]. Related to the work of finding the expansion of a given function by means of Bessel polynomials in the higher-dimensional context, see the work given in [29, 30]. Using the orthogonality property (46), one can easily represent a given function $f(x)$ over the interval $[0, b]$ by a series of Bessel functions such as

$$f(x) = \sum_{i=0}^{\infty} a_i J_n^\alpha(\lambda_i x), \quad 0 < x < b, \quad (59)$$

where $J_n^\alpha(\lambda_i b) = 0$, $i = 0, 1, 2, 3, \cdots$, and a_i are determined by

$$a_i = \frac{2\alpha}{b^{2\alpha}[J_{n+1}^\alpha(\lambda_i b)]^2}\int_0^b x^{2\alpha-1}f(x)J_n^\alpha(\lambda_i x)dx, \quad i = 0, 1, 2, 3, \cdots \quad (60)$$

As the topic of expansions of an arbitrary function, of either a real or a complex variable, into a series of polynomials has not been fully explored, we believe that several open problems remain untouched in particular in the framework of fractional calculus.

4.3. Applications. In this subsection, we intend to indicate the efficiency and applicability of the results developed in this study. Precisely, we construct a scheme which will be employed to solve some linear and nonlinear CFDEs. In this concern, we first define the m^{th} truncated CFBFs of the first kind. Then, we introduce the noninteger derivative in the conformable context of an approximated function expanded in terms of the CFBFs. Several important examples including famous FDEs have been comprehensively treated, and their solutions have been compared to other existing methods in the literature to show the consistency and accuracy of our proposed method.

We begin by considering the m^{th} truncated CFBFs of the first kind as follows:

$$\tilde{J}_m^{\alpha}(x) = \sum_{\kappa=0}^{\lfloor (\mathscr{M}-m)/2 \rfloor} \frac{(-1)^{\kappa}}{\kappa!\Gamma(m+\kappa+1)} \left(\frac{x^{\alpha}}{2}\right)^{2\kappa+m}, \quad 0 \le x < \infty, \tag{61}$$

where $\mathscr{M}$ is a positive integer such that $\mathscr{M} \ge m$ and $m = 0, 1, 2, \cdots, \mathscr{M}$. For $\mathscr{M} = 2$, we have

$$\begin{aligned} \tilde{J}_0^{\alpha}(x) &= 1 - \frac{x^{2\alpha}}{4}, \\ \tilde{J}_1^{\alpha}(x) &= \frac{x^{\alpha}}{2}, \\ \tilde{J}_m^{2}(x) &= \frac{x^{2\alpha}}{8}. \end{aligned} \tag{62}$$

Figures 1 and 2 show the graphs of the truncated CFBFs when $\mathscr{M} = 2$ and by taking various values of m and α.

Let $f(x)$ be a function defined over $[0, 1]$; then, $f(x)$ can be expanded in terms of CFBFs as follows:

$$f(x) = \sum_{i=0}^{\infty} a_i \tilde{J}_i^{\alpha}(x). \tag{63}$$

Thus, the following truncated series for $f(x)$ is supposed to be

$$f(x) = \sum_{m=0}^{\mathscr{M}} a_m \tilde{J}_m^{\alpha}(x). \tag{64}$$

Theorem 17. *The noninteger derivative of order $\gamma > 0$ of the CFBFs in the conformable sense is given by*

$$\mathscr{D}^{\gamma} \tilde{J}_m^{\alpha}(x) = \sum_{\kappa=0}^{\lfloor (\mathscr{M}-m)/2 \rfloor} \eta_{\kappa,m}^{\alpha,\gamma} x^{\alpha(2\kappa+m)-\gamma}, \tag{65}$$

where

$$\eta_{\kappa,\kappa}^{\alpha,\gamma} = \frac{(-1)^{\kappa}\Gamma(\alpha(2\kappa+m)+1)}{2^{2\kappa+m}k!\Gamma(m+\kappa+1)\Gamma(\alpha(2\kappa+m)-\lceil\gamma\rceil+1)}. \tag{66}$$

Proof. The linearity of the conformable derivative (see [12, 16]) leads to

$$\begin{aligned} \mathscr{D}^{\gamma} \tilde{J}_m^{\alpha}(x) &= \sum_{\kappa=0}^{\lfloor (\mathscr{M}-m)/2 \rfloor} \frac{(-1)^{\kappa}}{2^{2\kappa+m}\kappa!\Gamma(m+\kappa+1)} \mathscr{D}^{\gamma} x^{\alpha(2\kappa+m)} \\ &= \sum_{\kappa=0}^{\lfloor (\mathscr{M}-m)/2 \rfloor} \frac{(-1)^{\kappa}}{2^{2\kappa+m}\kappa!\Gamma(m+\kappa+1)} \\ &\quad \cdot \frac{\Gamma(\alpha(2\kappa+m)+1)}{\Gamma(\alpha(2\kappa+m)-\lceil\gamma\rceil+1)} x^{\alpha(2\kappa+m)-\gamma}, \end{aligned} \tag{67}$$

as required. □

Remark 18. If $\alpha(2\kappa+m) < \gamma$, where $\alpha(2\kappa+m) \in \mathbb{N}_0$, then, $\mathscr{D}^{\gamma} \tilde{J}_m^{\alpha}(x) = 0$.

Theorem 19. *Let $u_{\mathscr{M}}(x)$ be an approximated function given by means of the truncated formula of CFBFs (61). Then,*

$$\mathscr{D}^{\gamma} u_{\mathscr{M}}(x) = \sum_{m=0}^{\mathscr{M}} \sum_{\kappa=0}^{\lfloor (\mathscr{M}-m)/2 \rfloor} a_m \eta_{\kappa,m}^{\alpha,\gamma} x^{\alpha(2\kappa+m)-\gamma}. \tag{68}$$

Proof. The induction of Theorem 17 and in view of the linearity property leads to the required result. □

4.3.1. Proposed Scheme

(1) Linear Multiorder CFDEs. Suppose that the generalized linear multiorder CFDE is given in the form

$$\mathscr{D}^{\gamma} u(x) + \sum_{j=0}^{s} A_j \mathscr{D}^{\gamma_j} u(x) + A_{s+1} u(x) = A_{s+2} h(x), \in [0, 1], \tag{69}$$

subject to the initial conditions

$$\mathscr{D}^{(i)} u(x) = d_i, i = 0, 1, 2, \cdots, \lceil\gamma\rceil - 1, \tag{70}$$

where $\mathscr{D}^{\gamma}, 0 < \gamma_1 < \gamma_2 < \cdots < \gamma_s < \gamma$, denotes to the CFD of order $\gamma > 0$,$h(x)$ are known to be a continuous function, and $d_i, i = 0, 1, 2, \cdots, \lceil\gamma\rceil - 1$ are some constants.

Assume that the solution of the CFDE (69) can be given in the form

$$u_{\mathscr{M}}(x) = \sum_{m=0}^{\mathscr{M}} a_m \tilde{J}_m^{\alpha}(x). \tag{71}$$

Substituting (71) into (69) and using Theorem 19, we have

$$\begin{aligned} &\sum_{m=0}^{\mathscr{M}} \sum_{\kappa=0}^{\lfloor (\mathscr{M}-m)/2 \rfloor} a_m \eta_{\kappa,m}^{\alpha,\gamma} x^{\alpha(2\kappa+m)-\gamma} \\ &\quad + \sum_{j=0}^{s} A_j \left\{ \sum_{m=0}^{\mathscr{M}} \sum_{\kappa=0}^{\lfloor (\mathscr{M}-m)/2 \rfloor} a_m \eta_{\kappa,m}^{\alpha,\gamma_j} x^{\alpha(2\kappa+m)-\gamma_j} \right\} \\ &\quad + A_{s+1} \sum_{m=0}^{\mathscr{M}} a_m \tilde{J}_m^{\alpha}(x) = A_{s+2} h(x). \end{aligned} \tag{72}$$

Collocating Equation (72) at the points $x_q = q/\mathscr{M}$, $= 1, 2, 3, \cdots, \mathscr{M} + 1 - \lceil\gamma\rceil$, we get

$$\sum_{m=0}^{\mathscr{M}}\sum_{\kappa=0}^{\lfloor(\mathscr{M}-m)/2\rfloor} a_m \eta_{\kappa,m}^{\alpha,\gamma} x_q^{\alpha(2\kappa+m)-\gamma} + \sum_{j=0}^{s} A_j \left\{ \sum_{m=0}^{\mathscr{M}}\sum_{\kappa=0}^{\lfloor(\mathscr{M}-m)/2\rfloor} a_m \eta_{\kappa,m}^{\alpha,\gamma_j} x_q^{\alpha(2\kappa+m)-\gamma_j} \right\} + A_{s+1}\sum_{m=0}^{\mathscr{M}} a_m \tilde{J}_m^{\alpha}(x_q) = A_{s+2} h(x_q). \tag{73}$$

These equations give $(\mathscr{M}+1-\lceil\gamma\rceil)$ linear algebraic equations. Combining (71) and (70) produces $\lceil\gamma\rceil$-algebraic equations. Thus, we obtain a linear algebraic system of $\mathscr{M}+1$ equations in the unknown $a_m, m=0,1,2,\cdots,\mathscr{M}$. By solving this system, we obtain the solution of Equation (69) associated with the initial condition (70).

(2) Nonlinear Multiorder CFDEs. Consider the generalized nonlinear multiorder CFDE such that

$$\mathscr{D}^{\gamma}u(x) = F\big(x, u(x), \mathscr{D}^{\gamma_1}u(x), \mathscr{D}^{\gamma 2}u(x), \cdots, \mathscr{D}^{\gamma_s}u(x)\big), \quad x\in[0,1], \tag{74}$$

with the initial conditions

$$\mathscr{D}^{(i)}u(x) = c_i,\ i=0,1,2,\cdots,\lceil\gamma\rceil-1, \tag{75}$$

where $\mathscr{D}^{\gamma}, 0<\gamma_1<\gamma_2<\cdots<\gamma_s<\gamma$, stands for the CFD of order $\gamma>0$, F is a nonlinear operator, and $c_i, i=0,1,2,\cdots,\lceil\gamma\rceil-1$ are given constants. A similar procedure as in establishing (69) can be used to approximate $u(x)$ in terms of CFBFs. Thus, combining (71) with (74) and using Theorem 19 yield

$$\sum_{m=0}^{\mathscr{M}}\sum_{\kappa=0}^{\lfloor(\mathscr{M}-m)/2\rfloor} a_m \eta_{\kappa,m}^{\alpha,\gamma} x^{\alpha(2\kappa+m)-\gamma} = F\Bigg(x, \sum_{m=0}^{\mathscr{M}} a_m \tilde{J}_m^{\alpha}(x), \sum_{m=0}^{\mathscr{M}}\sum_{\kappa=0}^{\lfloor(\mathscr{M}-m)/2\rfloor} \cdot a_m \eta_{\kappa,m}^{\alpha,\gamma_1} x^{\alpha(2\kappa+m)-\gamma_1}, \sum_{m=0}^{\mathscr{M}}\sum_{\kappa=0}^{\lfloor(\mathscr{M}-m)/2\rfloor} \cdot a_m \eta_{\kappa,m}^{\alpha,\gamma_2} x^{\alpha(2\kappa+m)-\gamma_2}, \cdots, \sum_{m=0}^{\mathscr{M}}\sum_{\kappa=0}^{\lfloor(\mathscr{M}-m)/2\rfloor} \cdot a_m \eta_{\kappa,m}^{\alpha,\gamma_s} x^{\alpha(2\kappa+m)-\gamma_s} \Bigg). \tag{76}$$

Collocating Equation (76) at the points $x_q, = 1,2,3,\cdots, \mathscr{M}+1-\lceil\gamma\rceil$, thus, we have the following:

$$\sum_{m=0}^{\mathscr{M}}\sum_{\kappa=0}^{\lfloor(\mathscr{M}-m)/2\rfloor} a_m \eta_{\kappa,m}^{\alpha,\gamma} x_q^{\alpha(2\kappa+m)-\gamma} = F\Bigg(x_q, \sum_{m=0}^{\mathscr{M}} a_m \tilde{J}_m^{\alpha}(x_q), \sum_{m=0}^{\mathscr{M}}\sum_{\kappa=0}^{\lfloor(\mathscr{M}-m)/2\rfloor} \cdot a_m \eta_{\kappa,m}^{\alpha,\gamma_1} x_q^{\alpha(2\kappa+m)-\gamma_1}, \sum_{m=0}^{\mathscr{M}}\sum_{\kappa=0}^{\lfloor(\mathscr{M}-m)/2\rfloor} \cdot a_m \eta_{\kappa,m}^{\alpha,\gamma_2} x_q^{\alpha(2\kappa+m)-\gamma_2}, \cdots, \sum_{m=0}^{\mathscr{M}}\sum_{\kappa=0}^{\lfloor(\mathscr{M}-m)/2\rfloor} \cdot a_m \eta_{\kappa,m}^{\alpha,\gamma_s} x_q^{\alpha(2\kappa+m)-\gamma_s} \Bigg). \tag{77}$$

Equation (77) determines $(\mathscr{M}+1-\lceil\gamma\rceil)$ nonlinear equations. In virtue of (71) and the initial conditions (75), we get $\lceil\gamma\rceil$ equations. Immediately, one can get a system of $\mathscr{M}+1$ nonlinear equations in the unknown $a_m, m=0,1,2,\cdots,\mathscr{M}$. As usual, Newton's iterative method can be used to solve this system. Thus, the solution of the nonlinear CFDE (74) with (75) can be deduced.

We can briefly clarify the achieved advantages of employing the proposed method as follows. The fractional-order Bessel functions approximate the fractional function with more accuracy. This feature has made the FBFs more effective than Bessel functions in solving the fractional problems. As the values of coefficients in Bessel polynomials are smaller than the coefficients of Chebyshev, Legendre, and Bernoulli polynomials, the computational error in the current method is less. Furthermore, our detailed treatment to these FDEs using the collocation method is aimed at encouraging the use of such approach which allows reaching the required solutions with ease and accuracy.

In the following subsection, we discuss several numerical examples to demonstrate the consequences of the above-mentioned features.

4.4. Illustrative Examples. In view of the above arguments, it is interesting to employ the provided techniques to solve some useful FDEs, as we shall see through the following examples.

Example 20. Consider the famous Bagley-Torvik equation

$$\mathscr{D}^2u(x) + \mathscr{D}^{3/2}u(x) + u(x) = 1+x, \quad 0\le x\le 1, \tag{78}$$

subject to the initial conditions

$$u(0)=1,\ u'(0)=1. \tag{79}$$

This equation has been solved using Legendre polynomials in view of the conformable fractional sense in [14], as well as in [47–50] in the sense of Caputo derivative. The exact solution of (78) was given in ([47, 49]) as $u(x)=1+$

Table 1

Conformable fractional differential equation	$\mathscr{D}^3 u(x) + \mathscr{D}^{5/2} u(x) + u^2(x) = x^4, x \in [0, 1]$
Initial conditions	$u(0) = 0, u'(0) = 0$, and $u''(0) = 2$
Exact solution	x^2 (as given by various authors in [47–50])
Values of $\mathscr{M}$ and α, as indicated in relation (71)	$\mathscr{M} = 4$ and $\alpha = 1$
Coefficients to be determined in relation (71)	$a_i = 0$ for $i = 0, 1, 3$, $a_2 = 8$, and $a_4 = 32$
Solution	x^2

Table 2

Conformable fractional differential equation	$\mathscr{D}^4 u(x) + \mathscr{D}^{7/2} u(x) + u^3(x) = x^9,\ 0 < x \leq 1$
Initial conditions	$u(0) = 0, u'(0) = 0, u''(0) = 0$, and $u'''(0) = 6$
Exact solution	x^3 (as given in [51, 52])
Values of $\mathscr{M}$ and α, as is indicated in relation (71).	$\mathscr{M} = 4$ and $\alpha = 1$
Coefficients to be determined in relation (71)	$a_i = 0$ for $i = 0, 1, 2, 4$, $a_3 = 48$
Solution	x^3

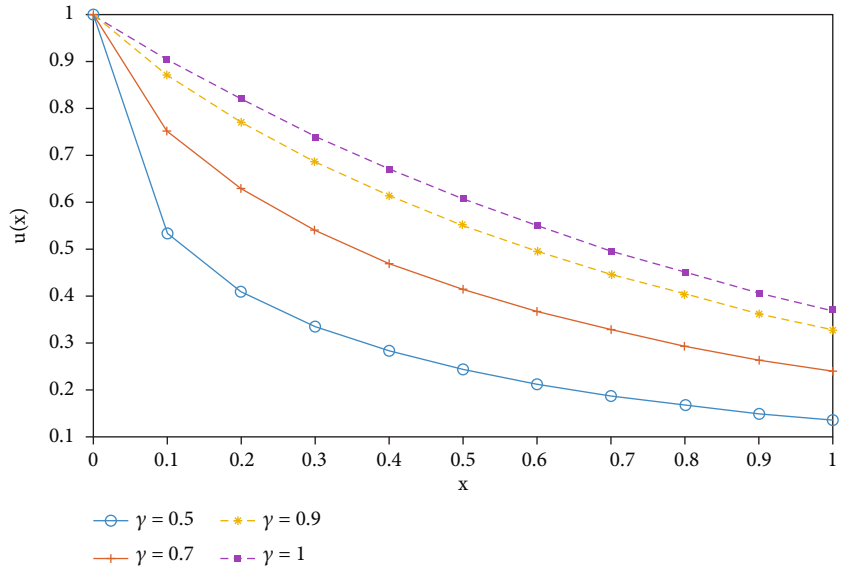

Figure 3: Graph of the approximate solutions of Example 22 when $\mathscr{M} = 5$ with $\gamma = \alpha = 0.5, 0.7, 0.9, 1$.

x; then for $\mathscr{M} = 2$ and $\alpha = 1$ in (71), one gets the approximated solution of (78) in the form

$$u_2(x) = \sum_{m=0}^{2} a_m \tilde{f}_m^{\alpha}(x). \tag{80}$$

Owing to initial condition (79), then (80) gives

$$a_0 = 1, a_1 = 2 \tag{81}$$

Using the collocation point $x = 0.5$ and in view of (81), one can get

$$0.3982 a_2 = 0.7964. \tag{82}$$

Hence, $a_2 = 2$. Therefore, we have $u(x) = 1 + x$, which coincides with the one given in ([47, 49]).

A similar procedure can be carried out as in Example 20, so that we may summarize the corresponding details for two different CFDEs as follows.

Remark 21.

(i) The problem in Table 1 has been treated in [47–50] with the Caputo fractional derivative using various methods such as Legendre polynomials, homotopy perturbation method, and homotopy analysis method

(ii) The problem in Table 2 has been manipulated in [51] by means of Legendre polynomials with conformable

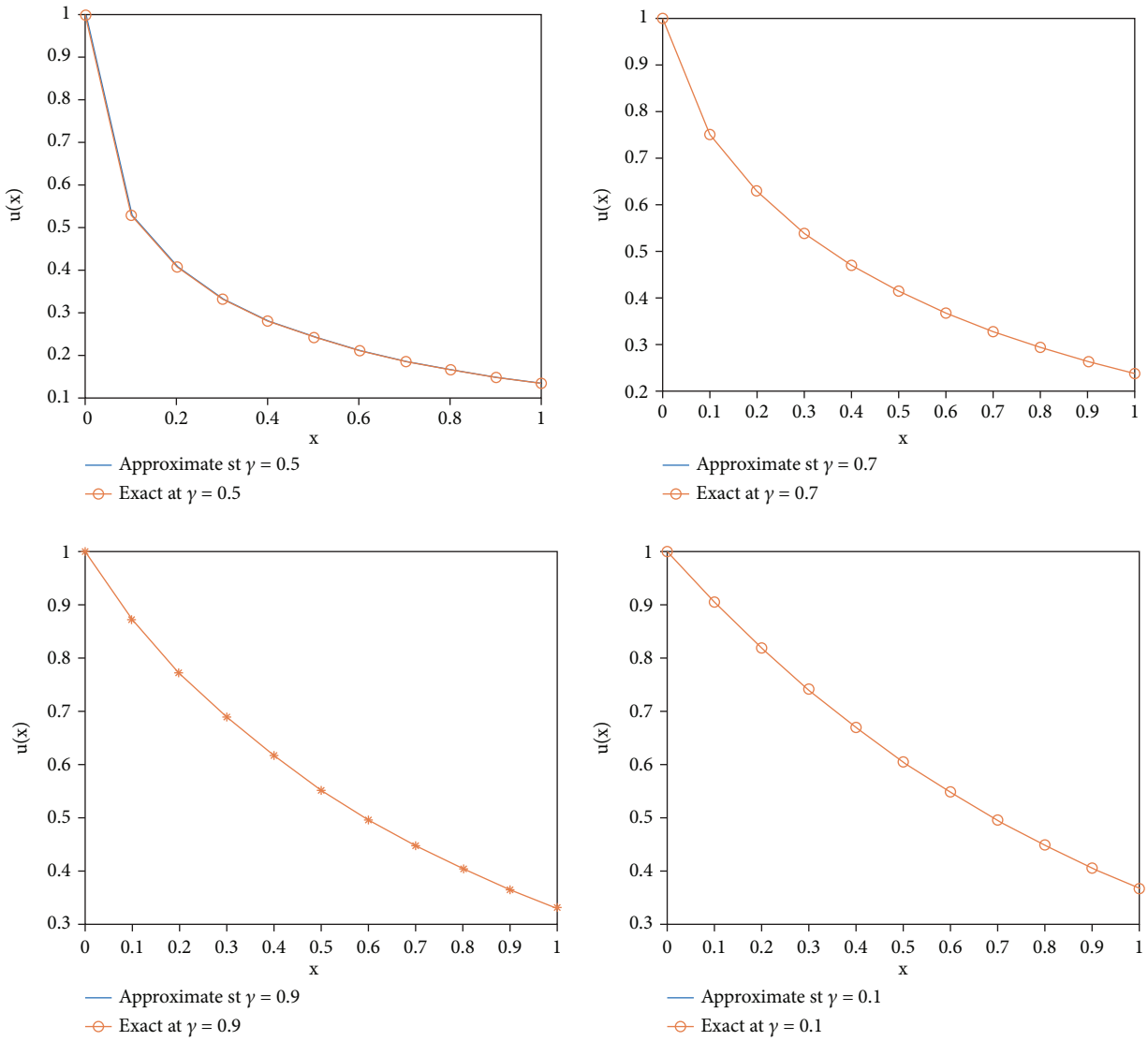

FIGURE 4: The comparison of the approximate solutions of Example 22 with the exact solution when $\mathscr{M} = 5$ and for $\gamma = \alpha = 0.5,0.7,0.9,1$.

derivative and in [52] in view of Laguerre polynomials involving Caputo derivative

Example 22. Suppose that we have the following linear fractional differential equation in the form

$$\mathscr{D}^{\gamma} u(x) + u(x) = 0, \quad 0 < \gamma \leq 1, \tag{83}$$

with the initial condition

$$u(0) = 1. \tag{84}$$

The exact solution of (83) is $u(x) = \exp(-(x^{\gamma}/\gamma))$ (see [47]). This problem has been evaluated using various methods (see for example [47, 49, 53]) in the sense of the Caputo fractional derivative. Putting $\mathscr{M} = 5$ in (71) with $\gamma = \alpha$, then using the presented technique, we computed the approximate solution of the problem (83) for the values $\gamma = \alpha = 0.5,0.7,0.9,1$. We indicate the approximate solution through Figure 3, while Figure 4 compares the obtained solution with the exact solution of (83). Moreover, the corresponding absolute errors of our approximate solution are displayed in Table 3. From Figure 4, it is clear that the approximate solutions converge to the exact solutions.

Example 23. It is well known that the theory of Bessel functions is connected with the Riccati equations. In fact, Bessel functions are defined as solutions of Bessel equations, which can be derived from the Riccati equations. This motivates us to consider the following the nonlinear Riccati fractional differential equation:

$$\mathscr{D}^{\gamma} u(x) + u^2(x) = 1, \quad 0 < \gamma, x \leq 1, \tag{85}$$

subject to the initial condition

$$u(0) = 0. \tag{86}$$

Table 3: Absolute errors for example 22 in the case of $\mathscr{M} = 5$ with various values of $\gamma = \alpha$.

x	$\alpha = 0.5$	$\alpha = 0.7$	$\alpha = 0.9$	$\alpha = 1$
0.1	$1.698913766905.10^{-3}$	$2.01482483935533.10^{-4}$	$2.55260108363852.10^{-5}$	$9.4292936385015.10^{-6}$
0.2	$1.341809039425.10^{-3}$	$1.80206291971352.10^{-4}$	$2.57393080246859.10^{-5}$	$1.0100445353045.10^{-5}$
0.3	$1.094073239144.10^{-3}$	$1.53118426981402.10^{-4}$	$2.22828517444373.10^{-5}$	$8.740914169325.10^{-6}$
0.4	$9.222016584745.10^{-4}$	$1.32711916546735.10^{-4}$	$1.9580499485472.10^{-5}$	$7.674994977578.10^{-6}$
0.5	$7.94771487391.10^{-4}$	$1.17204363458189.10^{-4}$	$1.77639190854228.10^{-5}$	$7.0847477455521.10^{-6}$
0.6	$6.94723214864.10^{-4}$	$1.04225706794691.10^{-4}$	$1.61290436707651.10^{-5}$	$6.5282543029262.10^{-6}$
0.7	$6.13410718572.10^{-4}$	$9.28101826830340.10^{-5}$	$1.43823651976849.10^{-5}$	$5.7858773236572.10^{-6}$
0.8	$5.46280728516.10^{-4}$	$8.30201804029595.10^{-5}$	$1.2815490789575.10^{-5}$	$5.0984705504265.10^{-6}$
0.9	$4.90369742377.10^{-4}$	$7.50420455738476.10^{-5}$	$1.18437600535870.10^{-5}$	$4.8554037531864.10^{-6}$
1	$4.42903116775.10^{-4}$	$6.82330917218671.10^{-5}$	$1.11289526305072.10^{-5}$	$4.7847594708325.10^{-6}$

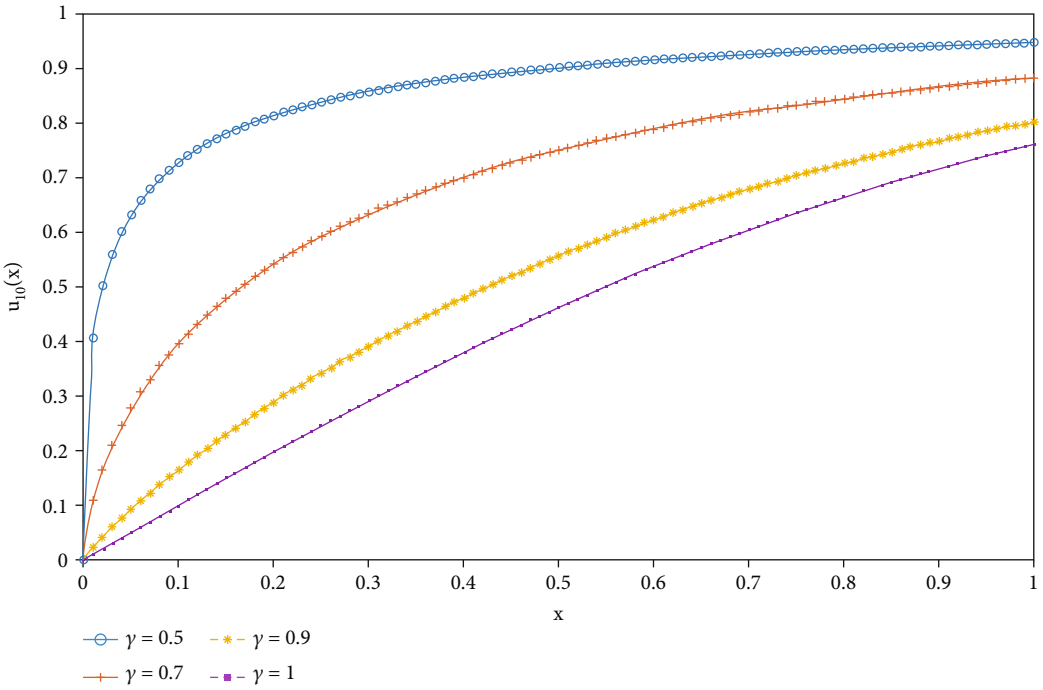

Figure 5: The approximate solutions for various values of $\gamma = \alpha$ in Example 23.

This problem has the exact solution $u_e(x) = [\exp(2x^\gamma/\gamma) - 1]/[\exp(2x^\gamma/\gamma) + 1]$ (see [21]), and it has been treated by many authors using various methods such as the collocation method, operational matrix method, homotopy perturbation Pade technique, homotopy analysis method, modified homotopy perturbation (MHP) method, modified variational iteration method, B-spline operational matrix method, and polynomial least squares method (see, for example, [54, 55]. In all these methods, the authors used the Caputo fractional derivative.

Now, regarding the proposed method here, the approximated analytical solution of the initial value problem (85) has been computed for $\mathscr{M} = 10$ with various values of $\gamma = \alpha$. Figure 5 shows the approximate solutions for $\mathscr{M} = 10$ and various values of $\gamma = \alpha = 0.5,0.7,0.9,1$. Table 4 illustrates both numerical and exact solutions of (85). The comparison between the obtained values of $u(x)$ by the presented method and the modified Homotopy perturbation method (MHPM) given in [55] for $\gamma = 1$ and $\mathscr{M} = 10$ is shown in Table 5. Table 5 illustrates that our method is more accurate compared to other methods.

Example 24. Suppose that a system of fractional differential equations is given in the form

$$\begin{aligned} \mathscr{D}^{\gamma_1} u_1(x) &= u_1(x) + u_2(x), \quad 0 < \gamma_1 \le 1, 0 \le x \le 1, \\ \mathscr{D}^{\gamma_2} u_2(x) &= -u_1(x) + u_2(x), \quad 0 < \gamma_2 \le 1, \end{aligned} \tag{87}$$

Table 4: Obtained values of $u(x)$ for Example 23 by the present method with $\mathscr{M} = 10$ and $\gamma = \alpha = 0.7$ and 0.9.

x	$\gamma = \alpha = 0.7$		$\gamma = \alpha = 0.9$	
	Exact solution $u_e(x)$	Appr. Sol $u_{10}(x)$	Exact solution $u_e(x)$	Appr. Sol $u_{10}(x)$
0.1	0.277560937258027	0.396329287768680	0.138975357216608	0.165142712549575
0.2	0.432562507032238	0.541472216303135	0.255255338098812	0.287926712330121
0.3	0.547648770236210	0.634513884465960	0.359212661331767	0.391527449696852
0.4	0.636470555494007	0.700774990734457	0.451905777263955	0.480439682175042
0.5	0.706113027676249	0.750534511840285	0.533789465005938	0.556914559531437
0.6	0.761214832718165	0.789171534868799	0.605386508611184	0.622580109650008
0.7	0.805098130420862	0.819896688293229	0.667388747653672	0.678810765325902
0.8	0.840237973205243	0.844771155592644	0.720626381374415	0.726831787717051
0.9	0.868514797371047	0.865206088424650	0.766006660708606	0.767744616102944
1	0.891373467734719	0.882214664339926	0.804454800298401	0.802541763903386

Table 5: Comparison of obtained values of $u_{10}(x)$ with MHPM in Example 23 with $\gamma = 1$.

x	MHPM [55]	Present method	Exact solution	Absolute error
0.1	0.099668	0.099667671416668	0.099667994624956	$3.232082876148868.10^{-7}$
0.2	0.197375	0.197375012267825	0.197375320224904	$3.079570785998806.10^{-7}$
0.3	0.291312	0.291312318874021	0.291312612451591	$2.935775703234479.10^{-7}$
0.4	0.379944	0.379948688365082	0.379948962255225	$2.738901430200881.10^{-7}$
0.5	0.462078	0.462116905688459	0.462117157260010	$2.515715507406561.10^{-7}$
0.6	0.536857	0.537049339939348	0.537049566998035	$2.270586874674282.10^{-7}$
0.7	0.603631	0.604367573599157	0.604367777117164	$2.035180060362447.10^{-7}$
0.8	0.661706	0.664036591419464	0.664036770267849	$1.788483853309343.10^{-7}$
0.9	0.709919	0.716297714005185	0.716297870199024	$1.561938393935934.10^{-7}$
1	0.746032	0.761594024015154	0.761594155955765	$1.319406113975582.10^{-7}$

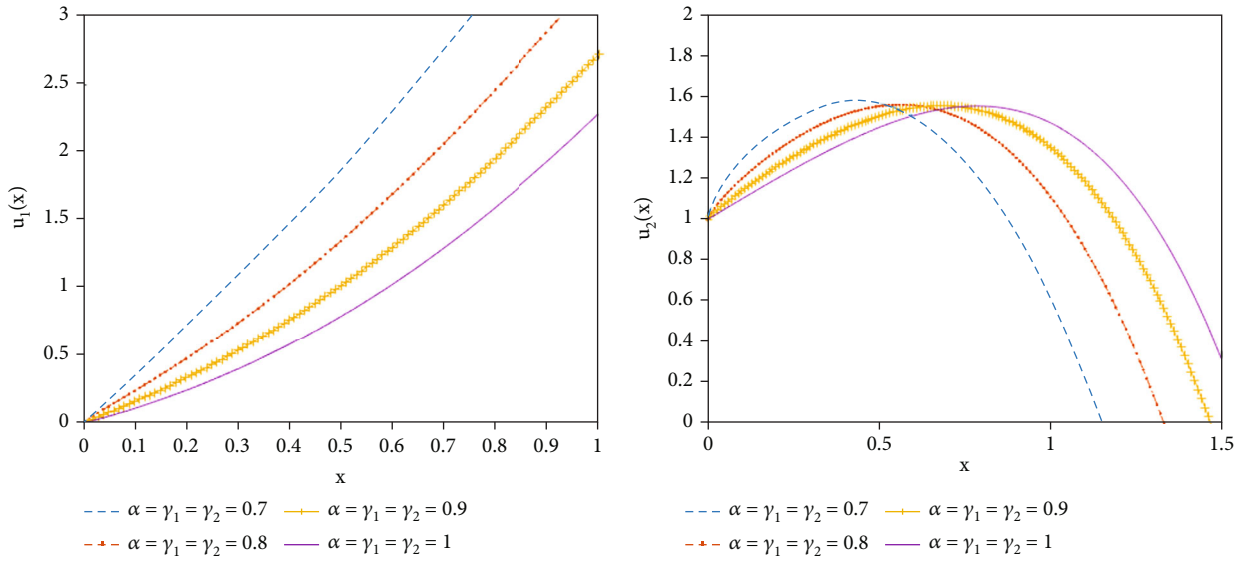

Figure 6: Graph of the approximate solutions $u_1(x)$ and $u_2(x)$ of Example 24 for $\mathscr{M} = 5$ and various values of $\alpha = \gamma_1 = \gamma_2 = 0.7, 0.8, 0.9, 1$.

Table 6: Absolute errors of $u_1(x)$ for various values of $\mathscr{M} = 5, 8, 10$ with $\alpha = \gamma_1 = \gamma_2 = 1$ in Example 24.

x	$\mathscr{M} = 5$	$\mathscr{M} = 8$	$\mathscr{M} = 10$
0.1	$2.175152855412623.10^{-4}$	$9.162421859512191.10^{-8}$	$1.758976284592979.10^{-10}$
0.2	$2.563542720906999.10^{-4}$	$1.010603222372797.10^{-7}$	$1.884819425658612.10^{-10}$
0.3	$2.455251579074233.10^{-4}$	$1.112064359635733.10^{-7}$	$2.046192475246368.10^{-10}$
0.4	$2.320713758760705.10^{-4}$	$1.218391399387871.10^{-7}$	$2.191098474404878.10^{-10}$
0.5	$2.201273528237466.10^{-4}$	$1.315382035648231.10^{-7}$	$2.333426724860480.10^{-10}$
0.6	$1.996737905732100.10^{-4}$	$1.409308454622984.10^{-7}$	$2.471041121886989.10^{-10}$
0.7	$1.643238206067162.10^{-4}$	$1.489432328394127.10^{-7}$	$2.648922750010470.10^{-10}$
0.8	$1.175657989381895.10^{-4}$	$1.556332410815428.10^{-7}$	$2.906084812992896.10^{-10}$
0.9	$6.701651870429315.10^{-5}$	$1.606609913492092.10^{-7}$	$3.310520786806953.10^{-10}$
1	$6.404833938994381.10^{-6}$	$1.601412220569667.10^{-7}$	$4.151750389509799.10^{-10}$

Table 7: Absolute errors of $u_2(x)$ for various values of $\mathscr{M} = 5, 8, 10$ with $\alpha = \gamma_1 = \gamma_2 = 1$ in Example 24.

x	$\mathscr{M} = 5$	$\mathscr{M} = 8$	$\mathscr{M} = 10$
0.1	$1.764442982358745.10^{-4}$	$1.289165400939913.10^{-8}$	$6.228629314555091.10^{-12}$
0.2	$2.483473612144735.10^{-4}$	$3.801071933089472.10^{-9}$	$1.613098247747954.10^{-11}$
0.3	$2.943918013066388.10^{-4}$	$6.996798181222391.10^{-9}$	$3.734106142077792.10^{-11}$
0.4	$3.463545496320502.10^{-4}$	$1.992154729449800.10^{-8}$	$6.483630453443810.10^{-11}$
0.5	$4.089060754978633.10^{-4}$	$3.538677484194269.10^{-8}$	$9.820822938741669.10^{-11}$
0.6	$4.761667760399912.10^{-4}$	$5.339426604651616.10^{-8}$	$1.410768556814162.10^{-10}$
0.7	$5.435609065997361.10^{-4}$	$7.429242006830613.10^{-8}$	$2.010920588084222.10^{-10}$
0.8	$6.132891968498514.10^{-4}$	$9.811361566232743.10^{-8}$	$2.860794615286945.10^{-10}$
0.9	$6.915106434315280.10^{-4}$	$1.250216107427356.10^{-7}$	$4.199493848745102.10^{-10}$
1	$7.750844548684034.10^{-4}$	$1.556557391707215.10^{-7}$	$6.201785524511703.10^{-10}$

with the primary conditions

$$u_1(0) = 0, u_2(0) = 1. \tag{88}$$

We proceed the solution as follows. When $\gamma_1 = \gamma_2 = 1$, the exact solution of this system was given in [56, 57] as $u_1(x) = e^x \sin x$, and $u_2(x) = e^x \cos x$. Applying the same technique described above and by putting $\mathscr{M} = 5$ in (71) with $\alpha = \gamma_1 = \gamma_2$, we have computed the approximate solution for the values $\alpha = \gamma_1 = \gamma_1 = 0.7,0.8,0.9,1$. Figure 6 shows the graphs of approximate solution for various values of $\alpha = \gamma_1 = \gamma_2$ with $\mathscr{M} = 5$. Tables 6 and 7 display the corresponding absolute error to our approximate solutions for $\alpha = \gamma_1 = \gamma_2 = 1$ and various values of $\mathscr{M}$. Note that the absolute error tends to zero when the terms $\mathscr{M}$ of CFBFs increase.

5. Conclusion

Exploring the multifaceted applications of Bessel functions in several fields of science with recognition of the growing impact conformable fractional calculus has in many applications, this paper exhibits further developments on the conformable fractional-order Bessel functions (CFBFs). The novelty of this research paper is determined by explaining the comparison between our obtained solutions (results) and the solutions in previously published articles by various authors. Such novelty may be described as follows. In the first part of the paper, some useful formulas concerning the properties of conformable fractional Laplace transforms are obtained. These formulas are successfully employed to obtain the solutions for a new type of fractional kinetic equations associated with the CFBFs in the conformable fractional sense which is generalized and developed in this study. These solutions are newly presented compared with those given by various authors (see [38, 58–61]).

In addition, an interesting orthogonal relation of the CFBFs is established. This gives rise to the discussion of functions expansions where we present a given function in a series of the CFBFs. Consequently, we investigate the analytical and approximate solutions of some linear and nonlinear CFDEs using a proposed scheme depending on the collocation method, involving CFBFs. Particular emphasis is paid to indicate that our approach, in some sense, is easily applicable and provides more accurate results with refined errors. The proposed scheme is used to approximate the solutions of linear, nonlinear CFDEs, and also systems of CFDEs. The numerical

examples show the validity and efficiency of the method. Notably, it is demonstrated that the presented method works well and achieves better accuracy compared with exact solutions and with results obtained using other methods. Our scheme is beneficial in the way that using the fractional-order Bessel functions leads to more accurate results in approximating the fractional function. Because of this characteristic, FBFs are more effective than Bessel functions in treating fractional problems. Because Bessel polynomials have smaller coefficients than Chebyshev, Legendre, and Bernoulli polynomials, the computational error in the current approach is less. Importantly, the employment of the collocation method provides convenient and accurate solutions. Furthermore, all the given solutions are obtained differently, unlike those established by the authors in [47–55] and the references therein where other fractional derivatives such as Caputo derivative were used.

Data Availability

The data used to support the findings of this study are included within the article.

Conflicts of Interest

The authors declare there is no conflict of interest.

Authors' Contributions

The authors have contributed equally to this work.

Acknowledgments

The authors extend their appreciation to the Deanship of Scientific Research at King Khalid University, Saudi Arabia, through research group program under grant R.G.P.1/86/42.

References

[1] S. Qureshi, "Effects of vaccination on measles dynamics under fractional conformable derivative with Liouville-Caputo operator," *The European Physical Journal Plus*, vol. 135, no. 1, 2020.

[2] M. Dalir and M. Bashour, "Applications of fractional calculus," *Applied Mathematical Sciences*, vol. 4, no. 21, pp. 1021–1032, 2010.

[3] A. A. Kilbas, H. M. Srivastava, and J. J. Trujillo, *Theory and Applications of Fractional Differential Equations, (Vol. 204)*, Elsevier, 2006.

[4] I. Podlubny, *Fractional Differential Equations: An Introduction to Fractional Derivatives, Fractional Differential Equations, to Methods of Their Solution and Some of Their Applications*, Elsevier, 1998.

[5] G. Montseny, J. Audounet, and B. Mbodje, "Optimal models of fractional integrators and application to systems with fading memory," in *Proceedings of IEEE Systems Man and Cybernetics Conference-SMC*, Le Touquet, France, 1993.

[6] T. Kaczorek and K. Rogowski, *Fractional Linear Systems and Electrical Circuits*, Springer International Publishing, Cham, Switzerland, 2015.

[7] F. Mirzaee and N. Samadyar, "On the numerical method for solving a system of nonlinear fractional ordinary differential equations arising in HIV infection of CD4 T cells," *Iranian Journal of Science and Technology, Transactions A: Science*, vol. 43, no. 3, pp. 1127–1138, 2019.

[8] Q. M. Al-Mdallal, "On fractional-Legendre spectral Galerkin method for fractional Sturm-Liouville problems," *Chaos, Solitons and Fractals*, vol. 116, pp. 261–267, 2018.

[9] Q. M. Al-Mdallal, H. Yusuf, and A. Ali, "A novel algorithm for time-fractional foam drainage equation," *Alexandria Engineering Journal*, vol. 59, no. 3, pp. 1607–1612, 2020.

[10] K. S. Miller and B. Ross, *An Introduction to the Fractional calculus and Fractional Differential Equations*, Wiley, 1993.

[11] M. F. Simões Patrício, H. Ramos, and M. Patrício, "Solving initial and boundary value problems of fractional ordinary differential equations by using collocation and fractional powers," *Journal of Computational and Applied Mathematics*, vol. 354, pp. 348–359, 2019.

[12] R. Khalil, M. Al Horani, A. Yousef, and M. Sababheh, "A new definition of fractional derivative," *Journal of Computational and Applied Mathematics*, vol. 264, pp. 65–70, 2014.

[13] V. E. Tarasov, "No violation of the Leibniz rule. No fractional derivative," *Communications in Nonlinear Science and Numerical Simulation*, vol. 18, no. 11, pp. 2945–2948, 2013.

[14] M. Abul-Ez, M. Zayed, A. Youssef, and M. De la Sen, "On conformable fractional Legendre polynomials and their convergence properties with applications," *Alexandria Engineering Journal*, vol. 59, no. 6, pp. 5231–5245, 2020.

[15] M. Abul-Ez, M. Zayed, and A. Youssef, "Further study on the conformable fractional Gauss hypergeometric function," *Aims Mathematics*, vol. 6, no. 9, pp. 10130–10163, 2021.

[16] T. Abdeljawad, "On conformable fractional calculus," *Journal of Computational and Applied Mathematics*, vol. 279, pp. 57–66, 2015.

[17] D. R. Anderson, E. Camrud, and D. J. Ulness, "On the nature of the conformable derivative and its applications to physics," *Journal of Fractional Calculus and Applications*, vol. 10, no. 2, pp. 92–135, 2019.

[18] H. W. Zhou, S. Yang, and S. Q. Zhang, "Conformable derivative approach to anomalous diffusion," *Physica A: Statistical Mechanics and its Applications*, vol. 491, pp. 1001–1013, 2018.

[19] A. Atangana, D. Baleanu, and A. Alsaedi, "New properties of conformable derivative," *Open Mathematics*, vol. 13, no. 1, pp. 889–898, 2015.

[20] O. T. Birgani, S. Chandok, N. Dedovic, and S. Radenovic, "A note on some recent results of the conformable fractional derivative," *Advances in the Theory of Nonlinear Analysis and its Application*, vol. 3, no. 1, pp. 11–17, 2018.

[21] E. Ünal and A. Gökdoğan, "Solution of conformable fractional ordinary differential equations via differential transform method," *Optik*, vol. 128, pp. 264–273, 2017.

[22] D. Zhao and M. Luo, "General conformable fractional derivative and its physical interpretation," *Calcolo*, vol. 54, no. 3, pp. 903–917, 2017.

[23] A. Younas, T. Abdeljawad, R. Batool, A. Zehra, and M. A. Alqudah, "Linear conformable differential system and its controllability," *Advances in Difference Equations*, vol. 2020, no. 1, 26 pages, 2020.

[24] A. Atangana and D. Baleanu, "New fractional derivatives with nonlocal and non-singular kernel: theory and application to heat transfer model," *Thermal Science*, vol. 20, no. 2, pp. 763–769, 2016.

[25] J. Niedziela, *Bessel Functions and Their Applications*, University of Tennessee, Knoxville, 2008.

[26] A. Gökdoğan, E. Ünal, and E. Çelik, "Conformable fractional Bessel equation and Bessel functions," 2015, https://arxiv.org/abs/1506.07382.

[27] H. Dehestani, Y. Ordokhani, and M. Razzaghi, "Fractional-order Bessel functions with various applications," *Applications of Mathematics*, vol. 64, no. 6, pp. 637–662, 2019.

[28] M. Izadi and C. Cattani, "Generalized Bessel polynomial for multi-order fractional differential equations," *Symmetry*, vol. 12, no. 8, 2020.

[29] M. A. Abul-Ez, "Bessel polynomial expansions in spaces of holomorphic functions," *Journal of Mathematical Analysis and Applications*, vol. 221, no. 1, pp. 177–190, 1998.

[30] M. Abdalla, M. Abul-Ez, and J. Morais, "On the construction of generalized monogenic Bessel polynomials," *Mathematical Methods in the Applied Sciences*, vol. 41, no. 18, pp. 9335–9348, 2018.

[31] Ş. Yüzbaşi, N. Şahin, and M. Sezer, "Numerical solutions of systems of linear Fredholm integro-differential equations with Bessel polynomial bases," *Computers & Mathematics with Applications*, vol. 61, no. 10, pp. 3079–3096, 2011.

[32] K. Parand, M. Nikarya, and J. A. Rad, "Solving non-linear lane-Emden type equations using Bessel orthogonal functions collocation method," *Celestial Mechanics and Dynamical Astronomy*, vol. 116, no. 1, pp. 97–107, 2013.

[33] E. Tohidi and H. Saberi Nik, "A Bessel collocation method for solving fractional optimal control problems," *Applied Mathematical Modelling*, vol. 39, no. 2, pp. 455–465, 2015.

[34] E. Grosswald, *Bessel Polynomials*, Springer-Verlag, Berlin Heidelberg, 1978.

[35] D. E. Rainville, *Special Functions*, Chelsea, New York, 1960.

[36] A. Wiman, "Über den fundamentalsatz in der teorie der funktionen $E_a(x)$," *Acta Mathematica*, vol. 29, pp. 191–201, 1905.

[37] H. J. Haubold and A. M. Mathai, "The fractional kinetic equation and thermonuclear functions," *Astrophysics and Space Science*, vol. 273, no. 1/4, pp. 53–63, 2000.

[38] R. K. Saxena and S. L. Kalla, "On the solutions of certain fractional kinetic equations," *Applied Mathematics and Computation*, vol. 199, no. 2, pp. 504–511, 2008.

[39] S. G. Samko, A. A. Kilbas, and O. I. Marichev, *Fractional Integrals and Derivatives, Yverdon-les-Bains*, Gordon and Breach Science Publishers, Yverdon, Switzerland, 1993.

[40] W. W. Bell, *Special Functions for Scientists and Engineers*, Courier Corporation, 2004.

[41] R. P. Boas and R. C. Buck, *Polynomial Expansions of Analytic Functions*, Springer-Verlag, Berlin Heidelberg, 1958.

[42] G. Faber, "Über polynomische Entwickelungen," *Mathematische Annalen*, vol. 57, no. 3, pp. 389–408, 1903.

[43] J. Whittaker and C. Gattegno, *Sur les Séries de Base de Polynbmes Quelconques*, Gauthier-Villars, Paris, 1949.

[44] M. A. Abul-ez and D. Constales, "Basic sets of pofynomials in Clifford analysis," *Complex Variables, Theory and Application: An International Journal*, vol. 14, no. 1-4, pp. 177–185, 1990.

[45] M. Zayed, M. Abul-Ez, and J. P. Morais, "Generalized derivative and primitive of Cliffordian bases of polynomials constructed through Appell monomials," *Computational Methods and Function Theory*, vol. 12, no. 2, pp. 501–515, 2012.

[46] M. Zayed, "Generalized Hadamard product bases of special monogenic polynomials," *Advances in Applied Clifford Algebras*, vol. 30, no. 1, 2020.

[47] S. Kazem, S. Abbasbandy, and S. Kumar, "Fractional-order Legendre functions for solving fractional-order differential equations," *Applied Mathematical Modelling*, vol. 37, no. 7, pp. 5498–5510, 2013.

[48] H. Jafari, S. Das, and H. Tajadodi, "Solving a multi-order fractional differential equation using homotopy analysis method," *Journal of King Saud University-Science*, vol. 23, no. 2, pp. 151–155, 2011.

[49] A. Saadatmandi and M. Dehghan, "A new operational matrix for solving fractional-order differential equations," *Computers and Mathematics with Applications*, vol. 59, no. 3, pp. 1326–1336, 2010.

[50] N. H. Sweilam, M. M. Khader, and R. F. Al-Bar, "Numerical studies for a multi-order fractional differential equation," *Physics Letters A*, vol. 371, no. 1-2, pp. 26–33, 2007.

[51] H. Çerdik Yaslan and F. Mutlu, "Numerical solution of the conformable differential equations via shifted Legendre polynomials," *International Journal of Computer Mathematics*, vol. 97, no. 5, pp. 1016–1028, 2020.

[52] M. M. Khader, T. S. El Danaf, and A. S. Hendy, "Efficient spectral collocation method for solving multi-term fractional differential equations based on the generalized Laguerre polynomials," *Journal of Fractional Calculus and Applications*, vol. 3, pp. 1–14, 2012.

[53] K. Parand and M. Nikarya, "Application of Bessel functions for solving differential and integro- differential equations of the fractional order," *Applied Mathematical Modelling*, vol. 38, no. 15-16, pp. 4137–4147, 2014.

[54] C. Bota and B. Căruntu, "Analytical approximate solutions for quadratic Riccati differential equation of fractional order using the polynomial least squares method," *Chaos, Solitons and Fractals*, vol. 102, pp. 339–345, 2017.

[55] Z. Odibat and S. Momani, "Modified homotopy perturbation method: application to quadratic Riccati differential equation of fractional order," *Chaos, Solitons & Fractals*, vol. 36, no. 1, pp. 167–174, 2008.

[56] M. Zurigat, S. Momani, Z. Odibat, and A. Alawneh, "The homotopy analysis method for handling systems of fractional differential equations," *Applied Mathematical Modelling*, vol. 34, no. 1, pp. 24–35, 2010.

[57] S. Momani and Z. Odibat, "Numerical approach to differential equations of fractional order," *Journal of Computational and Applied Mathematics*, vol. 207, no. 1, pp. 96–110, 2007.

[58] D. Kumar, S. D. Purohit, A. Secer, and A. Atangana, "On generalized fractional kinetic equations involving generalized Bessel function of the first kind," *Mathematical Problems in Engineering*, vol. 2015, Article ID 289387, 7 pages, 2015.

[59] P. Agarwal, M. Chand, D. Baleanu, D. O'Regan, and S. Jain, "On the solutions of certain fractional kinetic equations involving k-Mittag-Leffler function," *Advances in Difference Equations*, vol. 2018, no. 1, 2018.

[60] G. Singh, P. Agarwal, M. Chand, and S. Jain, "Certain fractional kinetic equations involving generalized k-Bessel function," *Transactions of A. Razmadze Mathematical Institute*, vol. 172, no. 3, pp. 559–570, 2018.

[61] P. Agarwal, M. Chand, and G. Singh, "Certain fractional kinetic equations involving the product of generalized k-Bessel function," *Alexandria Engineering Journal*, vol. 55, no. 4, pp. 3053–3059, 2016.

Hindawi
Journal of Function Spaces
Volume 2021, Article ID 4797955, 11 pages
https://doi.org/10.1155/2021/4797955

Research Article

Analytic Normalized Solutions of 2D Fractional Saint-Venant Equations of a Complex Variable

Najla M. Alarifi[1] **and Rabha W. Ibrahim**[2]

[1]*Department of Mathematics, Imam Abdulrahman Bin Faisal University, Dammam 31113, Saudi Arabia*
[2]*IEEE: 94086547, Kuala Lumpur 59200, Malaysia*

Correspondence should be addressed to Rabha W. Ibrahim; rabhaibrahim@yahoo.com

Received 14 July 2021; Accepted 4 August 2021; Published 10 September 2021

Academic Editor: Badr Saad. T. Alkaltani

Saint-Venant equations describe the flow below a pressure surface in a fluid. We aim to generalize this class of equations using fractional calculus of a complex variable. We deal with a fractional integral operator type Prabhakar operator in the open unit disk. We formulate the extended operator in a linear convolution operator with a normalized function to study some important geometric behaviors. A class of integral inequalities is investigated involving special functions. The upper bound of the suggested operator is computed by using the Fox-Wright function, for a class of convex functions and univalent functions. Moreover, as an application, we determine the upper bound of the generalized fractional 2-dimensional Saint-Venant equations (2D-SVE) of diffusive wave including the difference of bed slope.

1. Introduction

Newly, fractional calculus has expanded considerable attention primarily appreciations to the growing occurrence of investigation mechanisms in the life sciences, allowing for simulations found by fractional operators [1] including differential and integral formulas. Further, the mathematical investigation of fractional calculus has advanced, chief to connections with other mathematical areas such as probability theory, mathematical physics [2], and mathematical biology [3–7] and the investigation of stochastic processes in real cases. In addition, it appears in studies of complex analysis. Now the literature, several different definitions of fractional integrals and derivatives are presented. Some of them such as the Riemann-Liouville integral, the Caputo, and the Riemann-Liouville differential operators are extensively employed in mathematics and physics and actually utilized in applied structures, modeling systems in real cases. While, in complex analysis, especially the theory of geometric functions, the researchers are focusing on Srivastava-Owa integral and differential operators [8], Tremblay differential operator, and the most recent fractional operator in [9, 10]. A new investigation of the complex ABC-fractional operator is presented to formulate different classes of analytic functions [11]. Some definitions such as the Hilfer and Prabhakar results [12] (differential and integral operators) are essentially the theme of mathematical study.

Our study is aimed to extend the Prabhakar operator [13] to the open unit disk utilizing the class of normalized analytic functions. We formulate this operates in a linear convolution operator to study some important geometric behaviors. A class of integral inequalities is investigated involving special functions. The upper bound of the suggested operator is computed by using the Fox-Wright function, for a class of convex functions and univalent functions, and other studies are illustrated in the sequel.

2. Complex Prabhakar Operator (CPO)

The Prabhakar integral operator is defined for analytic function $\phi(z) \in \mathscr{H}[0,1] = \{\phi \in \cup : \phi_1 z + \phi_2 z^2 + \cdots\}$ by the

formula [14–20]

$$P_{\alpha,\beta}^{\gamma,\omega}\phi(z)=\int_0^z (z-\zeta)^{\beta-1}\Xi_{\alpha,\beta}^{\gamma}\left[\omega(z-\zeta)^{\alpha}\right]\phi(\zeta)d\zeta=\left(\phi\cdot\rho_{\alpha,\beta}^{\gamma,\omega}\right)(z),$$
$$(\alpha,\beta,\gamma,\omega\in\mathbb{C},\ z\in\cup\coloneqq\{z\in\mathbb{C}:|z|<1\},\ \Re(\alpha),\Re(\beta)>0), \tag{1}$$

where, [15]

$$\rho_{\alpha,\beta}^{\gamma,\omega}(z)\coloneqq z^{\beta-1}\Xi_{\alpha,\beta}^{\gamma}(\omega z^{\alpha}),$$
$$\Xi_{\alpha,\beta}^{\gamma}(\chi)=\sum_{n=0}^{\infty}\frac{\Gamma(\gamma+n)}{\Gamma(\gamma)\Gamma(\alpha n+\beta)}\frac{\chi^n}{n!}. \tag{2}$$

For example, let $\phi(z)=z^{\varepsilon-1}$ then in view of [21] Corollary 2.3, we have

$$P_{\alpha,\beta}^{\gamma,\omega}z^{\varepsilon-1}=\int_0^z (z-\zeta)^{\beta-1}\Xi_{\alpha,\beta}^{\gamma}\left[\omega(z-\zeta)^{\alpha}\right]\left(\zeta^{\varepsilon-1}\right)d\zeta$$
$$=\Gamma(\varepsilon)z^{\beta+\varepsilon-1}\Xi_{\alpha,\beta+\varepsilon}^{\gamma}(\omega z^{\alpha}). \tag{3}$$

The Prabhakar derivative can be computed by the formula [13]

$$D_{\alpha,\beta}^{\gamma,\omega}\phi(z)=\frac{d^k}{dz^k}\left(P_{\alpha,k-\beta}^{-\gamma,\omega}\phi(z)\right),\ z\in\cup. \tag{4}$$

To study the geometric indications of CPO, we introduce the following class of analytic function: a normalized analytic function $\phi(z)\in\wedge, z\in\cup$ achieving the power series

$$\phi(z)=z+\sum_{n=2}^{\infty}\phi_n z^n,\quad z\in\cup, \tag{5}$$

Two analytic functions f,g are called convoluted, denoting by $f*g$ if and only if

$$(f*g)(z)=\left(\sum_{n=0}^{\infty}a_n z^n\right)*\left(\sum_{n=0}^{\infty}g_n z^n\right)=\sum_{n=0}^{\infty}a_n g_n z^n. \tag{6}$$

Definition 1. Define a new function $\Omega:\cup\longrightarrow\cup$, such that

$$\Omega_{\alpha,\beta}^{\gamma,\omega}(z)\coloneqq\left(\frac{\Gamma(\alpha+\beta)}{\gamma\omega^{1/\alpha}}\right)z^{1-\beta}\rho_{\alpha,\beta}^{\gamma,\omega}\left(z^{\frac{1}{\alpha}}\right)$$
$$=\left(\frac{\Gamma(\alpha+\beta)}{\gamma\omega^{1/\alpha}}\right)\Xi_{\alpha,\beta}^{\gamma}\left(\omega^{\frac{1}{\alpha}}\left(z^{\frac{1}{\alpha}}\right)^{\alpha}\right)$$
$$=\left(\frac{\Gamma(\alpha+\beta)}{\gamma\omega^{1/\alpha}}\right)\sum_{n=0}^{\infty}\frac{\Gamma(\gamma+n)}{\Gamma(\gamma)\Gamma(\alpha n+\beta)}\frac{\left(\omega^{1/\alpha}z\right)^n}{n!} \tag{7}$$
$$=\left(\frac{\Gamma(\alpha+\beta)}{\gamma\omega^{1/\alpha}}\right)\sum_{n=0}^{\infty}\left(\frac{\Gamma(\gamma+n)\omega^{n/\alpha}}{\Gamma(\gamma)\Gamma(\alpha n+\beta)}\right)\frac{z^n}{n!},$$
$$\cdot(\alpha,\beta,\gamma,\omega\in\mathbb{C},z\in\cup,\Re(\alpha),\Re(\beta)>0).$$

Note that,

$$\left(\Omega_{1,1}^{1,1}\right)(z)=\sum_{n=0}^{\infty}\frac{z^n}{n!}=e^z, \tag{8}$$

where e^z is a transcendental function. Utilizing the functional $\Omega_{\alpha,\beta}^{\gamma,\omega}$, we define the modified complex linear Prabhakar operator

$$\mathbb{P}_{\alpha,\beta}^{\gamma,\omega}\phi(z)\coloneqq\Omega_{\alpha,\beta}^{\gamma,\omega}*\phi(z),\quad \phi\in\wedge. \tag{9}$$

We have the following result.

Proposition 2. *If $\phi\in\wedge$, then $\mathbb{P}_{\alpha,\beta}^{\gamma,\omega}\phi(z)=(\Omega_{\alpha,\beta}^{\gamma,\omega}*\phi)\in\wedge$, where $*$ indicates the convolution product.*

Proof. Let $\phi\in\wedge$, then we have

$$\left(\Omega_{\alpha,\beta}^{\gamma,\omega}*\phi\right)(z)=\Omega_{\alpha,\beta}^{\gamma,\omega}(z)*\phi(z)$$
$$=\left(\frac{\Gamma(\alpha+\beta)}{\gamma\omega^{1/\alpha}}\right)\left(\sum_{n=0}^{\infty}\frac{\Gamma(\gamma+n)\omega^{n/\alpha}}{\Gamma(\gamma)\Gamma(\alpha n+\beta)}\frac{z^n}{n!}\right)$$
$$*\left(z+\sum_{n=2}^{\infty}\phi_n z^n\right)=\left(\left(\frac{\Gamma(\alpha+\beta)}{\Gamma(\beta)\gamma\omega^{1/\alpha}}\right)\right.$$
$$\left.+\left(\frac{\Gamma(\alpha+\beta)}{\gamma\omega^{1/\alpha}}\right)\left(\frac{\gamma\omega^{1/\alpha}}{\Gamma(\alpha+\beta)}\right)z+\cdots\right)$$
$$*\left(0+z+\phi_2 z^2+\cdots\right)=z+\sum_{n=2}^{\infty}\left(\frac{\Gamma(\alpha+\beta)}{\gamma\omega^{1/\alpha}}\right)$$
$$\cdot\left(\frac{\Gamma(\gamma+n)\omega^{n/\alpha}}{\Gamma(\gamma)\Gamma(\alpha n+\beta)}\right)\frac{\phi_n}{n!}z^n\coloneqq z+\sum_{n=2}^{\infty}\Phi_n z^n, \tag{10}$$

where

$$\Phi_n=\left(\frac{\Gamma(\alpha+\beta)}{\gamma\omega^{1/\alpha}}\right)\left(\frac{\Gamma(\gamma+n)\omega^{n/\alpha}}{\Gamma(\gamma)\Gamma(\alpha n+\beta)}\right)\frac{\phi_n}{n!}$$
$$=\left(\frac{\Gamma(\alpha+\beta)}{\Gamma(\gamma+1)\omega^{1/\alpha}}\right)\left(\frac{\Gamma(\gamma+n)\omega^{n/\alpha}}{\Gamma(\alpha n+\beta)}\right)\frac{\phi_n}{n!}. \tag{11}$$

Hence, $\mathbb{P}_{\alpha,\beta}^{\gamma,\omega}\phi(z)=(\Omega_{\alpha,\beta}^{\gamma,\omega}*\phi)(z)\in\wedge$. ?

We need the following concepts to study the $\mathbb{P}_{\alpha,\beta}^{\gamma,\omega}\phi(z)$ geometrically.

Definition 3. A function $\phi\in\wedge$ is indicated to be starlike including the origin of the linear slice contains the origin to all further point of ϕ in $\phi(z\in\cup)$. A univalent function (one-one) ϕ is indicated to be convex in $\cup$ if the linear slice relating every two points of $\phi(z)$ lies completely in $\phi(z\in\cup)$. We indicate these classes by $\mathcal{S}^*$ and $\mathcal{C}$ for starlike and convex consistently. Consider the class $\mathcal{P}$ includes all mappings $\wp$ smooth in $\cup$ with a positive real part in $\cup$ realizing $\wp(0)=1$

, $\wp'(0) > 0$. Precisely, $\phi \in \mathcal{S}^* \Leftrightarrow z\phi'(z)/\phi(z) \in \mathcal{P}$ and $\phi \in \mathcal{C} \Leftrightarrow 1 + z\phi''(z)/\phi'(z) \in \mathcal{P}$. Regularly, $\Re(z\phi'(z)/\phi(z)) > 0$ for the starlikeness and $\Re(1 + z\phi''(z)/\phi'(z)) > 0$ for the convexity.

Two analytic functions f_1, f_2 in $\mathbb{U}$ are called subordinated [22] denoting by $f_1 \prec f_2$ or $f_1(z) \prec f_2(z), z \in \cup$, if there occurs an analytic function $\omega, |\omega| \leq |z| < 1$ satisfying

$$f_1(z) = f_2(\omega(z)), \quad z \in \cup. \tag{12}$$

Next, lemma can be located in [22], P138-140.

Lemma 4. *Let $h \in \wedge$. Then,*

(a) $h(z) + az\,h'(z) \prec (1+a)z + az^2 \Rightarrow h(z) \prec z$, *when* $a \in (0, 1/3]$

(b) $zh'(z)[1 + h(z)] + ah^2(z) \prec z + (1+a)z^2 \Rightarrow h(z) \prec z$, *when* $|1 + a| \leq 1/4$

(c) $[zh'(z) - h(z)]e^{a(h(z))} + e^{h(z)} \prec e^z \Rightarrow h(z) \prec z$, *when* $|a - 1| \leq \pi/2$

(d) $zh'(z)(1 + ah(z)) + h(z) \prec 2z + az^2 \Rightarrow h(z) \prec z$, *when* $|a| \leq 1/2$

(e) $zh'(z)e^{a\,h(z)} + h(z) \prec z(1 + aze^{az}) \Rightarrow h(z) \prec z$, *when* $|a| \leq 1$

(f) $h(z) + (zh'(z)/1 + ah(z)) \prec z \Rightarrow h(z) \prec z$, *when* $|a| \leq 1$

and the solution is sharp.

Definition 5. The Fox-Wright function ${}_p\mathscr{W}_q(z)$ (the extension function of hypergeometric function) is formulated by

$$\begin{aligned} {}_p\mathscr{W}_q\left[\begin{matrix}(x_1, X_1) & (x_2, X_2) & \cdots & (x_p, X_p) \\ (y_1, Y_1) & (y_2, Y_2) & \cdots & (y_q, Y_q)\end{matrix}; z\right] \\ = \sum_{n=0}^{\infty} \frac{\Gamma(x_1 + X_1 n) \cdots \Gamma(x_p + X_p n)}{\Gamma(y_1 + Y_1 n) \cdots \Gamma(y_q + Y_q n)} \frac{z^n}{n!}. \end{aligned} \tag{13}$$

And it normalized by

$$\begin{aligned} {}_p\mathscr{W}_q^*\left[\begin{matrix}(x_1, X_1) & (x_2, X_2) & \cdots & (x_p, X_p) \\ (y_1, Y_1) & (y_2, Y_2) & \cdots & (y_q, Y_q)\end{matrix}; z\right] \\ = \frac{\Gamma(y_1) \cdots \Gamma(y_q)}{\Gamma(x_1) \cdots \Gamma(x_p)} \sum_{n=0}^{\infty} \frac{\Gamma(x_1 + X_1 n) \cdots \Gamma(x_p + X_p n)}{\Gamma(y_1 + Y_1 n) \cdots \Gamma(y_q + Y_q n)} \frac{z^n}{n!}. \end{aligned} \tag{14}$$

Note that the series is converged when

$$\triangleright := \sum_{j=1}^{q} Y_j - \sum_{i=1}^{p} X_i \geq -1. \tag{15}$$

Moreover, it converges for all finite values z to the entire function provided $\triangleright < -1$. In addition, at the boundary $|z| = 1$, it has the convergence value (see [23])

$$\Re(\triangleleft) := \Re\left(\sum_{j=1}^{q} y_j - \sum_{i=1}^{p} x_i + \frac{p - q - 1}{2}\right) > 0. \tag{16}$$

The significance of the Fox-Wright function arises regularly from its part in fractional calculus (see [1]). Further fascinating applications correspondingly occur. Wright's original attentiveness in this function was connected to the asymptotic theory of partitions [24]. The formula $\triangleleft$ is generated in [23] by adding a positive parameter $\theta > 0$ as follows:

$$\triangleleft_\theta := \sum_{j=1}^{q} y_j + \theta - \sum_{i=1}^{p} x_i + \frac{p - q - 1}{2}. \tag{17}$$

Based on this generalization, the authors in [24] introduced the following lemma.

Lemma 6. *Assume that $\triangleright = -1, \theta > 0$ and $\Re(\triangleleft_\theta) > 0$. Then,*

$${}_p\mathscr{W}_q(z) = \Gamma(\theta) \int_0^1 \frac{H\left(\rho^{-1}t\right)dt}{t\left(1 - tz\rho^{-1}\right)^{\theta}}, \quad |z| < \rho, \tag{18}$$

where

$$H := \frac{1}{2\pi i} \int_{\cup} \Pi(\varsigma, \theta) z^{-\varsigma} / \Gamma(\varsigma + \theta) d\varsigma < \infty, \tag{19}$$

is the delta-neutral H function and Π indicates the Fox-Wright coefficients.

Proposition 7. *Let $\phi \in \mathcal{C}$ (convex in the open unit disk), then*

$$\begin{aligned} \left|\left(\Omega_{\alpha,\beta}^{\gamma,\omega} * \phi\right)'(z)\right| \leq {}_1\mathscr{W}_1^*\left[\begin{matrix}(1+\gamma, 1) \\ (\alpha + \beta, \alpha)\end{matrix}; \omega^{1/\alpha} r\right], \\ (\alpha > 0, \quad \beta > 0, \quad |z| := r < 1, \gamma, \omega \in \mathbb{R}_+), \end{aligned} \tag{20}$$

Proof. Since $\phi \in \mathcal{C}$, then for each $n \geq 2$, we have $|\phi_n| \leq 1$.

Then, a computation implies that

$$\begin{aligned}\left|\left(\Omega_{\alpha,\beta}^{\gamma,\omega} * \phi\right)(z)\right| &\le \left(\frac{\Gamma(\alpha+\beta)}{\Gamma(\gamma+1)\omega^{1/\alpha}}\right)\sum_{n=1}^{\infty}\left(\frac{\Gamma(\gamma+n)\omega^{n/\alpha}}{\Gamma(\alpha n+\beta)}\right)\frac{|\phi_n|}{n!}\, r^n \\ &\le \left(\frac{\Gamma(\alpha+\beta)}{\Gamma(\gamma+1)\omega^{1/\alpha}}\right)\sum_{n=1}^{\infty}\left(\frac{\Gamma(\gamma+n)\omega^{n/\alpha}}{\Gamma(\alpha n+\beta)}\right)\frac{r^n}{n!} \\ &= \left(\frac{\Gamma(\alpha+\beta)}{\Gamma(\gamma+1)\omega^{1/\alpha}}\right)\sum_{n=1}^{\infty}\left(\frac{\Gamma(\gamma+n)}{\Gamma(\alpha n+\beta)}\right)\frac{\left(\omega^{1/\alpha}r\right)^n}{n!} \\ &= \left(\frac{\Gamma(\alpha+\beta)}{\Gamma(\gamma+1)\omega^{1/\alpha}}\right)\sum_{n=0}^{\infty}\left(\frac{\Gamma(\gamma+1+n)}{\Gamma(\alpha n+\alpha+\beta)}\right)\frac{\left(\omega^{1/\alpha}r\right)^{n+1}}{(n+1)!} \\ &= \left(\omega^{1/\alpha}r\right)\left(\frac{\Gamma(\alpha+\beta)}{\Gamma(\gamma+1)\omega^{1/\alpha}}\right)\sum_{n=0}^{\infty} \\ &\quad\cdot\left(\frac{\Gamma(1+n)\Gamma(1+\gamma+n)}{\Gamma(2+n)\Gamma(\alpha n+\alpha+\beta)}\right)\frac{\left(\omega^{1/\alpha}r\right)^n}{(n)!} \\ &= r\left(\frac{\Gamma(\alpha+\beta)}{\Gamma(\gamma+1)}\right)\sum_{n=0}^{\infty}\left(\frac{\Gamma(1+n)\Gamma(1+\gamma+n)}{\Gamma(2+n)\Gamma(\alpha n+\alpha+\beta)}\right)\frac{\left(\omega^{1/\alpha}r\right)^n}{(n)!} \\ &= r\left(\frac{\Gamma(\alpha+\beta)}{\Gamma(\gamma+1)}\right)_2\mathscr{W}_2\left[\begin{matrix}(1,1) & (1+\gamma,1)\\ (2,1) & (\alpha+\beta,\alpha)\end{matrix};\omega^{1/\alpha}r\right] \\ &= r\left(\frac{\Gamma(2)\Gamma(\alpha+\beta)}{\Gamma(\gamma+1)\Gamma(1)}\right)_2\mathscr{W}_2\left[\begin{matrix}(1,1) & (1+\gamma,1)\\ (2,1) & (\alpha+\beta,\alpha)\end{matrix};\omega^{1/\alpha}r\right] \\ &= r_2\mathscr{W}_2^*\left[\begin{matrix}(1,1) & (1+\gamma,1)\\ (2,1) & (\alpha+\beta,\alpha)\end{matrix};\omega^{1/\alpha}r\right].\end{aligned} \tag{21}$$

Now, for the derivative, we have

$$\begin{aligned}\left|\left(\Omega_{\alpha,\beta}^{\gamma,\omega} * \phi\right)'(z)\right| &\le \sum_{n=1}^{\infty}\left(\frac{\Gamma(\alpha+\beta)}{\gamma\omega^{1/\alpha}}\right)\left(\frac{\Gamma(\gamma+n)\omega^{n/\alpha}}{\Gamma(\gamma)\Gamma(\alpha n+\beta)}\right)\frac{n|\phi_n|}{n!}\,|z|^{\wedge}\{n-1\} \\ &\le \sum_{n=0}^{\infty}\left(\frac{\Gamma(\alpha+\beta)}{\Gamma(\gamma+1)\omega^{1/\alpha}}\right)\left(\frac{\Gamma(\gamma+n+1)\omega^{(n+1)/\alpha}}{\Gamma(\alpha n+\alpha+\beta)}\right)\frac{r^n}{n!} \\ &= \sum_{n=0}^{\infty}\left(\frac{\Gamma(\alpha+\beta)}{\Gamma(\gamma+1)}\right)\left(\frac{\Gamma(\gamma+n+1)\omega^{n/\alpha}}{\Gamma(\alpha n+\alpha+\beta)}\right)\frac{r^n}{n!} \\ &= \left(\frac{\Gamma(\alpha+\beta)}{\Gamma(\gamma+1)}\right)_1\mathscr{W}_1\left[\begin{matrix}(1+\gamma,1)\\ (\alpha+\beta,\alpha)\end{matrix};\omega^{1/\alpha}r\right] \\ &= {}_1\mathscr{W}_1^*\left[\begin{matrix}(1+\gamma,1)\\ (\alpha+\beta,\alpha)\end{matrix};\omega^{1/\alpha}r\right].\end{aligned} \tag{22}$$

This completes the proof.

Remark 8.

(i) It is clear that the above upper bound of $(\Omega_{\alpha,\beta}^{\gamma,\omega} * \phi)(z), |z| \longrightarrow 1, \omega = 1$ converges at

$$\begin{aligned}\Re(\triangleleft) &= \Re\left(\sum_{j=1}^{q} y_j - \sum_{i=1}^{p} x_i + \frac{p-q-1}{2}\right) \\ &> 0 \longrightarrow \alpha+\beta-\gamma-1/2>0 \longrightarrow \alpha+\beta>\gamma+1/2.\end{aligned} \tag{23}$$

Moreover, the upper bound of $(\Omega_{\alpha,\beta}^{\gamma,\omega} * \phi)(z)$ converges, when

$$\begin{aligned}\Re(\triangleleft) &= \Re\left(\sum_{j=1}^{q} y_j - \sum_{i=1}^{p} x_i + \frac{p-q-1}{2}\right) \\ &> 0 \longrightarrow \alpha+\beta-\gamma-3/2>0 \longrightarrow \alpha+\beta>\gamma+3/2.\end{aligned} \tag{24}$$

(ii) For special case: by Proposition 7 and Lemma 6, we have

$$\begin{aligned}\left|\left(\Omega_{2,\beta}^{\gamma,1} * \phi\right)(z)\right| &\le r\left(\frac{\Gamma(2)\Gamma(2+\beta)}{\Gamma(\gamma+1)\Gamma(1)}\right)_2\mathscr{W}_2\left[\begin{matrix}(1,1) & (1+\gamma,1)\\ (2,1) & (2+\beta,2)\end{matrix};r\right] \\ &\le r\left(\frac{\Gamma(2+\beta)}{\Gamma(\gamma+1)}\right)\int_0^1\frac{\mathrm{H}\left(r^{-1}t\right)dt}{t(1-tzr^{-1})},\end{aligned} \tag{25}$$

provided that $5/2+\beta>\gamma$ and $\theta=1$.

Proposition 9. *Let ϕ be univalent in the open unit disk. Then,*

$$\begin{aligned}&\left|\left(\Omega_{\alpha,\beta}^{\gamma,\omega} * \phi\right)(z)\right| \le r_1\mathscr{W}_1^*\left[\begin{matrix}(1+\gamma,1)\\ (\alpha+\beta,\alpha)\end{matrix};\omega^{1/\alpha}r\right], \\ &\left|\left(\Omega_{\alpha,\beta}^{\gamma,\omega} * \phi\right)(z)\right| \le \left(r_1\mathscr{W}_1^*\left[\begin{matrix}(1+\gamma,1)\\ (\alpha+\beta,\alpha)\end{matrix};\omega^{1/\alpha}r\right]\right)' \\ &(\alpha\neq 0, r<1, \beta, \gamma\in\mathbb{R}_+).\end{aligned} \tag{26}$$

Proof. Since ϕ is univalent, then for each $n \ge 2$, we have $|\phi_n| \le n$. Then a calculation indicates that

$$\begin{aligned}\left|\left(\Omega_{\alpha,\beta}^{\gamma,\omega} * \phi\right)(z)\right| &\le \left(\frac{\Gamma(\alpha+\beta)}{\Gamma(\gamma+1)\omega^{1/\alpha}}\right)\sum_{n=1}^{\infty}\left(\frac{\Gamma(\gamma+n)\omega^{n/\alpha}}{\Gamma(\alpha n+\beta)}\right)\frac{|\phi_n|}{n!}\, r^n \\ &\le \left(\frac{\Gamma(\alpha+\beta)}{\Gamma(\gamma+1)\omega^{1/\alpha}}\right)\sum_{n=1}^{\infty} n\left(\frac{\Gamma(\gamma+n)\omega^{n/\alpha}}{\Gamma(\alpha n+\beta)}\right)\frac{r^n}{n!} \\ &= \left(\frac{\Gamma(\alpha+\beta)}{\Gamma(\gamma+1)\omega^{1/\alpha}}\right)\sum_{n=1}^{\infty}\left(\frac{\Gamma(\gamma+n)}{\Gamma(\alpha n+\beta)}\right)\frac{\left(\omega^{1/\alpha}r\right)^n}{(n-1)!} \\ &= \left(\frac{\Gamma(\alpha+\beta)}{\Gamma(\gamma+1)\omega^{1/\alpha}}\right)\sum_{n=0}^{\infty}\left(\frac{\Gamma(\gamma+1+n)}{\Gamma(\alpha n+\alpha+\beta)}\right)\frac{\left(\omega^{1/\alpha}r\right)^{n+1}}{(n)!} \\ &= r\left(\frac{\Gamma(\alpha+\beta)}{\Gamma(\gamma+1)}\right)\sum_{n=0}^{\infty}\left(\frac{\Gamma(1+\gamma+n)}{\Gamma(\alpha n+\alpha+\beta)}\right)\frac{\left(\omega^{1/\alpha}r\right)^n}{(n)!} \\ &= r\left(\frac{\Gamma(\alpha+\beta)}{\Gamma(\gamma+1)}\right)_1\mathscr{W}_1\left[\begin{matrix}(1+\gamma,1)\\ (\alpha+\beta,\alpha)\end{matrix};\omega^{1/\alpha}r\right] \\ &= r_1\mathscr{W}_1^*\left[\begin{matrix}(1+\gamma,1)\\ (\alpha+\beta,\alpha)\end{matrix};\omega^{1/\alpha}r\right].\end{aligned} \tag{27}$$

Now, we return to the upper bound of the derivative

$$\begin{aligned}
|\left(\Omega_{\alpha,\beta}^{\gamma,\omega} * \phi\right)(z)| &\leq \sum_{n=1}^{\infty} \left(\frac{\Gamma(\alpha+\beta)}{\gamma\omega^{1/\alpha}}\right)\left(\frac{\Gamma(\gamma+n)\omega^{n/\alpha}}{\Gamma(\gamma)\Gamma(\alpha n+\beta)}\right)\frac{n\phi_n}{n!}\,|z^{n-1}| \\
&\leq \sum_{n=1}^{\infty} \left(\frac{\Gamma(\alpha+\beta)}{\gamma\omega^{1/\alpha}}\right)\left(\frac{\Gamma(\gamma+n)\omega^{n/\alpha}}{\Gamma(\gamma)\Gamma(\alpha n+\beta)}\right)\frac{n\,|\,\phi_n\,|}{n!}\,r^{n-1} \\
&\leq \sum_{n=1}^{\infty} \left(\frac{\Gamma(\alpha+\beta)}{\gamma\omega^{1/\alpha}}\right)\left(\frac{\Gamma(\gamma+n)\omega^{n/\alpha}}{\Gamma(\gamma)\Gamma(\alpha n+\beta)}\right)\frac{n}{(n-1)!}\,r^{n-1} \\
&= \sum_{n=0}^{\infty} \left(\frac{\Gamma(\alpha+\beta)}{\Gamma(\gamma+1)}\right)\left(\frac{\Gamma(\gamma+n+1)}{\Gamma(\alpha n+\beta+\alpha)}\right)\frac{(n+1)}{n!}\left(\omega^{1/\alpha}r\right)^n \\
&= \left(\frac{\Gamma(\alpha+\beta)}{\Gamma(\gamma+1)}\right)\sum_{n=0}^{\infty} \left(\frac{\Gamma(1+\gamma+n)}{\Gamma(\alpha n+\alpha+\beta)}\right)\frac{(n+1)\left(\omega^{1/\alpha}r\right)^n}{(n)!} \\
&= \left(\frac{\Gamma(\alpha+\beta)}{\Gamma(\gamma+1)}\right)\left(r_1\mathscr{W}_1\left[\begin{matrix}(1+\gamma,1)\\(\alpha+\beta,\alpha)\end{matrix};\omega^{1/\alpha}r\right]\right)' \\
&= \left(r_1\mathscr{W}_1^*\left[\begin{matrix}(1+\gamma,1)\\(\alpha+\beta,\alpha)\end{matrix};\omega^{1/\alpha}r\right]\right)'.
\end{aligned} \tag{28}$$

This completes the proof. ?

More integral inequality results will consider in the following theorem.

Theorem 10. *Consider $\phi \in \wedge$ and the operator $(\Omega_{\alpha,\beta}^{\gamma,\omega} * \phi)(z)$, where $\alpha \neq 0, z \in \cup,\ \beta, \gamma \in \mathbb{R}_+$. If one of the following subordination inequalities hold*

$$\begin{gathered}
\left(\Omega_{\alpha,\beta}^{\gamma,\omega} * \phi\right)(z) + z\left(\Omega_{\alpha,\beta}^{\gamma,\omega} * \phi\right)(z)\left(1+\sigma\left(\Omega_{\alpha,\beta}^{\gamma,\omega} * \phi\right)(z)\right) \prec \sigma z^2 + 2z, \quad |\sigma| \leq \frac{1}{2}, \\
\left(\Omega_{\alpha,\beta}^{\gamma,\omega} * \phi\right)(z) + z\left(\Omega_{\alpha,\beta}^{\gamma,\omega} * \phi\right)(z)e^{\sigma z} \prec (1+\sigma z e^{\sigma z})z, \quad |\sigma| \leq 1, \\
\left(\Omega_{\alpha,\beta}^{\gamma,\omega} * \phi\right)(z) + \frac{z\left(\Omega_{\alpha,\beta}^{\gamma,\omega} * \phi\right)(z)}{1+\sigma\left(\Omega_{\alpha,\beta}^{\gamma,\omega} * \phi\right)(z)} \prec \frac{z(1+\sigma z)}{1+\sigma z}, \quad |\sigma| \leq 1, \\
\left(z\left(\Omega_{\alpha,\beta}^{\gamma,\omega} * \phi\right)(z) - \left(\Omega_{\alpha,\beta}^{\gamma,\omega} * \phi\right)(z)\right)e^{\sigma\left(\Omega_{\alpha,\beta}^{\gamma,\omega} * \phi\right)(z)} + e^{\sigma\left(\Omega_{\alpha,\beta}^{\gamma,\omega} * \phi\right)(z)} \prec e^z, \quad |\sigma - 1| \leq \frac{\pi}{2}, \\
\left(\Omega_{\alpha,\beta}^{\gamma,\omega} * \phi\right)(z) + \sigma z\left(\Omega_{\alpha,\beta}^{\gamma,\omega} * \phi\right)(z) \prec (1+\sigma z) + \sigma z^2, \quad 0 < |\sigma| \leq \frac{1}{3}, \\
\left(\Omega_{\alpha,\beta}^{\gamma,\omega} * \phi\right)(z) + z\left(\Omega_{\alpha,\beta}^{\gamma,\omega} * \phi\right)(z) \prec 2z, \\
\left(\Omega_{\alpha,\beta}^{\gamma,\omega} * \phi\right)(z)\left[1+\frac{z\left(\Omega_{\alpha,\beta}^{\gamma,\omega} * \phi\right)(z)}{\left(\Omega_{\alpha,\beta}^{\gamma,\omega} * \phi\right)(z)}\right] \prec 2z, \\
\left(\Omega_{\alpha,\beta}^{\gamma,\omega} * \phi\right)(z)\left[1+z\left(\left(\Omega_{\alpha,\beta}^{\gamma,\omega} * \phi\right)(z)\right)^2\right] \prec 2z,
\end{gathered} \tag{29}$$

then $\Psi(z) \coloneqq 1/e^{\sigma z}\int_0^z (\Omega_{\alpha,\beta}^{\gamma,\omega} * \phi)(\zeta)e^{\sigma\zeta}d\zeta \in \mathscr{H}[0,1]$ and

$$\left|\frac{1}{e^{\sigma z}}\int_0^z \left(\Omega_{\alpha,\beta}^{\gamma,\omega} * \phi\right)(\zeta)e^{\sigma\zeta}d\zeta\right| < \frac{1}{2-|\sigma|}, \quad |\sigma| < 2. \tag{30}$$

Proof. Suppose that the operator $(\Omega_{\alpha,\beta}^{\gamma,\omega} * \phi)$ achieves one of the subordination inequalities (a)-(h) then, in view of Proposition 2 and results in Lemma 4, we have

$$\left(\Omega_{\alpha,\beta}^{\gamma,\omega} * \phi\right)(z) \prec z, \quad z \in \cup. \tag{31}$$

Consequently, we obtain the upper bound inequality

$$\left|\left(\Omega_{\alpha,\beta}^{\gamma,\omega} * \phi\right)(z)\right| < 1, \quad z \in \cup. \tag{32}$$

The function $e^{\sigma z}$ achieves the real inequality

$$\Re\left(\frac{z(e^{\sigma z})'}{e^{\sigma z}} + 2\right) = \Re(\sigma z + 2) > 0, \tag{33}$$

provided that $|\sigma| < 2$. Moreover, we have superior inequality

$$\begin{aligned}
\chi &= \sup_{|z|<1}\left\{\frac{|e^{\sigma z}|}{|z(e^{\sigma z})' + 2e^{\sigma z}|}\right\} = \sup_{|z|<1}\left\{\frac{|e^{\sigma z}|}{|z\sigma e^{\sigma z} + 2e^{\sigma z}|}\right\} \\
&\leq \frac{1}{2-|\sigma|} < \infty, \quad |\sigma| < 2.
\end{aligned} \tag{34}$$

Hence, in view of [22] [Corollary 4.3a.2, P210], we conclude that

$$\left|\frac{1}{e^{\sigma z}}\int_0^z \left(\Omega_{\alpha,\beta}^{\gamma,\omega} * \phi\right)(\zeta)e^{\sigma\zeta}d\zeta\right| \leq \frac{|z|^2}{2-|\sigma|}, \quad |\sigma| < 2, \tag{35}$$

which yields

$$\begin{gathered}
\left|\frac{1}{e^{\sigma z}}\int_0^z \left(\Omega_{\alpha,\beta}^{\gamma,\omega} * \phi\right)(\zeta)e^{\sigma\zeta}d\zeta\right| < \frac{1}{2-|\sigma|}, \\
(|\sigma| < 2,\ z \in \cup,),
\end{gathered} \tag{36}$$

hence the proof. ?

Now, we investigate another integral inequality involving the operator $(\Omega_{\alpha,\beta}^{\gamma,\omega} * \phi)$ where $\phi \in \wedge$.

Theorem 11. *Consider $\phi \in \wedge$ and the operator $(\Omega_{\alpha,\beta}^{\gamma,\omega} * \phi)(z)$, where $\alpha, \beta, \gamma, \omega \in \mathbb{C}, z \in \cup, \Re(\alpha), \Re(\beta) > 0$. If one of the subordination inequalities in Theorem 10 holds, then*

$$\begin{aligned}
&G(z) \coloneqq \frac{1}{e^{\sigma z}}\int_0^z \left(\Omega_{\alpha,\beta}^{\gamma,\omega} * \phi\right)(\zeta)g(\zeta)\zeta^{\sigma-1}d\zeta \in \mathscr{H}[0,1], \\
&|\frac{1}{e^{\sigma z}}\int_0^z \left(\Omega_{\alpha,\beta}^{\gamma,\omega} * \phi\right)(\zeta)g(\zeta)d\zeta| < \frac{|g(z)|}{1-|\sigma|},\ |\sigma| < 1,
\end{aligned} \tag{37}$$

where $g \in \mathscr{H}[1,1], g \neq 0$.

Proof. Suppose that the operator $(\Omega_{\alpha,\beta}^{\gamma,\omega} * \phi)$ has one of the subordination inequalities (a)-(h) in Theorem 10 then, in view of Proposition 2, we have

$$\left(\Omega_{\alpha,\beta}^{\gamma,\omega} * \phi\right)(z) \prec z, \quad z \in \cup, \tag{38}$$

which implies that

$$\left|\left(\Omega_{\alpha,\beta}^{\gamma,\omega} * \phi\right)(z)\right| < 1, \quad z \in \cup. \tag{39}$$

As in Theorem 10, the function $e^{\sigma z}$ admits the real inequality

$$\Re\left(\frac{z(e^{\sigma z})'}{e^{\sigma z}} + 1\right) = \Re(\sigma z + 1) > 0, \tag{40}$$

provided that $|\sigma| < 1$. Moreover, we have superior inequality

$$\begin{aligned} \nu &= \sup_{|z|<1}\left\{\frac{|g(z)|}{\left|z(e^{\sigma z})' + (1+\sigma)e^{\sigma z}\right|}\right\} = \sup_{|z|<1}\left\{\frac{|g(z)|}{|z\sigma e^{\sigma z} + e^{\sigma z}|}\right\} \\ &= \sup_{|z|<1}\left\{\frac{|g(z)|}{1-|\sigma|}\right\}, \ |\sigma| < 1 < \infty, \end{aligned} \tag{41}$$

Thus, in view of [22] [Theorem 4.3a, P207], we indicate that then $G(z) \in \mathscr{H}[0, 1]$ and

$$\left|\frac{1}{e^{\sigma z}}\int_0^z \left(\Omega_{\alpha,\beta}^{\gamma,\omega} * \phi\right)(\zeta) g(\zeta) d\zeta\right| < \frac{|g(z)|}{1-|\sigma|}, \quad |\sigma| < 1, \tag{42}$$

where $g \in \mathscr{H}[1, 1]$, $g \neq 0$, hence the proof. ?

In addition, we have the following result by replacing $e^{\sigma z}$ by $ze^{\sigma z}$:

Theorem 12. *Consider $\phi \in \wedge$ and the operator $(\Omega_{\alpha,\beta}^{\gamma,\omega} * \phi)(z)$, where $\alpha \neq 0, z \in \cup\beta, \gamma \in \mathbb{R}_+$. If one of the subordination inequalities in Theorem 10 holds, then*

$$\begin{aligned} L(z) &:= \frac{1}{z^{\kappa} e^{\sigma z}}\int_0^z \left(\Omega_{\alpha,\beta}^{\gamma,\omega} * \phi\right)(\zeta)(1+\sigma\zeta)e^{\sigma\zeta}\zeta^{\kappa-1} d\zeta \in \mathscr{H}[0, 1], \\ &\left|\frac{1}{z^{\kappa} e^{\sigma z}}\int_0^z \left(\Omega_{\alpha,\beta}^{\gamma,\omega} * \phi\right)(\zeta)(1+\sigma\zeta)e^{\sigma\zeta}\zeta^{\kappa-1} d\zeta\right| \\ &< \left\{\frac{1+|\sigma|}{1-|\sigma|+\kappa}\right\}, \ \kappa > 0, |\sigma| \leq 1. \end{aligned} \tag{43}$$

Proof. Suppose that the operator $(\Omega_{\alpha,\beta}^{\gamma,\omega} * \phi)$ has one of the subordination inequalities (a)-(h) then, in view of Proposition 2 and results in [22], P138-140, we have

$$\left(\Omega_{\alpha,\beta}^{\gamma,\omega} * \phi\right)(z) \prec z, \quad z \in \cup, \tag{44}$$

which leads to

$$\left|\left(\Omega_{\alpha,\beta}^{\gamma,\omega} * \phi\right)(z)\right| < 1, \quad z \in \cup. \tag{45}$$

The function $ze^{\sigma z}$ admits the following properties

$$\begin{aligned} &ze^{\sigma z} \in \wedge, \\ &\frac{(ze^{\sigma z})'(ze^{\sigma z})}{z} = e^{2\sigma z} + \sigma z e^{2\sigma z} \neq 0, \ |\sigma| \leq 1; \\ &\Re\left(\frac{z(ze^{\sigma z})'}{(ze^{\sigma z})} + \kappa\right) = \Re(1 + \sigma z + \kappa) > 0. \end{aligned} \tag{46}$$

Moreover, we have superior inequality

$$\begin{aligned} S &= \sup_{|z|<1}\left\{\frac{|z(ze^{\sigma z})'|}{|z(ze^{\sigma z})' + \kappa(ze^{\sigma z})|}\right\} = \sup_{|z|<1}\left\{\frac{1+\sigma z}{1+\sigma z+\kappa}\right\} \\ &= \sup_{|z|<1}\left\{\frac{1+|\sigma|}{1-|\sigma|+\kappa}\right\}, \quad |\sigma| < 1, \kappa > 0 < \infty. \end{aligned} \tag{47}$$

Thus, in view of [22]-[Corollary 4.3a.1, P208], $L(z) \in \mathscr{H}[0, 1]$ and

$$\begin{aligned} &\left|\frac{1}{z^{\kappa} e^{\sigma z}}\int_0^z \left(\Omega_{\alpha,\beta}^{\gamma,\omega} * \phi\right)(\zeta)(1+\sigma\zeta)e^{\sigma\zeta}\zeta^{\kappa-1} d\zeta\right| < \left\{\frac{1+|\sigma|}{1-|\sigma|+\kappa}\right\}, \\ &(\kappa > 0, \quad \sigma| \leq 1, \quad z \in \cup, \phi \in \wedge). \end{aligned} \tag{48}$$

This completes the proof. ?

Theorem 13. *Consider that ϕ is convex univalent function in the open unit disk and the operator $(\Omega_{\alpha,\beta}^{\gamma,\omega} * \phi)(z)$, where $\alpha \neq 0, z \in \cup, \beta, \gamma \in \mathbb{R}_+$. Then,*

$$\Psi(z) \in \mathscr{H}[0, 1], \tag{49}$$

with

$$\begin{aligned} &\left|\frac{1}{e^{\sigma z}}\int_0^z \left(\Omega_{\alpha,\beta}^{\gamma,\omega} * \phi\right)(\zeta) e^{\sigma\zeta} d\zeta\right| \\ &< \frac{{}_2\mathscr{W}_2^*\left[\begin{matrix}(1,1) & (1+\gamma,1)\\ (2,1) & (\alpha+\beta,\alpha)\end{matrix}; \omega^{1/\alpha}\right]}{2-|\sigma|}, |\sigma| < 2. \end{aligned} \tag{50}$$

$G(z) \in \mathscr{H}[0, 1]$ *with*

$$\begin{aligned} &\left|\frac{1}{e^{\sigma z}}\int_0^z \left(\Omega_{\alpha,\beta}^{\gamma,\omega} * \phi\right)(\zeta) g(\zeta) d\zeta\right| \\ &< \frac{|g(z)|_2\mathscr{W}_2^*\left[\begin{matrix}(1,1) & (1+\gamma,1)\\ (2,1) & (\alpha+\beta,\alpha)\end{matrix}; \omega^{1/\alpha}\right]}{1-|\sigma|}, |\sigma| < 1, \end{aligned} \tag{51}$$

where $g \in \mathscr{H}[1, 1]$, $g \neq 0$.

$L(z) \in \mathcal{H}[0,1]$ *with*

$$\left|\frac{1}{z^{\kappa}e^{\sigma z}}\int_0^z \left(\Omega_{\alpha,\beta}^{\gamma,\omega} * \phi\right)(\zeta)(1+\sigma\zeta)e^{\sigma\zeta}\zeta^{\kappa-1}d\zeta\right| < \frac{(1+|\sigma|)_2\mathscr{W}_2^*\left[\begin{matrix}(1,1) & (1+\gamma,1)\\ (2,1) & (\alpha+\beta,\alpha)\end{matrix};\omega^{1/\alpha}\right]}{1+|\sigma|+\kappa}, \quad (\kappa>0,\ |\sigma|\le 1,\ z\in\cup). \tag{52}$$

Proof. Let ϕ be convex univalent in $\cup$. Then, in view of Proposition 7, we have

$$\left|\left(\Omega_{\alpha,\beta}^{\gamma,\omega} * \phi\right)(z)\right| < r_2\mathscr{W}_2^*\left[\begin{matrix}(1,1) & (1+\gamma,1)\\ (2,1) & (\alpha+\beta,\alpha)\end{matrix};\omega^{1/\alpha}r\right]. \tag{53}$$

Consequently, by assuming $r \longrightarrow 1$, we obtain

$$\left|\left(\Omega_{\alpha,\beta}^{\gamma,\omega} * \phi\right)(z)\right| < {}_2\mathscr{W}_2^*\left[\begin{matrix}(1,1) & (1+\gamma,1)\\ (2,1) & (\alpha+\beta,\alpha)\end{matrix};\omega^{1/\alpha}\right]. \tag{54}$$

By the proof of Theorem 10, we conclude that (A). Similarly, by using the proof in Theorems 11 and 12, we have (B) and (C), respectively. This ends the proof. ?

Theorem 14. *Consider that ϕ is univalent function in the open unit disk and the operator $(\Omega_{\alpha,\beta}^{\gamma,\omega} * \phi)(z)$, where $\alpha \neq 0, z \in \cup$, $\beta, \gamma \in \mathbb{R}_+$. Then*

$\Psi(z) \in \mathcal{H}[0,1]$ *with*

$$\left|\frac{1}{e^{\sigma z}}\int_0^z \left(\Omega_{\alpha,\beta}^{\gamma,\omega} * \phi\right)(\zeta)e^{\sigma\zeta}d\zeta\right| < \frac{{}_1\mathscr{W}_1^*\left[\begin{matrix}(1+\gamma,1)\\ (\alpha+\beta,\alpha)\end{matrix};\omega^{1/\alpha}\right]}{2-|\sigma|}, |\sigma|<2. \tag{55}$$

$G(z) \in \mathcal{H}[0,1]$ *with*

$$\left|\frac{1}{e^{\sigma z}}\int_0^z \left(\Omega_{\alpha,\beta}^{\gamma,\omega} * \phi\right)(\zeta)g(\zeta)d\zeta\right| < \frac{|g(z)|_1\mathscr{W}_1^*\left[\begin{matrix}(1+\gamma,1)\\ (\alpha+\beta,\alpha)\end{matrix};\omega^{1/\alpha}\right]}{1-|\sigma|}, |\sigma|<1, \tag{56}$$

where $g \in \mathcal{H}[1,1], g \neq 0$.

$L(z) \in \mathcal{H}[0,1]$ *with*

$$\left|\frac{1}{z^{\kappa}e^{\sigma z}}\int_0^z \left(\Omega_{\alpha,\beta}^{\gamma,\omega} * \phi\right)(\zeta)(1+\sigma\zeta)e^{\sigma\zeta}\zeta^{\kappa-1}d\zeta\right| < \frac{(1+|\sigma|)_1\mathscr{W}_1^*\left[\begin{matrix}(1+\gamma,1)\\ (\alpha+\beta,\alpha)\end{matrix};\omega^{1/\alpha}\right]}{1+|\sigma|+\kappa}, (\kappa>0,\ |\sigma|\le 1, z\in\cup). \tag{57}$$

Proof. Let ϕ be convex univalent in $\cup$. Then, in view of Proposition 9, we have

$$\left|\left(\Omega_{\alpha,\beta}^{\gamma,\omega} * \phi\right)(z)\right| < r_1\mathscr{W}_1^*\left[\begin{matrix}(1+\gamma,1)\\ (\alpha+\beta,\alpha)\end{matrix};\omega^{1/\alpha}r\right]. \tag{58}$$

Consequently, by assuming $r \longrightarrow 1$, we have

$$\left|\left(\Omega_{\alpha,\beta}^{\gamma,\omega} * \phi\right)(z)\right| < {}_1\mathscr{W}_1^*\left[\begin{matrix}(1+\gamma,1)\\ (\alpha+\beta,\alpha)\end{matrix};\omega^{1/\alpha}\right]. \tag{59}$$

By the proof of Theorem 10, we conclude that (A). Similarly, by using the proof in Theorems 11 and 12, we have (B) and (C), respectively. This ends the proof. ?

In the next result, we discuss the starlikeness of the operator $(\Omega_{\alpha,\beta}^{\gamma,\omega} * \phi)$.

Theorem 15. *Consider the operator $(\Omega_{\alpha,\beta}^{\gamma,\omega} * \phi), \phi \in \wedge$.*

(A) If $|(\Omega_{\alpha,\beta}^{\gamma,\omega} * \phi)(z)/e^{\sigma z}(\sigma z+1)-1| < 0.04$, where $|\sigma| < 1/2(\sqrt{13}-3) \approx 0.3027$ then $(\Omega_{\alpha,\beta}^{\gamma,\omega} * \phi) \in \mathcal{S}^*$

(B) If $|z\phi'(z)/\phi(z)-1| < 0.374$ and $\sup\{|(\Omega_{\alpha,\beta}^{\gamma,\omega} * \phi)(z)/(\Omega_{\alpha,\beta}^{\gamma,\omega} * \phi)(z)|\} \equiv |\sigma|, |\sigma| < 1$ then

$$\int_0^z \left(\Omega_{\alpha,\beta}^{\gamma,\omega} * \phi\right)(z)\phi'(z)dz \in \mathcal{S}^*. \tag{60}$$

(C) If $|(\Omega_{\alpha,\beta}^{\gamma,\omega} * \phi)(z)| < 2/\sqrt{5}$ then $(\Omega_{\alpha,\beta}^{\gamma,\omega} * \phi)(z) \in \mathcal{S}^*$

Proof. For part (A), assume that $g(z) = ze^{\sigma z}$ then

$$\sup\left\{\left|\frac{g''(z)}{g'(z)}\right|\right\} = \sup\left\{\left|\frac{2\sigma+z\sigma^2}{1+z\sigma}\right|\right\}. \tag{61}$$

Consequently, we have

$$\sup\left\{\left|\frac{2\sigma+z\sigma^2}{1+z\sigma}\right|\right\} \le \frac{2|\sigma|+|\sigma|^2}{1-|\sigma|} < 1,\ |\sigma|<1. \tag{62}$$

The value $|\sigma| < 1/2(\sqrt{13}-3) \approx 0.3027$ implies that $2|\sigma|+|\sigma|^2/1-|\sigma| \approx 0.98 < 1$. Since

$$\left|\frac{\left(\Omega_{\alpha,\beta}^{\gamma,\omega} * \phi\right)(z)}{e^{\sigma z}(\sigma z+1)}-1\right| < 0.04, \tag{63}$$

then in view of [22]-[Theorem 5.5c, P296], we conclude that $(\Omega_{\alpha,\beta}^{\gamma,\omega} * \phi) \in \mathcal{S}^*$.

For part (B), since

$$\left|\frac{z\phi'(z)}{\phi(z)} - 1\right| < 0.374, \tag{64}$$

where the number 0.374 is a solution of the equation $(1+x)e^x = 2$ then by [22] [Theorem 5.5g, P299], we have $|\phi'(z) - 1| < 1$. Moreover, in terms of $|\sigma|$, we have

$$\left|\phi'(z) - 1\right| < \frac{(2-|\sigma|)\sqrt{2(2-2|\sigma|)+1}-|\sigma|}{(2-|\sigma|)^2+1} < 1, |\sigma| < 1,$$
$$\lim_{|\sigma|\longrightarrow 1} \frac{(2-|\sigma|)\sqrt{2(2-2|\sigma|)+1}-|\sigma|}{(2-|\sigma|)^2+1} \approx 0. \tag{65}$$

by [22] [Theorem 5.5d, P298] then

$$\int_0^z \left(\Omega_{\alpha,\beta}^{\gamma,\omega} * \phi\right)(z)\phi'(z)dz \in \mathcal{S}^*. \tag{66}$$

The last part immediately comes from [22] [Corollary5.5.a,P294]. This ends the proof. ?

Theorem 16. *Consider the operator* $(\Omega_{\alpha,\beta}^{\gamma,\omega} * \phi)$, $\phi \in \wedge$.

(A) If the following inequality holds

$$\frac{z\left(\Omega_{\alpha,\beta}^{\gamma,\omega} * \phi\right)(z)}{\left(\Omega_{\alpha,\beta}^{\gamma,\omega} * \phi\right)(z)} \prec e^z - 1, \quad z \in \cup, \tag{67}$$

then

$$\left(\Omega_{\alpha,\beta}^{\gamma,\omega} * \phi\right)(z) \prec \exp\left(\int_0^z \left(e^\zeta - 1\right)\zeta^{-1}d\zeta\right), \quad z \in \cup, \tag{68}$$

(B) If the subordination occurs

$$\frac{z\left(\Omega_{\alpha,\beta}^{\gamma,\omega} * \phi\right)(z)}{\left(\Omega_{\alpha,\beta}^{\gamma,\omega} * \phi\right)(z)} - 1 \prec e^z - 1, \quad z \in \cup, \tag{69}$$

then

$$\frac{\left(\Omega_{\alpha,\beta}^{\gamma,\omega} * \phi\right)(z)}{z} \prec \exp\left(\int_0^z \left(e^\zeta - 1\right)\zeta^{-1}d\zeta\right), \quad z \in \cup, \tag{70}$$

(C) If the next relation exists

$$z\left(\Omega_{\alpha,\beta}^{\gamma,\omega} * \phi\right)(z) \prec e^z - 1, \quad z \in \cup, \tag{71}$$

then

$$\left(\Omega_{\alpha,\beta}^{\gamma,\omega} * \phi\right)(z) \prec \int_0^z \left(e^\zeta - 1\right)\zeta^{-1}d\zeta. \tag{72}$$

Proof. It is clear that the function

$$f(z) = e^z - 1 = z + \frac{z^2}{2} + \frac{z^3}{6} + \frac{z^4}{24} + \frac{z^5}{120} + O(z^6), \tag{73}$$

satisfies $f(0) = 0$ and it is convex in the open unit disk. Consequently, it is starlike. By Proposition 2, the operator $(\Omega_{\alpha,\beta}^{\gamma,\omega} * \phi)(z) \in \wedge$ and hence $(\Omega_{\alpha,\beta}^{\gamma,\omega} * \phi)(0) = 1$ that is $(\Omega_{\alpha,\beta}^{\gamma,\omega} * \phi)(z) \in \mathcal{H}[1,1]$. Similarly for the function

$$\frac{\left(\Omega_{\alpha,\beta}^{\gamma,\omega} * \phi\right)(z)}{z} \in \mathcal{H}[1,1]. \tag{74}$$

Thus, in view of [22]-[Corollary 3.1d.1, P76], we have the desire results.

For the last part (C), $z(\Omega_{\alpha,\beta}^{\gamma,\omega} * \phi)(z) \in \mathcal{H}[0,1]$; thus, in virtue of [22]-[Theorem 3.1d, P76], where $a = 0$, we conclude the last subordination. ?

2.1. Fractional Saint-Venant Equations. By using the fractional calculus of the construction, we formulate the fractional 2D-Saint-Venant equations utilizing the functional convolution operator $\Omega_{\alpha,\beta}^{\gamma,\omega} * \phi$, $\phi \in \Lambda$, and $z \in \cup$.

Example 1. We investigate the upper bound of the 2-dimensional Saint-Venant equations (2D-SVE) of diffusive wave (this equation has measured the level of the water). This equation simply presents the formula

$$\frac{d\Theta(z)}{dz} - \Delta(z) = 0, \tag{75}$$

where Θ is the height deviation of the horizontal pressure surface at two-dimensional position $z = x + iy$ and $\Delta(\varsigma)$ represents the difference of bed slope. By using the convolution operator, we generalize 2D-SVE into the form

$$\left(\Omega_{\alpha,\beta}^{\gamma,\omega} * \phi\right)(z) - \Delta(z) = 0, \quad z \in \cup. \tag{76}$$

Multiplying both sides of Eq. (76) by z and let

$$\Delta(z) = \frac{e^z - 1}{z} = 1 + \frac{z}{2} + \frac{z^2}{6} + \frac{z^3}{24} + \frac{z^4}{120} + \frac{z^5}{720} + O(z^6), \tag{77}$$

we have

$$z\left(\Omega_{\alpha,\beta}^{\gamma,\omega} * \phi\right)(z) = e^z - 1, \quad z \in \cup. \tag{78}$$

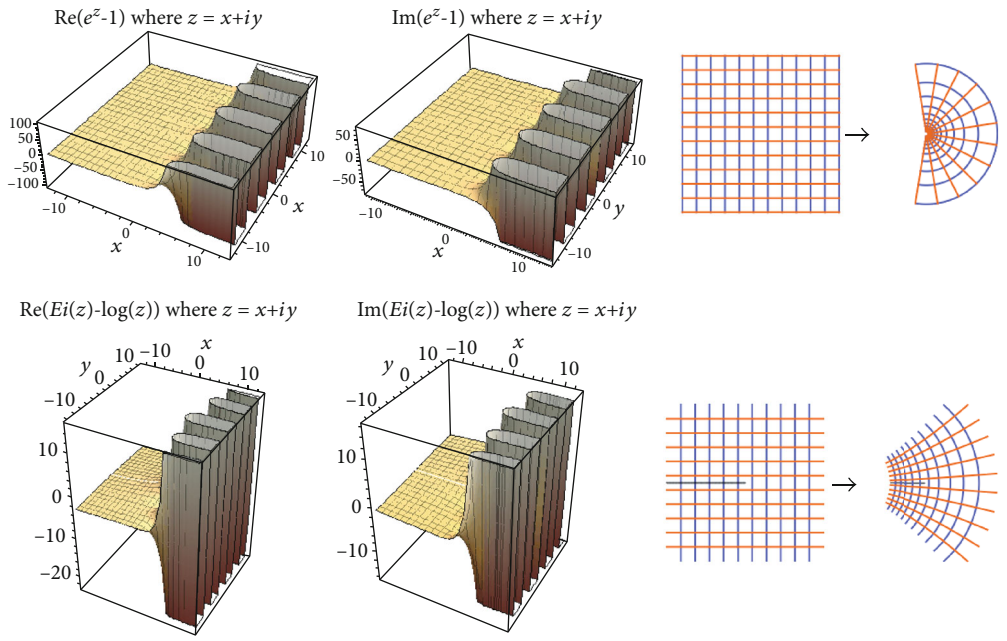

(a) The first row represents the function $f(z) = (e^z) - 1$ and the second row indicates the solution (79) of the extended 2D-SVE

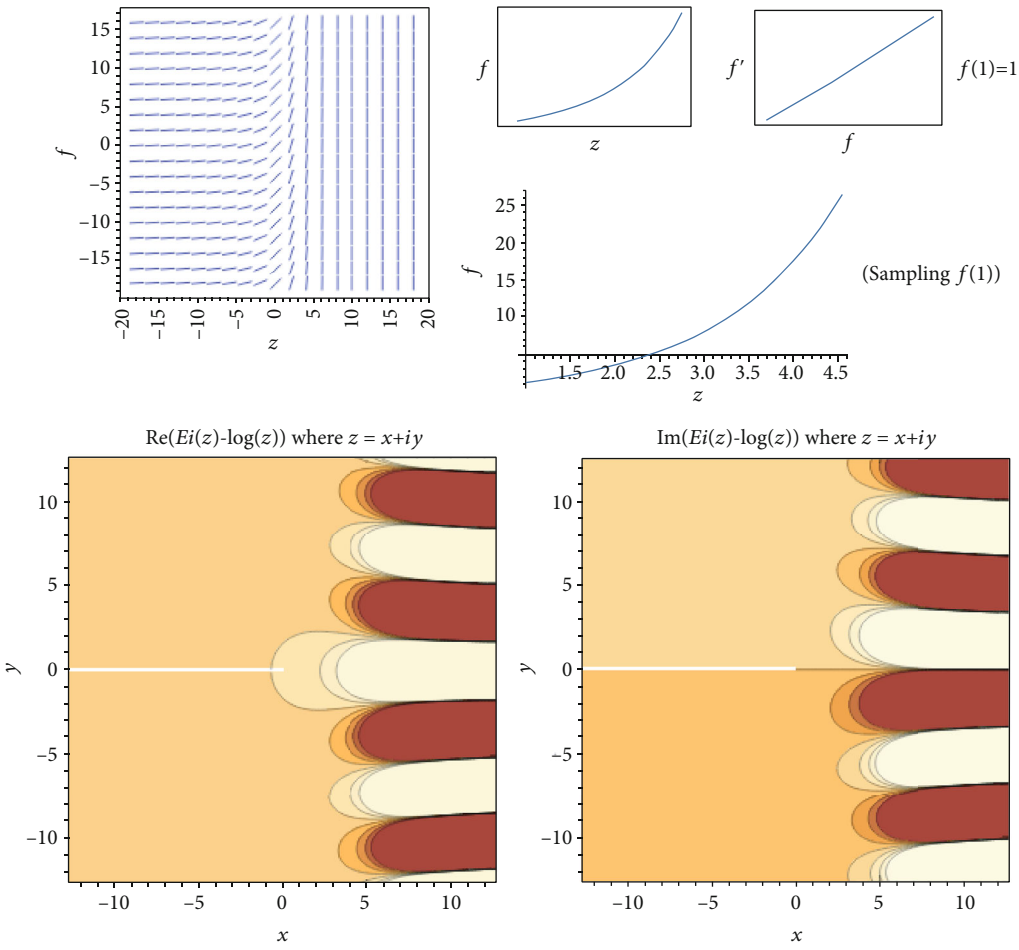

(b) The solution $f(z) \coloneqq (\Omega_{\alpha,\beta}^{\gamma,\omega} * \phi)(z)$

FIGURE 1: Saint-Venant equations (2D-SVE) of diffusive wave.

Thus, in view of Theorem 16-(C), we conclude the upper solution of Eq. (78) is given by (see Figure 1, second row)

$$\left(\Omega_{\alpha,\beta}^{\gamma,\omega} * \phi\right)(z) \prec \int_0^z \left(e^{\zeta} - 1\right)\zeta^{-1} d\zeta. \tag{79}$$

Hence, we obtain

$$\begin{aligned}\left(\Omega_{\alpha,\beta}^{\gamma,\omega} * \phi\right)(z) &= c + Ei(z) - \log(z) = c + 0.577 + z + \frac{z^2}{4} \\ &+ \frac{z^3}{18} + \frac{z^4}{96} + \frac{z^5}{600} + \frac{z^6}{4320} + O\left(z^7\right) \\ &- i\pi\left[\frac{(\arg(z) + \pi)}{(2\pi)}\right],\end{aligned} \tag{80}$$

where c is a constant and

$$Ei(z) = 0.577 + \ln(z) + z + \cdots, \tag{81}$$

indicates the exponential integral. Assuming that

$$c = i\pi\left[\frac{(\arg(z) + \pi)}{(2\pi)}\right] - 0.577, \tag{82}$$

we get

$$\left(\Omega_{\alpha,\beta}^{\gamma,\omega} * \phi\right)(z) = z + \frac{z^2}{4} + \frac{z^3}{18} + \frac{z^4}{96} + \frac{z^5}{600} + \frac{z^6}{4320} + O\left(z^7\right) \in \wedge. \tag{83}$$

By the convexity of e^z (see [22]-P139), we confirm that the solution is normalized analytic convex in $\cup$. Note that the term $(\Omega_{\alpha,\beta}^{\gamma,\omega} * \phi)(z)$ is called the convective acceleration term. Figure 1 shows the behavior of solutions of 2D-SVE of diffusive wave.

3. Conclusion

From above, we have extended the Prabhakar operator in the open unit disk. We formulated it in a linear convolution operator with a normalized function. A class of integral inequalities is investigated involving special functions. The upper bound of the suggested operator is computed by using the Fox-Wright function, for a class of convex functions and univalent functions. Moreover, we applied the operator to generalize the 2D-SVE. A solution of the extended 2D-SVE is computed by using recent result (Theorem 16).

For future woks, one can consider extra studies in the geometric function theory by considering the operator in different classes of analytic functions, such as normalized functions, harmonic functions, and meromorphic functions.

Data Availability

Data sharing is not applicable to this article as no datasets were generated or analyzed during the current study.

Conflicts of Interest

The authors declare no conflict of interest.

Authors' Contributions

All authors contributed equally and significantly to writing this article. All authors read and agreed to the published version of the manuscript.

References

[1] A. A. Kilbas, H. M. Srivastava, and J. J. Trujillo, "Theory and applications of the fractional differential equations," *North-Holland Mathematics Studies*, vol. 204, 2006.

[2] H. K. Nashine, R. W. Ibrahim, R. Arab, and M. Rabbani, "Solvability of fractional dynamic systems utilizing measure of noncompactness," *Nonlinear Analysis: Modelling and Control*, vol. 25, no. 4, pp. 618–637, 2020.

[3] S. Momani, R. Ibrahim, and S. Hadid, "Susceptible-infected-susceptible epidemic discrete dynamic system based on Tsallis entropy," *Entropy*, vol. 22, no. 7, p. 769, 2020.

[4] R. W. Ibrahim and D. Altulea, "Controlled homeodynamic concept using a conformable calculus in artificial biological systems," *Chaos, Solitons & Fractals*, vol. 140, article 110132, 2020.

[5] P. A. Naik, M. Yavuz, S. Qureshi, J. Zu, and S. Townley, "Modeling and analysis of COVID-19 epidemics with treatment in fractional derivatives using real data from Pakistan," *Nuovo cimento della Società italiana di fisica B*, vol. 135, no. 10, pp. 1–42, 2020.

[6] A. Atangana and S. İ. Ğ. araz, "A novel Covid-19 model with fractional differential operators with singular and non-singular kernels: analysis and numerical scheme based on Newton polynomial," *Alexandria Engineering Journal*, vol. 60, no. 4, pp. 3781–3806, 2021.

[7] A. Atangana and B. S. T. Alkahtani, "A novel double integral transform and its applications," *Journal of Nonlinear Sciences and Applications*, vol. 9, no. 2, pp. 424–434, 2016.

[8] H. M. Srivastava and S. Owa, *Univalent Functions, Fractional Calculus, and Their Applications*, Halsted Press, Wiley, New York, 1989.

[9] R. W. Ibrahim, "On generalized Srivastava-Owa fractional operators in the unit disk," *Advances in Difference Equations*, vol. 2011, no. 1, 2011.

[10] R. W. Ibrahim and J. M. Jahangiri, "Boundary fractional differential equation in a complex domain," *Boundary Value Problems*, vol. 2014, no. 1, 11 pages, 2014.

[11] R. W. Ibrahim and D. Baleanu, "Symmetry breaking of a time-2D space fractional wave equation in a complex domain," *Axioms*, vol. 10, no. 3, p. 141, 2021.

[12] R. Garra, R. Gorenflo, F. Polito, and Ž. Tomovski, "Hilfer-Prabhakar derivatives and some applications," *Applied Mathematics and Computation*, vol. 242, pp. 576–589, 2014.

[13] T. R. Prabhakar, "A singular integral equation with a generalized Mittag-Leffler function in the kernel," *Yokohama Mathematical Journal*, vol. 19, pp. 7–15, 1971.

[14] R. Garrappa and E. Kaslik, "Stability of fractional-order systems with Prabhakar derivatives," *Nonlinear Dynamics*, vol. 102, no. 1, pp. 567–578, 2020.

[15] R. Garra and R. Garrappa, "The Prabhakar or three parameter Mittag-Leffler function: theory and application," *Communications in Nonlinear Science and Numerical Simulation*, vol. 56, pp. 314–329, 2018.

[16] A. Giusti and I. Colombaro, "Prabhakar-like fractional viscoelasticity," *Communications in Nonlinear Science and Numerical Simulation*, vol. 56, pp. 138–143, 2018.

[17] M. H. Derakhshan, "New numerical algorithm to solve variable-order fractional integrodifferential equations in the sense of Hilfer-Prabhakar derivative," *Abstract and Applied Analysis*, vol. 2021, Article ID 8817794, 10 pages, 2021.

[18] S. Eshaghi, A. Ansari, and R. K. Ghaziani, "Generalized Mittag-Leffler stability of nonlinear fractional regularized Prabhakar differential systems," *International Journal of Nonlinear Analysis and Applications*, vol. 12, no. 2, pp. 665–678, 2021.

[19] N. Eghbali, A. Moharramnia, and J. Rassias, "Mittag-Leffler-Hyers-Ulam stability of Prabhakar fractional integral equation," *International Journal of Nonlinear Analysis and Applications*, vol. 12, no. 2, pp. 25–33, 2021.

[20] T. M. Michelitsch, F. Polito, and A. P. Riascos, "On discrete time Prabhakar-generalized fractional Poisson processes and related stochastic dynamics," *Physica A: Statistical Mechanics and its Applications*, vol. 565, article 125541, 2021.

[21] A. A. Kilbas, M. Saigo, and R. K. Saxena, "Generalized Mittag-Leffler function and generalized fractional calculus operators," *Integral Transforms and Special Functions*, vol. 15, no. 1, pp. 31–49, 2004.

[22] S. S. Miller and P. T. Mocanu, *Differential Subordinations: Theory and Applications*, CRC Press, 2000.

[23] D. B. Karp and E. G. Prilepkina, "The Fox-Wright function near the singularity and the branch cut," *Journal of Mathematical Analysis and Applications*, vol. 484, no. 1, article 123664, 2020.

[24] Y. Luchko, "The Wright function and its applications," in *Handbook of Fractional Calculus with Applications, Volume 1: Basic Theory*, A. Kochubei and Y. Luchko, Eds., pp. 241–268, De Gruyter, 2019.

Hindawi
Journal of Function Spaces
Volume 2021, Article ID 3484482, 10 pages
https://doi.org/10.1155/2021/3484482

Research Article

Numerical Analysis of Fractional-Order Parabolic Equations via Elzaki Transform

Muhammad Naeem,[1] **Omar Fouad Azhar**,[1] **Ahmed M. Zidan**,[2,3] **Kamsing Nonlaopon**,[4] **and Rasool Shah**[5]

[1]*Deanship of Joint First Year Umm Al-Qura University Makkah, Saudi Arabia*
[2]*Department of Mathematics, College of Science, King Khalid University, 9004 Abha, Saudi Arabia*
[3]*Department of Mathematics, Faculty of Science, Al-Azhar University, 71524 Assiut, Egypt*
[4]*Department of Mathematics, Faculty of Science, Khon Kaen University, Khon Kaen 40002, Thailand*
[5]*Department of Mathematics, Abdul Wali Khan University, Mardan 23200, Pakistan*

Correspondence should be addressed to Kamsing Nonlaopon; nkamsi@kku.ac.th and Rasool Shah; rasoolshah@awkum.edu.pk

Received 10 June 2021; Revised 1 August 2021; Accepted 11 August 2021; Published 1 September 2021

Academic Editor: Badr Saad T. Alkaltani

This research article is dedicated to solving fractional-order parabolic equations, using an innovative analytical technique. The Adomian decomposition method is well supported by Elzaki transformation to establish closed-form solutions for targeted problems. The procedure is simple, attractive, and preferred over other methods because it provides a closed-form solution for the given problems. The solution graphs are plotted for both integer and fractional-order, which shows that the obtained results are in good contact with problems' exact solution. It is also observed that the solution of fractional-order problems is convergent to the integer-order problem. Moreover, the validity of the proposed method is analyzed by considering some numerical examples. The theory of the suggested approach is fully supported by the obtained results for the given problems. In conclusion, the present method is a straightforward and accurate analytical technique that can solve other fractional-order partial differential equations.

1. Introduction

The present research work is dedicated to studying the analytical solution of fractional-order parabolic equations. The literature is well recognized that a broad range of physics, engineering, nuclear physics, and mathematics problems can be defined as unique boundary and initial value problems. Homogeneous beam's transverse vibrations are controlled by fractional single fourth-order parabolic partial differential equations (PDEs). Such problem types occur in viscoelastic and inelastic flow mathematical modeling, layer deflection theories, and beam deformation [1–12]. Analyses of these problems have taken several physicist's and mathematician's attention [13–15].

The time fractional parabolic PDEs with variable coefficient:

$$\frac{\partial^{\beta}\mu}{\partial\tau^{\beta}} + \kappa(\phi,\varphi,\psi)\frac{\partial^{4}\mu}{\partial\phi^{4}} + \frac{1}{\varphi}\mu(\phi,\varphi,\psi)\frac{\partial^{4}\mu}{\partial\varphi^{4}} + \frac{1}{\psi}\rho(\phi,\varphi,\psi)\frac{\partial^{4}\mu}{\partial\psi^{4}} = g(\phi,\varphi,\psi,\tau), \quad 1<\beta\le 2, \tau\ge 0, \tag{1}$$

where $\kappa(\phi,\varphi,\psi)$, $\mu(\phi,\varphi,\psi)$, and $\rho(\phi,\varphi,\psi)$ are positive. With initial conditions,

$$\mu(\phi,\varphi,\psi,\tau)=f_0(\phi,\varphi,\psi),$$
$$\mu_\tau(\phi,\varphi,\psi,\tau)=k_0(\phi,\varphi,\psi), \tag{2}$$

with boundary conditions

$$\begin{aligned}
&\mu(a,\varphi,\psi,\tau)=h_0(\varphi,\psi,\tau),\ \mu(b,\varphi,\psi,\tau)=h_1(\varphi,\psi,\tau),\\
&\mu(\phi,a,\psi,\tau)=g_0(\varphi,\psi,\tau),\ \mu(\phi,b,\psi,\tau)=g_1(\varphi,\psi,\tau),\\
&\mu(\phi,\varphi,a,\tau)=k_0(\varphi,\psi,\tau),\ \mu(\phi,\varphi,b,\tau)=k_1(\varphi,\psi,\tau),\\
&\mu_{\phi\phi}(a,\varphi,\psi,\tau)=\bar{h}_0(\varphi,\psi,\tau),\ \mu_{\phi\phi}(b,\varphi,\psi,\tau)=\bar{h}_1(\varphi,\psi,\tau),\\
&\mu_{\varphi\varphi}(\phi,a,\psi,\tau)=\bar{g}_0(\varphi,\psi,\tau),\ \mu_{\varphi\varphi}(\phi,b,\psi,\tau)=\bar{g}_1(\varphi,\psi,\tau),\\
&\mu_{\psi\psi}(\phi,\varphi,a,\tau)=\bar{k}_0(\varphi,\psi,\tau),\ \mu_{\psi\psi}(\phi,\varphi,b,\tau)=\bar{k}_1(\varphi,\psi,\tau).
\end{aligned} \tag{3}$$

For which, h_ℓ, g_ℓ, k_ℓ, h_ℓ, g_ℓ, and k_ℓ are continuous variables, and ℓ differs between 0 and 1 and beam's flexural stiffness ratio [1] in its volume per unit mass, like, and its mentions [1, 3, 4, 6, 8, 10, 11]. Many researchers [10, 16, 17] have attempted to study the analytical solutions of the parabolic equation of the fourth-order. Different techniques have been suggested recently, such as the B-spline method [18], decomposition method [19], the implicit scheme [20], the explicit scheme [11], and the spline method [21] to analyze the solution of the partial differential fourth-order parabolic equation. Biazar and Ghazvini [22] have used He's iterative technique for the solution of parabolic PDE's. The modified version of this method was introduced in [23] to solve singular fourth-order parabolic PDEs. The fourth-order parabolic PDE analytical solution was examined in [24]. The modified Laplace discussed variational iteration technique [25] to solve singular fourth-order parabolic PDEs.

G. Adomian is an American scientist who has developed the Adomian decomposition method. It focuses on the search for a set of solutions and the decomposition of the nonlinear operator into a sequence in which Adomian polynomials [26] are recurrently computed to use the terms. This method is improved with the aid of Elzaki transformation such that the improved method is known as the Elzaki decomposition method (EDM). Elzaki Transform (ET) is a modern integral transform introduced by Tarig Elzaki in 2010. ET is a modified transform of Sumudu and Laplace transforms. It is important to note that there are many differential equations with variable coefficients that Sumudu and Laplace cannot accomplish transforms but can be conveniently done by using ET [27–30]. Many mathematicians have been solving differential equations with the aid of ET, such as Navier-Stokes equations [30], heat-like equations [31] and Burgers–Huxley equation [32].

2. Preliminaries

2.1. Definition. The Abel-Riemann of fractional operator D^β of order β is given as [27–30]

$$D^\beta \nu(\zeta)=\begin{cases}\dfrac{d^j}{d\zeta^j}\nu(\zeta), & \beta=j,\\ \dfrac{1}{\Gamma(j-\beta)}\dfrac{d}{d\zeta^j}\displaystyle\int_0^\zeta \frac{\nu(\zeta)}{(\zeta-\psi)^{\beta-j+1}}d\psi, & j-1<\beta<j,\end{cases} \tag{4}$$

where $j\in Z^+$, $\beta\in R^+$, and

$$D^{-\beta}\nu(\zeta)=\frac{1}{\Gamma(\beta)}\int_0^\zeta(\zeta-\psi)^{\beta-1}\nu(\psi)d\psi,\quad 0<\beta\le 1. \tag{5}$$

2.2. Definition. The fractional-order Abel-Riemann integration operator J^β is defined as [27–30]

$$J^\beta\nu(\zeta)=\frac{1}{\Gamma(\beta)}\int_0^\zeta(\zeta-\psi)^{\beta-1}\nu(\zeta)d\zeta,\quad \zeta>0,\beta>0. \tag{6}$$

The operator of basic properties:

$$\begin{aligned}
J^\beta\zeta^j&=\frac{\Gamma(j+1)}{\Gamma(j+\beta+1)}\zeta^{j+\psi},\\
D^\beta\zeta^j&=\frac{\Gamma(j+1)}{\Gamma(j-\beta+1)}\zeta^{j-\psi}.
\end{aligned} \tag{7}$$

2.3. Definition. The Caputo fractional operator D^β of β is defined as [27–30]

$${}^{C}D^\beta\nu(\zeta)=\begin{cases}\dfrac{1}{\Gamma(j-\beta)}\displaystyle\int_0^\zeta\frac{\nu^j(\psi)}{(\zeta-\psi)^{\beta-j+1}}d\psi, & j-1<\beta<j,\\ \dfrac{d^j}{d\zeta^j}\nu(\zeta), & j=\beta.\end{cases} \tag{8}$$

3. Idea of NDM

The general fractional-order PDE is given as

$$D^\beta\mu(\phi,\tau)+L\mu(\phi,\tau)+N\mu(\phi,\tau)=q(\phi,\tau),\quad \phi,\tau\ge 0,1<\beta\le 1, \tag{9}$$

In Equation (9), we represent the linear part of the equation with L and the nonlinear part with N, and $D^\beta=\partial^\beta/\partial\tau^\beta$ denotes the Caputo fractional derivatives.

With initial condition,

$$\mu(\phi,0)=k(\phi), \tag{10}$$

We have applied the Elzaki transformation to Equation (9)

$$\mathbb{E}\left[D^\beta\mu(\phi,\tau)\right]+\mathbb{E}[L\mu(\phi,\tau)+N\mu(\phi,\tau)]=\mathbb{E}[q(\phi,\tau)], \tag{11}$$

and using Elzaki Transform's differentiation property, we

get

$$\frac{1}{s^{\beta}}\mathbb{E}[\mu(\phi,\tau)] - s^{2-\beta}\mu(\phi,0) = \mathbb{E}[q(\phi,\tau)] - \mathbb{E}[L\mu(\phi,\tau) + N\mu(\phi,\tau)],$$
$$\mathbb{E}[\mu(\phi,\tau)] = s^{2}\mu(\phi,0) + s^{\beta}\mathbb{E}[q(\phi,\tau)] - s^{\beta}\mathbb{E}[L\mu(\phi,\tau) + N\mu(\phi,\tau)]. \tag{12}$$

Now, $\mu(\phi,0) = k(\phi)$.

$$\mathbb{E}[\mu(\phi,\tau)] = s^{2}k(\phi) + s^{\beta}\mathbb{E}[q(\phi,\tau)] - s^{\beta}\mathbb{E}[L\mu(\phi,\tau) + N\mu(\phi,\tau)]. \tag{13}$$

The following infinite series represent the EDM solution $\mu(\phi,\tau)$.

$$\mu(\phi,\tau) = \sum_{j=0}^{\infty}\mu_{j}(\phi,\tau), \tag{14}$$

and Adomian polynomials as

$$N\mu(\phi,\tau) = \sum_{j=0}^{\infty}A_{j}, \tag{15}$$

$$A_{j} = \frac{1}{j!}\left[\frac{d^{j}}{d\lambda^{j}}\left[N\sum_{j=0}^{\infty}\left(\lambda^{j}\mu_{j}\right)\right]\right]_{\lambda=0}, \quad j = 0, 1, 2, \cdots. \tag{16}$$

We get replacement Equation (14) and Equation (15) in Equation (13).

$$\mathbb{E}\left[\sum_{j=0}^{\infty}\mu_{j}(\phi,\tau)\right] = s^{2}k(\phi) + s^{\beta}\mathbb{E}[q(\phi,\tau)] - s^{\beta}\mathbb{E}\left[L\sum_{j=0}^{\infty}\mu_{j}(\phi,\tau) + \sum_{j=0}^{\infty}A_{j}\right]. \tag{17}$$

Applying the Elzaki transformation's linearity,

$$\mathbb{E}[\mu_{0}(\phi,\tau)] = s^{2}k(\phi) + s^{\beta}\mathbb{E}[q(\phi,\tau)], \tag{18}$$

$$\mathbb{E}[\mu_{1}(\phi,\tau)] = -s^{\beta}\mathbb{E}[L\mu_{0}(\phi,\tau) + A_{0}]. \tag{19}$$

We can generally write

$$\mathbb{E}\left[\mu_{j+1}(\phi,\tau)\right] = -s^{\beta}\mathbb{E}\left[L\mu_{j}(\phi,\tau) + A_{j}\right], \quad j \geq 1. \tag{20}$$

Equation (18) and Equation (20) implement the inverse Elzaki transformation

$$\mu_{0}(\phi,\tau) = k(\phi) + \mathbb{E}^{-1}\left[s^{\beta}\mathbb{E}[q(\phi,\tau)]\right],$$
$$\mu_{j+1}(\phi,\tau) = -\mathbb{E}^{-1}\left[s^{\beta}\mathbb{E}\left[L\mu_{j}(\phi,\tau) + A_{j}\right]\right]. \tag{21}$$

4. Numerical Implementation

4.1. Problem. Consider fractional-order one-dimensional parabolic equation:

$$\frac{\partial^{\beta}\mu}{\partial\tau^{\beta}} + \left(\frac{1}{\phi} + \frac{\phi^{4}}{120}\right)\frac{\partial^{4}\mu}{\partial\phi^{4}} = 0, \quad 1 < \beta \leq 2, \tau \geq 0, \tag{22}$$

with initial conditions

$$\mu(\phi,0) = 0, \mu_{\tau}(\phi,0) = 1 + \frac{\phi^{5}}{120}, \tag{23}$$

with boundary conditions

$$\mu\left(\frac{1}{2},\tau\right) = \left(1 + \frac{(1/2)^{5}}{120}\right)\sin(\tau), \mu(1,\tau) = \left(\frac{121}{120}\right)\sin(\tau),$$
$$\frac{\partial^{2}\mu}{\partial\phi^{2}}\left(\frac{1}{2},\tau\right) = \frac{1}{6}\left(\frac{1}{2}\right)^{3}\sin(\tau), \frac{\partial^{2}\mu}{\partial\phi^{2}}(1,\tau) = \frac{1}{6}\sin(\tau). \tag{24}$$

The Elzaki transform of Equation (22):

$$\frac{1}{s^{\beta}}\mu(\phi,s,u) - s^{2-\beta}\mu(\phi,0) - s^{3-\beta}\mu_{\tau}(\phi,0) = -\mathbb{E}\left[\left(\frac{1}{\phi} + \frac{\phi^{4}}{120}\right)\frac{\partial^{4}\mu}{\partial\phi^{4}}\right]. \tag{25}$$

Simplify and replace Equation (23) condition.

$$\mu(\phi,s,u) = s^{2}(0) + s^{3}\left(1 + \frac{\phi^{5}}{120}\right) - \mathbb{E}\left[\left(\frac{1}{\phi} + \frac{\phi^{4}}{120}\right)\frac{\partial^{4}\mu}{\partial\phi^{4}}\right]. \tag{26}$$

Use of inverse Elzaki transformation

$$\mu(\phi,\tau) = \mathbb{E}^{-1}\left[s^{3}\left(1 + \frac{\phi^{5}}{120}\right) - s^{\beta}\mathbb{E}\left[\left(\frac{1}{\phi} + \frac{\phi^{4}}{120}\right)\frac{\partial^{4}\mu}{\partial\phi^{4}}\right]\right], \tag{27}$$

$$\mu(\phi,\tau) = \left(1 + \frac{\phi^{5}}{120}\right)\tau - \mathbb{E}^{-1}\left[s^{\beta}\mathbb{E}\left[\left(\frac{1}{\phi} + \frac{\phi^{4}}{120}\right)\frac{\partial^{4}\mu}{\partial\phi^{4}}\right]\right]. \tag{28}$$

Equation (28) correction function is provided by

$$\sum_{\ell=0}^{\infty}\mu_{\ell+1}(\phi,\tau) = \left(1 + \frac{\phi^{5}}{120}\right)\tau - \mathbb{E}^{-1}\left[s^{\beta}\mathbb{E}\left[\left(\frac{1}{\phi} + \frac{\phi^{4}}{120}\right)\sum_{\ell=0}^{\infty}\frac{\partial^{4}\mu_{\ell}}{\partial\phi^{4}}\right]\right], \tag{29}$$

the first term

$$\mu_{0}(\phi,\tau) = \left(1 + \frac{\phi^{5}}{120}\right)\tau, \tag{30}$$

then we got

$$\mu_{\ell+1}(\phi,\tau) = -\mathbb{E}^{-1}\left[s^{\beta}\mathbb{E}\left[\left(\frac{1}{\phi}+\frac{\phi^4}{120}\right)\sum_{\ell=0}^{\infty}\frac{\partial^4\mu_{\ell}}{\partial\phi^4}\right]\right], \tag{31}$$

for $j=0$,

$$\mu_1(\phi,\tau) = -\mathbb{E}^{-1}\left[s^{\beta}\mathbb{E}\left[\left(\frac{1}{\phi}+\frac{\phi^4}{120}\right)\frac{\partial^4\mu_0}{\partial\phi^4}\right]\right],$$
$$\mu_1(\phi,\tau) = -\mathbb{E}^{-1}\left[\frac{\left(1+\left(\phi^5/120\right)\right)u^{\beta}}{s^{\beta+2}}\right] = -\left(1+\frac{\phi^5}{120}\right)\frac{\tau^{\beta+1}}{\Gamma(\beta+2)}. \tag{32}$$

The following terms are

$$\mu_2(\phi,\tau) = -\mathbb{E}^{-1}\left[s^{\beta}\mathbb{E}\left[\left(\frac{1}{\phi}+\frac{\phi^4}{120}\right)\frac{\partial^4\mu_1}{\partial\phi^4}\right]\right] = \left(1+\frac{\phi^5}{120}\right)\frac{\tau^{2\beta+1}}{\Gamma(2\beta+2)},$$
$$\mu_3(\phi,\tau) = -\mathbb{E}^{-1}\left[s^{\beta}\mathbb{E}\left[\left(\frac{1}{\phi}+\frac{\phi^4}{120}\right)\frac{\partial^4\mu_2}{\partial\phi^4}\right]\right] = -\left(1+\frac{\phi^5}{120}\right)\frac{\tau^{3\beta+1}}{\Gamma(3\beta+2)},$$
$$\vdots \tag{33}$$

The series form of problem (1) such as:

$$\mu(\phi,\tau) = \mu_0(\phi,\tau)+\mu_1(\phi,\tau)+\mu_2(\phi,\tau)+\mu_3(\phi,\tau)+\mu_4(\phi,\tau)\cdots,$$
$$\mu(\phi,\tau) = \left(1+\frac{\phi^5}{120}\right)\left\{\tau-\frac{\tau^{\beta+1}}{\Gamma(\beta+2)}+\frac{\tau^{2\beta+1}}{\Gamma(2\beta+2)}-\frac{\tau^{3\beta+1}}{\Gamma(3\beta+2)}+\frac{\tau^{4\beta+1}}{\Gamma(4\beta+2)}\cdots\right\}, \tag{34}$$

when $\beta=2$, then integer EDM solution is

$$\mu(\phi,\tau) = \left(1+\frac{\phi^5}{120}\right)\left\{\tau-\frac{\tau^3}{3!}+\frac{\tau^5}{5!}-\frac{\tau^7}{7!}+\frac{\tau^9}{9!}\cdots\right\}. \tag{35}$$

The exact result is given as

$$\mu(\phi,\tau) = \left(1+\frac{\phi^5}{120}\right)\sin(\tau). \tag{36}$$

In Figure 1, the exact and the EDM solutions of problem 1 at $\beta=1$ are shown by subgraphs, respectively. From the given figure, it can be seen that both the EDM and exact results are in close contact with each other. In Figure 2, the EDM solutions of problem 1 are investigated at different fractional order $\beta=0.8$ and 0.6. It is analyzed that time-fractional problem results are convergent to an integer-order effect as time-fractional analysis to integer order.

4.2. Problem. Consider fractional-order two-dimensional parabolic equation:

$$\frac{\partial^{\beta}\mu}{\partial\tau^{\beta}}+2\left(\frac{1}{\phi^2}+\frac{\phi^4}{6!}\right)\frac{\partial^4\mu}{\partial\phi^4}+2\left(\frac{1}{\varphi^2}+\frac{\varphi^4}{6!}\right)\frac{\partial^4\mu}{\partial\varphi^4}=0,\quad 1<\beta\le 2,\tau\ge 0, \tag{37}$$

with initial conditions

$$\mu(\phi,\varphi,0)=0,\mu_{\tau}(\phi,\varphi,0)=2+\frac{\phi^6}{6!}+\frac{\varphi^6}{6!}, \tag{38}$$

with boundary conditions

$$\mu\left(\frac{1}{2},\varphi,\tau\right)=\left(2+\frac{(1/2)^6}{6!}+\frac{\varphi^6}{6!}\right)\sin(\tau),\mu\left(\frac{1}{2},\varphi,\tau\right)=\left(2+\frac{(1)^6}{6!}+\frac{\varphi^6}{6!}\right)\sin(\tau),$$
$$\mu_{\phi\phi}\left(\frac{1}{2},\varphi,\tau\right)=\left(\frac{(1/2)^4}{4!}\right)\sin(\tau),\mu_{\phi\phi}\left(\frac{1}{2},\varphi,\tau\right)=\frac{1}{24}\sin(\tau),$$
$$\mu_{\varphi\varphi}\left(\phi,\frac{1}{2},\tau\right)=\frac{(1/2)^4}{4!}\sin(\tau),\mu_{\varphi\varphi}\left(\phi,\frac{1}{2},\tau\right)=\frac{1}{24}\sin(\tau). \tag{39}$$

In the Elzaki transformation of Equation (37), we get

$$\frac{1}{s^{\beta}}\mu(\phi,\varphi,s,u)-s^{2-\beta}\mu(\phi,0)-s^{3-\beta}\mu_{\tau}(\phi,0) = -\mathbb{E}\left[2\left(\frac{1}{\phi^2}+\frac{\phi^4}{6!}\right)\frac{\partial^4\mu}{\partial\phi^4}+2\left(\frac{1}{\varphi^2}+\frac{\varphi^4}{6!}\right)\frac{\partial^4\mu}{\partial\varphi^4}\right], \tag{40}$$

Simplify and replace Equation (38) condition.

$$\mu(\phi,\varphi,s,u) = s^2(0)+s^3\left(2+\frac{\phi^6}{6!}+\frac{\varphi^6}{6!}\right) - s^{\beta}\mathbb{E}\left[2\left(\frac{1}{\phi^2}+\frac{\phi^4}{6!}\right)\frac{\partial^4\mu}{\partial\phi^4}+2\left(\frac{1}{\varphi^2}+\frac{\varphi^4}{6!}\right)\frac{\partial^4\mu}{\partial\varphi^4}\right], \tag{41}$$

using inverse Elzaki transformation

$$\mu(\phi,\varphi,\tau)=\mathbb{E}^{-1}\left[s^3\left(2+\frac{\phi^6}{6!}+\frac{\varphi^6}{6!}\right)-s^{\beta}\mathbb{E}\left\{2\left(\frac{1}{\phi^2}+\frac{\phi^4}{6!}\right)\frac{\partial^4\mu}{\partial\phi^4}+2\left(\frac{1}{\varphi^2}+\frac{\varphi^4}{6!}\right)\frac{\partial^4\mu}{\partial\varphi^4}\right\}\right], \tag{42}$$

$$\mu(\phi,\varphi,\tau) = \left(2+\frac{\phi^6}{6!}+\frac{\varphi^6}{6!}\right)\tau-\mathbb{E}^{-1} \cdot\left[s^{\beta}\mathbb{E}\left\{2\left(\frac{1}{\phi^2}+\frac{\phi^4}{6!}\right)\frac{\partial^4\mu}{\partial\phi^4}+2\left(\frac{1}{\varphi^2}+\frac{\varphi^4}{6!}\right)\frac{\partial^4\mu}{\partial\varphi^4}\right\}\right], \tag{43}$$

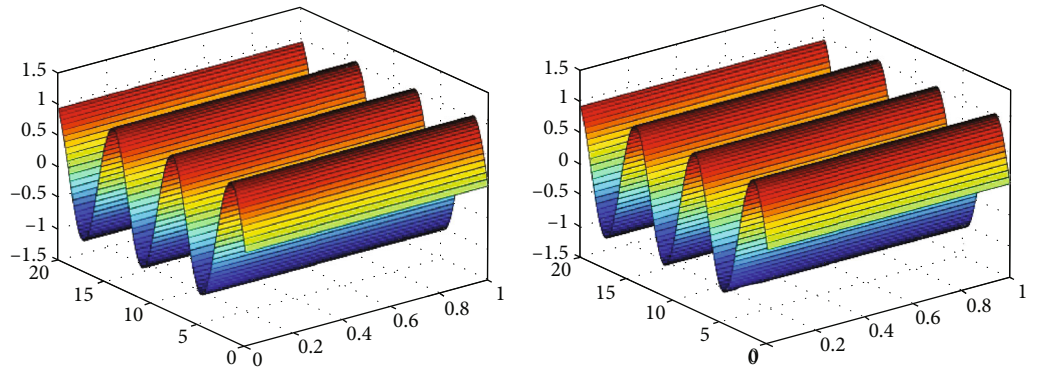

Figure 1: The graphs of exact and EDM result for $\beta = 2$ of problem 1.

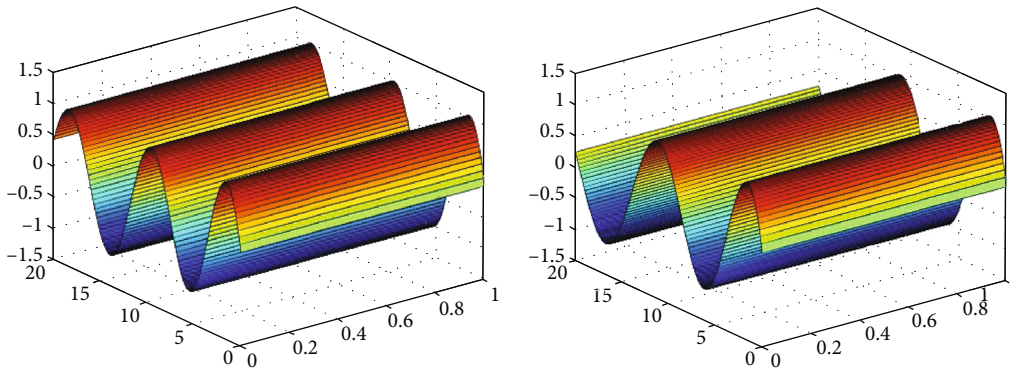

Figure 2: The fractional-order graphs of $\beta = 0.8$ and 0.6 of problem 1.

Equation (43) correction function is provided by

$$\sum_{\ell=0}^{\infty}\mu_{\ell+1}(\phi,\varphi,\tau) = \left(2+\frac{\phi^6}{6!}+\frac{\varphi^6}{6!}\right)\tau - \mathbb{E}^{-1} \cdot \left[s^{\beta}\mathbb{E}\left\{2\left(\frac{1}{\phi^2}+\frac{\phi^4}{6!}\right)\sum_{\ell=0}^{\infty}\frac{\partial^4\mu_\ell}{\partial\phi^4}+2\left(\frac{1}{\varphi^2}+\frac{\varphi^4}{6!}\right)\sum_{\ell=0}^{\infty}\frac{\partial^4\mu_\ell}{\partial\varphi^4}\right\}\right], \tag{44}$$

the first term

$$\mu_0(\phi,\varphi,\tau) = \left(2+\frac{\phi^6}{6!}+\frac{\varphi^6}{6!}\right)\tau, \tag{45}$$

then we get

$$\mu_{\ell+1}(\phi,\varphi,\tau) = -\mathbb{E}^{-1}\left[s^{\beta}\mathbb{E}\left\{2\left(\frac{1}{\phi^2}+\frac{\phi^4}{6!}\right)\sum_{\ell=0}^{\infty}\frac{\partial^4\mu_\ell}{\partial\phi^4}+2\left(\frac{1}{\varphi^2}+\frac{\varphi^4}{6!}\right)\sum_{\ell=0}^{\infty}\frac{\partial^4\mu_\ell}{\partial\varphi^4}\right\}\right], \tag{46}$$

for $j = 0$,

$$\mu_1(\phi,\varphi,\tau) = -\mathbb{E}^{-1}\left[s^{\beta}\mathbb{E}\left\{2\left(\frac{1}{\phi^2}+\frac{\phi^4}{6!}\right)\frac{\partial^4\mu_0}{\partial\phi^4}+2\left(\frac{1}{\varphi^2}+\frac{\varphi^4}{6!}\right)\frac{\partial^4\mu_0}{\partial\varphi^4}\right\}\right],$$
$$\mu_1(\phi,\tau) = -\mathbb{E}^{-1}\left[\left(2+\frac{\phi^6}{6!}+\frac{\varphi^6}{6!}\right)\frac{u^{\beta}}{s^{\beta+2}}\right] = -\left(2+\frac{\phi^6}{6!}+\frac{\varphi^6}{6!}\right)\frac{\tau^{\beta+1}}{\Gamma(\beta+2)}. \tag{47}$$

The following terms are

$$\mu_2(\phi,\varphi,\tau) = -\mathbb{E}^{-1}\left[s^{\beta}\mathbb{E}\left\{2\left(\frac{1}{\phi^2}+\frac{\phi^4}{6!}\right)\frac{\partial^4\mu_1}{\partial\phi^4}+2\left(\frac{1}{\varphi^2}+\frac{\varphi^4}{6!}\right)\frac{\partial^4\mu_1}{\partial\varphi^4}\right\}\right],$$
$$\mu_2(\phi,\varphi,\tau) = \left(2+\frac{\phi^6}{6!}+\frac{\varphi^6}{6!}\right)\frac{\tau^{2\beta+1}}{\Gamma(2\beta+2)},$$
$$\mu_3(\phi,\varphi,\tau) = -\mathbb{E}^{-1}\left[s^{\beta}\mathbb{E}\left\{2\left(\frac{1}{\phi^2}+\frac{\phi^4}{6!}\right)\frac{\partial^4\mu_2}{\partial\phi^4}+2\left(\frac{1}{\varphi^2}+\frac{\varphi^4}{6!}\right)\frac{\partial^4\mu_2}{\partial\varphi^4}\right\}\right],$$
$$\mu_3(\phi,\varphi,\tau) = -\left(2+\frac{\phi^6}{6!}+\frac{\varphi^6}{6!}\right)\frac{\tau^{3\beta+1}}{\Gamma(3\beta+2)},$$
$$\vdots \tag{48}$$

In the series form of problem (2), we get

$$\mu(\phi,\varphi,\tau) = \mu_0(\phi,\varphi,\tau)+\mu_1(\phi,\varphi,\tau)+\mu_2(\phi,\varphi,\tau)+\mu_3(\phi,\varphi,\tau)+\mu_4(\phi,\varphi,\tau)\cdots,$$

$$\mu(\phi,\varphi,\tau) = \left(2+\frac{\phi^6}{6!}+\frac{\varphi^6}{6!}\right)\left\{\tau-\frac{\tau^{\beta+1}}{\Gamma(\beta+2)}+\frac{\tau^{2\beta+1}}{\Gamma(2\beta+2)}-\frac{\tau^{3\beta+1}}{\Gamma(3\beta+2)}+\frac{\tau^{4\beta+1}}{\Gamma(4\beta+2)}\cdots\right\}. \tag{49}$$

Then, $\beta = 2$, the integer EDM result as

$$\mu(\phi, \varphi, \tau) = \left(2 + \frac{\phi^6}{6!} + \frac{\varphi^6}{6!}\right)\left\{\tau - \frac{\tau^3}{3!} + \frac{\tau^5}{5!} - \frac{\tau^7}{7!} + \frac{\tau^9}{9!} \cdots\right\}. \tag{50}$$

The exact solution is

$$\mu(\phi, \varphi, \tau) = \left(2 + \frac{\phi^6}{6!} + \frac{\varphi^6}{6!}\right)\sin(\tau). \tag{51}$$

In Figure 3, the exact and the EDM solutions of problem 2 at $\beta = 1$ are shown by subgraphs, respectively. From the given figure, it can be seen that both the EDM and exact results are in close contact with each other. In Figure 4, the EDM solutions of problem 2 are investigated at different fractional order $\beta = 0.8$ and 0.6. It is analyzed that time-fractional problem results are convergent to an integer-order effect as time-fractional analysis to integer order.

4.3. Problem. Consider fractional-order three-dimensional parabolic equation:

$$\frac{\partial^\beta \mu}{\partial \tau^\beta} + 2\left(\frac{\varphi + \psi}{2\cos\phi} - 1\right)\frac{\partial^4 \mu}{\partial \phi^4} + 2\left(\frac{\phi + \psi}{2\cos\varphi} - 1\right)\frac{\partial^4 \mu}{\partial \varphi^4} + 2\left(\frac{\varphi + \phi}{2\cos\psi} - 1\right)\frac{\partial^4 \mu}{\partial \psi^4} = 0, \tag{52}$$

$$1 < \beta \le 2, \tau \ge 0, \tag{53}$$

with initial conditions

$$\mu(\phi, \varphi, \psi, 0) = \phi + \varphi + \psi - (\cos(\phi) + \cos(\varphi) + \cos(\psi)), \tag{54}$$

$$\mu_\tau(\phi, \varphi, \psi, 0) = (\cos(\phi) + \cos(\varphi) + \cos(\psi)) - (\phi + \varphi + \psi), \tag{55}$$

with boundary conditions

$$\begin{aligned}
\mu(0, \varphi, \psi, \tau) &= (-1 + \varphi + \psi - \cos(\varphi) - \cos(\psi))e^{-\tau},\\
\mu\left(\frac{\pi}{3}, \varphi, \psi, \tau\right) &= \left(\frac{2\pi - 3}{6} + \varphi + \psi - \cos(\varphi) - \cos(\psi)\right)e^{-\tau},\\
\mu(\phi, 0, \psi, \tau) &= (-1 + \phi + \psi - \cos(\phi) - \cos(\psi))e^{-\tau},\\
\mu\left(\phi, \frac{\pi}{3}, \psi, \tau\right) &= \left(\frac{2\pi - 3}{6} + \phi + \psi - \cos(\phi) - \cos(\psi)\right)e^{-\tau},\\
\mu(\phi, \varphi, 0, \tau) &= (-1 + \phi + \varphi - \cos(\phi) - \cos(\varphi))e^{-\tau},\\
\mu\left(\phi, \varphi, \frac{\pi}{3}, \tau\right) &= \left(\frac{2\pi - 3}{6} + \phi + \varphi - \cos(\phi) - \cos(\varphi)\right)e^{-\tau},\\
\mu_\phi(0, \varphi, \psi, \tau) &= \mu_\varphi(\phi, 0, \psi, \tau) = \mu_\psi(\phi, \varphi, 0, \tau) = e^{-\tau},\\
\mu_\phi\left(\frac{\pi}{3}, \varphi, \psi, \tau\right) &= \mu_\varphi\left(\phi, \frac{\pi}{3}, \psi, \tau\right) = \mu_\psi\left(\phi, \varphi, \frac{\pi}{3}, \tau\right) = \left(\frac{\sqrt{3} + 2}{2}\right)e^{-\tau}.
\end{aligned} \tag{56}$$

In the Elzaki transformation of Equation (52), we get

$$\begin{aligned}
&\frac{1}{s^\beta}\mu(\phi, \varphi, \psi, s, u) - s^{2-\beta}\mu(\phi, \varphi, \psi, 0) - s^{3-\beta}\mu_\tau(\phi, \varphi, \psi, 0)\\
&= -\mathbb{E}\left[2\left(\frac{\varphi + \psi}{2\cos\phi} - 1\right)\frac{\partial^4 \mu}{\partial \phi^4} + 2\left(\frac{\phi + \psi}{2\cos\varphi} - 1\right)\frac{\partial^4 \mu}{\partial \varphi^4}\right.\\
&\left. + 2\left(\frac{\varphi + \phi}{2\cos\psi} - 1\right)\frac{\partial^4 \mu}{\partial \psi^4}\right],
\end{aligned} \tag{57}$$

Simplify and replace Equation (54) condition.

$$\begin{aligned}
\mu(\phi, \varphi, \psi, s, u) &= s^2\{\phi + \varphi + \psi - (\cos(\phi) + \cos(\varphi) + \cos(\psi))\}\\
&+ s^3\{(\cos(\phi) + \cos(\varphi) + \cos(\psi)) - (\phi + \varphi + \psi)\}\\
&- s^\beta\mathbb{E}\left[2\left(\frac{\varphi + \psi}{2\cos\phi} - 1\right)\frac{\partial^4 \mu}{\partial \phi^4} + 2\left(\frac{\phi + \psi}{2\cos\varphi} - 1\right)\frac{\partial^4 \mu}{\partial \varphi^4}\right.\\
&\left. + 2\left(\frac{\varphi + \phi}{2\cos\psi} - 1\right)\frac{\partial^4 \mu}{\partial \psi^4}\right],
\end{aligned} \tag{58}$$

using the inverse Elzaki transform

$$\begin{aligned}
\mu(\phi, \varphi, \psi, \tau) &= \mathbb{E}^{-1}\left[s^2\{\phi + \varphi + \psi - (\cos(\phi) + \cos(\varphi) + \cos(\psi))\}\right.\\
&\left. + s^3\{(\cos(\phi) + \cos(\varphi) + \cos(\psi)) - (\phi + \varphi + \psi)\}\right]\\
&- \mathbb{E}^{-1}\left[s^\beta\mathbb{E}\left[2\left(\frac{\varphi + \psi}{2\cos\phi} - 1\right)\frac{\partial^4 \mu}{\partial \phi^4} + 2\left(\frac{\phi + \psi}{2\cos\varphi} - 1\right)\frac{\partial^4 \mu}{\partial \varphi^4}\right.\right.\\
&\left.\left. + 2\left(\frac{\varphi + \phi}{2\cos\psi} - 1\right)\frac{\partial^4 \mu}{\partial \psi^4}\right]\right],
\end{aligned} \tag{59}$$

$$\begin{aligned}
\mu(\phi, \varphi, \psi, \tau) &= \{\phi + \varphi + \psi - (\cos(\phi) + \cos(\varphi) + \cos(\psi))\}(1 - \tau)\\
&- \mathbb{E}^{-1}\left[s^\beta\mathbb{E}\left[2\left(\frac{\varphi + \psi}{2\cos\phi} - 1\right)\frac{\partial^4 \mu}{\partial \phi^4} + 2\left(\frac{\phi + \psi}{2\cos\varphi} - 1\right)\frac{\partial^4 \mu}{\partial \varphi^4}\right.\right.\\
&\left.\left. + 2\left(\frac{\varphi + \phi}{2\cos\psi} - 1\right)\frac{\partial^4 \mu}{\partial \psi^4}\right]\right].
\end{aligned} \tag{60}$$

Equation (59) correction function is provided by

$$\begin{aligned}
\sum_{\ell=0}^{\infty}\mu_{\ell+1}(\phi, \varphi, \tau) &= \{\phi + \varphi + \psi - (\cos(\phi) + \cos(\varphi) + \cos(\psi))\}(1 - \tau)\\
&- \mathbb{E}^{-1}\left[s^\beta\mathbb{E}\left[2\left(\frac{\varphi + \psi}{2\cos\phi} - 1\right)\sum_{\ell=0}^{\infty}\frac{\partial^4 \mu_\ell}{\partial \phi^4} + 2\left(\frac{\phi + \psi}{2\cos\varphi} - 1\right)\sum_{\ell=0}^{\infty}\frac{\partial^4 \mu_\ell}{\partial \varphi^4}\right.\right.\\
&\left.\left. + 2\left(\frac{\varphi + \phi}{2\cos\psi} - 1\right)\sum_{\ell=0}^{\infty}\frac{\partial^4 \mu_\ell}{\partial \psi^4}\right]\right],
\end{aligned} \tag{61}$$

the first term

$$\mu_0(\phi, \varphi, \psi, \tau) = \{\phi + \varphi + \psi - (\cos(\phi) + \cos(\varphi) + \cos(\psi))\}(1 - \tau), \tag{62}$$

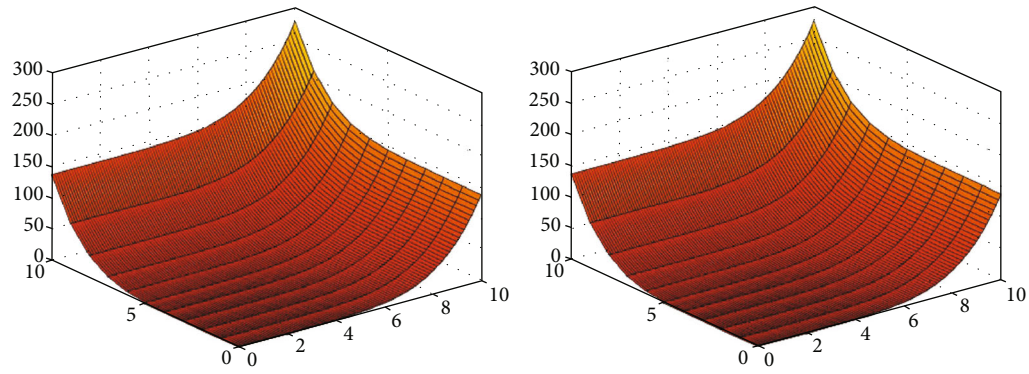

Figure 3: The exact and EDM solution for $\beta = 2$ of problem 2.

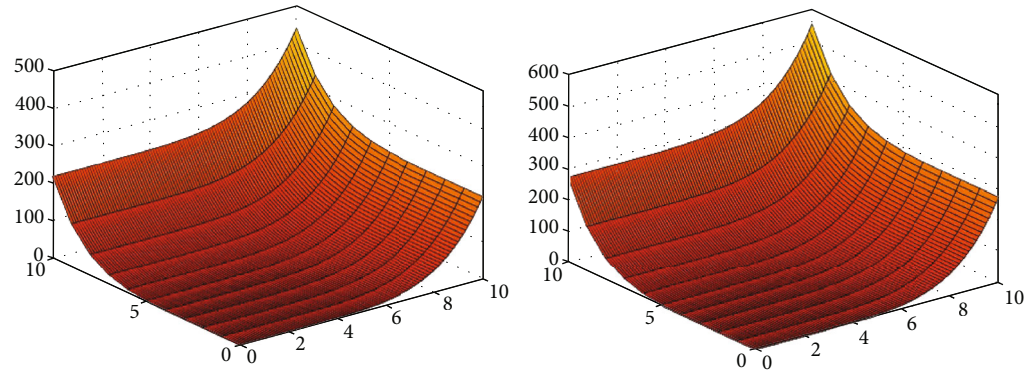

Figure 4: The fractional-order graphs of $\beta = 0.8$ and 0.6 of problem 2.

then we get

$$\mu_{\ell+1}(\phi,\varphi,\psi,\tau) = -\mathbb{E}^{-1}\left[s^{\beta}\mathbb{E}\left\{2\left(\frac{\varphi+\psi}{2\cos\phi}-1\right)\sum_{\ell=0}^{\infty}\frac{\partial^4\mu_\ell}{\partial\phi^4} + 2\left(\frac{\phi+\psi}{2\cos\varphi}-1\right)\sum_{\ell=0}^{\infty}\frac{\partial^4\mu_\ell}{\partial\varphi^4} + 2\left(\frac{\varphi+\phi}{2\cos\psi}-1\right)\sum_{\ell=0}^{\infty}\frac{\partial^4\mu_\ell}{\partial\psi^4}\right\}\right], \tag{63}$$

for $j = 0$,

$$\mu_1(\phi,\varphi,\psi,\tau) = -\mathbb{E}^{-1}\left[s^{\beta}\mathbb{E}\left\{2\left(\frac{\varphi+\psi}{2\cos\phi}-1\right)\frac{\partial^4\mu_0}{\partial\phi^4} + 2\left(\frac{\phi+\psi}{2\cos\varphi}-1\right)\frac{\partial^4\mu_0}{\partial\varphi^4} + 2\left(\frac{\varphi+\phi}{2\cos\psi}-1\right)\frac{\partial^4\mu_0}{\partial\psi^4}\right\}\right],$$

$$\mu_1(\phi,\varphi,\psi,\tau) = \mathbb{E}^{-1}\left[\phi+\varphi+\psi-(\cos(\phi)+\cos(\varphi)+\cos(\psi))\left(\frac{u^{\beta}}{s^{\beta+1}}-\frac{u^{\beta}}{s^{\beta+2}}\right)\right],$$

$$\mu_1(\phi,\varphi,\psi,\tau) = \{\phi+\varphi+\psi-(\cos(\phi)+\cos(\varphi)+\cos(\psi))\}\left(\frac{\tau^{\beta}}{\Gamma(\beta+1)}-\frac{\tau^{\beta+1}}{\Gamma(\beta+2)}\right). \tag{64}$$

The following terms are

$$\mu_2(\phi,\varphi,\psi,\tau) = -\mathbb{E}^{-1}\left[s^{\beta}\mathbb{E}\left\{2\left(\frac{\varphi+\psi}{2\cos\phi}-1\right)\frac{\partial^4\mu_1}{\partial\phi^4} + 2\left(\frac{\phi+\psi}{2\cos\varphi}-1\right)\frac{\partial^4\mu_1}{\partial\varphi^4} + 2\left(\frac{\varphi+\phi}{2\cos\psi}-1\right)\frac{\partial^4\mu_1}{\partial\psi^4}\right\}\right],$$

$$\mu_2(\phi,\varphi,\psi,\tau) = \{\phi+\varphi+\psi-(\cos(\phi)+\cos(\varphi)+\cos(\psi))\}\cdot\left(\frac{\tau^{2\beta}}{\Gamma(2\beta+1)}-\frac{\tau^{2\beta+1}}{\Gamma(2\beta+2)}\right),$$

$$\mu_3(\phi,\varphi,\psi,\tau) = \mathbb{E}^{-1}\left[s^{\beta}\mathbb{E}\left\{2\left(\frac{\varphi+\psi}{2\cos\phi}-1\right)\frac{\partial^4\mu_2}{\partial\phi^4} + 2\left(\frac{\phi+\psi}{2\cos\varphi}-1\right)\frac{\partial^4\mu_2}{\partial\varphi^4} + 2\left(\frac{\varphi+\phi}{2\cos\psi}-1\right)\frac{\partial^4\mu_2}{\partial\psi^4}\right\}\right],$$

$$\mu_3(\phi,\varphi,\psi,\tau) = \{\phi+\varphi+\psi-(\cos(\phi)+\cos(\varphi)+\cos(\psi))\}\cdot\left(\frac{\tau^{3\beta}}{\Gamma(3\beta+1)}-\frac{\tau^{3\beta+1}}{\Gamma(3\beta+2)}\right),$$

$$\vdots \tag{65}$$

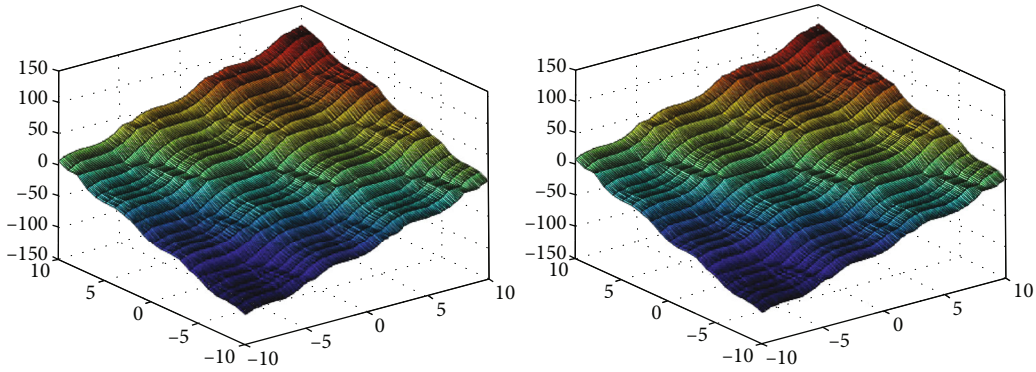

Figure 5: The exact and EDM solution for $\beta = 2$ of problem 3.

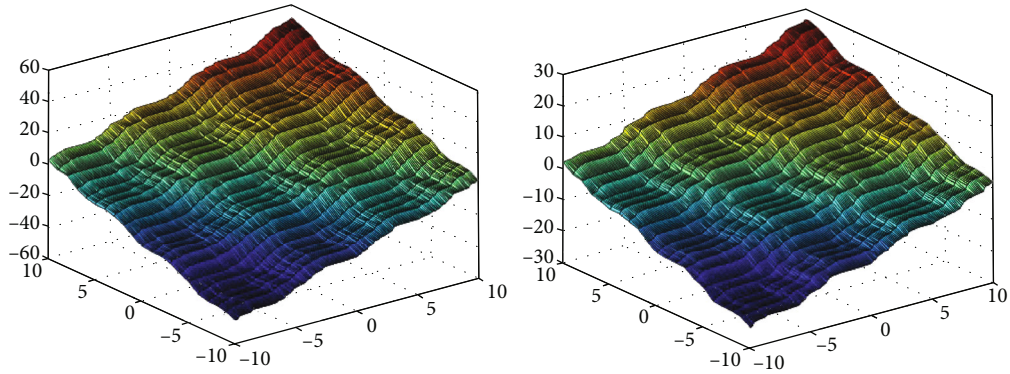

Figure 6: For fractional-order graphs of $\beta = 0.8$ and 0.6 of problem 3.

The series form of problem (3) such as

$$\mu(\phi,\varphi,\psi,\tau) = \mu_0(\phi,\varphi,\psi,\tau) + \mu_1(\phi,\varphi,\psi,\tau) + \mu_2(\phi,\varphi,\psi,\tau) + \mu_3(\phi,\varphi,\psi,\tau) + \mu_4(\phi,\varphi,\psi,\tau)\cdots,$$

$$\mu(\phi,\varphi,\psi,\tau) = \{\phi+\varphi+\psi-(\cos(\phi)+\cos(\varphi)+\cos(\psi))\} \cdot \left\{1-\tau+\frac{\tau^{\beta}}{\Gamma(\beta+1)}-\frac{\tau^{\beta+1}}{\Gamma(\beta+2)}+\frac{\tau^{2\beta}}{\Gamma(2\beta+1)} - \frac{\tau^{2\beta+1}}{\Gamma(2\beta+2)}+\frac{\tau^{3\beta}}{\Gamma(3\beta+1)}-\frac{\tau^{3\beta+1}}{\Gamma(3\beta+2)}\cdots\right\}. \tag{66}$$

In the integer-order solution of EDM of Equation (52) at $\beta = 2$, we get

$$\mu(\phi,\varphi,\psi,\tau) = \{\phi+\varphi+\psi-(\cos(\phi)+\cos(\varphi)+\cos(\psi))\} \cdot \left\{1-\tau+\frac{\tau^2}{2!}-\frac{\tau^3}{3!}+\frac{\tau^4}{4!}-\frac{\tau^5}{5!}+\frac{\tau^6}{6!}-\frac{7}{7!}\cdots\right\}. \tag{67}$$

The exact solution is given as

$$\mu(\phi,\varphi,\psi,\tau) = (\phi+\varphi+\psi-(\cos(\phi)+\cos(\varphi)+\cos(\psi)))e^{-\tau}. \tag{68}$$

In Figure 5, the exact and the EDM solutions of problem 3 at $\beta = 1$ are shown by subgraphs, respectively. From the given figure, it can be seen that both the EDM and exact results are in close contact with each other. In Figure 6, the EDM solutions of problem 3 are investigated at different fractional order $\beta = 0.8$ and 0.6. It is analyzed that time-fractional problem results are convergent to an integer-order effect as time-fractional analysis to integer order.

5. Conclusion

In the present article, an efficient analytical technique is used to solve fractional-order parabolic equations. The present method is the combination of two well-known methods, namely, Elzaki transform and Adomian decomposition method. The Elzaki transform is applied to the given problem, which makes it easier. After this, we implemented Adomian decomposition method and then inverse Elzaki transform to get closed form analytical solutions for the given problems. The proposed method required small number of calculation to attain closed form solutions and is therefore considered to be one of the best analytical method to solve fractional-order partial differential equations.

Data Availability

The numerical data used to support the findings of this study are included within the article.

Conflicts of Interest

The authors declare that there are no conflicts of interest regarding the publication of this article.

Acknowledgments

One of the coauthors (A. M. Zidan) extends his appreciation to the Deanship of Scientific Research at King Khalid University, Abha, 61413, Saudi Arabia, for funding this work through a research group program under grant number R.G.P.-2/142/42. The authors would like to thank Deanship Scientific Research at the Umm Al-Qura University for supporting this research work under grant code 19-SCI-1-01-0041.

References

[1] A. Q. M. Khaliq and E. H. Twizell, "A family of second order methods for variable coefficient fourth order parabolic partial differential equations," *International Journal of Computer Mathematics*, vol. 23, no. 1, pp. 63–76, 1987.

[2] H. Jafari, J. G. Prasad, P. Goswami, and R. S. Dubey, "Solution of the local fractional generalized KDV equation using homotopy analysis method," *Fractals*, vol. 29, no. 5, article 2140014, 2021.

[3] D. J. Gorman, "Free vibration analysis of beams and shafts (book)," in *Research supported by the National Research Council of Canada*, p. 395, Wiley-Interscience, New York, 1975.

[4] C. Andrade and S. McKee, "High accuracy A.D.I. methods for fourth order parabolic equations with variable coefficients," *Journal of Computational and Applied Mathematics*, vol. 3, no. 1, pp. 11–14, 1977.

[5] R. S. Dubey, B. S. T. Alkahtani, and A. Atangana, "Analytical solution of space-time fractional Fokker-Planck equation by homotopy perturbation Sumudu transform method," *Mathematical Problems in Engineering*, vol. 2015, Article ID 780929, 7 pages, 2015.

[6] S. D. Conte, "A stable implicit finite difference approximation to a fourth order parabolic equation," *Journal of the ACM*, vol. 4, no. 1, pp. 18–23, 1957.

[7] V. Gill and R. S. Dubey, "New analytical method for Klein-Gordon equations arising in quantum field theory," *European Journal of Advances in Engineering and Technology*, vol. 5, no. 8, pp. 649–655, 2018.

[8] W. C. Royster and S. D. Conte, "Convergence of finite difference solutions to a solution of the equation of the vibrating rod," *Proceedings of the American Mathematical Society*, vol. 7, no. 4, pp. 742–749, 1956.

[9] V. B. L. Chaurasia and R. S. Dubey, "Analytical solution for the differential equation containing generalized fractional derivative operators and Mittag-Leffler-type function," *International Scholarly Research Notices*, vol. 2011, Article ID 682381, 9 pages, 2011.

[10] D. J. Evans, "A stable explicit method for the finite-difference solution of a fourth-order parabolic partial differential equation," *The Computer Journal*, vol. 8, no. 3, pp. 280–287, 1965.

[11] D. J. Evans and W. S. Yousif, "A note on solving the fourth order parabolic equation by the AGE method," *International journal of computer mathematics*, vol. 40, no. 1-2, pp. 93–97, 1991.

[12] A.-M. Wazwaz, "On the solution of the fourth order parabolic equation by the decomposition method," *International Journal of Computer Mathematics*, vol. 57, no. 3-4, pp. 213–217, 1995.

[13] M. A. Almuqrin, P. Goswami, S. Sharma, I. Khan, R. S. Dubey, and A. Khan, "Fractional model of Ebola virus in population of bats in frame of Atangana-Baleanu fractional derivative," *Results in Physics*, vol. 26, article 104295, 2021.

[14] A. Kilicman, R. Shokhanda, and P. Goswami, "On the solution of (n+1)-dimensional fractional M-Burgers equation," *Alexandria Engineering Journal*, vol. 60, no. 1, pp. 1165–1172, 2021.

[15] I. Malyk, M. M. A. Shrahili, A. R. Shafay, P. Goswami, S. Sharma, and R. S. Dubey, "Analytical solution of nonlinear fractional Burger's equation in the framework of different fractional derivative operators," *Results in Physics*, vol. 19, article 103397, 2020.

[16] W. Liao, J. Zhu, and A. Q. M. Khaliq, "An efficient high-order algorithm for solving systems of reaction-diffusion equations," *Numerical Methods for Partial Differential Equations*, vol. 18, no. 3, pp. 340–354, 2002.

[17] M. K. Jain, S. R. K. Iyengar, and A. G. Lone, "Higher order difference formulas for a fourth order parabolic partial differential equation," *International Journal for Numerical Methods in Engineering*, vol. 10, no. 6, pp. 1357–1367, 1976.

[18] H. Caglar and N. Caglar, "Fifth-degree B-spline solution for a fourth-order parabolic partial differential equations," *Applied Mathematics and Computation*, vol. 201, no. 1-2, pp. 597–603, 2008.

[19] A.-M. Wazwaz, "Analytic treatment for variable coefficient fourth-order parabolic partial differential equations," *Applied Mathematics and Computation*, vol. 123, no. 2, pp. 219–227, 2001.

[20] J. Rashidinia and R. Mohammadi, "Sextic spline solution of variable coefficient fourth-order parabolic equations," *International Journal of Computer Mathematics*, vol. 87, no. 15, pp. 3443–3454, 2010.

[21] T. Aziz, A. Khan, and J. Rashidinia, "Spline methods for the solution of fourth-order parabolic partial differential equations," *Applied Mathematics and Computation*, vol. 167, no. 1, pp. 153–166, 2005.

[22] J. Biazar and H. Ghazvini, "He's variational iteration method for fourth-order parabolic equations," *Computers and Mathematics with Applications*, vol. 54, no. 7-8, pp. 1047–1054, 2007.

[23] M. A. Noor, K. I. Noor, and S. T. Mohyud-Din, "Modified variational iteration technique for solving singular fourth-order parabolic partial differential equations," *Nonlinear Analysis: Theory, Methods and Applications*, vol. 71, no. 12, pp. e630–e640, 2009.

[24] M. Dehghan and J. Manafian, "The solution of the variable coefficients fourth-order parabolic partial differential equations by the homotopy perturbation method," *Zeitschrift für Naturforschung A*, vol. 64, no. 7-8, pp. 420–430, 2009.

[25] M. Nadeem, F. Li, and H. Ahmad, "Modified Laplace variational iteration method for solving fourth-order parabolic partial differential equation with variable coefficients," *Computers and Mathematics with Applications*, vol. 78, no. 6, pp. 2052–2062, 2019.

[26] G. Adomian, "Solving frontier problems of physics: the decomposition method; with a preface by Yves Cherruault," *Fundamental Theories of Physics*, vol. 60, 1994.

[27] T. M. Elzaki, "The new integral transform Elzaki transform," *Global Journal of Pure and Applied Mathematics*, vol. 7, no. 1, pp. 57–64, 2011.

[28] T. M. Elzaki, "On the connections between Laplace and Elzaki transforms," *Advances in Theoretical and Applied Mathematics*, vol. 6, no. 1, pp. 1–11, 2011.

[29] T. M. Elzaki, "On the new integral transform "Elzaki transform" fundamental properties investigations and applications," *Global Journal of Mathematical Sciences: Theory and Practical*, vol. 4, no. 1, pp. 1–13, 2012.

[30] R. M. Jena and S. Chakraverty, "Solving time-fractional Navier-Stokes equations using homotopy perturbation Elzaki transform," *SN Applied Sciences*, vol. 1, no. 1, p. 16, 2019.

[31] A. K. H. Sedeeg, "A coupling Elzaki transform and homotopy perturbation method for solving nonlinear fractional heat-like equations," *American Journal of Mathematical and Computer Modelling*, vol. 1, no. 1, pp. 15–20, 2016.

[32] A. C. Loyinmi and T. K. Akinfe, "An algorithm for solving the Burgers–Huxley equation using the Elzaki transform," *SN Applied Sciences*, vol. 2, no. 1, pp. 1–17, 2020.